

Crosslinking Approaches towards Self-Healing Polymers: “Click”-Crosslinking and Supramolecular Clustering

Dissertation

zur Erlangung des
Doktorgrades der Naturwissenschaften (Dr. rer. nat.)

der

Naturwissenschaftlichen Fakultät II
Chemie, Physik und Mathematik

der Martin-Luther-Universität
Halle-Wittenberg

vorgelegt

von Frau Diana Döhler
geb. am 01.03.1988 in Werdau

Gutachter

1. Prof. Dr. Wolfgang H. Binder
2. Prof. Dr. Ulrich S. Schubert

Verteidigung: 01.10.2015

Halle (Saale), 16.06.2015

DANKSAGUNG

Ich danke Prof. Dr. Wolfgang Binder für die Überlassung des interessanten Themas verbunden mit den vielen Ausgestaltungsmöglichkeiten, die ich mir im Rahmen des Themas selbst wählen konnte, für die langjährige Betreuung und Zusammenarbeit seit 2009 und für die vielen eingeräumten Möglichkeiten, meine Forschungsergebnisse im In- und Ausland präsentieren zu können.

Des Weiteren danke ich der gesamten Arbeitsgruppe und ihren ehemaligen Mitgliedern für die gemeinsame Zeit und die entgegengebrachte Unterstützung. Mein besonderer Dank geht hierbei an Susanne Tanner, Norman Diedrich und Julia Weichhold für durchgeführte GPC-, ESI- und MALDI-Messungen und für die Bestellung und Bereitstellung von Chemikalien und Arbeitsmitteln, sowie an Anke Hassi für ihre Unterstützung bei allen administrativen Angelegenheiten. Außerdem danke ich der Mittagsrunde, allen jetzigen und ehemaligen Mitgliedern des Labors 3.03.0 und des Büros 3.10.0, insbesondere jedoch Philipp Michael, für die fachlichen Diskussionen, die Hilfe und für das offene Ohr in allen nur vorstellbaren Situationen.

Des Weiteren danke ich Dr. Anja Stojanovic-Marinow, Dr. Sravendra Rana und Dr. Johanna Akbarzadeh für ihre Unterstützung und ihre Ratschläge beim Erstellen meiner Dissertation.

Mein Dank geht auch an die Arbeitsgruppe von Prof. Alfred Blume und Prof. Dariush Hinderberger für die Bereitstellung des Rheometers und des Fluoreszenzspektrometers und die damit verbundenen fachlichen Diskussionen und an Dr. Ströhl und sein Team für die Anfertigung von unzähligen NMR-Spektren. In diesem Zusammenhang möchte ich auch Stefan Gröger für NMR-Messungen am Institut für Physik danken.

Zusätzlich danke ich Prof. Herwig Peterlik und Prof. Thomas Thurn-Albrecht und ihren Mitarbeitern sowie Dr. Sigrid Bernstorff und ihrem Team für die Durchführung von SAXS-Messungen und die damit verbundenen fachlichen Diskussionen.

Ich möchte mich auch bei Dr. Daniel Crespy und seinen Mitarbeitern für die Ermöglichung eines Forschungsaufenthaltes am Max-Planck-Institut für Polymerforschung in Mainz und die Betreuung vor Ort bedanken.

Außerdem danke ich meiner Familie und meinen Freunden für ihre ständige Motivation und Unterstützung, den von mir eingeschlagenen Weg weiter zielstrebig zu verfolgen. Danke, dass ihr immer für mich da seid und ich auch weiterhin auf Euch zählen kann!

Für meinen Vater.

Ich weiß, dass Du stolz auf mich gewesen wärst.

TABLE OF CONTENTS

1. ABSTRACT	VI
2. KURZDARSTELLUNG	VII
3. ABBREVIATIONS	VIII
4. INTRODUCTION	1
4.1. Self-healing polymers – from concepts to market	1
4.1.1. Definition and general considerations towards self-healing materials	1
4.1.2. (Pre-)commercial applications	2
4.1.3. Overview of self-healing concepts	3
4.2. Self-healing polymers <i>via</i> covalent crosslinking under ambient conditions	4
4.2.1. Initial self-healing approaches	6
4.2.2. Self-healing approaches based on click-chemistry	7
4.2.3. Metal-adhesives based on click chemistry	8
4.2.4. Polymer particles and polymer gels prepared <i>via</i> click chemistry	9
4.2.5. Degradable polymer networks prepared <i>via</i> click chemistry	9
4.2.6. Metal-free click reactions	10
4.2.7. Self-healing approaches based on Diels–Alder / retro Diels–Alder (DA / rDA) reactions	10
4.2.8. Thiol and radical based self-healing concepts	12
4.3. Self-healing concepts based on supramolecular interactions	12
4.3.1. Overview of different supramolecular interactions and their application potential towards self-healing polymers	12
4.3.2. Importance of phase segregation phenomena on the self-healing response	15
4.3.3. Hydrogen bonding interactions towards self-healing polymers	16
4.3.4. Hydrogen bonding interactions between ureidopyrimidone (UPy) synthons	17
4.3.5. Hydrogen bonding interactions between UPy and 2,7-diamido-1,8-naphthyridine (DAN) synthons	21
4.3.6. Hydrogen bonding interactions between ureido-7-deazaguanine (DeUG) or the butylurea of guanosine (UG) and DAN synthons	21
4.3.7. Bis(urea) based hydrogen bonding interactions	22
4.3.8. Fatty acid based formation of thermoplastic elastomers (TPEs)	23
4.3.9. Hydrogen bonding interactions between acid-, phenyl urazole acid- or phenyl urazole-functionalized polymers	23
4.3.10. Hydrogen bonding interactions between nucleobases and tailor-made hydrogen bonding wedges	24
4.4. Combined self-healing principles based on interwoven network structures <i>via</i> supramolecular and covalent network formation	26
4.4.1. Challenges for the further development of self-healing concepts	26
4.4.2. Overview of self-healing concepts based on interwoven network structures	26
4.4.3. Combined irreversible-reversible self-healing concepts	29
4.4.4. Combined reversible-reversible self-healing concepts	31
5. SCOPE OF THE THESIS	37
5.1. Objective	37
5.2. Concept	38

6. RESULTS AND DISUCSSION	41
6.1. Autocatalysis in the Room Temperature Copper(I)-Catalyzed Alknyne-Azide "Click" Cycloaddition of Multivalent Poly(acrylate)s and Poly(isobutylene)s	41
6.2. Hyperbranched poly(isobutylene)s for self-healing polymers	59
6.3. A dual crosslinked self-healing system: Supramolecular and covalent network formation of four-arm star polymers	72
7. SUMMARY AND OUTLOOK	89
8. REFERENCES	94
9. APPENDIX	XI
9.1. Preparation of initiators and quenching agents for living carbocationic polymerization of isobutylene and preparation of supramolecular moieties	XI
9.2. Autocatalysis during copper(I)-catalyzed alkyne-azide "click" cycloaddition crosslinking reactions	XIV
9.3. Characterization of hyperbranched poly(isobutylene)s and kinetic investigations of inimer-type living carbocationic polymerization <i>via</i> inline FTIR-measurements	XVI
9.4. Characterization of four-arm star poly(isobutylene)s and analysis of SAXS-data according to the Percus-Yevick model	XIX
CURRICULUM VITAE	XXII
EIGENSTÄNDIGKEITSERKLÄRUNG	XXV

1. ABSTRACT

The exploration of self-healing materials, which has started in 2001 inspired by the nature's inherent self-healing ability, supersedes the formerly damage management concept based on a continuous technical progress of artificial man-made materials. Thus, self-healing triggered by an external stimulus or the damage event itself includes the restoration of material properties and their mechanical performance while using inherently available resources in order to generate at least in theory an everlasting and unfailling material.

For the development of self-healing polymers, efficient and fast crosslinking processes working under ambient conditions in an autonomous fashion play a key role in order to close crack-induced damages while restoring the (mechanical) properties without any loss in functionality. Therefore, in the scope of this thesis, autocatalytic effects within a copper(I)-catalyzed alkyne-azide “click” cycloaddition (CuAAC) reaction based click-crosslinking approach suitable for room temperature self-healing applications have been investigated. Accordingly, liquid three-arm star azide- and alkyne-telechelic poly(isobutylene)s (PIBs) have been prepared *via* living carbocationic polymerization (LCCP). The click-crosslinking kinetics has been studied in dependence on the molecular weight and therefore on the functional group density, linking molecular mobility to the CuAAC reactivity. 1,3-Triazole ring formation was observed as a promoter for further click reactions showing an autocatalytic effect up to a factor of 3.8. Thus, formed 1,3-triazole rings subsequently acted as internal ligands preorientating functional groups near the active Cu(I) centers, hence accelerating the crosslinking process.

The so developed design of a fast and highly efficient crosslinking approach has been extended to hyperbranched azide- and alkyne-functionalized PIBs prepared *via* inimer (initiator-monomer) type LCCP. Thus, enhanced formation of triazole rings and improved network densities were envisioned while tuning the molecular architecture related to a higher functional group density per single molecule. Therefore, direct end quenching of living polymer chain ends using 3-(bromopropoxy)benzene (BPB) or trimethyl(3-phenoxy-1-propynyl)silane (TMPSS) has been optimized to yield bromide- and trimethylsilyl-protected alkyne-functionalized hyperbranched PIBs which were subsequently converted in the according azide- and alkyne-functionalized hyperbranched polymers with up to ≈ 10 endgroups. Click-crosslinking of so obtained highly functionalized spherical PIBs resulted in strongly crosslinked polymeric materials within 30 to 50 minutes emphasizing the great potential of a CuAAC reaction mediated development of room temperature self-healing polymers.

Accordingly, the fast and efficient covalent click-crosslinking approach was combined with a multiple time healing concept based on supramolecular cluster formation in order to create a dual self-healing material with an interwoven network structure, able to remain mechanical integrity. Therefore, four-arm star PIBs functionalized with both reactive azide-endgroups suitable for click-crosslinking and thymine-moieties undergoing reversible supramolecular network formation have been prepared *via* LCCP in combination with various endgroup transformation steps including microwave-assisted click chemistry to introduce supramolecular tie points. Thus, four-arm star PIB with averaging 1.7 azide endgroups and 2.3 thymine-endgroups per polymer was click-crosslinked with three-arm star alkyne-telechelic PIB resulting in a weakly crosslinked covalent network additionally supported by hydrogen bonding interactions. In comparison to four-arm star thymine-telechelic PIB which was obtained as tough supramolecular rubber click-crosslinking reduced the amount of clustered hydrogen bonds from ≈ 10 to ≈ 8 . Thus, tunable four-arm star polymers with mixed endgroups enabled the design of a multiple time room temperature self-healing system based on dual network formation due to supramolecular cluster formation and click-crosslinking.

2. KURZDARSTELLUNG

Die Erforschung selbstheilender Materialien, die 2001 inspiriert durch die Natur begann, löst das bisher bestehende Konzept der Schadenstoleranz, basierend auf der kontinuierlichen technischen Weiterentwicklung von kommerziellen Materialien, ab. Dem entsprechend beinhaltet Selbstheilung, ausgelöst durch einen externen Stimulus oder durch den auftretenden Schaden selbst, die Wiederherstellung der Materialeigenschaften und der mechanischen Leistung, um zumindest theoretisch ein immerwährendes, unfehlbares Material zu schaffen.

Für die Entwicklung selbstheilender Polymere spielen effiziente und schnelle Vernetzungsprozesse, die unter den vorherrschenden Umgebungsbedingungen ablaufen, eine Schlüsselrolle, um auftretende Risse zu schließen und die (mechanischen) Eigenschaften ohne Verlust der Funktionalität wiederherzustellen. In diesem Zusammenhang wurden im Rahmen dieser Dissertation autokatalytische Effekte in der Kupfer(I)-katalysierten Azid-Alkin-Klickreaktion und deren Anwendungspotential für die Selbstheilung bei Raumtemperatur untersucht. Dafür wurden flüssige, sternförmige Polyisobutylene funktionalisiert mit jeweils drei Azid- oder Alkin-gruppen mittels lebender karbokationischer Polymerisation synthetisiert. Die Kinetik des Klick-basierten Vernetzungsprozesses wurde in Abhängigkeit vom Molekulargewicht und der daraus resultierenden Konzentration an funktionellen Gruppen untersucht, um einen Zusammenhang zwischen der Reaktivität der Kupfer(I)-katalysierten Azid-Alkin-Klickreaktion und der molekularen Mobilität herstellen zu können. Durch die im Reaktionsverlauf voranschreitende Bildung von 1,3-Triazolringen, die als interne Liganden fungierten, wurden die nachfolgenden Klickreaktionen begünstigt, sodass ein autokatalytischer Effekt mit einem Faktor von bis zu 3.8 beobachtet wurde.

Das entwickelte Design der schnellen und effizienten Klick-basierten kovalenten Vernetzung wurde auf hyperverzweigte Azid- und Alkin-funktionalisierte Polyisobutylene, die mittels Initiator-Monomer vermittelter lebender karbokationischer Polymerisation hergestellt wurden, ausgedehnt. Aufgrund der Anpassung der molekularen Architektur, verbunden mit einer erhöhten Dichte an funktionellen Gruppen (3.04 bis 9.91), wurde eine vermehrte Bildung von Triazolringen und eine Erhöhung der daraus resultierenden Netzwerkichten erreicht. Dafür wurden die Reaktionsbedingungen des direkten Quenchs der lebenden Polymerketten mit 3-(Bromopropoxy)benzen und Trimethyl(3-phenoxy-1-propynyl)silan optimiert, um vollständig Bromid- und Trimethylsilyl-geschützte Alkin-funktionalisierte hyperverzweigte Polymere zu erhalten, die dann in die entsprechenden Azid- und Alkin-funktionalisierten Polymere umgewandelt wurden. Die Klick-basierte Vernetzung der stark funktionalisierten, kugelförmigen Polyisobutylene verlief innerhalb von 30 bis 50 Minuten unter Bildung hochvernetzter polymerer Materialien, die das Potential der Kupfer(I)-katalysierten Azid-Alkin-Klickreaktion für die Entwicklung von Raumtemperatur-basierten selbstheilenden Polymeren unterstreicht.

Der Ansatz der Klick-basierten Vernetzung wurde mit einem multiplen Heilungskonzept basierend auf der Bildung von supramolekularen Clustern kombiniert, um ein duales selbstheilendes Material mit einer verflochtenen Netzwerkstruktur und damit verbundener mechanischer Integrität zu entwickeln. Dafür wurden sternförmige Polyisobutylene mit reaktiven Azid-gruppen, die sich für die Klick-basierte Vernetzung eignen, und mit Thymin-gruppen, die reversible supramolekulare Netzwerke ausbilden, hergestellt. Sternförmige Polyisobutylene mit ca. 1.7 Azid-gruppen und 2.3 Thymin-gruppen pro Polymer wurden mit sternförmigen Alkin-funktionalisierten Polymeren zur Reaktion gebracht, wobei sich – unterstützt durch die Ausbildung von Wasserstoffbrückenbindungen – ein schwach vernetztes kovalentes Netzwerk ausbildete. Im Vergleich zu sternförmigen Thymin-funktionalisierten Polymeren, reduzierte der Klick-basierte Vernetzungsprozess die Anzahl der Wasserstoffbrückenbindungen im supramolekularen Cluster von ≈ 10 auf ≈ 8 , wobei Selbstheilung bei Raumtemperatur gezeigt wurde. Dem entsprechend ermöglicht die Synthese der sternförmigen Polyisobutylene mit gemischten Endgruppen durch Kombination von supramolekularer Clusterbildung und Klick-basierter kovalenter Vernetzung die Entwicklung eines Raumtemperatur-basierten, multiplen Selbstheilungssystems.

3. ABBREVIATIONS

A	Acceptor
ATMS	Allyltrimethylsilane
ATR	Attenuated total reflectance
bipy	Bipyridine
BPB	3-(Bromopropoxy)benzene
BPTCC	Biphenyl tetracumyl chloride
cal.	Calculated
CuAAC	Copper(I)-catalyzed alkyne–azide “click” cycloaddition
D	Donor
DA	Diels–Alder
DAN	2,7-Diamido-1,8-naphthyridine
DCM	Dichloromethane
DCPD	Dicyclopentadiene
DCTB	<i>Trans</i> -2-[3-(4- <i>tert</i> -butyl-phenyl)-2-methyl-2-propenylidene]malononitrile
DeUG	Ureido-7-deazaguanine
DIPEA	<i>N,N</i> -Diisopropylethylamine
DMA	<i>N,N</i> -Dimethylacetamide
DMF	<i>N,N</i> -Dimethylformamide
DMSO	Dimethyl sulfoxide
DSC	Differential scanning calorimetry
<i>Dt</i> BP	2,6-Di- <i>tert</i> -butylpyridine
EA	Ethyl acetate
ESI	Electrospray ionization
FTIR spectroscopy	Fourier transform infrared spectroscopy
GPC	Gel permeation chromatography
IB	Isobutylene
Inimer	Initiator-monomer
IR	Infrared
LA	Lewis acid
LCCP	Living carbocationic polymerization
MALDI	Matrix assisted laser desorption and ionization
Mebip	2,6-Bis(<i>N</i> -methylbenzimidazolyl)pyridine
MeOH	Methanol
MS	Mass spectrometry
<i>n</i> BA	<i>N</i> -butyl acrylate
NMP	Nitroxide mediated polymerization
NMR	Nuclear magnetic resonance
OMebip	4-Oxy-2,6-bis(<i>N</i> -methylbenzimidazolyl)pyridine
PA	Propargyl acrylate
PCL	Poly(ϵ -caprolactone)
PDI	Polydispersity index
PDMS	Poly(dimethyl siloxane)
PEG	Poly(ethylene glycol)
PEO	Poly(ethylene oxide)
PIB	Poly(isobutylene)
PMMA	Poly(methyl acrylate)
<i>Pn</i> BA	Poly(<i>n</i> -butyl acrylate)

PPO	Poly(propylene oxide)
PS	Poly(styrene)
pTHF	Poly(tetrahydrofuran)
PVA	Poly(vinyl alcohol)
rDA	Retro Diels–Alder
ROMP	Ring-opening metathesis polymerization
RT	Room temperature
SAXS	Small-angle X-ray scattering
SDS	Sodium dodecyl sulfonate
SEM	Scanning electron microscopy
TAD	1,2,4-Triazoline-3,5-dione
TBAF	Tetrabutylammonium fluoride
TBTA	Tris[(1-benzyl-1 <i>H</i> -1,2,3-triazol-4-yl)methyl]amine
T_g	Glass transition temperature
TGA	Thermogravimetric analysis
THF	Tetrahydrofuran
TIPNO	2,2,5-Trimethyl-4-phenyl-3-azahexane-3-nitroxide
TLC	Thin-layer chromatography
TMPPS	Trimethyl(3-phenoxy-1-propynyl)silane
TMS	Trimethylsilyl
TMSPA	3-(Trimethylsilyl)prop-2-ynyl acrylate
TOF	Time of flight
TPE	Thermoplastic elastomer
tpy	2,2':6',2''-Terpyridine
UPy	Ureidopyrimidone
UV	Ultraviolet

IR-spectroscopy

w	Weak
m	Middle
s	Strong

NMR-spectroscopy

d	Doublet
dt	Doublet of a triplet
dd	Doublet of a doublet
m	Multiplet
qu	Quintet
s	Singlet
t	Triplet

Parts of the introduction have been published in the book chapter "Principles of Self Healing Polymers" (D. Döhler, P. Michael, W. H. Binder*, in *Self Healing Polymers: from Principle to Application* (Ed.: W. H. Binder), Wiley-VCH Verlag GmbH & Co. KGaA, Weinheim, **2013**, pp. 7. <http://www.wileyvch.de/publish/dt/books/bySubjectCH00/forthcomingTitles/3527334394/?sID=4lc2dgtgl51e02a336i57dj356>) Text parts and tables have been reprinted and adapted with permission from John Wiley and Sons (Copyright 2013).

The results of the *Results and Discussion* part of this thesis are based on several publications. Thus, the first section is dedicated to covalent click-crosslinking approaches towards the design of a once-a-time self-healing system acting at room temperature, therefore dealing with the "Autocatalysis in the Room Temperature Copper(I)-Catalyzed Alkyne-Azide "Click" Cycloaddition of Multivalent Poly(acrylate)s and Poly(isobutylene)s" (D. Döhler, P. Michael, W. H. Binder, *Macromolecules* **2012**, *45*, 3335. <http://dx.doi.org/10.1021/ma300405v>), while the second section shows the extension of this approach to hyperbranched polymers investigating "Hyperbranched poly(isobutylene)s for self-healing polymers" (D. Döhler, P. Zare, W. H. Binder, *Polym. Chem.* **2014**, *5*, 992. <http://dx.doi.org/10.1039/C3PY01151H>). Text and figures have been adapted with permission from the American Chemical Society (Copyright 2012) and by the Royal Society of Chemistry (Copyright 2014).

In the third section of the main part of the thesis the results related the design of interwoven network structures *via* simultaneously proceeding covalent and supramolecular network formation towards a multivalent room temperature based self-healing concept combining sufficient chain dynamics and mechanical integrity can be found dealing with "A dual crosslinked self-healing system: Supramolecular and covalent network formation of four-arm star polymers" (D. Döhler, H. Peterlik, W. H. Binder, *Polymer* **2015**, doi:10.1016/j.polymer.2015.01.073. <http://dx.doi.org/10.1016/j.polymer.2015.01.073>). Text and figures have been adapted with permission from Elsevier Ltd. (Copyright 2015).

4. INTRODUCTION

4.1. Self-healing polymers – from concepts to market

4.1.1. Definition and general considerations towards self-healing materials

Self-healing is defined as the ability to restore (partially) degraded material properties, function and performance like wear resistance, adhesion strength, hardness, corrosion protection, thermal or electrical conductivity, reflectivity etc. as well as to recover the mechanical performance of the material by repairing the damage under usage of inherently available resources triggered by the damage event itself or by external stimuli like heat, light or pressure^[1].

Although self-healing is a well known phenomena in nature and furthermore found unconsciously application in natural building materials like mortar and adobe for the construction of impressive and therefore everlasting buildings like the Pantheon in Rome, up to now usually the design of new materials with improved (mechanical) properties and an increased robustness as well as the development of nondestructive material inspection and evaluation methods played a major role^[1b, 1d]. Now, with the investigation of self-healing materials this formerly damage prevention approach limited by a confined development potential was superseded by newly developed damage management concepts (see Figure 1)^[1b, 1d, 2].

Accordingly, self-healing concepts offer new routes towards longer-lasting and therefore safer, fault tolerant products across a broad range of material classes for a magnitude of potential applications^[1b, 1d], whereas in an ideal multiple self-healing material the service lifetime is abundantly extended without loss of the initial material properties (see Figure 1, curve d). Thus, self-healing materials were listed as one of the ten emerging technologies by the World Economic Forum in 2013^[3].

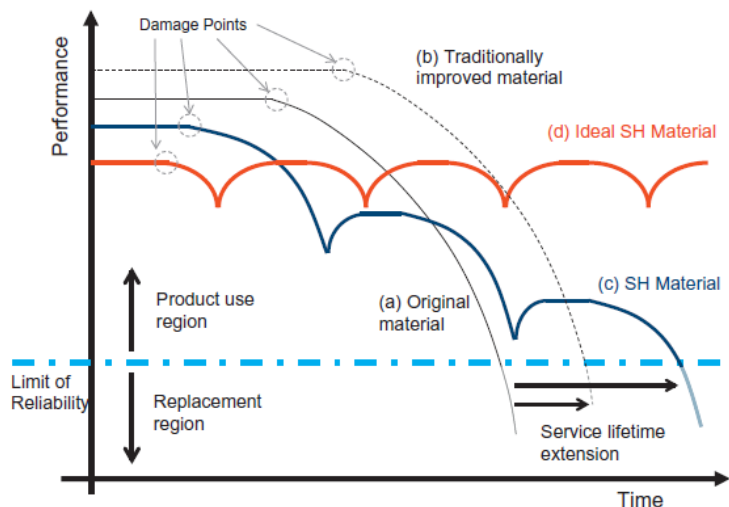


Figure 1: Implementation of self-healing principles in engineered materials for service lifetime extension. Figure reprinted from reference^[1d] with permission from Elsevier Ltd. (Copyright 2014).

In general, all classes of polymers ranging from elastomers over thermosets to thermoplastics have the potential for self-healing^[1b], whereas within all material classes polymers exhibit the greatest self-healing potential due to their outstanding molecular mobility and their enormous development opportunities towards chemical functionalization and modification^[1e].

Polymers displaying self-healing properties need the ability to transform physical energy into a chemical and / or physical response able to heal the damage – a process which is inspired by nature^[4] and which normally is not present in conventional polymers. Thus, the polymer needs to identify the state of structural integrity and to "sense" the damage while transforming it autonomously (without further external stimulus)^[1b, 1e] into a healing event at the damaged site in order to maintain the mechanical integrity of the material^[1d].

Thus, a self-healing polymer, is supposed to heal an occurring damage at a local site in time^[1e] by either physical processes alone or *via* a combination of chemical and physical processes, whereas the healing process should be faster than crack propagation^[1e]. The design of self-healing polymers, therefore, is a multidisciplinary process involving chemists, physicists and material scientists, requiring knowledge about the polymer structure, its individual dynamics, as well as a deep knowledge of chemical processes. Thus, the design of self-healing polymers needs a thorough understanding of the polymer's individual dynamics, including also the dynamics of each segment interacting with a specific part of the newly created interface or other polymeric / monomeric molecules^[1a].

A great challenge for chemists and material scientists involved in the evolution of self-healing polymers is the development of self-healing concepts that, in a fast and preferably simple way, form highly crosslinked networks. Therefore, investigated approaches display different features with respect to external conditions under which self-healing takes place such as the required stress for activation, the temperature of healing as well as other external constraints imposed by the mechanism of the healing concept. Often, the properties of the self-healing agents have been tuned so that damage healing is occurring under ambient conditions, like low temperatures, or humid and oxygen-containing environments. Moreover, some scientists explore catalytic self-healing methods to accomplish a fast network formation at ambient temperatures, while others pursue higher temperature methods.

Besides, a large diversity of protection methods for healing agents, such as encapsulation or *in situ* activation of catalysts, was developed, also preventing undesired premature crosslinking reactions. Furthermore, the number of healing-cycles thus implying either a once-a-time-healing response after a single stress event, or the possibility to repeatedly heal damage at the same position of the material as well as the timescale on which the self-healing process is taking place can be tuned.

Another challenging task is to achieve a healing reaction only in direct response to a damage event. Therefore, reversible reactions shiftable to a "broken" stage and cured subsequently by re-shifting to the "healed" stage can be used. Hence, a large body of work has been dedicated to develop a diversity of self-healing concepts while optimizing the healing conditions like the operating temperature, required additives, and the applied catalysts as well as the technical realization of the concept, thus being able to fabricate and produce technically useful self-healing polymers at reasonable costs^[1-2].

4.1.2. (Pre-)commercial applications

Some self-healing products are already at a (pre-)commercialization level including self-healing asphalt triggered by induction-heating^[5], self-healing bacteria-containing concrete^[6] as well as self-healing clear coatings^[7] (see Figure 2).

Thus, self-healing asphalt consisting of porous asphalt concrete and incorporated steel wool fibers was developed at Delft University and was used for building a test track on the A58 near Vlissingen in the Netherlands. A self-healing response is obtained by induction heating of steel wool fibers resulting in the closure of microcracks and in the reduction of stone loss at an early stage. Thus, an 85 % recovery of the original bending strength and therefore, an improvement of the driving safety especially during rainy weather and an extension of the service lifetime of the freeway were obtained^[5].

Self-healing concrete was designed by adding a specific group of spore-forming and alkaline-resistant bacteria (*Bacillus*) as self-healing agent. In case of a rupture event related to the penetration of water the bacteria become active and convert their incorporated "food" namely calcium lactate to calcium carbonate or calcium carbonate-based minerals thus closing the crack^[6].

Self-healing clear coatings based on poly(urethane)s find application in automotive industry as protection layer against scratches while providing resistance and elasticity to automotive paints.

Self-healing is achieved either *via* elastic poly(urethane) networks with a molecular memory and thus, deforming under mechanical impact while reforming their old structure afterwards or *via* incorporation of hydrogen bonding interactions allowing self-healing under sunlight-induced heating^[7].

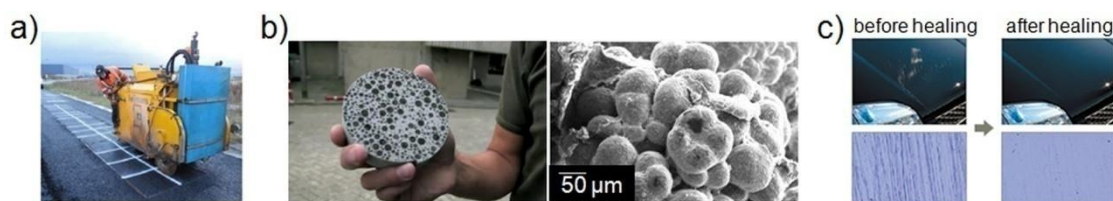


Figure 2: a) Rotating surface abrasion test slaps preparation process, figure reprinted from reference^[5b] with permission from Elsevier Ltd. (Copyright 2014), b) self-healing concrete containing bacteria spores (left), a bacteria-induced mineral deposit (right), figure reprinted from reference^[6a, 6b], c) automotive paint of an engine bonnet before (left) and after self-healing (right), figure reprinted from reference^[7c].

4.1.3. Overview of self-healing concepts

Similar to biochemical healing processes, the initial damage generates a free, usually fresh and non-equilibrated interface, which in turn can act as a site for molecular processes, including swelling, patching or simple molecular diffusion, which can therefore induce a welding process, subsequently leading to crack closure *via* surface rearrangement, surface approach, wetting, diffusion, and randomization and thus a "self-healing" response^[8]. Furthermore, nanoparticles or small up to even large molecules can diffuse to the interface, thus leading to changes in the local concentration, and in the individual local mobility of the molecules resulting in turn to a (crack) healing ability.

Chemical healing processes always need a combination of physical and chemical healing principles, as a chemical reaction can only take place after achieving contact between the liquid reactants. In general, after transfer of healing agents *via* diffusion, self-sealing and conversion of the reactive healing components, the crack is filled by a newly generated and mechanically stable network^[1d, 1e], formed by a crosslinking reaction of individual polymer chains, either *via* purely physical and therefore supramolecular forces, or by action of truly chemical forces resulting in reversible or stable covalent bonds.

Moreover, often an inherent "switch" such as light or an electrochemical stimulus can be used to trigger a (reversible) network formation within the polymer and thus a self-healing response.

Purely supramolecular interactions, well known from molecular self-assembly, can reform, thus generating a network with intrinsic dynamic properties and thus an – at least in theory – multiple time self-healing ability.

In contrast, covalent chemistry is able to form new networks by a plethora of chemical crosslinking reactions involving various kinds of functional groups, often well known and well optimized by technical processes of resin-chemistry ("thermosets"). In particular, Diels-Alder (DA) reactions^[9], epoxide chemistry^[10], "click-based" chemistry^[11], isocyanate chemistry^[12], ring opening metathesis polymerization^[10m, 13], and thiol chemistry^[11a-g] have gained significance in the development of self-healing concepts.

Choice of the therefore applied chemical reactions usually takes into account the efficiency ("free energy") of the reactants as a major selection tool also for a specific application, besides the stability and selective incorporation of the respective functional groups into the final material, for example, *via* encapsulation or enchanneling strategies allowing sufficient protection during processing while releasing the self-healing agents on demand in case of a rupture event^[1e, 4a].

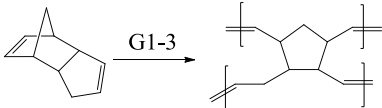
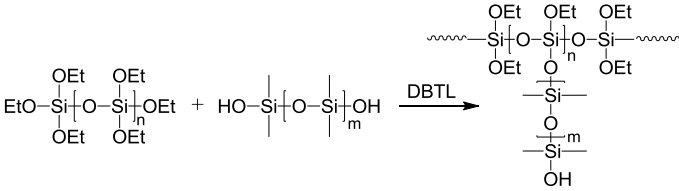
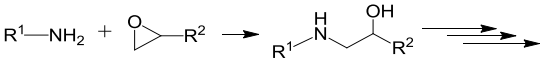
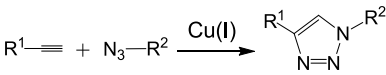
Moreover, self-healing concepts using mechanochemical activation of molecules can be designed. Thereby, the physical energy of a damage is directly transformed by a mechanophore^[14] into an activated chemical state, which in turn allows self-healing. These specially designed groups are intrinsically connected to the polymer chains, acting as a "handle", which by definition allows the conversion of applied mechanical energy into the actual chemical reaction^[15] and thus in a self-healing response. Therefore, especially, ring-opening reactions^[14c, 14d, 16] and carbene-based catalyst activation^[17] have become prominent for realizing the concept of self-healing polymers.

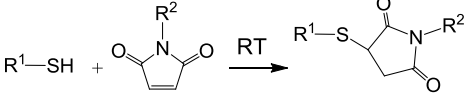
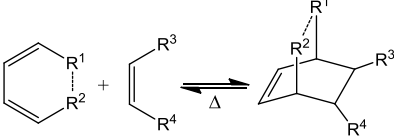
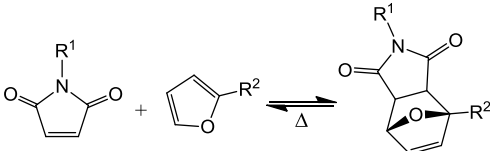
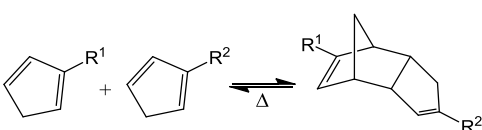
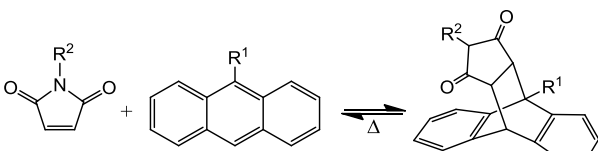
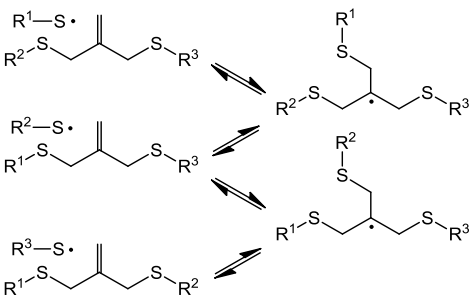
4.2. Self-healing polymers *via* covalent crosslinking under ambient conditions

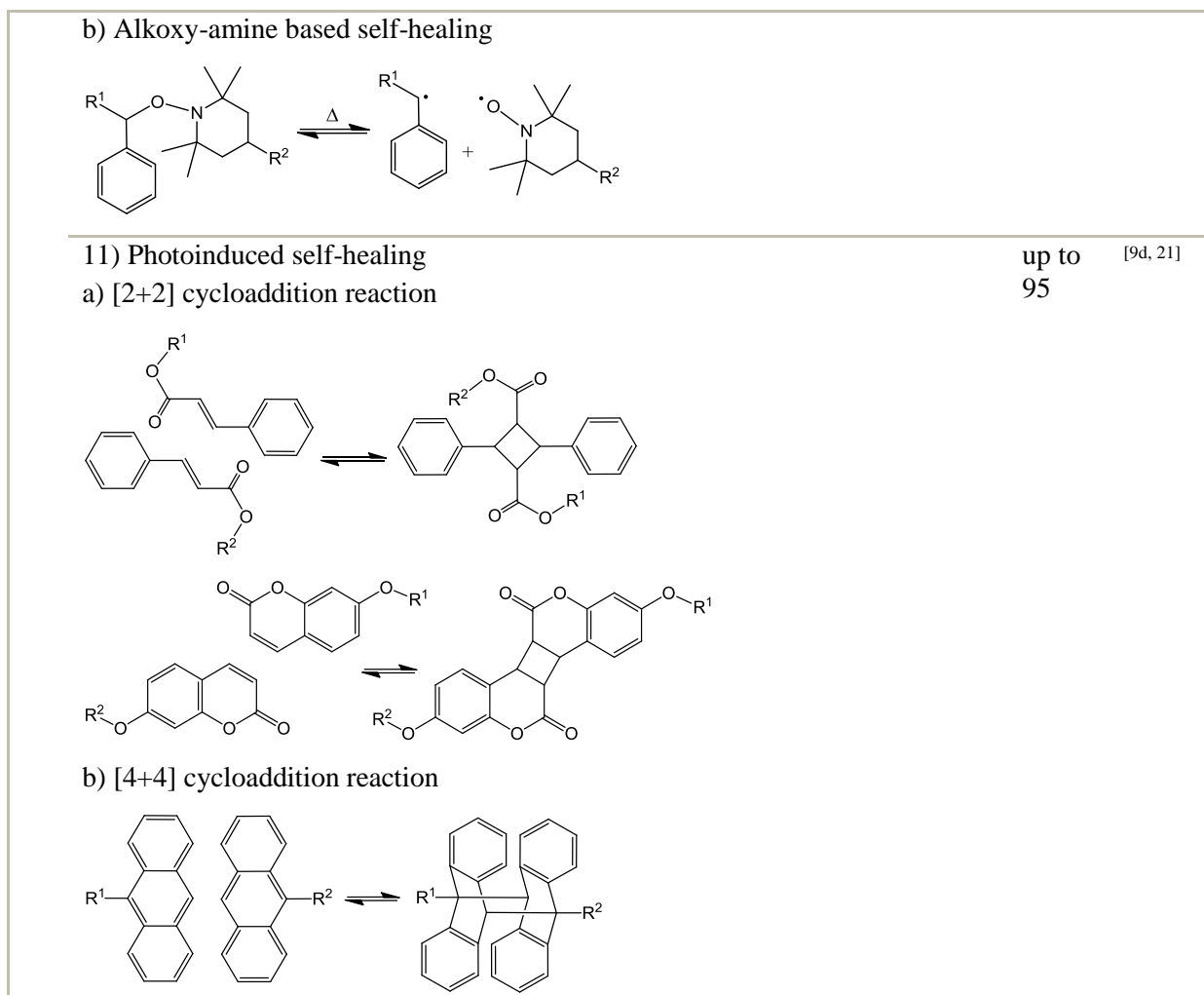
Chemical self-healing principles can be classified into two main categories, based either on covalent or on supramolecular network formation. In the case of covalent network formation chemical bonds between functional groups are generated and thus a permanent, but sometimes also reversible, network is established. In contrast, supramolecular networks are commonly reversible associates of polymers connected *via* supramolecular interactions thus showing a high dynamic behavior.

In self-healing concepts based on covalently crosslinked networks, covalently linked network points are generated in a chemical reaction. They exist in a large diversity and can be subdivided into reversible and irreversible reactions (see Table 1). Reversible methods, like DA / rDA reactions^[9] or polycondensation reactions and poly(siloxane)-based self-healing approaches^[18] provide the opportunity for multiple healing cycles, while irreversible methods, like the microcapsule-based ROMP concept^[10m, 13], epoxides^[10], or various click approaches^[11], cannot heal a once ruptured area a second time.

Table 1: Self-healing concepts based on covalently crosslinked networks *via* I) reversible network formation or II) irreversible network formation.

Self-healing concept	η_{SH} [%]	Ref.
I) 1) Ring opening metathesis polymerization (ROMP) 	up to 99	[10m, 13]
2) Polycondensation reactions of poly(siloxane)s and poly(siloxane)-based self-healing approaches 	24	[18a-d, 18g-k]
3) Epoxide curing 	up to 100	[10]
4) CuAAC "click" reactions 	up to 100	[11g-ad]

5) Thiol-ene / thiol-yne "click" reactions	up to 93	[11a-g]
$R^1-C\equiv C + HS-R^2 \xrightarrow{h\nu} R^1-CH_2-CH_2-S-R^2$		
6) Michael addition	up to 121	[11ae, 11af]
		
II 7) Diels-Alder / retro-Diels-Alder reactions (DA / rDA reactions)	up to 100	[9]
		
a) furan-maleimide based DA / rDA reactions	at RT: 70	
		
b) cyclopentadiene based DA / rDA reactions		
		
c) anthracene based DA / rDA reactions		
		
8) Thiol-disulfide linkages	50 - 104	[19]
$R^1-SH + HS-R^2 \xrightleftharpoons[\text{reduction}]{\text{oxidation}} R^1-S-S-R^2$		
9) Disulfide exchange		
$R^1-S-S-R^2 + R^3-S-S-R^4 \xrightleftharpoons{RT} R^1-S-S-R^4 + R^2-S-S-R^3$		
10) Radical based self-healing concepts	60 - 105	[20]
a) RAFT-like reactions		
		



4.2.1. Initial self-healing approaches

The most prominent self-healing concept using irreversible covalent network formation based on the ROMP of dicyclopentadiene was developed in 2001^[13a]. The healing agent was encapsulated and subsequently embedded into an epoxy-matrix with incorporated Grubbs catalyst (see Table 1, Entry 1). In case of a damage event cyclopentadiene was released into the crack plane, resulting in network formation *via* ROMP after getting into contact with the Grubbs catalyst^[13a-d]. Thus, the material properties were recovered, while achieving self-healing efficiencies up to 99 %^[13e]. Other monomers which were applied as healing agent for a ROMP-based self-healing system include norbornene^[13f], 5-(chloromethyl) norbornene^[13h], 5-(bromomethyl) norbornene^[13h], 5-ethylidene-2-norbornene^[13g], norbornene carboxylic acid ethyl ester^[13h] and *endo*-1,2-dihydrodicyclopentadiene^[13f].

In a similar approach, the organotin-catalyzed polycondensation reaction between poly(diethoxysiloxane)s and hydroxyl-functionalized poly(dimethylsiloxane)s (see Table 1, Entry 2) has been studied due to the higher catalyst stability against oxygen and humidity and due to better and cheaper technical availability of therefore required components. To prevent premature crosslinking reactions, the tin catalyst had to be encapsulated. However, only a healing efficiency of 24 % was achieved limiting technical realization^[18g, 18h].

Irreversible covalent network formation can also be realized by epoxides undergoing fast coupling reactions^[10f-p] due to their high ring strain. Thus, they react with a hardener, which is a substrate usually containing activated hydrogen atoms, including amines, maleimides, acid anhydrides, alcohols, carboxylic acids as well as mercaptans (see Table 1, Entry 3). Embedded as encapsulated

healing agents covalent bond formation, related to conversions up to 100 %, is taking place in case of a rupture event resulting in the release of reactive components. Thereby, crosslinking can proceed either under ambient conditions ("cold curing") or at high temperatures ("hot curing") resulting in the formation of a three-dimensional and insoluble thermoset network, thus filling the crack while restoring the original material properties. For the design of self-healing composites, especially primary and secondary aliphatic amines find application due to their increased low temperature reactivity. By choosing the hardener and therefore the curing conditions the properties of the final resin including its morphology and crosslinking density can be adopted to the desired demands. Furthermore, epoxy curing possesses a great advantage towards the development of self-healing resins bringing them close to technical realization: as during the self-healing reaction the same kind of material is generated, good adhesion between the newly formed thermoset and the matrix is ensured while enabling a full recovery of strength without introducing any tension.

4.2.2. Self-healing approaches based on click-chemistry

Several once-a-time crosslinking concepts acting at ambient temperatures based on CuAAC reactions^[11h-n] (see Table 1, Entry 4), as well as on the thiol-ene / thiol-yne reactions^[11a-gl] (see Table 1, Entry 5) have been investigated. However, the used set-up of reactions can be generalized by the term click chemistry^[22] characterized by the generation of only one, mostly regiospecific pure product under simple reaction conditions and in high yields. Accordingly, their capability for self-healing applications is primed by a thermodynamic driving force greater than 20 kcal·mol⁻¹^[23] related to a fast and complete conversion.

Thus, a one-time self-healing concept based on the CuAAC of multivalent azide- and alkyne-functionalized PIBs and poly(acrylate)s was investigated^[11h-k]. Therefore, polymers with different molecular weights and different functional group densities were synthesized *via* living polymerization techniques as at least three functional groups per polymer are needed to obtain a conversion of 50 to 66 % at the gel point^[24]. While using Cu⁽⁰⁾Br(PPh₃)₃ crosslinking of equimolar polymer mixtures proceeded at room temperature achieving gelation times, determined as crossover of the storage and loss modulus^[25], within the range of 2 - 15 hours^[11h, 11k]. The crosslinking behavior – investigated *via in situ* rheology as appropriate tool to get information about the dynamics of network formation^[26] – was studied in dependence on the starting viscosity of equimolar polymer mixtures, on the molecular weight and on the concentration of functional groups as kinetic quantities can be calculated on the basis of changes in the viscosity up to the gel point^[25] related to the degree of conversion^[27]. While analyzing the change of the viscosity during the progress of the click reaction, increasing reaction rates with increasing concentration of functional groups were observed, while demonstrating an autocatalytic effect within the reaction up to a factor of 4.3. The acceleration of further click reactions was correlated to clustering effects of formed triazole rings, acting as internal ligands while preorientating the reactive endgroups near to the active copper(I) center. Thus, a polymeric room temperature self-healing approach predicated on a deeper understanding of catalytic effects throughout the CuAAC was developed^[11h].

Previously, the successful encapsulation of a liquid and highly reactive, three-arm star azide-telechelic PIB healing agent was shown for the first time. After embedding μm-sized capsules filled with multivalent alkynes and three-arm star azide-telechelic PIB in a high-molecular weight PIB matrix together with finely dispersed Cu⁽⁰⁾Br(PPh₃)₃, reactive components were released by shear force induced rupture. Due to the subsequently proceeding network formation *via* CuAAC, dynamic mechanical analysis showed a 91 % recovery of the tensile storage modulus at room temperature, proving the concept of a PIB-based one-time self-healing approach.^[11i]

In a very similar self-healing approach based on the CuAAC^[11i, 11m] a bisphenol-A based bisazide and bisphenol-E or tetraethylene glycol based diynes have been used, thus ensuring flow of the components into the crack plane. After triggering the CuAAC by the copper(I) catalyst the network filled the crack and restored the material properties. However, due to the usage of bivalent monomers, solely linear polymers were generated forming networks only *via* physical chain entanglements.

4.2.3. Metal-adhesives based on click chemistry

Metal-adhesive materials^[11q-s] with a comparable or even improved outstanding strength to commercial glues have been prepared by click-crosslinking of stock solutions of various low molecular weight multivalent azides and alkynes directly on a metal surface^[11r, 11s]. Thus, the Cu(I) ions needed to enable the crosslinking reaction have been provided directly by the pure metal surface^[11r, 11s]. Adhesives with an outstanding high crosslinking density were obtained for starting materials with a higher degree of functionality and if mixed in an exact 1:1 ratio^[11r, 11ab]. Accordingly, the highest network density was obtained for crosslinking a trivalent azide and a tetravalent alkyne. Thereby, a raise in the temperature enhanced the click reaction, whereas the time required for adhesive formation strongly depended on the nature of the investigated monomers^[11s]. In contrast, the maximum adhesive strength was not affected by the curing temperature^[11s]. Furthermore, the presence of amines assisted the production of the Cu-acetylide intermediate while productively contributing to the chelating interactions with the metal center. Thus, longer polymer chains with improved adhesive properties were obtained^[11r]. Load testing of prepared materials showed a load bearing capacity of 27 - 268 kg load per g adhesive comparable to commercial glues with a load bearing capacity between 212 - 248 kg load per g glue^[11r] (see Figure 3). In a modified peel test even improved mechanical properties have been reported with a better adhesion strength compared to commercial glue formulations. Thus, the force at failure was between 4 - 92 N for prepared adhesives compared to 49 - 55 N for commercial glues^[11s], whereas the strong adhesion ability was explained by the formation of three-dimensional high molecular weight thermosets remaining bound to Cu(0)-centers^[11t].



Figure 3: Determination of the load bearing capacity of adhesives *via* peel test with crossed copper plates. Figure reprinted from reference^[11r] with permission from John Wiley and Sons (Copyright 2004).

In a similar approach, low molecular weight bisazides and trisalkynes^[11u] in the presence of an amine, $\text{CuSO}_4 \cdot 5\text{H}_2\text{O}$ and sodium ascorbate, whereas some azide groups remained in hindered regions. Thus, further click-crosslinking did not proceed and the obtained materials showed a swelling and deswelling behavior exclusively in strong acidic media (TFA in DCM) resulting in a 18 times weight increase within the first 10 minutes. An even more swellable triazole polymer was obtained under more diluted conditions by crosslinking a 3:2 mixture of 1,6-diazidohexane and tripropargylamine^[11u].

4.2.4. Polymer particles and polymer gels prepared *via* click chemistry

Azide-functionalized poly(styrene-*co*-chloromethyl styrene) co-polymers^[11o] with different amounts of incorporated azide-groups per chain underwent a room temperature click crosslinking reaction with various low molecular weight bivalent alkyne-components. Accordingly, cyclic polymers and particle-like structures were observed in solution, whereas investigations in the solid state as well as self-healing tests have not been performed^[11o].

Similarly, bioconjugable polymeric nanoparticles (5 - 20 nm) out of poly[MMA-*co*-(3-azidopropyl methacrylate)-*co*-(3-trimethylsilyl-propyn-1-yl methacrylate)] terpolymers with different composition have been prepared by a room temperature based single-chain intramolecular click crosslinking approach in solution while adding CuBr and TBAF in a one-pot reaction^[11p].

Polyester nanoparticles have been prepared either *via* a CuAAC reaction or *via* a thiol-ene reaction^[11g]. Thus, an alkyne-functionalized polyester was crosslinked with 1,8-diazide-3,5-dioxaoctane in the presence of CuBr at room temperature or 45 °C, whereas the size of the nanoparticles strongly depended on the amount of added equivalents of the azide component as well as on the reaction temperature (at 45 °C: 40 +/- 4 nm for 2 equivalents, 88 +/- 5 nm for 4 equivalents and 183 +/- 14 nm for 8 equivalents). A similar equivalent-dependent size evaluation of polyester nanoparticles was observed while applying thiol-ene-chemistry^[11g].

Biodegradable PEG-peptide hydrogels for cell-based wound healing applications^[11v] have been prepared by reacting four-arm star alkyne-telechelic PEG with an azide-modified Arg-Gly-Asp (RGD-sequence) containing peptide in the presence of CuSO₄·5H₂O and sodium ascorbate. Thus, obtained hydrogels characterized by a swelling degree between 20 - 30 % and a quasi-equilibrium modulus ranging from 83 - 285 Pa showed an improved cell attachment as well as greater cell proliferation rates^[11v]. Similar, PEG-based hydrogels have been obtained by room temperature crosslinking of four-arm star azide-telechelic and bivalent alkyne-telechelic PEGs.^[11w] Remaining functional groups were used for subsequent chemical tailoring resulting in diverse crosslinked materials. Hydrogel formation proceeded within minutes while obtaining a gel fraction of 95 % or higher. Thus, PEG-based hydrogels showed a higher gel fraction, a higher swelling degree and consequently a higher extension to break than comparable photochemically crosslinked hydrogels^[11w]. Click-crosslinking of multivalent azide- and alkyne-modified PVAs in the presence of CuSO₄·5H₂O and sodium ascorbate resulted in the formation of PVA-based hydrogels^[11x] with a gel fraction up to 89 %, a storage modulus up to 1013 Pa and a 3 to 4 fold swelling ability. Furthermore, polyfunctional PVAs showed a higher gelation capacity than bivalent functionalized PEG crosslinkers with a gel fraction of 64 %^[11x].

Hyaluronic acid based hydrogels for drug-delivery systems with an elastic plateau moduli between 1490 - 6700 Pa were prepared by crosslinking of an azide-functionalized hyaluronan and different bisalkyne components with varying length^[11aa]. Click-crosslinking proceeded at room temperature in the presence of CuSO₄·5H₂O and sodium ascorbate, whereas the degree of swelling was an inverse function of the bisalkyne length^[11aa]. Similarly, highly porous hydrogels as scaffolds for tissue engineering have been synthesized by click-crosslinking of azide- and alkyne-amide derivated hyaluronic acids^[11ac].

4.2.5. Degradable polymer networks prepared *via* click chemistry

By click-crosslinking of a four-arm star azide-terminated PEI^[11y] with a disulfide containing low molecular weight bisalkyne crosslinker in the presence of CuBr a reducibly degradable disulfid-containing polymeric material was obtained. The so introduced reduction-responsiveness was investigated by testing either glutathione or 1,4-dithio-DL-threitol while mimicking the reductive

intracellular environment. Thus, a high gene transfection efficiency and the ability to condense plasmid DNA into positively charged polymeric nanoparticles was proven^[11y].

Ozonizable and thus degradable three-dimensional polymer networks were obtained by combining an ATRP approach using 1,4-bis(bromoisobutyryloxy)-2-butene as initiator with click crosslinking^[11z]. Thus, prepared linear azide-modified poly(*tert*-butylacrylate) was reacted with tetravalent low molecular weight alkyne components, whereas cleavage and dissolution of solid triazole-containing materials was achieved by ozonolysis of incorporated double bonds^[11z].

4.2.6. Metal-free click reactions

Hyperbranched poly(aroyltriazole)s with film forming capability have been obtained *via* a metal-free click reaction between trisazides and bis(aroylacetylene)s^[11ad] (see Figure 4). Due to remaining free azide- and alkyne-groups in the periphery, repeatable healing of cut films was observed while heating up to 110 °C for four hours. Although a reduced amount of unreacted azide groups within healed films was observed, healing was mainly attributed to the reflow of the material as the applied healing temperature exceeded its T_g ^[11ad].

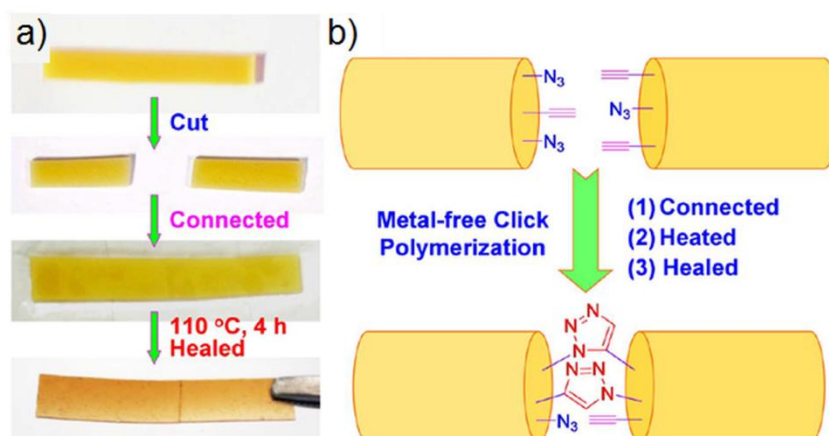


Figure 4: a) Self-healing of poly(aroyltriazole) films at 110 °C, b) proposed self-healing mechanism *via* metal-free click polymerization. Figure reprinted from reference^[11ad] with permission from the Nature Publishing Group (Copyright 2013).

Other interesting potential self-healing approaches based on click chemistry might be the strain-promoted azide-alkyne cycloaddition reaction or the photochemically triggered thiol-ene or thiol-yne click reactions^[11a-g]. Thereby, the absence of biotoxic copper salts affords application in living systems. Moreover, thiol-ene and thiol-yne click reactions enable a spatially and temporally controlled light-triggered self-healing process.

An alternative self-healing concept uses the Michael addition (see Table 1, Entry 6) of multivalent thiols and maleimides^[11ae, 11af] and can be applied for the damage healing of epoxy amino resins due to the crosslinking between maleimide moieties and residual amino groups at the crack surface. Therefore, the healing efficiency strongly depends on the used matrix resin and the applied curing conditions^[11ae].

4.2.7. Self-healing approaches based on DA / rDA reactions

Reversible and therefore multiple time self-healing concepts based on covalent carbon-carbon bond formation in high yields and without the incorporation of additional healing agents can be realized by versatile DA cycloaddition reactions^[9] (see Table 1, Entry 7). In the course of the reaction (bi)cyclic

products are formed in a specific manner *via* a [4+2] cycloaddition of a diene and a dienophile. Self-healing in this context is based on the usually thermally induced [4+2] cycloreversion, called rDA reaction. Thus, in case of a damage event, the rDA reaction is taking place, whereas the previously formed bond between the diene and the dienophile is probably broken due to its relatively low bond strength^[9e]. During commonly applied heating the mobility of the reactive (end)groups is enhanced, accelerating the reconnection of the diene and the dienophile *via* the DA reaction related to a self-healing response^[9d, 9e].

DA / rDA reactions working under ambient conditions^[9p] are also known often using dithioesters as outstanding reactive dienophiles^[9o, 9q]. In order to permit a fast DA reaction at lower temperatures the HOMO of the diene and the LUMO of the dienophile have to be brought closer together. Accordingly, dienes are often functionalized with electron-donating groups at the 1-position, whereas commonly cyclic components like furan or cyclopentadiene find application due to their conjugation trapping them in the *cis*-position. As suitable reaction partners, conjugated dienophiles with a lowered LUMO are used. Thus, furan groups are normally reacted with maleimide groups^[9d-f, 9h, 9j] (see Table 1, Entry 7a) while cyclopentadiene itself acts as diene and conjugated dienophile^[9d, 9g] (see Table 1, Entry 7b). Furthermore, DA / rDA reactions between anthracene-modified polymers^[9d, 9i, 9l, 9m, 9r] (see Table 1, Entry 7c) find application for the development of self-healing materials.

For a room temperature self-healing concept based on DA chemistry a main-chain functionalized bio-based furan-polymer, namely poly(2,5-furandimethylene succinate) was prepared and was crosslinked with varying equivalents of several low molecular weight bismaleimide linkers^[9b, 9c] (see Figure 5). Thus, while using shorter and stiffer bismaleimides e.g. containing phenylene rings better mechanical properties of the final materials including an enhanced tensile strength were observed resulting simultaneously in a hindered self-healing response with healing efficiencies below 20 %^[9b]. In contrast, longer and more flexible chain bismaleimides showed healing efficiencies of around 70 % after 5 days, whereas no further improvement was observed for prolonged healing times^[9b, 9c]. Furthermore, the adjusted furan / maleimide ratio determined the mechanical properties related to the network densities of the final materials^[9c]. Accordingly, increased healing efficiencies were observed for adjusting the furan / maleimide ratio from 2 / 1 up to 6 / 1, whereas more than 50 % of incorporated furan moieties remained unreacted, therefore promoting the healing process by increasing the opportunity for reconnection during the rDA reaction^[9b, 9c].

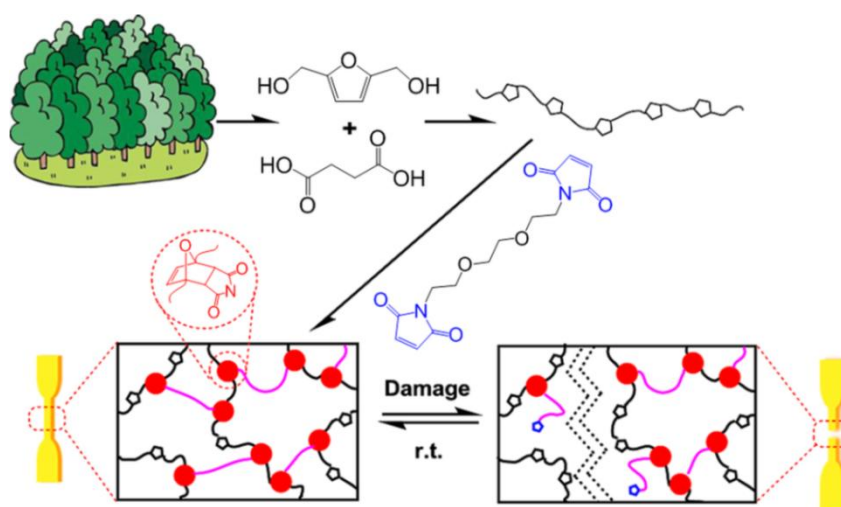


Figure 5: Preparation of a room temperature (r.t.) self-healing DA-system consisting of bio-based poly(2,5-furandimethylene succinate) crosslinked with various bismaleimides. Figure reprinted and adapted with permission from reference^[9c]. Copyright 2013, American Chemical Society.

4.2.8. Thiol and radical based self-healing concepts

Further reversible self-healing concepts are based on disulfide linkages which can be cleaved off under reductive conditions resulting in the formation of thiols while releasing accumulated stress^[19a-m] (see Table 1, Entry 8). Healing, and therefore the restoration of the initial materials performance can proceed *via* re-formation of disulfide linkers under oxidative conditions. Similarly, self-healing can occur *via* simple disulfide exchange reactions^[19n] (see Table 1, Entry 9) or by reversible photoinduced cleavage of allyl sulfide linkers^[20b, 20c] (see Table 1, Entry 10a). The so generated thiyl radicals introduce chain mobility resulting in the release of stress due to homolytic photolysis followed by the rearrangement of polymer chains and therefore the reformation of rubber-like materials without changing the initial material properties. Similarly, stress can be released by the reversible and thermally induced homolytic cleavage of alkoxyamine bonds (see Table 1, Entry 10b) suitable for self-healing applications^[20a, 20d, 20h-m].

Furthermore, several self-healing concepts using light, external force, an electrochemical stimulus or a pH-change as trigger^[9d, 21, 28] and therefore based on switchable network formation have been developed. Accordingly, an incorporated functionality within the polymer backbone is controlled on the molecular level. Due to turning the switch in a highly selective manner^[9a, 21p] the dynamics of the underlying chemistry is changed on demand playing a key role for sufficient self-healing^[9a, 29]. Other self-healing approaches based on clean and cheap light-induced switching involve reversible cycloaddition reactions^[9d, 21]. Thus, self-healing occurs due to the opening and closing of crosslinked ring structures within polymer networks. Accordingly, especially the [2+2] cycloaddition reaction between cinnamoyl groups^[9d, 21a, 21m, 21n, 21q, 21s, 21u] (see Table 1, Entry 11a) as well as between coumarin groups^[9d, 21a, 21j-l, 21o, 21t] (see Table 1, Entry 11b) and the [4+4] cycloaddition reaction of anthracene groups^[9d, 21a-i, 21v] (see Table 1, Entry 11c) find application for self-healing investigations.

4.3. Self-healing concepts based on supramolecular interactions

4.3.1. Overview of different supramolecular interactions and their application potential towards self-healing polymers

Supramolecular polymers^[21a, 30] are built up by reversible, non-covalent interactions like hydrogen bonding interactions^[31], metal-ligand interactions^[32], ionic interactions^[33] or π - π -stacking^[34] between low molecular weight compounds, functionalized oligomers or modified polymer chains resulting in materials with properties routinely related to covalent polymers with high molecular weight or even to (crosslinked) elastomeric materials^[35], whereas the monomeric and polymeric forms within the assembly are in equilibrium^[35b, 36] (see Table 2).

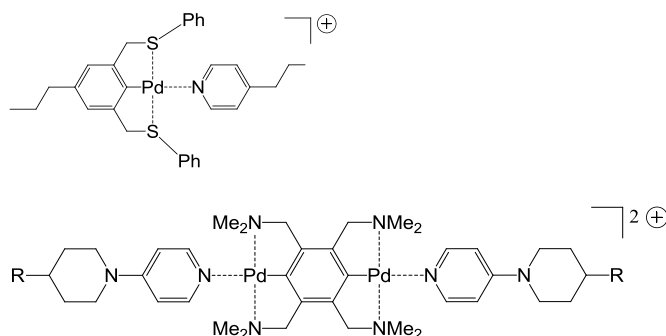
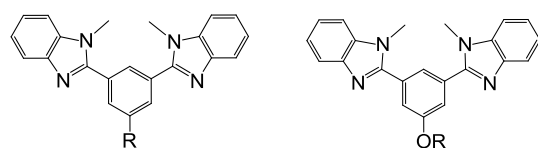
Table 2: Self-healing concepts based on supramolecular interactions.

Self-healing concept	Reference
1) Hydrogen bonding interactions	[31]

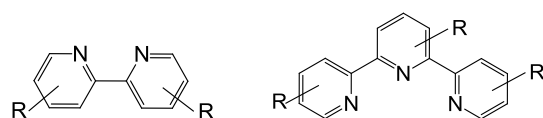
2) Metal-ligand interactions

[32]

a) Pd / Pt pincer complexes

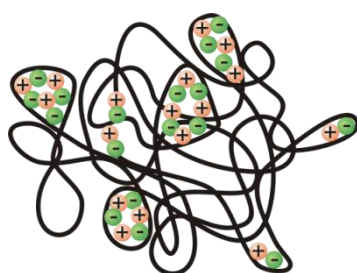
b) 2,6-Bis(*N*-methylbenzimidazolyl)pyridine (Mebip) and 4-oxy-2,6-bis(*N*-methylbenzimidazolyl)pyridine (OMebip) ligands

c) Bipyridine (bipy) and terpyridine (tpy) ligands

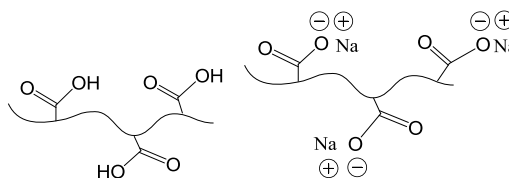


3) Ionomers

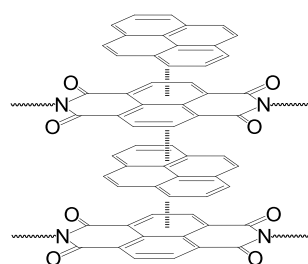
[33]



EMAA and partially neutralized EMMA

4) π - π -stacking interactions

[34]



The exploration of supramolecular chemistry has already started in the 1980s and was additionally kicked off by awarding the Nobel Prize to Jean-Marie Lehn, Donald Cram and Charles Pedersen for their work on cryptands and establishing the term "supramolecular chemistry as the chemistry beyond the molecule", in 1987^[37]. Thus, already a magnitude of several hydrogen bonding synthons have been investigated in solution, whereas the geometry and the shape of the hydrogen bonding motifs played an important role in the self-assembly process^[38]. Due to the semiflexible and reversible nature and the dynamic properties which can be freely tuned by the variation of the virtual degree of polymerization, the strength and the direction of the interaction supramolecular polymers find applications as smart,

adaptive and stimuli-responsive materials^[35b, 36b, 39]. Beside, their application potential is additionally stated by their easy producibility and processability due to a low melt viscosity while eliminating the need of additionally added reactive and toxic chemicals due to their inherent reversibility^[35b, 40].

Supramolecular polymers display ideal candidates for multiple time self-healing materials as applied stresses resulting from a damage event can be released by breaking and reforming of supramolecular (weak) bonds.^[41]

Nevertheless, the prediction of their (self-)association behavior and the resulting (self-)assembly in the bulk material is still challenging as a direct transfer of the characteristics observed in solution is not possible. In strong contrast to the solution behavior, where outstanding strong hydrogen bonding interactions usually result in a slow dynamics^[35b, 42], the amount and the strength of the hydrogen bonding interactions in the bulk phase is not necessarily important^[43]. Accordingly, weak interactions in solution might become strong in the bulk material, whereas suddenly homo-dimerization is more favored than hetero-dimerization^[43].

Thus, for the design and the fine-tuning of a self-healing supramolecular polymer^[34g, 35a, 40-41, 44] the knowledge of the solid-state properties and the related morphology plays a key-role as the self-healing performance depends not only on a sufficient and dynamic chain mobility, good mechanical bulk properties and the stickiness of the hydrogen bonding moieties but usually also on micro- or nanophase separation phenomena or on the crystallization of supramolecular moieties within the bulk, whereas disentangled domains crystallize earlier to due faster intramolecular homogeneous nucleation^[30b, 30c, 34a, 41a, 45].

Therefore, two or more associating groups with a supramolecular bond lifetime in the range of μs to s ^[30d, 33e, 35b, 41a, 46] enabling flow and therefore relaxation on long timescales are needed to introduce (self-healable) supramolecular network structures or branches, whereas the thermodynamically most stable conformation is formed often resulting in improved mechanical properties^[47] or even in rubbery materials^[35, 48]. Thus, the intrinsic ordering of the polymer chains related to the viscosity and the flow behavior of the material as well as the strength of the material is directly influenced by introducing supramolecular interactions, whereas their association dynamics^[49], their reversibility and thus the binding strength can be tuned over a large range of orders of magnitude by controlling the design of the supramolecular moieties^[39, 41a] and by tailoring the selective telechelic functionalization of polymers^[50].

As the binding energy of supramolecular interactions is generally weak ($0.5 - 50 \text{ kJ}\cdot\text{mol}^{-1}$ ^[51]) the supramolecular bond will fail during a damage event while dissipating the energy allowing the bond segment and therefore the whole polymer to move^[52]. Thus, within the formerly equilibrated bulk material fresh and sticky surfaces with free supramolecular binding sites in a non-equilibrium state are created during the rupture event^[53]. In order to achieve self-healing^[41a] these free binding sites have to be brought into contact to find a new partner in order to re-associate either *via* (self-)complementary interactions or *via* cluster formation (see Figure 6). Thus, stress relaxation related to breaking and reforming of supramolecular weak bonds with the dissociation being the rate-determining step^[54] proceeds by the reptation mechanism^[55], whereas chain relaxation at the surface usually proceeds faster than in bulk^[56].

Accordingly, the healing response at least depends on two timescales: 1st) the recombination of supramolecular moieties and 2nd) the chain dynamics required to enable the mobility of supramolecular motifs within the bulk material^[41a] related to the time required to renew the chain conformation under unstrained conditions and to reestablish the equilibrium^[57]. Thus, the motion of the chain according to the hindered reptation model or sticky reptation model is controlled by the lifetime and the concentration of supramolecular tie points, whereas the chain can diffuse just at timescales longer than the lifetime of the supramolecular interactions^[58]. Nevertheless, the applicability of the sticky reptation

model is limited for strong supramolecular associations, thus providing only the basis for more sophisticated self-healing models^[58b].

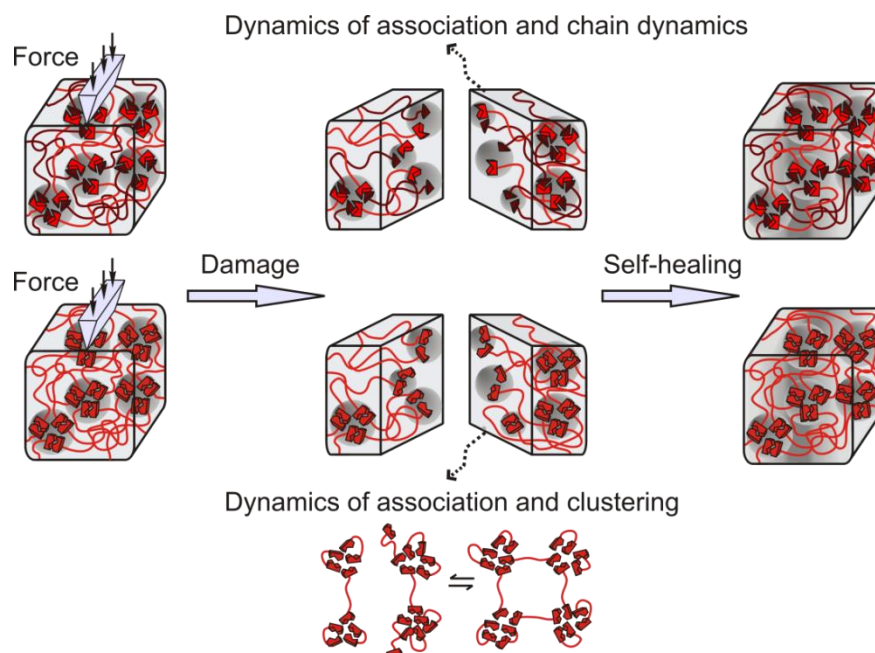


Figure 6: Self-healing of a supramolecular rubber after a force-induced damage event *via* re-association of (self-)complementary hydrogen bonding interactions (upper bank) or *via* cluster formation (bottom bank). Figure reprinted and adopted from reference^[48a] with permission from John Wiley and Sons (Copyright 2013).

4.3.2. Importance of phase segregation phenomena on the self-healing response

Nanophase separation between hard and soft domains within a polymer or composite material or the crystallization of introduced supramolecular moieties can introduce a self-healing response based on the autonomous rearrangement between hard and soft phases after an occurring damage event. While getting the inspiration from the design of self-healing polymers with exchangeable and therefore weak covalent bonds^[19b, 59] hybrid computational models^[60] can be applied to predict the influence of the fraction of permanent and labile bonds as well as to simulate the mechanism of strain recovery.

Thus, a competitive effect between the extent and the rate of strain recovery was proven *via* calculations, whereas with increasing labile bond energy related to an increased time scale necessary for strain recovery a tougher material with improved mechanical properties was obtained. In contrast, an increasing amount in permanent bonds provided a better and faster strain recovery after performing several stretch-relaxation cycles.

Accordingly, already the incorporation of a small fraction of labile bonds (20 - 30 %) resulted in a significant improvement of the tensile strength while incorporating additionally a self-healing response to tensile deformation. Thus, labile bonds acted as sacrificial species while dissipating the energy emerging to a rupture event due to structural rearrangements and preserving the overall mechanical integrity^[59, 61].

Further computational studies of flexible polymer composites containing nanoparticles^[62], nanoscopic polymer gel particles^[59], copolymer nanoparticle blends^[63] and particle-filled microcapsules^[64] for the design of a "repair and go" system exploited the interplay between entropic and enthalpic contributions. Thus, the distribution of incorporated nanoparticles was directed while tailoring morphologies and thus controlling the macroscopic performance of the resulting composite material.

Incorporated nanoparticles migrate to fractured surfaces forming patches which can act as "band aids"^[62c] for the composite materials resulting in multiple healing events related to a 75 - 100 % restoration of the mechanical properties dependent on the density of the incorporated nanoparticles and the dimensions of the fractured surface.

Furthermore, supramolecular multiphase TPEs can be built up by nanophase-separation between a hard and a soft domain, whereas the stiff phase acts as scaffold preserving the mechanical integrity while the mobile phase can introduce a self-healing ability within the material. Thus, a tough and self-healable rubber system with a prominent high modulus was created by incorporating a hard PS polymer backbone within a soft polyacrylate-amide matrix^[65]. Room temperature self-healing of cut surfaces was observed within 24 hours resulting in a recovery of 92 % due to hydrogen bonding interactions within amide groups of the matrix^[65].

Similarly, multiphase polymers consisting of a glassy and hard PS backbone and soft imidazole-containing brushes formed self-healable TPEs^[32ab]. The mechanical properties could be tuned by adjusting the degree of polymerization, the backbone composition and the metal to ligand ratio. Thus, a nearly quantitative recovery of the tensile toughness was observed within 3 hours at room temperature due to metal-ligand interactions between imidazole-brushes and zinc ions^[32ab].

Quantitative room temperature healing due to dynamic hydrogen bonding interactions was reported for hard-soft core-shell two-phase nanoparticles built up by crosslinked PS nanoparticles covered with a grafted poly(acrylate amide) shell^[66].

Similarly, ABA-type supramolecular block copolymers were prepared consisting of hard PS blocks and a soft PnBA middle block connected *via* dimerization of UPy groups. After healing for 18 hours at 45 °C a 90 % recovery in the tensile strength was observed^[67].

4.3.3. Hydrogen bonding interactions towards self-healing polymers

Supramolecular self-healing concepts offer the possibility to create multiple time self-healing materials, whereas especially hydrogen bonding interactions play a key role due to their dynamic nature and flexibility to external stimuli in combination with a tunable and directed association strength^[68]. Accordingly, supramolecular polymers with incorporated hydrogen bonding moieties were put on the frontline for industrial applications and a variety of hydrogen bonding synthons are highlighted in Figure 7.

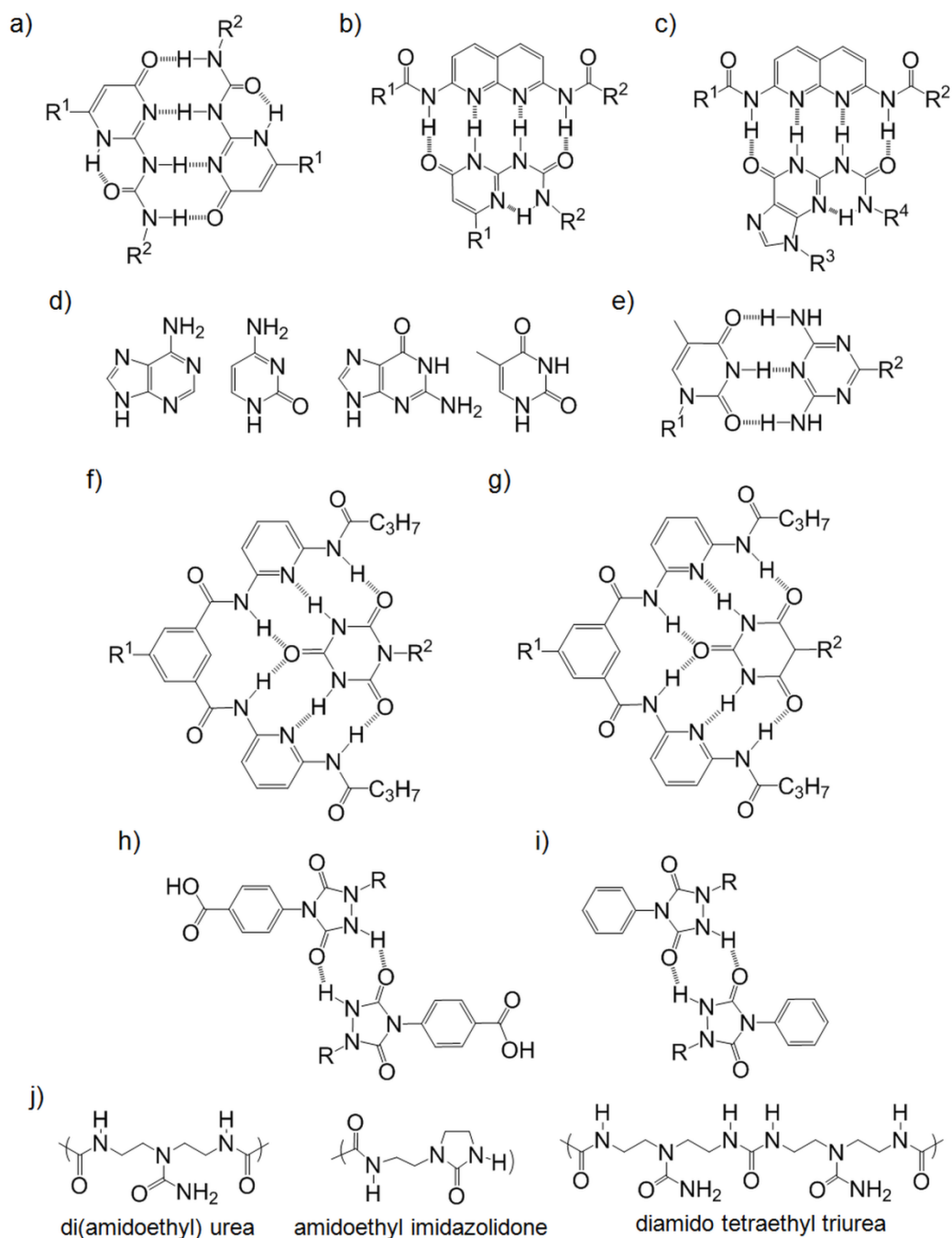


Figure 7: Hydrogen bonding interactions between a) two ureidopyrimidones (UPy), b) UPy and 2,7-diamido-1,8-naphthyridine (DAN), c) DAN and ureido-7-deazaguanine (DeUG), d) nucleobases: adenine, cytosine, guanine and thymine, e) thymine and diaminotriazine, f) Hamilton wedge and cyanuric acid wedge, g) Hamilton wedge and barbituric acid wedge, h) two phenyl urazole acids, i) two phenyl urazoles and j) components forming the Leibler rubber.

4.3.4. Hydrogen bonding interactions between ureidopyrimidone (UPy) synthons

Supramolecular polymers have been intensely studied in solution^[69] and their dynamic properties in semi-diluted entangled solutions are in good agreement with predictions according to the sticky reptation model^[70] as reptation is the dominant diffusion mechanism^[55, 71]. Especially, supramolecular polymers functionalized with UPy moieties have been of interest due to their high dimerization constant (K_{dim} , $\text{CHCl}_3 = 10^6 \text{ M}^{-1}$)^[72]. Consequently, investigations in the bulk phase have followed in

order to generate supramolecular polymers, polymer networks or polymeric nanoparticles^[73]. Furthermore, self-healable polymers as well as supramolecular rubbers based on UPy hydrogen bonding interactions have been commercialized under the trade name SupraBTM and Kraton® by SupraPolix BV^[48b, 68].

The formation of supramolecular polymer networks was observed *via* hydrogen bonding interactions between trivalent UPy-functionalized PPE-PEO blockcopolymers and bivalent UPy-modified PDMS^[74], whereas the resulting supramolecular crosslinked materials behaved similarly like entangled linear polymers. Furthermore, gel formation in solution and crystallization in the bulk phase was observed due to the directionality of the supramolecular interactions^[74]. Thus, UPy-telechelic PDMS formed TPEs with a rubbery plateau and a high activation enthalpy for stress relaxation^[75] due to lateral stacking of formed UPy dimers additionally reinforced by π - π interactions. The so observed aggregation behavior resulting in the assembly of spherical aggregates or fibers was attributed to the incompatibility of the hard block consisting of microcrystalline domains of associated UPy dimers and the soft PDMS backbone leading to microphase separation^[75].

Also dendronized polymers formed by UPy dendritic macromonomers assembled into fibrous superbundles due to hydrogen bonding interactions additionally facilitated by π - π -stacking^[76].

Similarly, UPy-telechelic PnBA, PS and poly(butadiene) formed micellar clusters of UPy aggregates in the solid state. Their size decreased due to the presence of triazole rings taking part in the endgroup association while leading to a higher storage modulus and a higher viscosity within the polymers^[77].

Bivalent UPy-telechelic PEG (see Figure 8) phase separated in hydrophobic hydrogen bonding domains consisting of UPy moieties and the PEG backbone resulting in the formation of solid-like hydrogels. Self-healing of so obtained materials was observed at 50 °C by switching the initial properties to a viscous liquid^[40, 78].

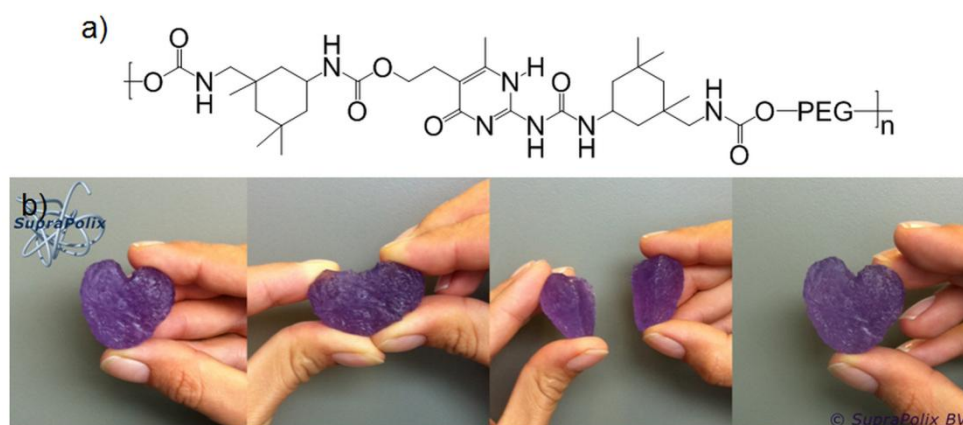


Figure 8: a) UPy-functionalized PEG, b) Self-healing of an UPy-functionalized PEG heart (colored by adding a purple dye, 15 wt% in water): initial heart shape was reestablished after pressing cut halves together. Figure reprinted and adopted from reference^[40] with permission from SupraPolix BV and John Wiley and Sons (Copyright 2012).

Self-healing hydrogels have also been prepared by copolymerizing 2-(*N'*-methacryloyloxyethylureido)-6-(1-adamantyl)-4[1*H*]-pyrimidinone with *N,N*-dimethylacrylamide, whereas hydrogen bonding was protected against the disruption by water molecules due to the presence of hydrophobic adamantyl groups^[79].

Copolymers prepared of poly(2-ethylhexyl methacrylate) and an UPy-modified methacrylate showed an increase in the complex viscosity as well as an increase and a lengthening of the plateau modulus with increasing UPy content. In contrast, the tensile strength increased to a constant level above an

UPy content of 3 mol%^[80]. Similar copolymers composed of *n*BA and an UPy-functionalized acrylate (UPy-content of 7.2 %) showed a recovery of the self-adhesion strength of fractured surfaces up to 100 % after a healing time of 50 hours^[81].

TPEs were received by copolymerizing an UPy-modified *n*BA with a Boc-protected amine functionalized monomer^[82]. So obtained copolymers showed a more prominent plateau modulus than high-molecular weight entangled *Pn*BA, whereas the bulk properties depended on the distance between stacked aggregates of UPy dimers. Furthermore, with increasing UPy content a linear increase in the plateau modulus was observed while the effective bond lifetime of hydrogen bonded aggregates increased proving that every UPy side group was active within the network for UPy contents of 7 mol% or higher^[82].

By comparing copolymers consisting of *n*BA and an UPy functionalized acrylate, acrylamidopyridine, acrylic acid or carboxyethylacrylate^[83] it was found that copolymers containing weak hydrogen bonding interactions behaved like unentangled melts with a hydrogen bonding dynamics faster than rheological chain relaxation. In contrast, copolymers with strong hydrogen bonding interactions behaved like entangled polymer networks resulting in soft and elastic solids, while the flow activation energies increased linearly with the increasing amount of hydrogen bonding moieties showing a dimer lifetime larger than 10 s^[83].

Similarly, supramolecular polymers formed by UPy-modified model compounds showed a persistence of multiple hydrogen bonding interactions on a timescale of 100 μ s related to the timescale of NMR investigations^[84]. Furthermore, it was found that the activation energy depended on the dissociation of hydrogen bonded domains and the tautomeric rearrangement of the supramolecular polymer from the keto- into the enol-form related to the formation of weaker hydrogen bonding interactions due to less dense packed protons^[84].

Due to clustering of hydrogen bonding units bivalent UPy-modified poly(ethylene butylene)s behave like soft rubbers at room temperature showing a broad rubbery plateau with a plateau modulus of 10⁶ Pa, whereas time-temperature superposition failed at low frequencies^[85].

Similarly, multi-functionalized poly(ethylene butylene)s carrying urethane, urea and UPy groups form TPEs^[86] due to microphase separation between the polymer backbone and hydrogen bonding moieties. By combining end to end and lateral aggregation of hydrogen bonding motifs the obtained materials showed long-living crosslinks related to an outstanding high melting point and enhanced mechanical properties^[86a].

α -Benzene-1,3,5-dicarboxamide- ω -UPy functionalized poly(ethylene-*co*-butylene) showed elastomeric properties due do crosslinking of nanofibrils formed by stacked UPy dimers and phase-segregated nanorods built up by helical, columnar aggregates of benzene-1,3,5-dicarboxamide units^[87].

TPE formation was also observed for UPy-functionalized amorphous polyesters showing a nearly unaffected rubbery plateau up to 50 °C due to nanophase separation between crystalline nanoscopic rods formed by stacked UPy dimers and the soft polymer block^[88].

By investigating crystalline UPy-modified poly(ethylene adipate)^[89] it was shown that the self-healing performance depended on the connection unit between the polymer backbone and the hydrogen bonding moiety. Thus, self-healing at room temperature was observed for polymers containing hexamethylene linkers related to a slower recovery in crystallinity. In contrast, tolylene linkers allowed a faster recovery of crystallinity while shifting the healing temperature above the melt temperature^[89].

UPy-functionalized poly(urethane)s^[90] found application as stress-sensing systems by incorporating spiropyran units into the polymer backbone able to undergo a stress-induced ring-opening resulting in the merocyanine form highlighted by a color change. Furthermore, such UPy-modified polymers able

to dissipate strain energy were used to mimic the modular structure within titin as the dissociation of hard UPy domains consisting of stacked dimers is working similarly like the unfolding process of sacrificial bonds in modular biomacromolecules^[90].

Similarly, UPy-modified diolefin monomers were polymerized *via* ADMET^[91] to create a titin-mimicking modular polymer with a high toughness and an adaptive behavior including a self-healing ability. Thus, a full recovery of toughness and strength was observed at 80 °C within 30 s^[91].

Furthermore, polyolefin elastomers were prepared *via* Ziegler-Natta copolymerization of 1-hexene with an UPy modified comonomer^[92]. Thus, a branched high molecular weight supramolecular polymer was obtained due to dimerization of UPy hydrogen bonding moieties and chain walking throughout the polymerization itself^[92].

Bivalent UPy-telechelic perfluoropolyethers^[93] recovered their storage modulus within two minutes after shearing at 130 °C due to the formation of hard crystalline UPy domains related to phase-separation between the soft polymer backbone and the hydrogen bonding moieties. In contrast, perfluoropolyethers functionalized with alkylated UPy groups showed a suppressed crystallization resulting in an increased recovery time of the storage modulus of 18 minutes after shearing at 110 °C^[93] (see Figure 9).

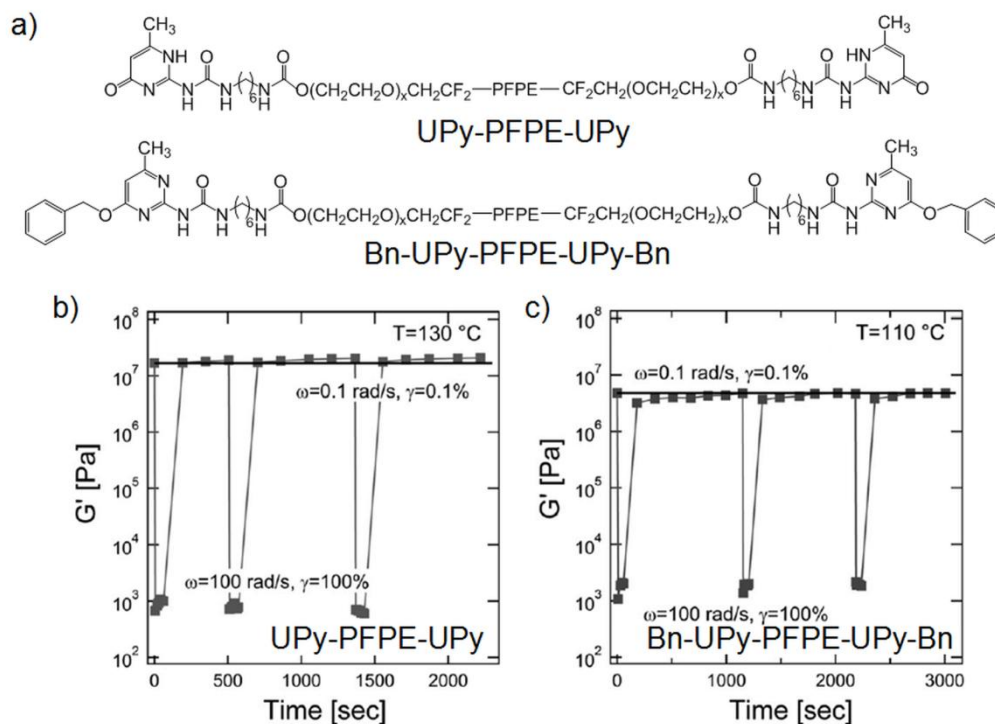


Figure 9: a) Structures of bivalent UPy-telechelic PFPE and bivalent Bn-UPy-telechelic PFPE, Multiple deformation-recovery cycles of b) bivalent UPy-telechelic PFPE and c) bivalent Bn-UPy-telechelic PFPE. Figure reprinted from reference^[93] with permission from John Wiley and Sons (Copyright 2013).

In bivalent UPy-modified PCL stacking of UPy dimers supported by hydrogen bonding interactions between urethane linker groups was observed, whereas chain scission proceeded faster than reptation. Thus, the so obtained materials showed a rubbery plateau zone even at low frequencies and viscous flow due to supramolecular network formation^[94]. In contrast, for tri- and tetravalent UPy-urethane modified PCLs no rubbery plateau was observed as the crystallization and stacking of UPy dimers was prevented by the polymer architecture resulting in a too short lifetime of the supramolecular

network^[95]. Similarly, large and bulky substituents interfered with the supramolecular assembly due to steric hindrance^[94].

4.3.5. Hydrogen bonding interactions between UPy and 2,7-diamido-1,8-naphthyridine (DAN) synthons

By investigating 2,7-diamido-1,8-naphthyridine (DAN) and UPy end functionalized PnBAs and poly(benzyl methacrylate)s it was found that the phase behavior and therefore the present microstructure in the bulk was controlled by hydrogen bonding interactions^[96]. Thus, UPy dimerization led to compatibilization, whereas complementary hydrogen bonding interactions resulted in a dramatic reduction of macroscopic phase separation^[96] and in the formation of supramolecular diblock copolymers^[97] or graft polymers^[98]. Furthermore, low molecular weight polymers formed homogeneous microstructures, whereas phase-separated domains were rapidly increasing for higher molecular weight polymers and with increasing temperature due to the increasing incompatibility of the phases^[97].

Supramolecular alternating copolymers were formed by hydrogen bonding interactions between a 1:1 mixture of a bisUPy-functionalized pTHF and a bisDAN-functionalized low molecular weight linker^[99]. By increasing the bisDAN linker content the virtual degree of polymerization decreased as the bisDAN linker acted as chain stopper^[99]. Accordingly, by the use of chain stoppers the concentration dependency of the virtual degree of polymerization and thus the chain length can be blocked in a defined concentration range which allows to draw conclusions about the hydrogen bonding interaction itself corrected by concentration effects^[41b, 47, 100]. Furthermore, chain stoppers were used to break-up supramolecular networks formed by strong hydrogen bonding interactions like in trifunctional UPy-telechelic polyether polyols. In contrast, in case of weaker hydrogen bonding interactions in urea modified polyether polyols no break-up of the supramolecular assembly was observed as the polymer ends were incorporated in the microphase separated hydrogen bonding arrays resulting in the formation of phase-separated TPES^[101].

4.3.6. Hydrogen bonding interactions between ureido-7-deazaguanine (DeUG) or the butylurea of guanosine (UG) and DAN synthons

The hydrogen bonding interaction between ureido-7-deazaguanine (DeUG) and DAN as well as between the butylurea of guanosine (UG) and DAN have been intensely studied in solution^[102]. Thus, it was found that DAN showed a redox-responsive behavior and thus a chemically and electrochemically switchable high affinity to DeUG in its reduced form and a low affinity to the oxidized form of DeUG^[103].

Accordingly, bivalent DAN-telechelic poly(butyl methacrylate)s and bivalent UG-telechelic PEG formed alternating supramolecular copolymers, whereas the virtual degree of the polymerization depended on the block ratio within the mixture and on the concentration^[104].

In contrast, a supramolecular network structure resulted from hydrogen bonding interactions between bivalent DAN-telechelic poly(butyl methacrylate) and bivalent UG-telechelic PS as the interacting blocks showed no miscibility^[105]. Consequently, nearly exclusively DAN-UG hydrogen bonding interactions have been observed, whereas self-association played only a minor role^[51].

Thus, PS functionalized with DAN showed good adhesion properties to a DeUG modified glass surface due to quadruple hydrogen bonding interactions. Thus, a recovery up to 55 % was reported, whereas no healing was observed in the case of adhesion loss^[106].

4.3.7. Bis(urea) based hydrogen bonding interactions

*Pn*BAs functionalized with a bis(urea) group in the middle showed viscoelastic properties, whereas the viscosity increased with decreasing molecular weight up to a molecular weight of 20 kg/mol attributed to hydrogen bonding interactions completely determining the rheological properties. In contrast, for functionalized *Pn*BAs with a molecular weight higher than 20 kg/mol polymers behaved nearly like unfunctionalized high molecular weight *Pn*BAs and their rheology was controlled by the polymer dynamics itself while incorporated supramolecular stickers simply increased the terminal relaxation time due to hydrogen bonding interactions^[107].

PDMS crafted with bis(urea) moieties formed TPEs due to supramolecular crosslinking related to (partial) self-organization of incorporated bis(urea) units in crystal-like domains^[108].

Furthermore, supramolecular silicones prepared by crosslinking of tris(urea) modified PDMS with hydrazine units^[109] *via* sextuple hydrogen bonding interactions formed single or double strand like structures. The so obtained materials showed a self-healing ability of cut films within several hours, whereas no self-healing was observed after keeping apart cut surfaces for more than 10 minutes due to equilibrating and reassembling of hydrogen bonding moieties^[109].

Several poly(urethane)-based TPEs containing a soft poly(ethylene-*co*-butylene) middle block^[110] have been prepared, whereas an increased microphase separation in the bulk correlated to an increased hydrogen bonding potential. Thus, an increase of the scattering intensity within SAXS experiments and an increase of the storage modulus was observed with changing the endgroup from dibutyl < morpholine < diol^[110].

Polyurea-urethanes with triuret-blocks showed a crosslinked structure at room temperature due to hydrogen bonding interactions, whereas de-crosslinking was observed between 105 - 135 °C^[111]. In contrast, tetrauret-block containing polyurea-urethanes resulted in a folded structure due to the present zigzag conformation stable up to 170 - 190 °C^[111].

Strong primary and secondary hydrogen bonding interactions between low molecular weight *N,N'*-disubstituted ureas resulted in the formation of supramolecular polymers comparable to high molecular weight poly(urethane)s^[112]. Accordingly, 2-ethyl-hexyl-3-[3-(3-(2-ethylhexyl)ureido)-4-methyl-phenyl]urea based supramolecular polymers behaved like organogels showing viscoelastic properties. Due to hydrogen bonding interactions within entangled single-strand filaments as well as scission of tubular structures a relaxation time in the magnitude of several seconds was observed^[112a].

Low molecular weight bis(urea) moieties as well as PIBs containing bis(urea) functionalities within the polymer backbone formed comb-shaped supramolecular assemblies resulting in the formation of filaments or tubes, whereas their length was tuned by varying the concentration and / or the solvent^[113]. Although the resulting structures just have been investigated in solution, a self-healing ability within the bulk material was estimated^[113b]. Thus, they showed self-organization behavior over a timescale of days resulting in viscoelastic soft gels at room temperature which disrupted at 80 °C but retrieved their structure after 20 hours of annealing highlighting their potential as soft adhesives and self-healing materials^[114].

The formation of transient networks and flower-like structures was also observed for adamantylurea-functionalized poly(propylene imine) dendrimers interacting with ureido-acetic acid functionalized oligoTHF^[115].

4.3.8. Fatty acid based formation of thermoplastic elastomers (TPEs)

Thermoreversible supramolecular polymers with a low T_g have been formed by hydrogen bonding interactions between polyamide oligomers prepared from fatty diacids treated with sulfonyl isocyanate and ethylenediamine^[116]. The so obtained materials exhibited a high rubbery plateau, whereas the introduced rubber elasticity resulted in a 88 % recovery of the tensile strength after keeping samples at 50 °C for 18 hours^[116].

Similarly, the preparation of a soft supramolecular rubber^[117] has been reported by condensing diethylene triamine and urea with a mixture of multiple functionalized fatty acids, whereas the degree of branching was controlled by the choice of fatty acids and adjusting their ratio. Thus, complementary hydrogen bonding units were incorporated in the resulting oligomeric material plasticized with dodecane (11 wt%) in order to lower its T_g to 8 °C. Accordingly, complete self-healing of cut pieces was observed within 3 hours at room temperature. The maximal waiting time of keeping cut samples apart from each other before self-healing was determined to be 48 hours at 48 °C^[117a] but healing could be completely suppressed by annealing at 90 °C due to equilibrating hydrogen bonding moieties^[118]. Consequently, the required healing time related to re-association of hydrogen bonding interactions strongly depends on the mobility of the whole polymer backbone as a reorganization over a larger length scale within the bulk material is required^[118]. Furthermore, it was shown that it was more difficult to separate a formerly cracked and therefore sticky and subsequently healed surface than a melt-pressed sample due to an enhanced self-adhesive strength^[118].

By investigating the rubber in more detail by various rheology and NMR techniques it was proven that it behaves like a nanophase-separated system. Consequently, the rubber consisted of a less mobile part (85 %) with a T_g shortly below RT therefore showing ongoing mechanical relaxations and a more mobile part (15 %). Furthermore, it was found that above 110 °C irreversible (chemical) crosslinking occurred resulting in an aging effect and therefore in a weakening of the self-healing ability^[119].

In a very similar approach supramolecular elastomers associated *via* multi-hydrogen bonding interactions have been prepared from multivalent acid-functionalized PDMS reacted with diethylene triamine and urea. Thus, a low temperature self-healing response was observed, whereas deformations recovered in the magnitude of seconds after releasing stress due to a real rubber-like elastic behavior^[120].

4.3.9. Hydrogen bonding interactions between acid-, phenyl urazole acid- or phenyl urazole-functionalized polymers

By reacting maleic polyisoprene with 3-amino-1,2,4-triazoles possible six-point hydrogen bonding interactions within the formed amide triazole-carboxylic acid unit have been incorporated showing comparable mechanical properties to sulfur-vulcanized rubber^[121].

Similarly, the properties of poly(butadiene)s with incorporated sulfonyl urethane groups can be tuned from rubbery materials to TPEs due to the formation of supramolecular self-complementary hydrogen bonding networks^[122].

Furthermore, the formation of three-dimensional supramolecular networks was observed for tetrapyrrolyl and diacid species^[123].

Supramolecular TPEs have also been prepared by functionalization of poly(butadiene) with carboxyphenylurazoles resulting in multiphased structures due to phase separation effects between the polymer backbone and introduced hydrogen bonding groups^[124]. Thus, time-temperature superposition of rheology data failed even for low concentrations of hydrogen bonding synthons^[124b].

A similar behavior was observed for (phenyl)urazole-functionalized poly(butadiene)s, resulting in thermoreversible elastomeric networks with a rubbery plateau shifted to lower frequencies and higher

temperatures^[125]. Due to the formation of hydrogen bonding interactions related to a hindrance of local flow processes, a broadening of the relaxation time up to seconds and the failure of time-temperature superposition was observed. Furthermore an increase in the activation enthalpy was attributed to an increasing degree of functionalization and thus, to the formation of supramolecular clusters with higher stability^[125].

Furthermore, it was shown that the incorporation of urazole groups resulted in an improved phase adhesion behavior in thermoplastic blends^[126].

Mannitol-based diols acted as organogelators showing self-healing properties due to the self-assembly in solution resulting in fibril formation and further aggregation into 3D spaghetti-like networks^[127]. Similarly, low molecular weight gelators capable of hydrogen bonding interactions were applied as coating material towards hydrophobic and slippery surfaces with self-cleaning and self-healing properties^[128].

Oligomeric poly(tetramethylene oxide) endcapped with a phthalic half-ester^[129] formed crystalline aggregates of carboxyl acid groups due to hydrogen bonding interactions. Nonetheless, hydrogen bonding was proved to be present in crystalline and amorphous regions related to two relaxation times and thus a good recovery to large strains and an elasticity-dominated response to small strains^[129].

4-Urazoylbenzoic acid modified bivalent PIBs^[130] able to form hydrogen bonded dimers of urazole moieties and incorporated acids showed a melting of ordered hydrogen bonding clusters between 110 - 120 °C. Within this temperature range a transition from elastic to viscous behavior was observed related to the reorientation and breaking of ordered supramolecular clusters into disordered multiplets of associated hydrogen bonding chains. Thus, time-temperature superposition failed and stress relaxation within the polymer was attributed to the relaxation of multiplets and the deformation of supramolecular clusters^[130].

4.3.10. Hydrogen bonding interactions between nucleobases and tailor-made hydrogen bonding wedges

Supramolecular blockcopolymers have been prepared by linking low molecular weight compounds functionalized by a diaminopyridine substituted isophthalamide receptor and a Janus-type cyanuric wedge. The so created blockcopolymers assembled into large fibrous structures suggesting a self-healing ability^[131].

Similarly, heterocomplementary monomers formed rigid fibers with their length dependent on the concentration of incorporated sextuple hydrogen bonding moieties namely a DAD-DAD array and a cyanuric acid wedge^[132].

Supramolecular polymers formed by copolymerization of norbornene with a cyanuric acid wedge functionalized norbornene-based monomer interacting with a ditopic Hamilton wedge linker behaved like a highly viscous fluid, whereas hydrogen bonding interactions with a ditopic diaminotriazine linker resulted in elastic polymer gels^[133].

In contrast, a similarly thymine-modified poly(norbornene)^[134] in combination with either the ditopic Hamilton wedge linker or the ditopic diaminotriazine linker stayed liquid. Accordingly, the mechanical properties of the self-assembled supramolecular polymer networks could be varied over five orders of magnitude^[134].

Similarly, bivalent thymine-telechelic PPOs behaved like viscoelastic solids forming lamellar structures due to microphase segregation below their order-disorder-transition temperature while strong complementary hydrogen bonding interactions between bivalent thymine- and diaminotriazine-telechelic PPOs suppressed microphase segregation and were therefore obtained as liquids^[31].

2,4,6-Triaminopyrimidines and benzyl- and octyl-substituted barbiturates have been incorporated into a PS and a PMMA matrix^[135]. Consequently, the formation of a nanoscaled superstructure was introduced within the PS matrix by the addition of 3 or more wt% octyl-substituted hydrogen bonding moiety. In contrast, no superstructure formation was observed within the PMMA matrix. Thus, it was concluded that the incompatibility between the hydrogen bonding moieties is a prerequisite for the formation of superstructures^[135].

In this context, the formation of wormlike lamellae was reported for α - ω -adenine-uracil-functionalized PCL due to phase segregation between the soft polymer backbone and the hard domains of stacked hydrogen bonding moieties^[136].

Furthermore, low molecular weight compounds bifunctionalized with ureidotriazine moieties dimerizing *via* self-complementary quadruple hydrogen bonding moieties were found to form helical structures due to a columnar assembly of stacked hydrogen bonding dimers^[137].

By investigating adenine-, thymine- and cytosine-modified low molecular weight pTHFs^[138] it was found that only the adenine- and the cytosine-terminated polymers showed film- and fiber-forming capabilities due to hydrogen bonding interactions. As the present supramolecular interactions are generally weak, it was assumed that a second driving force namely π - π -stacking interactions of hard crystalline nucleobase chain ends in combination with phase segregation between the soft polymer backbone and the hard hydrogen bonding moieties additionally contributed to this self-assembly behavior^[138]. Thus, self-healing applications of adenine-modified pTHFs were mentioned due to the temperature stability of the resulting supramolecular network structures up to 90 - 120 °C^[138b] (see Figure 10).

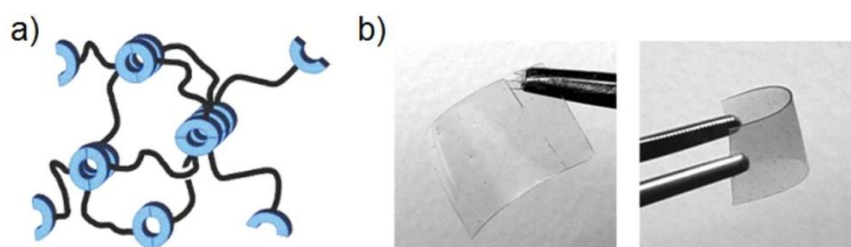


Figure 10: a) Schematic representation of a supramolecular polymer network composed of nucleobase-functionalized pTHF, b) Films of pTHF functionalized with adenine (left hand side) and cytosine (right hand side). Figure reprinted and adopted with permission from reference^[138b]. Copyright 2005, American Chemical Society.

The synthesis of bivalent PIBs functionalized with barbituric acid moieties and a Hamilton Wedge was reported^[46a], whereas their dynamics and hence the self-healing behavior has been studied in the melt state. Thus, pure PIBs and equimolar polymer mixtures of barbituric acid and Hamilton Wedge modified samples were investigated *via* temperature-dependent melt rheology. Surprisingly, strong and tough self-healing supramolecular rubbers showing an increased thermal stability were observed for acid telechelic PIBs. Rubber formation and the introduced self-healing response was related to a thermoreversible formation of larger aggregates enhanced by microphase separation between the polar hydrogen bonding synthons and the nonpolar PIB backbone. The formation of dynamic supramolecular junction points was additionally confirmed by rheology investigations showing terminal flow at low frequencies but a rubbery plateau zone at high frequencies as well as by SAXS measurements^[46a, 139]. Consequently, cut pieces of PIBs modified with barbituric acid groups were completely healed within 48 hours after cutting bringing them into contact again proving possible application as room temperature self-healing material. In contrast, PIBs bearing Hamilton Wedges and barbituric acid moieties behaved like brittle rubbers, whereas terminal flow was only observed at temperatures above 100 °C^[46a].

4.4. Combined self-healing principles based on interwoven network structures *via* supramolecular and covalent network formation

4.4.1. Challenges for the further development of self-healing concepts

A lot of effort has been dedicated to the design of once-a-time healing concepts as well as multiple healing approaches based on supramolecular or reversible covalent chemistry. Nevertheless, for the (further) development of self-healing concepts three important as well as challenging issues have to be carefully considered in order to reach the market: i) multiple self-healing materials showing shape persistency, ii) improved stress-sensing and simultaneously self-healing materials and iii) void-filling self-healing materials tailored for large volume restoration^[140].

Referring to the first issue supramolecular approaches realizing a self-healing response due to their inherent dynamic reorganization ability and remendability have been combined with additional structuring principles *via* partial (covalent) crosslinking^[19d, 32ai, 46b, 141], cluster formation^[46a, 139, 142] often related to nano- or microphase separation^[32ab, 65-67, 91] as well as *via* incorporation of nano-composites^[1f, 34e, 60b, 143] thus, providing shape persistence^[140, 144]. Accordingly, also the timescale of healing which has to be significantly shorter than global changes within the material including macroscopic deformation culminating in shape loss^[1d] and which depends on the sensing of a damage event while triggering the transport of reactive healing agents as well as on the timescale of the healing reaction itself can be further addressed^[1b]. Therefore, the combination of a fast and a slow healing mechanism allows subsequent crack closure in the first step while regaining the mechanical integrity in the second step^[145].

Stress-sensing due to a damage in combination with a site-directed self-healing response can be realized by stress-induced chemical reactions^[146]. Therefore, the careful adjustment of the required stress to activate and break a preferential bond (chemically labile bonds or supramolecular bonds) able to undergo a self-healing reaction plays an important role. Accordingly, additionally introduced network points required for a successful transfer of force have to be adjusted in the interplay with all other material properties like the presence of crystalline and therefore stiff domains in order to develop stress-sensing self-healing materials^[140].

Void-filling highlights one of the most difficult tasks throughout the development of self-healing materials as damage-induced voids always have to be filled related to a transport of additionally needed material to the void before healing can take place anyway. Thus, the incorporation of continuous channel structures containing liquid healing agents^[147], as well as shape-memory polymers^[148] found application in order to restore contact between ruptured crack planes – a prerequisite for subsequent successful healing^[140].

4.4.2. Overview of multiple self-healing concepts based on interwoven network structures

In the following part some approaches towards hybrid polymer architectures^[1d, 140] useful for the creation of shape-persistent multiple-time healing materials with increased mobility and flexibility and improved mechanical performance should be highlighted. Therefore, either a reversible and a permanent network structure or two reversible network structures prepared *via* a combination of supramolecular and / or reversible covalent self-healing concepts have been combined (see Table 3).

Table 3: Multiple self-healing concepts based on interwoven networks structures to effect self-healing polymers with shape-persistent properties: I) irreversible / reversible self-healing concepts, II) reversible / reversible self-healing concepts.

Ent.	Self-healing concept	1 st Self-healing principle	2 nd Self-healing principle	Healing conditions	η_{SH} [%]	Ref.	
I)	1)	Thiol-ene polymer networks	Thiol-ene click reaction	Hydrogen bonding	UV light (16 mW/cm ²)	-	[149]
	2)	Oxetane-substituted chitosan poly(urethane) networks	Chitosan chain scission and radical recombination	Hydrogen bonding	UV light (302 nm, 120 W)	-	[150]
	3)	Oxolane-substituted chitosan poly(urethane) networks	Chitosan chain scission and radical recombination, conformational changes	Hydrogen bonding	UV light (302 nm, 120 W)	-	[151]
	4)	Random terpolymer consisting of an oxetane-functionalized acrylate, a terpyridine-functionalized acrylate and <i>n</i> -BA	UV curing <i>via</i> free radical polymerization (1 st step) and cationic polymerization (2 nd step)	Metal-ligand interactions	UV light (1 st step: > 380 nm, 2 nd step: 350 - 450 nm)	-	[152]
	5)	Agar-based hydrogel	Photocrosslinking of acrylamide and stearyl methacrylate	Hydrogen bonding	UV light (365 nm, 8 W)	40	[153]
	6)	UPy-functionalized pTHF and polycarbonate mixed with acrylates	Photocrosslinking of mono- and diacrylates	Hydrogen bonding	UV light (320 - 400 nm, 5 W/cm ²)	-	[154]
	7)	Epoxy resins reinforced by DA crosslinking	Epoxide crosslinking	DA / rDA reaction	$T_{SH} = 70 - 150 \text{ }^\circ\text{C}$	quant. ¹	[10f, 155]
					$T_{SH} = RT$	70 - 90 %	[156]
					$T_{SH} = 175 \text{ }^\circ\text{C}$	-	[157]
	8)	Adhesion promotion of a self-healing epoxy matrix	ROMP	Hydrogen bonding	$T_{SH} = 25 - 50 \text{ }^\circ\text{C}$	-	[158]
	9)	CuAAC-based networks	CuAAC	Ionic interactions	$T_{SH} = RT$	-	[159]
Hydrogen bonding				$T_{SH} = RT$	quant. ¹	[46b]	
10)	Thermoreversible organogels	CuAAC	Hydrogen bonding	$T_{SH} = RT$	-	[160]	
11)	Polybenzoxazine precursor-based network formation	Friedel-Crafts reaction	Hydrogen bonding	$T_{SH} = 160 \text{ }^\circ\text{C}$	55	[161]	
II)	12)	TAD based poly(urethane)s	DA / rDA reaction	Ene-type reaction	$T_{SH} = 120 \text{ }^\circ\text{C}$	-	[162]

13)	Coumarin-functionalized poly(urethane)s	[2+2] Cycloaddition	Hydrogen bonding	UV light (254 nm photocleavage, 350 nm photodimerization)	quant. ¹	[163]
14)	Redox- and photoresponsive hydrogels	[2+2] Cycloaddition	Disulfide exchange	UV light (> 300 nm, 450 W)	-	[21c]
15)	PH- and photoresponsive hydrogels	Acyldiazide exchange	Disulfide exchange	T _{SH} = RT	> 50	[164]
16)	Poly(triazole)s	Acyldiazide exchange	Disulfide exchange	T _{SH} = 40 °C	70	[165]
17)	PDMS-based networks <i>via</i> dynamic exchange reactions	Acyldiazide exchange	Hydrogen bonding	T _{SH} = RT	90	[166]
18)	Cyclooctene-based polyolefin networks	Olefin crossmetathesis	Hydrogen bonding	T _{SH} = 50 °C	90-100	[167]
19)	Epoxy resins reinforced by hydrogen bonding interactions	Epoxide crosslinking	Hydrogen bonding	T _{SH} = RT	75	[168]
				-	-	[169]
				T _{SH} = 35 - 80 °C	40 - 212	[170]
20)	Poly(urethane)s with hard peptide segments	DA / rDA reactions	Hydrogen bonding	T _{SH} = 100 °C	-	[171]
21)	Interpenetrating nitrile butadiene rubbers	Rubber formation	Hydrogen bonding	-	-	[172]
22)	Maleated ethylene propylene diene rubber	Rubber formation	Hydrogen bonding	-	-	[173]
23)	Acrylate-based networks	Radical crosslinking	Metal-ligand interactions	-	-	[174]
24)	PH-responsive hydrogels	Schiff-base reaction	Hydrogen bonding	T _{SH} = 25 °C	quant. ¹	[175]
25)	Urea-urethane-based networks	Reversible urea bond formation	Hydrogen bonding	T _{SH} = 37 °C	87	[176]
		Disulfide exchange	Hydrogen bonding	T _{SH} = RT	quant. ¹	[19d, 19e]
		π - π stacking	Hydrogen bonding	T _{SH} = 100 °C	95	[177]
26)	Cholesteryl-based molecular gels	π - π stacking	Hydrogen bonding	T _{SH} = RT	quant. ¹	[178]
27)	Organogels based on poly(benzyl ether) dendrimers	π - π stacking	Hydrogen bonding	-	-	[179]
28)	Catechol-based healing of hydrogels	Hydrogen bonding	Metal-ligand interaction	T _{SH} = RT	-	[180]
				-	70	[181]
				T _{SH} = RT	99	[32ai]
29)	PH-responsive heterodifunctional telechelic polymers	Hydrogen bonding	Metal-ligand interaction	-	-	[182]
30)	Random poly(norbornene)-based terpolymers	Hydrogen bonding	Metal-ligand interaction	-	-	[183]
31)	Acrylamide-based hydrogels	Hydrogen bonding	Ionic interactions	T _{SH} = 25 - 45 °C	60 - 100	[184]

32)	Supramolecular ion gels	Hydrogen bonding	Ionic interactions	-	-	[185]
33)	Host-guest polymer networks	Metal-ligand interaction	Host-guest interaction: crown ether based molecular recognition	$T_{SH} = RT$	quant. ¹	[186]
34)	Host-guest polymer networks	Metal-ligand interaction	Host-guest interaction: cucurbit[8]uril based molecular recognition	-	-	[187]

¹quant. \equiv quantitative healing of the materials property.

4.4.3. Combined irreversible – reversible self-healing concepts

A simple but efficient dual network architecture was designed by incorporating dopamine acrylamide into bio-inspired and photo-curable thiol-ene networks^[149] (see Table 3, Entry 1). Improved mechanical properties as well as improved macroscopic adhesion were observed with increasing the content of incorporated dopamine acrylamide. This change in properties was related to additionally present hydrogen bonding interactions, whereas on the other hand a reduced crosslinking density within the thiol-ene network was noticed^[149].

Poly(urethane) networks with incorporated oxetane-substituted chitosan^[150] (see Table 3, Entry 2) showed complete scratch healing when irradiated with UV light for 20 to 60 minutes. The self-healing response and thus the restoration of the materials properties were attributed to chitosan chain scission followed by irreversible crosslinking reactions between the resulting reactive radicals and the present oxetane ends. Thus, repeated scratch healing was limited by the consumption of oxetane rings within previous healing events^[150]. In a similar approach, the light-induced scratch healing of oxolane-chitosan-polyurethane networks^[151] (see Table 3, Entry 3) has been investigated, whereas the four-membered oxetane ring was replaced by the five-membered oxolane ring. Although the repair process was slowed down due to the decreased ring strain, similar self-healing efficiencies (irradiation up to 120 minutes) were achieved based on the ring opening of incorporated oxolane rings, conformational changes within the backbone and a radically catalyzed polyurea-to-polyurethane conversion^[151].

Similarly, a random terpolymer^[152] built up by an oxetane-functionalized acrylate, a terpyridine-functionalized acrylate and *n*-BA could be cured *via* dual UV-irradiation, whereas the formation of permanent crosslinks proceeded due to free radical polymerization followed by cationic polymerization (see Table 3, Entry 4). Additionally, a supramolecular crosslinking reaction was accomplished by the addition of FeCl₂ and the consecutive formation of metal-ligand interactions which are assumed to incorporate a self-healing ability within the random terpolymer^[152].

Photocrosslinking was also applied for the formation of agar-based self-healable hydrogels^[153] (see Table 3, Entry 5). During heating agar macromolecules were formed aggregating into helical bundles upon cooling due to hydrogen bonding interactions. Subsequently, photopolymerization of incorporated stearyl methacrylate and acrylamide created a second physical network interpenetrating into the present agar-helices due to hydrophobic interactions between formed SDS micelles and the alkyl groups of stearyl methacrylate. The so introduced self-healing ability resulted in a maximum

self-healing efficiency of 40 % independent from the applied healing treatment as well as the healing time^[153].

Films of bivalent UPy-functionalized pTHF or polycarbonate were mixed with varying amounts of mono- and diacrylates undergoing photocuring by irradiation with UV-light^[154] (see Table 3, Entry 6). Due to photopolymerization microphase separation was induced, whereas with increasing diacrylate content the crystallinity of the supramolecular phase was decreased. Simultaneously, the length scale of microphase separation was decreased due to a shorter timescale before starting vitrification. The mechanical properties of the so obtained photocrosslinked hydrogen bonded polymers were comparable to high molecular weight covalent polymers^[154].

A relatively simple approach towards the generation of self-healable or thermally remendable epoxy resins for coating applications can be realized by the incorporation of DA chemistry (see Table 3, Entry 7). Thus, furan-functionalized epoxides mixed with bismaleimide linkers were cured in the presence of anhydrides^[10f] or amine curing agents^[155a-c], whereas the flexural and tensile properties of the obtained materials were comparable to traditional epoxy resins^[10f]. Repeatable healing of scratches was introduced by the rDA reaction taking usually place between 70 to 150 °C^[10f, 155].

Similarly, epoxy systems based on diglycidyl ether of bisphenol A and a newly designed diamine crosslinker prepared *via* DA reaction of a furan-functionalized amine and a bismaleimide have been reported^[155d, 155e]. Thus, the curing temperature had to be reduced to 60 °C in order to avoid premature rDA reactions producing maleimide groups which can react with free amine in a Michael-type addition while reducing curing and the self-healing response starting above 80 °C^[155d, 155e]. Furthermore, self-healable epoxy-amine coating systems showing a very fast self-healing ability within 30 s at 175 °C were obtained by incorporating furfuryl methacrylate, butyl methacrylate as well as a bismaleimide linker^[157].

By applying bismaleimide solutions directly injected to the crack plane the temperature of the rDA reaction and thus of self-healing was decreased to room temperature due to wetting and swelling effects^[156] related to an improved diffusion of the bismaleimide linker within the matrix. Such tests were performed in order to evaluate the self-healing performance of several bismaleimide solutions which later on should be encapsulated and embedded in an epoxy resin with incorporated DA chemistry^[156a, 156c].

The encapsulation of DCPC in combination with dimethylnorbornene ester^[158] possessing hydrogen bonding donor as well as acceptor sites followed by copolymerization in case of a rupture event resulted in nearly two to three times improved healing efficiencies. Furthermore it was shown that dimethylnorbornene ester^[158] as well as 5-norbornene-2-exo,3-exo-dimethanol and 5-norbornene-2-methanol^[188] can act as non-covalent adhesion promoter (see Table 3, Entry 8) thus improving the adhesion ability to the epoxy matrix^[158, 188].

Self-healing concepts acting at room temperature can also be designed by using efficiently covalent crosslinking approaches. Following this strategy, the CuAAC^[22a, 22b] (see Table 3, Entry 9) of multivalent azides and alkynes resulted in irreversibly crosslinked rubbery materials^[11h-j] due to active Cu(I) catalysis. Thus, highly mobile hyperbranched alkyne- and azide-functionalized PIBs have been reported resulting in highly crosslinked materials within times below 1 hour^[159]. Furthermore, four-arm star-shaped PIBs containing both, azide and thymine-endgroups have been prepared enabling a "click" crosslinking approach reinforced by additional hydrogen bonding interactions. Consequently, self-healing investigations showed a multiple recovery of cut specimen within 24 hours at room temperature^[46b].

Organogels were prepared by click-crosslinking of various low molecular weight bivalent alkyne and azide components in the presence of an organogelator suitable for hydrogen bonding interactions^[160] (see Table 3, Entry 10). Although stabilized by the formation of triazole rings, the well-ordered

arrangements due to hydrogen bonding interactions was disturbed proven by the subsequent loss of the previous thermoreversible behavior^[160].

For high-temperature applications a very stable and tough single-time self-healing concept based on the incorporation of poly(bisphenol-hexamine benzoxazine) into a polysulfone matrix was created^[161] (see Table 3, Entry 11). Irreversible network formation proceeded due to the thermally triggered ring-opening reaction of the incorporated polybenzoxazine precursors in combination with a Friedel-Crafts type reaction. Thus, self-healing of cut samples with a toughness recovery of 55 % was realized within 4 hours at 160 °C mainly attributed to hydrogen bonding interactions between hydroxyl and sulfone groups^[161].

4.4.4. Combined reversible - reversible self-healing concepts

For the preparation of crosslinked rubbery poly(urethane)s 1,2,4-triazoline-3,5-diones (TADs) were used as crosslinkers favoring both DA and ene-type reaction in the presence of a suitable reaction partner (see Table 3, Entry 12 and Figure 11), whereas both reactions are reversible at elevated temperatures (120 °C)^[162]. Therefore, appropriate reaction partners for TADs were incorporated in the polymer backbone by using indole diol and 2,4-hexadiene-1,6-diol treated with propylene oxide or hexamethylene diisocyanate. Accordingly, TAD crosslinked poly(urethane)s showed a self-healing response at 120 °C within 1 hour due to the proceeding rDA reaction subsequently followed by an ene-type reaction^[162].

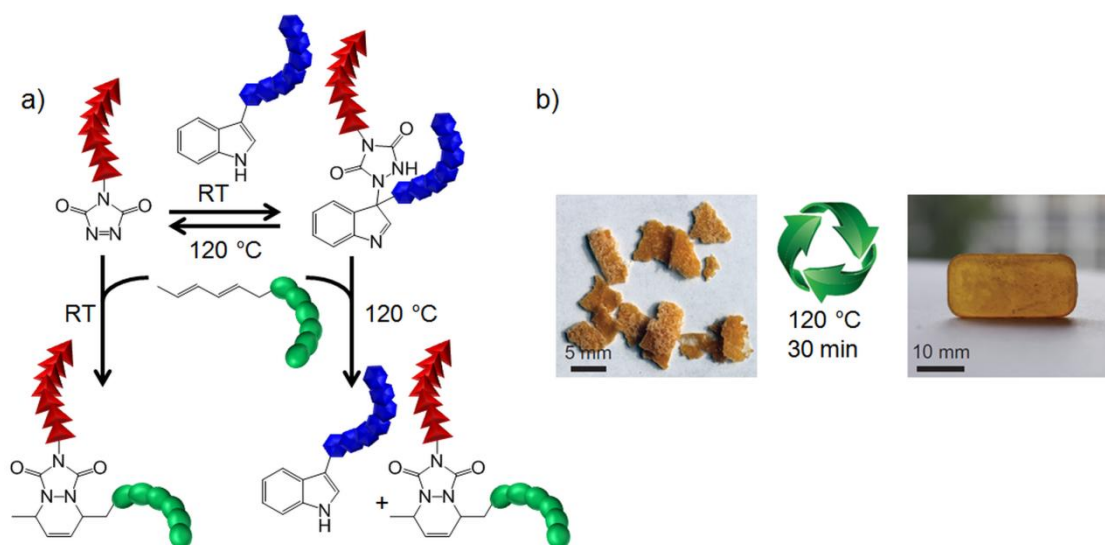


Figure 11: a) Overview of TAD based click reactions between TAD and indoles as well as between TAD and dienes. Concept applied to low molecular weight compounds and polymers. b) Image of a crosslinked PU sample, which was heated at 120 °C for 30 minutes. Figure reprinted and adopted from reference^[162] with permission from the Nature Publishing Group (Copyright 2014).

Photo-responsive poly(urethane)s were prepared by reacting tri-functional homopolymers of hexamethylene diisocyanate^[163a] or isophorone diisocyanate^[163b] with a soft PEG block and a coumarin-moiety to incorporate pendant hard coumarin segments (see Table 3, Entry 13). The formation of smooth films was realized by photodimerization of coumarin groups *via* irradiation at 350 nm. Thus, cracks were repeatedly healed by irradiating at 254 nm for 1 minute (photocleavage) followed by photodimerization at 350 nm for 90 minutes. Self-healing related to photo-remending was additionally promoted by hydrogen bonding interactions, whereas the corresponding efficiency depended on the formation of microphase separated rubbery domains as well as on the chain mobility.

Thus, the best healing efficiencies of 100 % after the first, 90 % after the second and 61 % after the third healing cycle related to a reduced photoreversibility were reported for polymers with a low content of coumarin groups related to a low T_g ^[163].

Redox- and photo-sensitive hydrogels have been prepared by incorporating disulfide and anthracene moieties suitable for photodimerization in bulk (see Table 3, Entry 14). Thus, the swelling degree was controlled by adjusting the irradiation time, whereas the cleavage of disulfide crosslinks was applied under reductive conditions using sodium borohydride^[21c].

Similar pH- and redox-responsive hydrogels were reported by introducing disulfide linkages and dynamic acylhydrazone units^[164] (see Table 3, Entry 15). Consequently, a self-healing response was observed within 48 hours under basic conditions based on disulfide exchange reactions. Under acidic conditions or *via* addition of aniline self-healing was accomplished due to acylhydrazone exchange^[164].

In line with this a 70 % self-healing efficiency of poly(triazole)s containing disulfide groups and acylhydrazone synthons was reached after keeping cut samples at 40 °C for 48 hours^[165] (see Table 3, Entry 16).

A double self-healing system based on exchangeable acylhydrazone units and hydrogen bonding interactions was prepared by polycondensating a soft siloxane-based dialdehyde and a carbohydrazide containing bis-iminourea-type synthons^[166] (see Table 3, Entry 17 and Figure 12). Thus, multiple self-healing within several hours related to a 90 % recovery of strain was observed while preserving the mechanical integrity. It was shown that the healing response mainly resulted from supramolecular interactions as no increased healing efficiencies were observed by adding an acidic catalyst suitable to accelerate the acylhydrazone exchange^[166]. Similar dynamers^[189] based on reversible acylhydrazone exchange and hydrogen bonding interactions formed branched fibrous aggregates in solution due to double crosslinking of polymers resulting in "dial-in" properties^[190].

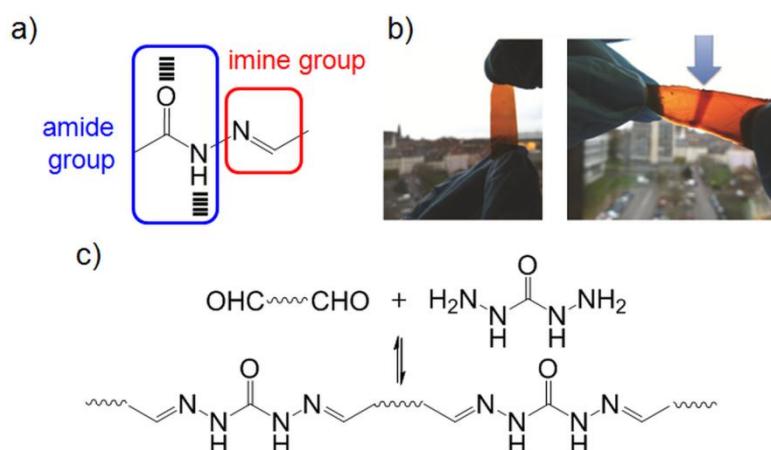


Figure 12: a) Chemical structure of the acylhydrazone functionality combining a reversible imine bond and a hydrogen bonding amide group, b) left – virgin polymer film; right – cut polymer film which was healed within the overlapping domain (see arrow), c) equilibrium between a bis-aldehyde and a carbohydrazide and the formed acylhydrazone. Figure reprinted and adopted from reference^[166] with permission from John Wiley and Sons (Copyright 2014).

Secondary amide side chains have been incorporated into polymer networks prepared *via* olefin cross-metathesis^[167, 191] of cyclooctene-based olefins (see Table 3, Entry 18 and Figure 13). Accordingly, introduced hydrogen bonds were capable of dissipating energy thus leading to improved mechanical properties and a self-healing response. Interestingly, the initial stiffness of the polymer

networks was nearly unaffected by hydrogen bonding interactions which was attributed to their relatively short lifetime making them "mechanically invisible" at timescale of the tensile experiments. Self-healing tests of cut samples performed at 50 °C resulted in a 90 % recovery of toughness after 3 hours and a complete recovery of the Young's modulus already after 1 hour^[167]. Similarly, the selective olefin cross-metathesis of Napy and UPy modified monomers resulted in the formation of supramolecular copolymers due to intermolecular hydrogen bonding interactions between UPy-moieties and UPy- and Napy-endgroups^[192].

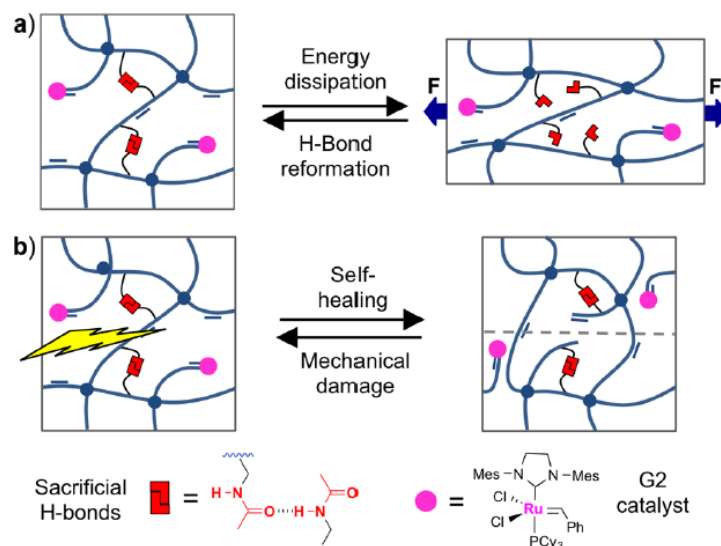


Figure 13: Self-healable polymer networks with incorporated hydrogen bonding interactions prepared *via* olefin cross-metathesis. Figure reprinted with permission from reference^[167]. Copyright 2015, American Chemical Society.

The incorporation of a self-healing ability within an epoxy resin was realized by using supramolecular and thus, reversible interactions like hydrogen bonds^[168-170, 193] (see Table 3, Entry 19). Thus, supramolecular chemistry has been implemented by embedding glycidyl methacrylate filled microcapsules in an epoxy matrix^[168]. In the case of a rupture event rebonding of the cracked surfaces was realized due to wetting and hydrogen bonding interactions. Accordingly, a healing efficiency of 75 % at 25 °C was observed due to the ring-opening reaction of epoxy groups followed by a nucleophilic addition to residual amine functionalities within the resin^[168]. Similarly, supramolecular chemistry of heterocyclic ureas was combined with epoxide crosslinking by catalyzed esterification of various fatty di- and triacids with multifunctional epoxides^[169]. Furthermore, hydrogen bonding interactions resulted in a fracture toughness healing efficiency ranging from 40 to 200 % within ureido-amide based thermoplastic elastomers prepared *via* crosslinking of diglycidylether of bisphenol A and an ureido-amide thermoplastic^[170]. Moreover, epoxy resins are reported to be reinforced by the incorporation of chitosan re-bridging cracked surfaces probably due to hydrogen bonding interactions^[193].

High-performance poly(urethane) films showing enhanced mechanical properties were prepared by introducing maleimide units into a poly(urethane) built up by hard peptide segments^[171] (see Table 3, Entry 20). Thus, hydrogen bonding interactions were additionally reinforced by reversible covalent network formation due to DA chemistry resulting in recycling with 5 to 20 minutes at relatively high temperatures between 160 - 180 °C due to the strong polymer backbone^[171].

Interpenetrating polymer networks with a viscoelastic behavior have been prepared by the incorporation of tetrakis [methylene-3-(3,5-di-tert-butyl-4-hydroxy phenyl)propionyloxy] methane which can form hydrogen bonding interactions within nitrile butadiene rubbers^[172] (see Table 3, Entry

21). Consequently, microphase separation and the induction of micro-pores within the material were observed. While performing long-time investigation it was shown that the supramolecular network was weakened due to progressed phase separation and crystallization of hydrogen bonding moieties related to a loose of the formerly induced viscoelasticity^[172].

In contrast, a maleated ethylene propylene diene rubber blended with 3-amino-1,2,4-triazole capable of hydrogen bonding interactions showed an improved stiffness as well as an improved heat shrinkability, whereas the hydrogen bonding interactions hindered crystal growth resulting in a decreased crystallinity of the rubber blend^[173] (see Table 3, Entry 22).

Polymer networks persisting of covalent and thus permanent crosslinks have been created by crosslinking ethylene glycol dimethacrylate, ethylene glycole, hydroxyethylmethacrylate and 4-vinylpyridine by the addition of sodium metabisulphite and ammonium persulphate^[174]. Furthermore, reversible metal-ligand interactions have been introduced by the coordination of bifunctional Pt(II) or Pd(II) pincer complexes with pyridine ligands located within side chains of the polymer network^[174] (see Table 3, Entry 23).

PH-responsive, hydrogels have been prepared by self-crosslinking of oxidized dialdehyde functionalized alginate and acrylamide-modified chitin functionalized with amino groups^[175]. Due to the introduction of dynamic linkages through a Schiff base reaction complete recovery was observed within 1 to 3 hours depending on the pH-value and the ratio of the polymers. Interestingly, it was shown that the self-healing ability was storable by freeze-drying and could be reactivated by rehydration. Furthermore, even stale cut surfaces showed complete self-healing after 3 hours^[175] (see Table 3, Entry 24).

The introduction of SH properties within poly(urethane)s and poly(urea)s (see Table 3, Entry 25) highlights a major prospect due to their importance in a magnitude of feasible applications. Thus, poly(urea)s and poly(urea urethane)s (containing DMF as swelling agent) have been functionalized with bulky substituents at the nitrogen atom of the urea unit^[176]. Due to the resulting weakening of the carbonyl-amine bond the reversible dissociation into isocyanate- and amine-groups was promoted. Supported by hydrogen bonding interactions, repairing was accomplished at low temperatures (37 °C) within several hours, whereas a maximal 87 % recovery of breaking strain was observed after 12 hours^[176]. Quantitative healing of poly(urea urethane)s with incorporated bis(4-aminophenyl) disulfide groups was observed at room temperature within 24 hours. Self-healing was accomplished by quadruple hydrogen bonding interactions between urea groups and reversible disulfide exchange while showing easy (re)processability at 150 °C by hot-pressing at 30 bar^[19d, 19e].

Self-healing concepts based on combinations of various supramolecular interactions solely have been reported as well^[32ai, 177-187, 194]. Thus, a repeatable double self-healing elastomer was prepared by blending a chain-folding polyimide and a pyrenyl-functionalized poly(urethane)^[177] (see Table 3, Entry 25). Cut samples were repeatedly healed at 100 °C within 240 minutes while observing a 95 % recovery of the tensile modulus due to aromatic π - π interactions between π -electron-deficient diimide units and π -electron-rich pyrenyl units additionally reinforced by hydrogen bonding interactions^[177].

Similarly, molecular gels of 7-nitrobenzo-2-oxa-1,3-diazol-4-yl appended cholesteryl derivatives self-assembled into fibrous structures or ball-like structures while showing a repeatable self-healing performance^[178] due to combined hydrogen bonding interactions and π - π -stacking (see Table 3, Entry 26). Thus, cut samples completely recovered their structure under ambient conditions, whereas the cholesteryl derivative with the shortest spacer length revealed the best gelation^[178].

Furthermore, organogelators based on poly(benzyl ether) dendrimers (see Table 3, Entry 27) were reported which self-assemble into one-dimensional nanostructures due to a combination of π - π -interactions, hydrogen bonding interactions and solvophobic interactions^[179].

Many recently reported adhesives and self-healable hybrid hydrogels^[32ai, 180-181, 194b, 194c] working under harsh environmental conditions have been mimicked by naturally occurring mussel adhesive proteins. In order to create a self-healing ability based on reversible metal-ligand interactions a high content of 3,4-dihydroxyphenylalanine (DOPA) as well as the presence of an Fe^{3+} source is required^[194b, 194c]. While performing a typical mussel-mimetic pH change from acidic to alkaline the formerly present covalent Fe^{3+} -catechol network was additionally reinforced by introducing corresponding Fe^{3+} -catechol coordination bonds able to dynamically respond to a rupture event^[180a] (see Table 3, Entry 28).

Similarly, self-assembled structures were obtained from heterodifunctional PS functionalized with UPy and tpy endgroups^[182] in the presence of a nickel(II), iron(II) or zinc(II) source (see Table 3, Entry 29). While changing the pH the hydrogen bonding interactions between supramolecular building blocks were disrupted. In contrast, the metal-ligand interactions were still present proving its higher tolerance against pH change^[182].

Random terpolymers have been prepared in solution *via* ROMP of norbornene and norbornene-based comonomers modified with palladated-pincer complexes and a diaminopyridine moiety or a cyanuric acid wedge moiety suitable for complementary hydrogen bonding interactions^[183] (see Table 3, Entry 30 and Figure 14). Due to the self-assembling of hydrogen bonding recognition units just a weak increase of the solution viscosity was monitored. In contrast, metal-ligand interactions resulted in a dramatic increase in viscosity. Thus, the strength of the final crosslinked polymer network could be tuned by adjusting the concentration of the crosslinking motifs^[183a].

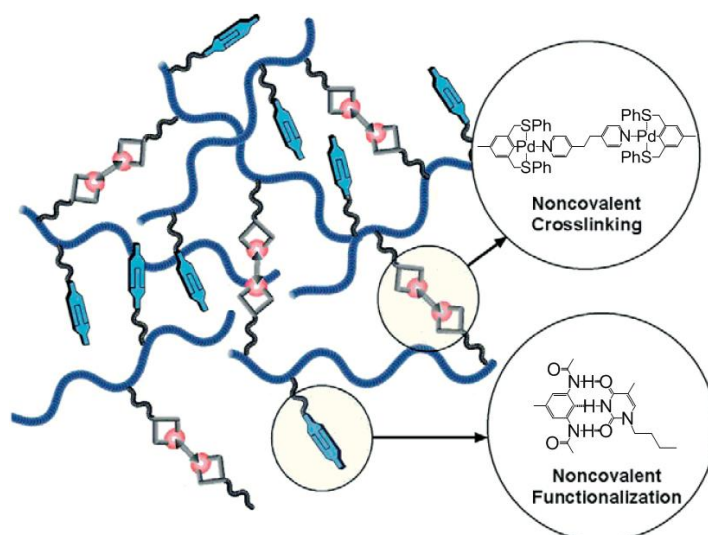


Figure 14: Multi-step self-assembly of random terpolymers *via* hydrogen bonding interactions and metal-ligand interactions of palladated-pincer complexes. Figure reprinted from reference^[183a] with permission from Elsevier Ltd. (Copyright 2004).

A repeatable self-healable hydrogel was reported based on poly(acrylamide-*co*-3-((2-(methacryloyloxy)ethyl)dimethylammonio)propane-1-sulfonate)^[184] displaying hydrogen bonding interactions between acrylamide parts as well as electrostatic interactions due to its zwitterionic nature. Thus, healing efficiencies up to 100 % were observed with recovery times below 1 minute^[184] (see Table 3, Entry 31).

Viscoelastic and thermoreversible supramolecular ion gels (see Table 3, Entry 32) have been prepared by dissolving ABA triblock copolymers in an ionic liquid^[185]. Supramolecular network formation related to a distinct rubbery plateau due to an increasing number of hydrogen bonding interactions was observed for cooling mixtures consisting of either poly(2-vinylpyridine)-*b*-poly(ethyl acrylate)-*b*-poly(2-vinylpyridine) and poly(4-hydroxystyrene)^[185b] or poly(2-vinylpyridine)-*b*-PEO-*b*-poly(2-vinylpyridine)^[185a] and poly(4-vinylphenol) in 1-ethyl-3-methylimidazolium bis(trifluoromethylsulfonyl)imide below the gel point (120 - 160 °C). Thus, the terminal relaxation dynamics was directly related to the amount of involved hydrogen bonds showing retardation with increasing the molecular weight of the A-block within the ABA triblock copolymer^[185].

Polymer network gels^[195] with good mechanical properties were created by multiple stimuli-responsive host-guest interactions based on a bis(benzo-21-crown-7)-based monomer and a bis(dialkylammonium salt)-based monomer^[186b] and metal-ligand interactions between added [PdCl₂(PhCN)₂] and incorporated triazole rings (see Table 3, Entry 33). The interplay of the two dynamically reversible interactions resulted in orthogonal self-assembly of the polymer gels showing a self-healing response within several minutes^[186b].

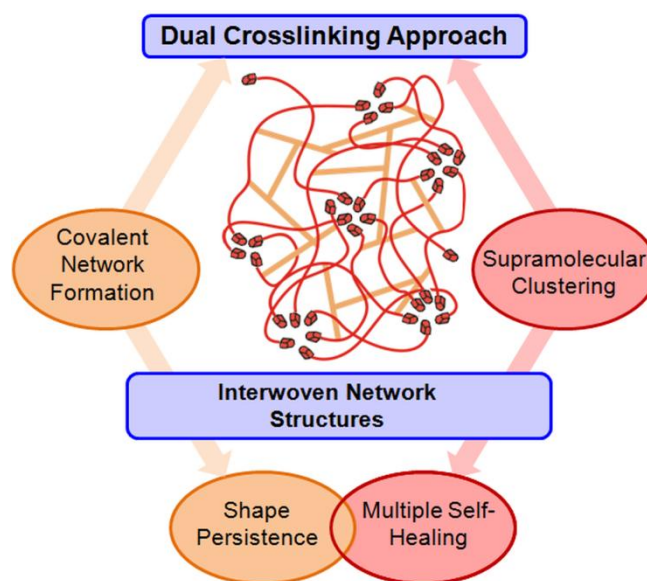
Similarly, a temperature- and pH-responsive supramolecular polymer network with a fast self-healing ability was created by the host-guest interaction between dibenzo-24-crown-8 and a dibenzylammonium salt^[186c] and by various metal-ligand interactions between Zn(OTf)₂, [PdCl₂(PhCN)₂], terpyridine ligands and triazole rings^[186c]. In a related approach crosslinked supramolecular networks were created by the addition of [PdCl₂(PhCN)₂] to a bis(meta-phenylene)-[32]crown-10 host and a paraquat guest^[186a] which have been linked by a CuAAC click reaction. Thus, supramolecular crosslinking was achieved *via* a combination of host-guest interactions and metal-ligand interactions formed between triazole rings and the added metal salt^[186a].

Furthermore, ternary complex / metal-organic polymer networks have been reported based on host-guest interactions between cucurbit[8]uril (see Table 3, Entry 34), a boronic acid modified viologen derivative and a naphthol- as well as catechol-functionalized chitosan and metal-ligand interactions in the presence of Fe³⁺^[187].

5. SCOPE OF THE THESIS

5.1. Objective

In the scope of this thesis embedded in the framework of the DFG SPP 1568 "Design and Generic Principles of Self-Healing Materials" the main objective was the development of an interwoven network structure based on covalent network formation *via* click chemistry and supramolecular network formation *via* clustering of hydrogen bonding moieties towards the design of a multiple self-healing polymer acting at room temperature. Thus, the optimization problem of self-healing as an inherent material property to respond to a damage event related to contrary demands including the fast closure of (crack-)induced damages while keeping the mechanical integrity in order to persist the shape of the material should be addressed by the preparation of an interwoven network structure and the investigation of its self-healing performance (see Scheme 1).



Scheme 1: A dual crosslinking approach by combination of covalent network formation and supramolecular clustering towards multiple self-healing polymers with interwoven network structures able to respond to a damage event in an autonomous fashion while addressing contrary demands like the fast closure of (crack-)induced damage and the shape persistence of the material.

Therefore, in the first step a room temperature once-a-time self-healing concept based on the copper(I)-catalyzed alkyne–azide “click” cycloaddition (CuAAC) reaction of azide- and alkyne-functionalized polymers with a star-shaped or hyperbranched architecture and a low glass transition temperature (T_g) had to be developed. Thus, the influence of the molecular weight, the functional group density, the starting viscosity of the investigated polymer mixtures as well as the architecture on the kinetics of the click-crosslinking approach should be studied aiming at a deeper understanding of (auto-)catalytic effects in the course of the reaction towards their application in self-healing materials.

In the second step, liquid, star-shaped polymers with mixed endgroups, containing reactive azide-endgroups suitable for click-crosslinking and hydrogen-bonding moieties acting as supramolecular tie points had to be prepared to create dual crosslinked network structures *via* simultaneously proceeding covalent and supramolecular network formation in the presence of an appropriate multivalent alkyne-functionalized polymer. Therefore, four-arm star polymers with different degree of functionality should be synthesized to study the proceeding dual network formation and the final network properties including their self-healing performance.

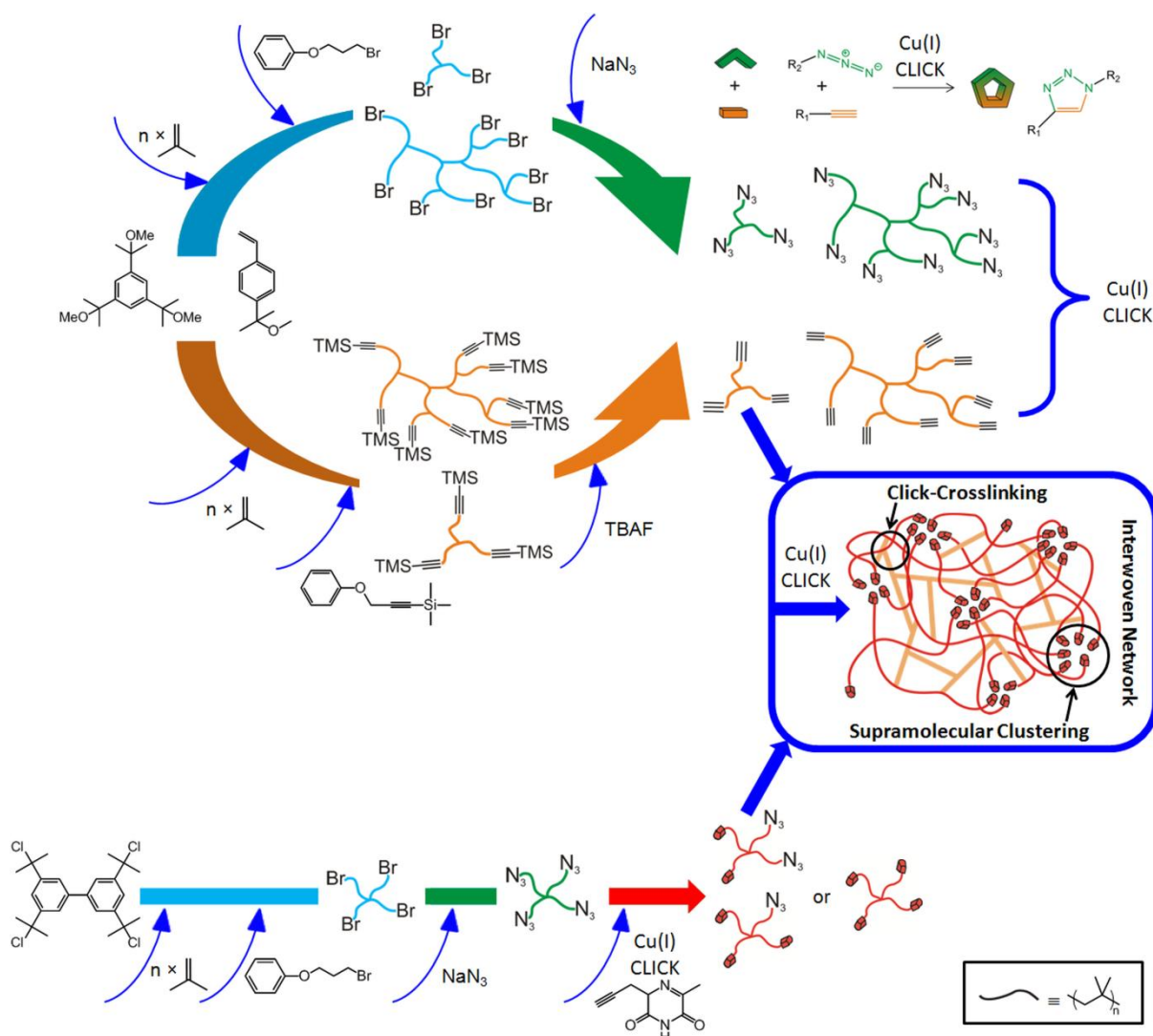
5.2. Concept

For the design of a multiple self-healing polymer with an interwoven network structure working under ambient conditions a covalent crosslinking approach based on the copper(I)-catalyzed alkyne–azide “click” cycloaddition (CuAAC) reaction and supramolecular network formation *via* clustering of hydrogen bonding moieties had to be combined.

Accordingly, in the first step, a room temperature once-a-time self-healing concept based on the CuAAC reaction of liquid and multivalent azide- and alkyne-functionalized polymers was investigated to study the influence of several parameters on the kinetics of the click-crosslinking approach including the molecular weight, the functional group density, the starting viscosity of the investigated polymer mixtures as well as the architecture of the reactive polymers while aiming at a deeper understanding of (auto-)catalytic effects in the course of the reaction.

In order to design such an autonomous once-a-time self-healing concept living carbocationic polymerization (LCCP) of isobutylene was performed to prepare liquid three-arm star and hyperbranched azide- and alkyne-functionalized poly(isobutylene)s (PIBs) with a low glass transition temperature (T_g) suitable for subsequent click-crosslinking at room temperature in the presence of an appropriate copper(I) catalyst.

Therefore, 1,3,5-tris(2-methoxy-2-propyl)benzene was applied as initiator for the synthesis of three-arm star PIBs, whereas 4-(2-methoxyisopropyl)styrene was used as inimer-type initiator for the preparation of hyperbranched polymers. For the quenching of living chain ends related to the direct introduction of bromide- or trimethylsilyl-protected alkyne-endgroups 3-(bromopropoxy)benzene (BPB) or trimethyl(3-phenoxy-1-propynyl)silane (TMPPS) was used as quenching agent. Desired three-arm star and hyperbranched azide- and alkyne-functionalized PIBs were obtained by subsequent endgroup modification in the presence of sodium azide or tetrabutylammonium fluoride (TBAF), respectively (see Scheme 2).



Scheme 2: Design of a multiple self-healing polymer with an interwoven network structure working under ambient conditions by combining a covalent crosslinking approach based on the CuAAC reaction and supramolecular network formation *via* clustering of hydrogen bonding moieties: Three-arm star and hyperbranched azide- and alkyne-functionalized PIBs were synthesized *via* LCCP using 1,3,5-tris(2-methoxy-2-propyl)benzene as initiator for the preparation of three-arm star PIBs, whereas for the preparation of hyperbranched polymers 4-(2-methoxyisopropyl)styrene was applied as inimer-type initiator. For the direct introduction of bromide- or trimethylsilyl-protected alkyne-endgroups BPB or TMPPS were used as quenching agents, subsequently followed by endgroup modification in the presence of sodium azide or TBAF, respectively, in order to obtain the desired azide- and alkyne-modified polymers. Four-arm star thymine-functionalized PIBs with complete or partial endgroup functionalization were synthesized *via* LCCP using biphenyl tetracumyl chloride as initiator in combination with BPB as quenching agent. Subsequently, bromide-telechelic polymers were converted into the corresponding four-arm star azide-telechelic PIBs in the presence of sodium azide, which were further reacted with an alkyne-functionalized thymine-moiety *via* a microwave-assisted CuAAC reaction. Finally, polymers containing both, azide- and thymine-moieties, were click-crosslinked with a three-arm star alkyne-telechelic PIB towards the development of a multiple self-healing polymer with an interwoven network structure working under ambient conditions due to combined covalent network formation and supramolecular clustering.

Thus, azide- and alkyne-functionalized polymers with two different architectures, various molecular weights and therefore various functional group densities and different starting viscosities have been prepared to study the influence of these parameters on the reaction rate of the CuAAC-based click-crosslinking approach *via* melt rheology and differential scanning calorimetry (DSC) measurements.

In order to obtain deeper insights into the (auto)catalysis of the CuAAC reaction of multivalent azide- and alkyne-functionalized polymers in the melt state while proving its suitability for room temperature self-healing applications, especially the required gelation times as well as the achieved network strand densities of finally crosslinked polymers have been investigated.

The related results can be found in the first and second section of the *Results and Discussion* part of this thesis dealing with the "Autocatalysis in the Room Temperature Copper(I)-Catalyzed Alkyne-Azide "Click" Cycloaddition of Multivalent Poly(acrylate)s and Poly(isobutylene)s" (D. Döhler, P. Michael, W. H. Binder, *Macromolecules* **2012**, *45*, 3335.) and with "Hyperbranched poly(isobutylene)s for self-healing polymers" (D. Döhler, P. Zare, W. H. Binder, *Polym. Chem.* **2014**, *5*, 992.).

In the second step, liquid, star-shaped PIBs with mixed endgroups, containing reactive azide-endgroups suitable for click-crosslinking and hydrogen-bonding moieties acting as supramolecular tie points had to be prepared to create a dual crosslinked network structure *via* simultaneously proceeding covalent and supramolecular network formation. Therefore, four-arm star polymers with different degree of functionality were synthesized to study the proceeding dual network formation and the final network properties including their self-healing performance.

For the synthesis of four-arm star thymine-functionalized PIBs with complete or partial endgroup functionalization LCCP was performed using biphenyl tetracumyl chloride as initiator while applying BPB as quenching agent. The so obtained four-arm star bromide-telechelic polymer was treated with sodium azide to obtain the corresponding four-arm star azide-telechelic PIB, which was further converted in a microwave-assisted CuAAC reaction in the presence of an alkyne-functionalized thymine-moiety to prepare desired thymine-modified PIBs with a different amount of remaining azide endgroups (see Scheme 2).

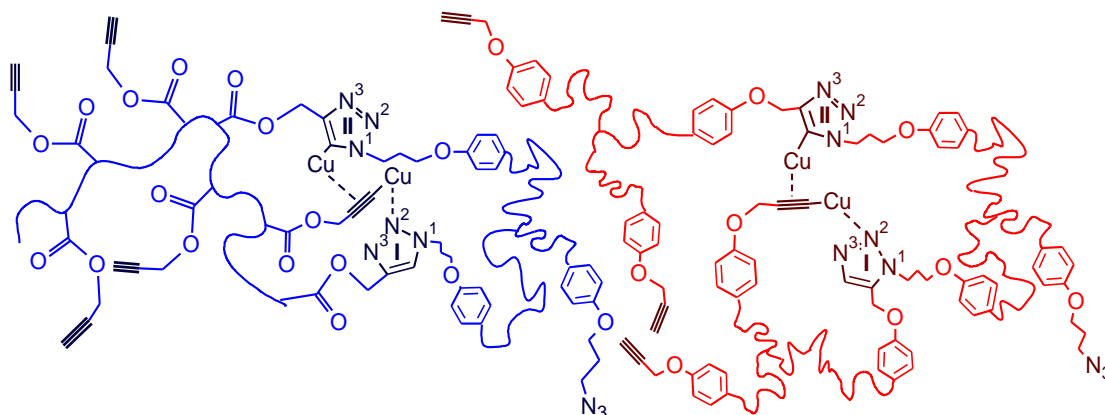
So obtained four-arm star thymine-modified PIBs with different degree of functionality suitable for click-crosslinking and supramolecular network formation *via* clustering of hydrogen bonding moieties were separated *via* column chromatography and further purified by dialysis.

Subsequently, they have been crosslinked with three-arm star alkyne-telechelic PIB to investigate the influence of the degree of functionality on the kinetics of the click-crosslinking reaction and on the supramolecular network formation *via* melt rheology. Furthermore, obtained interwoven network structures were studied *via* SAXS measurements to investigate supramolecular cluster formation while analyzing the amount of hydrogen bonding moieties within formed supramolecular clusters as well as their size and distribution. Finally, macroscopic self-healing tests have been performed to study the self-healing response of dual crosslinked polymers.

The results of this dual crosslinking approach based on the design of an interwoven network structure *via* simultaneously proceeding covalent and supramolecular network formation can be found in the third chapter of this thesis dealing with "A dual crosslinked self-healing system: Supramolecular and covalent network formation of four-arm star polymers" (D. Döhler, H. Peterlik, W. H. Binder, *Polymer* **2015**, doi:10.1016/j.polymer.2015.01.073.).

6. RESULTS AND DISCUSSION

6.1. Autocatalysis in the Room Temperature Copper(I)-Catalyzed Alkyne-Azide "Click" Cycloaddition of Multivalent Poly(acrylate)s and Poly(isobutylene)s



ABSTRACT

The concept of self-healing polymers requires fast and efficient crosslinking processes, ideally based on catalytic reactions. We investigate autocatalytic effects in crosslinking processes based on the copper(I)-catalyzed alkyne–azide “click” cycloaddition reaction (CuAAC), taking advantage of the 1,3-triazole rings formed during the CuAAC-based crosslinking, which act as ligands for subsequent “click”-reactions in turn accelerating the reaction rate of subsequent CuAAC-reactions. Catalysis during the crosslinking reactions of multivalent polymeric alkynes and azides (nine atactic random poly(propargyl acrylate-*co*-*n*-butyl acrylate)s, $M_n = 7000\text{--}23400$ g/mol) prepared *via* nitroxide mediated polymerization (NMP) and displaying alkyne-contents ranging from 2.7 mol % to 14.3 mol % per chain were studied *via* melt-rheology and differential scanning calorimetry (DSC), revealing significant increases of the reaction rate with increasing alkyne-concentrations. A kinetic analysis showed autocatalytic effects (up to a factor of 4.3) now enabling a deeper understanding of the catalysis as well as on the achievement of a “click”-crosslinking concept acting at room temperature. Effects exerted by the molecular weight were investigated by reacting five three-arm star azide-telechelic poly(isobutylene)s (PIBs) ($M_n = 5500\text{--}30000$ g/mol) and one three-arm star alkyne-telechelic PIB ($M_n = 6300$ g/mol) in the crosslinking-reaction, thus linking molecular mobility to changes in CuAAC-reactivity revealing faster network formation with lower molecular weights. The now designable significant autocatalytic effects together with the optimized reaction rate *via* the lowest molecular weight compounds enabled the design of a new, highly efficient and fast crosslinking system acting at room temperature.

INTRODUCTION

Network formation based on crosslinking and post-crosslinking reactions is of great interest for materials scientists as these reactions can be used to build up new complex architectures or to improve existing materials in their physicochemical and thermomechanical properties, most of all self-healing polymeric materials. Therefore, a permanent strive for reactions enabling crosslinking under mild reaction conditions as well as the quest for new reactants has been generating efficient

reactions such as Diels–Alder (DA) reactions, or “click”-type-reactions like the CuAAC,^{1–7} which proceed at moderate temperature^{1,2} with high efficiency and substrate insensitivity. The “click”-type reactions in particular are valuable tools for the design of self-healing polymers,^{8–11} which to a large extent rely on efficient and insensitive crosslinking chemistry. In contrast to the previously used epoxide^{12–14} or metathesis^{8,10,15–21} based crosslinking reactions, many approaches using DA-type reactions have been investigated,

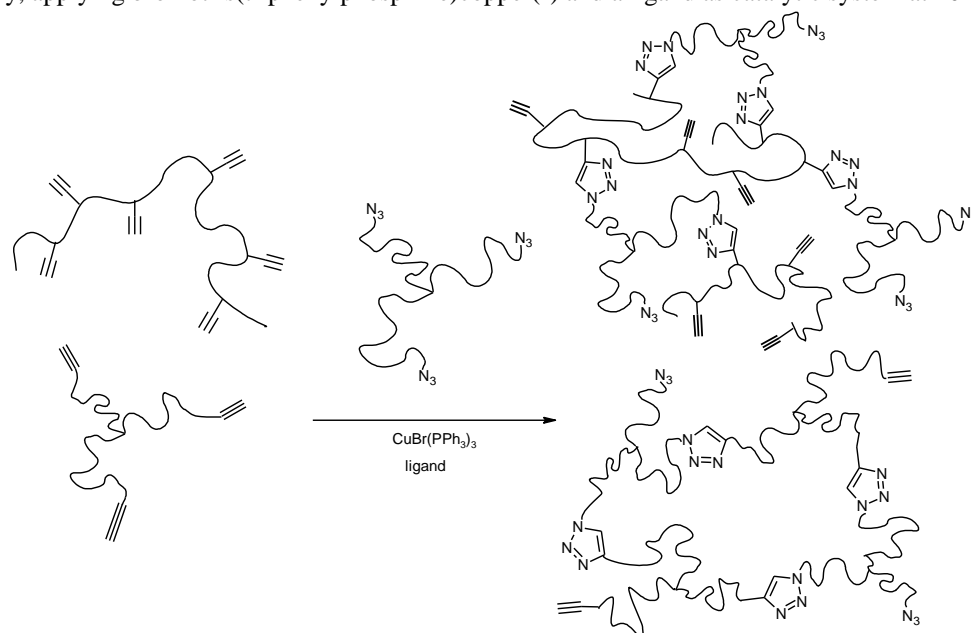
featuring furan/maleimide linkers²² or other maleimides,^{23–28} thus generating polymers with switchable mechanical properties.^{29–32} However, in most of these cases the underlying DA reactions proceeded at temperatures significantly above room temperature, often at 80–100 °C, leading to cross-linked materials such as hydrogels, shape-memory materials, in nanoscale probe lithography, adhesives or coatings.^{33–40}

To overcome the described disadvantage of required high temperatures we intensely investigated the use of the CuAAC as crosslinking reaction, specifically for the purpose of self-healing polymers.^{41,42} The CuAAC in particular opens suitable pathways for crosslinking approaches that have been used for the preparation of hydro- or microgels based on poly(vinyl alcohol)s,⁴³ poly(ethylenimine)s,⁴⁴ poly(ethylene glycol)s,^{43,45,46} hyaluronic acids,^{47–49} or for the stabilization of organogels.⁵⁰ For this purpose copper(II) sulfate pentahydrate/sodium ascorbate or ascorbic acid in aqueous conditions as well as CuBr, CuI, or CuCl in organic solutions were used as catalytic systems^{43–50} and the corresponding “click” reactions proceeded at moderate, but still elevated temperatures.^{43–50} In other concepts,

the CuAAC has been applied to synthesize cellulose nanoplatelet gels⁵¹ and polyester nanoparticles⁵² as well as particle-like structures⁵³ and polymeric nanoparticles⁵⁴ *via* intramolecular crosslinking reactions, often by use of crosslinking reactions based on low-molecular-weight⁵⁵ or polymeric precursors.^{41,42}

Our concept of using the CuAAC as crosslinking-principle relies on the use of liquid monovalent or three-arm star azide-telechelic polymers, namely PIBs with different liquid multivalent alkynes for their use in self-healing materials.^{41,42} When studying different copper-catalysts the resulting kinetic behavior of the crosslinking reaction in solution and in the solid state revealed that bromotris(triphenylphosphine)copper(I) was the best catalyst for a crosslinking reaction, also observing an acceleration of the reaction rate in solution when using NMR-spectroscopy.^{41,42} Therefore, we hypothesized that the autocatalytic effects observed in solution should operate in the melt-state of polymers as well, in particular for the herein described crosslinking of multivalent poly(acrylate)s and PIBs *via* “click” chemistry. Ligands containing

Scheme 1 CuAAC of multivalent poly(acrylate)s and PIBs functionalized with alkyne and azide groups, respectively, applying bromotris(triphenylphosphine)copper(I) and a ligand as catalytic system at 20 °C.



triazole rings and accelerating the reaction rate of the CuAAC are known in literature,⁵⁶ with TBTA (tris[(1-benzyl-1*H*-1,2,3-triazol-4-yl)methyl]amine)⁵⁶ being one prominent example completely encasing the catalytically active copper(I) center and protecting it against degradation. Such tetradentate ligands seem to be so effective because of their tertiary amine accelerating the catalytic process while increasing the electron density on the copper(I) center.

Within this publication we report on the catalysis during the crosslinking reaction of multivalent polymeric alkynes and azides *via* a CuAAC-process (see Scheme 1), aiming at a deeper understanding of the catalytic effects as well as on the achievement of a “click”-crosslinking concept acting at room temperature. Beside this we focus on the autocatalysis during the crosslinking reaction due to the *in situ* formation of triazole rings, investigating their influence with respect to density when present in various amounts within a random copolymer of propargyl acrylate (PA) and *n*-butyl acrylate (*n*BA). Furthermore, we evaluate autocatalytic effects with respect to the molecular weight of five three-arm star azide-telechelic PIBs and one three-arm star alkyne-telechelic PIB on the crosslinking-reaction, trying to link molecular mobility to changes in CuAAC-reactivity.

EXPERIMENTAL SECTION

Materials

The destabilization of commercial available *n*BA was done by passing through a short column of neutral alumina into a flask with calcium hydride and stored overnight into freezer. Before using, *n*BA was distilled freshly. PA and TMSPA were prepared according to Thelakkat et al.⁵⁷ 1,3,5-Tris(2-methoxy-2-propyl)benzene was synthesized according to previous descriptions.^{58,59} Trimethyl(3-phenoxy-1-propynyl)silane was synthesized according to Morgan et al.⁶⁰ Tris[(1-benzyl-1*H*-1,2,3-triazol-4-yl)methyl]amine (TBTA) was prepared according to Lee et al.⁶¹ All other

chemicals were purchased from Sigma-Aldrich and used without further purification.

Instrumentation

NMR spectra were recorded on a Varian Gemini 2000 (400 MHz) or on a Varian Unity Inova 500 (500 MHz) at 27 °C. Deuterated chloroform (CDCl₃) was used as solvent. All chemical shifts were given in ppm. MestRec-C software (version 4.9.9.6) was used for interpretation of the NMR-spectra.

ATR-IR spectra were performed on a Bruker Tensor VERTEX 70 equipped with a Golden Gate Heated Diamond ATR Top-plate. Opus 6.5 was used for analyzing data.

Gel permeation chromatography (GPC) measurements were performed on a Viscotek GPCmax VE 2002 using a H_{HR}H Guard-17369 and a GMH_{HR}-N-18055 column in THF at 40 °C and *via* detection of the refractive index with a VE 3580 RI detector of Viscotek. For external calibration PIB-standards (320 g/mol to 578000 g/mol) or PS-standards (1050 g/mol to 115000 g/mol) from Viscotek were used. The concentration of all samples was 3 mg/mL and the flow rate was 1 mL/min.

Rheological measurements were performed on an oscillatory plate rheometer MCR 501/SN 80753612 from Anton Paar (Physica). For all measurements a PP08 measuring system (parallel plated, diameter 8 mm) was used. Measurements were performed at 20 °C and the sample temperature was regulated by thermoelectric heating and cooling. For evaluation of data the RheoPlus/32 software (V 3.40) and OriginPro7 was used. For sample preparation a 1 : 1 mixture of an azido-functionalized polymer and an alkyne-functionalized polymer was placed in a flask (100.0–150.0 mg) and was dissolved in THF (approximately 3.0 mL). The solvent was removed and the sample was dried in high vacuo. The frequency sweep of the pure polymer mixture which was used as basic measurement was performed with a strain γ of 10.0% and with an angular frequency ω ranging from 100 to 1 rad/s. TBTA (0.2 equiv per functional group) was added to the

polymer mixture in case of poly(acrylate)s. $\text{CuBr}(\text{PPh}_3)_3$ (0.1 equiv per functional group) was dissolved in CHCl_3 (40.0 μL) and was added as a stock solution to all investigated polymer mixtures. Subsequently, the reaction mixture was mixed with a spatula and was immediately put on the rheometer plate. Measurements were performed with a strain γ of 0.1% or 0.5% and with an angular frequency ω ranging from 100 to 1 rad/s. A frequency sweep was performed every 20 minutes. All samples were measured at 20 °C. For samples **1a–i** + **3** a measurable torque could be achieved after approximately 100 min whereas in case of samples **4a,b** + **2** a reliable torque was observed only after reaction times of approximately 200 min. The gelation time⁶² was determined as crossover of the storage (G') and loss modulus (G''). Measurements were stopped after a total time (46–160 h) when the values of the storage and the loss modulus stayed constant (second decimal place) for at least 60 min. The plateau moduli corresponded to the storage moduli measured at 100 Hz and total time and were in the range of soft technical rubbers or soft natural gums.⁶² The rate constants k were analyzed over time up to the gel point. The factor of autocatalysis was determined by comparing the rate constant k_0 and the rate constant $k_{\text{crossover}}$ corresponding to the gelation time.

Differential scanning calorimetry (DSC) measurements were performed on a differential scanning calorimeter 204F1/ASC Phoenix from Netzsch. Crucibles and lids made of aluminum were used. Measurements were performed in a temperature range from 20 to 200 °C using heating rates of 2, 5, and 10 K/min. As purge gas a dry nitrogen flow of 20 mL/min was used for all experiments. For evaluation of data the Proteus Thermal Analysis Software (version: 5.2.1) and OriginPro7 was used. For sample preparation a 1: 1 mixture of an azido-functionalized polymer and an alkyne-functionalized polymer was placed in a flask (100.0–150.0 mg) and was dissolved in THF (approximately 3.0 mL). The solvent was removed and the sample was dried in high vacuo. $\text{CuBr}(\text{PPh}_3)_3$ (0.1 equiv

per functional group) and in case of poly(acrylate)s TBTA (0.2 equiv per functional group) was added to the polymer mixture which was mixed with a spatula and immediately put in a crucible and closed with a pinhole-pricked lid.

General Procedure for the NMP of Random Copolymers Consisting of PA and *n*BA (Poly(propargyl acrylate-co-ran-*n*-butyl acrylate)) (1a–i).

The polymerization was performed according to a general procedure with modifications as described by Thelakkat et al.⁵⁷ Previously destabilized *n*BA (687 μL , 4.77 mmol), TMSPA (91 μL , 0.47 mmol) and alkoxyamine 2,2,5-trimethyl-3-phenylethoxy-4-phenyl-3-azahexane (7.5 mg, 23.1 μmol) were added to a Schlenk tube. The free nitroxide TIPNO (0.1 mol equiv based on alkoxyamine, 2.31 μmol , 21 μL) was added by means of a stock-solution with a concentration of 25 mg/mL in *o*-dichlorobenzene. Further *o*-dichlorobenzene (557 μL) was added to achieve a monomer concentration of 9 mol/L. The Schlenk tube was sealed, degassed with argon for at least 30 min, subjected to four freeze–thaw cycles and immersed into a previously on 125 °C heated oil bath. Subsequently, the polymerization was quenched after 42 h by cooling to 0 °C, the solvent and the residual monomers were removed by precipitating two times into cold MeOH. After drying in high vacuum a colorless, highly viscous polymer was obtained. The deprotection of the alkyne groups was accomplished by dissolving the polymer (767 mg, 0.52 mmol based on TMSPA units) into 40 mL dry THF and the reaction mixture was degassed with argon for 30 min. After being cooled to –20 °C, a likewise degassed solution of 1.0 M tetrabutylammonium fluoride (TBAF) solution in THF (1.57 mL, 1.57 mmol) and acetic acid (90 μL , 1.57 mmol) in 10 mL dry THF was added. The reaction mixture was stirred for 30 min at –20 °C and further 24 h at room temperature. The final product (**1e**) was obtained as viscous, slightly yellow polymer after three times of precipitation into cold

MeOH and drying in high vacuum. The obtained polymer was stored under an inert gas in the dark. ¹H-NMR (400 MHz, CDCl₃): δ (ppm) 4.66 (2H, OCH₂ of PA), 4.04 (2H, OCH₂ of *n*BA), 2.52 (1H, C≡CH of PA), 2.29–1.39 (7H, CHCH₂ of polymer backbone and CH₂CH₂ of *n*BA), 0.95 (3H, CH₃ of *n*BA). *T*_g = –45.6 °C

Polymerization of Isobutylene (IB) and End Group Modification.

All PIB syntheses were done according to Binder et al.⁶³ and Morgan et al.^{60,64} and were further modified to obtain three-arm star PIBs. Polymerizations were done under an atmosphere of argon. Total reaction volumes (80–120 mL, DCM and *n*-hexane v/v = 40/60) were placed in a 250 mL round-bottom flask equipped with mechanical stirrer, septum and stopcock. The solution was started to cool down and during the cooling DiBP (5.0 mM), DMA (5.0 mM) and 1,3,5-tris(2-methoxy-2-propyl)benzene (2.0–16.0 mM, dissolved in 1.0–3.0 mL *n*-hexane) was added. At –80 °C isobutylene (0.75–1.0 M) was added and the polymerization was started by addition of TiCl₄ (10.0–15.0 mM). After 15 min the corresponding alkoxybenzene quenchers were added. To yield trimethylsilyl protected three-arm star alkyne-telechelic PIB, trimethyl(3-phenoxy-1-propynyl)silane (4.0 equiv per chain end) was used as quencher and quenching proceeded during 18 hours at –70 °C, however, only when using an extra portion of TiCl₄ (3 equiv of initial portion) to accelerate the quenching reaction. In order to obtain three-arm star bromine-telechelic PIB 3-(bromopropoxy)benzene (2.5 equiv per chain end) was used as quencher and quenching proceeded for 150 min at –60 °C. After quenching an excess of MeOH was added and the solvent was removed. The crude polymer was dissolved in *n*-hexane and precipitated in a 10 to 15 time excess of MeOH for three times. Obtained trimethylsilyl protected three-arm star alkyne-telechelic PIB was converted into compound 2 and obtained three-arm star bromine-telechelic PIBs were transformed in compounds 3 and 4a–d.

Synthesis of Three-arm star Alkyne-Telechelic PIB (2).

Under an atmosphere of nitrogen trimethylsilyl protected three-arm star alkyne-telechelic PIB (1 equiv, 1.1 mmol, 4.6 g) was dissolved in THF (24 mL) and TBAF (1.0 M solution in THF, 13.6 equiv, 15.0 mmol, 15 mL). The reaction mixture was stirred at room temperature overnight. The polymer solution was extracted with water (50 mL) and the desired polymer precipitated. It was subsequently dissolved in DCM (35 mL) and extracted with water (two times 50 mL). The organic layer was separated and dried over Na₂SO₄ and the solvent was removed. The crude polymer was dissolved in *n*-hexane, precipitated into a 10 to 15 time excess of MeOH and dried in high vacuo. ¹H-NMR (CDCl₃, 400 MHz): δ 7.13 (s, 3H, Ar–H of initiator), 6.89 (d, 6H, Ar–H of quenching agent), 4.66 (d, 6H, O–CH₂), 2.50 (t, 3H, C–CH), 1.41 (s, CH₂ of repetitive unit), 1.11 (s, CH₃ of repetitive unit), 0.79 (s, 18H, CH₃ of initiator part). ¹³C-NMR (CDCl₃, 100 MHz): δ 155.4, 148.4, 143.7, 127.2, 117.6, 114.2, 79.0, 77.9, 77.4, 76.6, 75.4, 61.9, 59.7, 59.2, 58.7, 57.5, 56.0, 51.0, 48.3, 39.1, 38.5, 38.4, 38.3, 38.2, 38.2, 38.1, 38.1, 38.0, 32.6, 32.3, 31.7, 31.4, 31.3, 31.2, 30.8, 29.2, 27.1.

Synthesis of Three-arm star Azide-telechelic PIBs (3, 4a–d).

Under an atmosphere of nitrogen three-arm star bromine-telechelic PIB (1.0 equiv, 775.0 mg, 126.0 μmol) was dissolved in a 1:1 mixture of *n*-heptane (30 mL) and DMF (30 mL). Sodium azide (30.0 equiv, 246.0 mg, 3.8 mmol) was added to the reaction mixture subsequently heating to 90 °C for 8 h. After the reaction mixture was cooled down, the *n*-heptane layer was separated and extracted with water (three times, 50 mL). The organic layer was dried over Na₂SO₄ and the solvent was removed, obtaining the crude polymer which was dissolved in *n*-hexane and was then precipitated into a 10 to 15 time excess of MeOH for three times and dried in high vacuo. ¹H-NMR (CDCl₃, 500 MHz): δ 6.81 (d, 6H, Ar–H of quenching agent), 4.03 (t, 6H,

O-CH₂), 3.49 (t, 6H, CH₂-N₃), 2.04 (q, 6H, CH₂-CH₂-CH₂), 1.80 (m, 6H, CH₂ next to repetitive unit), 1.41 (s, CH₂ of repetitive unit), 1.11 (s, CH₃ of repetitive unit), 0.80 (s, 18H, CH₃ of initiator part). ¹³C-NMR (CDCl₃, 125 MHz): δ 156.2, 148.4, 142.8, 127.1, 127.0, 126.9, 113.6, 113.6, 64.4, 59.6, 59.5, 59.4, 58.4, 48.3, 38.2, 38.1, 38.0, 37.9, 37.8, 32.1, 31.3, 31.2, 31.1, 30.9, 30.6, 28.9. IR (cm⁻¹): 2950, 2893, 2098, 1470, 1389, 1366, 1231, 950, 924, 827, 668, 630

RESULTS AND DISCUSSION

The investigation of catalysis during crosslinking *via* the CuAAC is based on liquid telechelic and orthogonal functionalized polymers, all of them displaying the reactive groups (azide/alkyne) as well as a glass transition temperature (T_g) below room temperature in order to ensure molecular mobility. The polymers are based on poly(acrylate)s as well as PIBs using living polymerization techniques, namely NMP and LCCP for their preparation. In order to understand the influence of functional-group density and molecular weight in relation to catalysis, nine atactic random poly(propargyl acrylate-*co*-*n*-butyl acrylate)s were prepared *via* NMP, gradually changing the composition of the alkyne bearing copolymers with respect to the alkyne content from 2.7 to 14.3 mol % PA per chain.

The newly generated 1,3-triazole functionalities during the CuAAC are expected to provide more labile N-donor atoms which in turn can bind to the catalytic copper(I) center strongly while allowing to open coordination sites temporarily for the formation of the copper(I)-acetylide/ligand complex. A related effect is known experimentally by acceleration of a “click”-process,⁶⁵ enabling preferential formation of a bistriazole product *via* catalysis of the monotriazole product based on spatial proximity of the just formed triazole ring to the reactive center. On the basis of these two

aspects a preorientation of functional groups (azide/alkyne) and therefore an autocatalytic effect within the “click” reaction seems to be possible due to the *in situ* formation of triazole rings acting as internal ligands and therefore as N-donors as well.

Preparation of Multivalent Functionalized Poly-(acrylate)s and PIBs.

The synthesis of poly(propargyl acrylate-*co*-*n*-butyl acrylate) *via* NMP and of three-arm star alkyne- and three-arm star azide-telechelic PIBs *via* LCCP is illustrated in Scheme 2.

Synthesis of Random Copolymers Consisting of PA and *n*BA *via* NMP.

NMP of random poly(propargyl acrylate-*co*-*n*-butyl acrylate)s (**1a-i**) was performed according to a modified procedure described in literature⁵⁷ adapted to the synthesis of copolymers using an alkoxyamine-initiator in *o*-dichlorobenzene. Important for the achievement of low polydispersities was the dilution with *o*-dichlorobenzene in order to prevent restricted diffusion and to minimize the impact of the increasing viscosity. Deprotection of trimethylsilyl protected poly(propargyl acrylate-*co*-*n*-butyl acrylate) was done according to literature⁵⁷ using a mixture of TBAF and acetic acid, in order to suppress the decomposition of the propargyl ester under alkaline conditions. The pure product (**1e**) showed a T_g of -45.6 °C proving the applicability of random copolymers consisting of PA and *n*BA for self-healing materials. In Table 1 the theoretical molecular weights calculated for 100% conversion as well as the molecular weights determined *via* GPC and NMR are listed, together with the average number of functional groups/chain, the PDIs and the yields of the synthesized multivalent poly(acrylate)s and PIBs.

Scheme 2 Synthesis of poly(propargyl acrylate-*co*-*n*-butyl acrylate)s (**1a–i**) via NMP and of three-arm star alkyne- (**2**) and three-arm star azide-telechelic (**3**, **4a–d**) PIBs via LCCP.

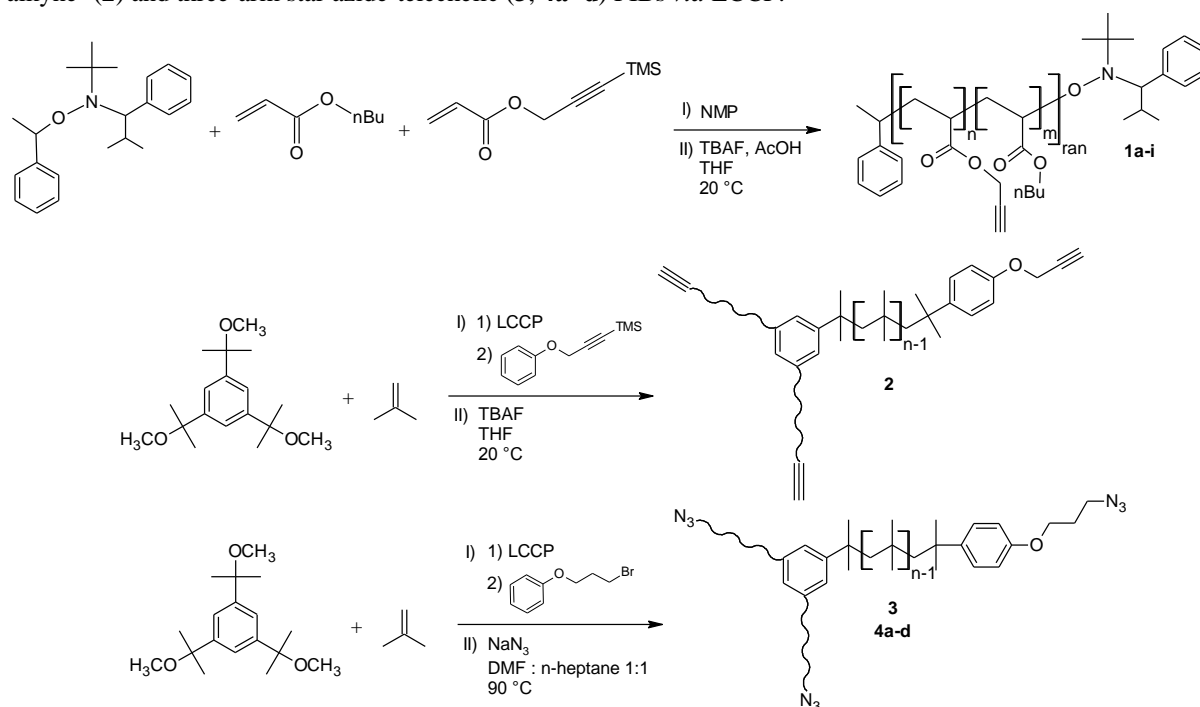


Table 1 Characterization of the poly(propargyl acrylate-*co*-*n*-butyl acrylate)s (**1a–i**) prepared via NMP and of the three-arm star alkyne- (**2**) and three-arm star azide-telechelic (**3**, **4a–d**) PIBs via LCCP.

Entry	Polymer	Polymer composition PA- <i>n</i> BA ^a	$M_{n,theor}$ [g/mol]	$M_{n,GPC}^b$ [g/mol]	$M_{n,NMR}^c$ [g/mol]	number of functional groups / chain ^d	PDI ^e	Yield ^f [%]
1	1a	1:6	30 000	7 000	-	7.6	1.8	30
2	1b	1:6	30 000	18 000	-	20.1	1.8	53
3	1c	1:12	50 000	9 600	-	5.6	1.4	45
4	1d	1:12	30 000	12 500	-	7.4	1.6	48
5	1e	1:12	30 000	19 100	-	11.4	1.8	70
6	1f	1:24	30 000	15 200	-	4.7	1.5	85
7	1g	1:24	50 000	22 200	-	6.9	2.3	69
8	1h	1:36	75 000	14 200	-	2.9	3.5	57
9	1i	1:36	30 000	23 400	-	4.9	1.6	91
10	2		6 000	6 300	5 700	3	1.3	90
11	3		5 000	6 200	6 300	3	1.2	87
12	4a		6 000	6 500	5 500	3	1.4	86
13	4b		12 000	10 400	11 600	3	1.5	85
14	4c		18 000	16 700	23 600	3	1.3	87
15	4d		30 000	20 200	30 000	3	1.4	88

^a determined via ¹H-NMR: integration of O-CH₂-resonance of PA at 4.62 ppm and O-CH₂-resonance of *n*BA at 4.02 ppm. ^b PS standards were used for polymers **1a–i**; PIB standards were used for polymers **2**, **3**, **4a–d**. ^c determination for polymers **1a–i** not possible due to overlapping resonances; for polymers **2**, **3**, **4a–d** determined via ¹H-NMR: integration of resonances of initiator at 0.78 ppm to 0.82 ppm and of polymer at 1.08 ppm to 1.10 ppm or at 1.37 ppm to 1.40 ppm. ^d for **1a–i** calculated from $M_{n, GPC}$ subtracted by the molecular weight of head and end group, divided by the average molecular weight of the monomers and divided by the ratio of PA to *n*BA detected via NMR. ^e determined via GPC. ^f yield of isolated product.

The molecular weights of the prepared polymers were in a range between 7000–23400 g/mol. Although increasing PDIs with increasing conversion are a well-known issue for NMP reactions,⁶⁶ acceptable low PDIs also at higher conversions could be achieved up to a theoretical molecular weight of 30000 g/mol

by using the described procedure. In case of polymers **1g** and **1h** higher PDIs were observed because of higher theoretical molecular weights and therefore longer reaction times. In general, the copolymerization was limited by the amount of TMSPA (1: 6 molar ratio of TMSPA to *n*BA)

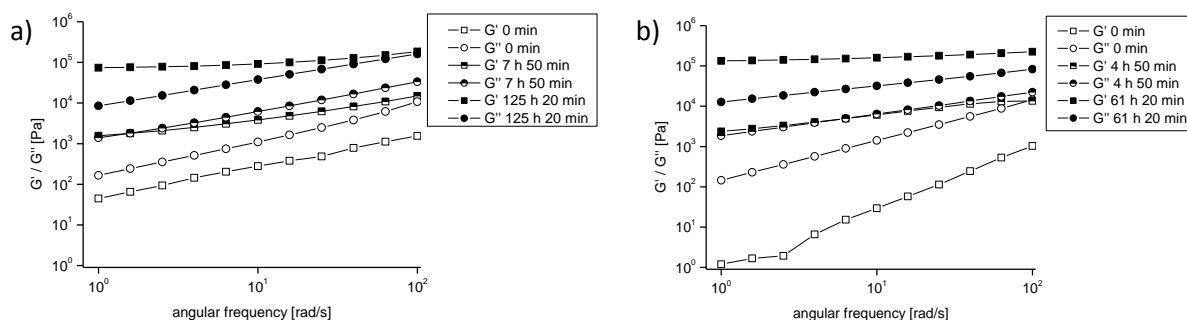


Fig. 1 *In situ* rheology for crosslinking a) **1e** (1:12, 19100 g/mol) and **3** applying bromotris(triphenylphosphine)copper(I) and TBTA as catalytic system at 20 °C and b) **2** and **4a** (5500 g/mol) applying bromotris(triphenylphosphine)copper(I) as catalyst at 20 °C.

in the copolymer because of increasing reaction times. The average number of functional groups/chain (2.9–20.1) was calculated from the molecular weight determined *via* GPC and the ratio of PA to *n*BA investigated *via* NMR spectroscopy providing a large range for studying the influence of the alkyne density (and thus of the subsequently formed triazole rings) on the kinetic behavior of the crosslinking reaction.

Synthesis of Three-arm star Functionalized PIBs *via* LCCP and End Group Functionalization.

For the synthesis of three-arm star functionalized PIBs^{60,63,64} LCCP was used, applying 1,3,5-tris(2-methoxy-2-propyl)benzene as initiator in all cases. In order to obtain polymer **2**, trimethyl(3-phenoxy-1-propynyl)silane was added as quenching agent leading to trimethylsilyl protected three-arm star alkyne-telechelic PIB. Although already described in literature⁶⁰ this approach was applied to the synthesis of three-arm star PIBs for the first time, requiring a quenching reaction at –70 °C for 18 h. In order to shift the equilibrium of the quenching reaction to the side of the final product, an additional portion of TiCl₄ had to be added during the quenching reaction. For deprotection of the trimethylsilyl group an excess of TBAF was used as deprotecting agent.⁶⁰ In a similar mode, 3-(bromopropoxy)-benzene was applied as quencher in order to synthesize three-arm star bromide-telechelic PIBs as developed by Storey et al.⁶⁴ for

bivalent telechelic PIB. During the quenching reaction the temperature was adjusted to –60 °C as the quencher was hardly soluble at the needed high concentrations for the three-arm star quenching reaction. Subsequently, the polymers **3** and **4a–d** were obtained by treating bromide functionalized PIBs with an excess of sodium azide in a 1:1 mixture of DMF and *n*-heptane and heating up to 90 °C.⁶⁴ In contrast to literature⁶⁴ the reaction time had to be increased from 2 to 8 h to achieve quantitative end group functionalization. Results of the synthesis of **2**, **3**, and **4a–d** are shown in Table 1 proving living polymerization conditions with a good match between desired and observed molecular weights.

Crosslinking Experiments *via in Situ* Rheology.

In situ rheology was performed to investigate the network formation as illustrated in Scheme 1 depending on the alkyne content, the molecular weight and the absolute concentration of functional groups. Of peculiar interest was the determination of the gelation time⁶² to draw conclusions about the rate of the catalytic process even at room temperature.

Copolymers **1a–i** (bearing 20.1–2.9 alkyne moieties/chain) were mixed with the three-arm star azide-telechelic PIB polymer **3**; alternatively the PIB-alkyne polymer **2** was reacted with the polymers **4a–d** using bromotris(triphenylphosphine)-copper(I) (stock solution) as catalyst. Figure 1a and 1b show the graphs obtained *via in situ* rheology,

as illustrated as example for crosslinking **1e** with **3** and **2** with **4a**.

With progressing network formation due to the “click” reaction, the crossover of the storage and the loss modulus could be observed after 7 h and 50 min in case of crosslinking **1e** and **3** or after 4 h and 50 min in case of crosslinking **2** and **4a** corresponding to the gelation times (gelation point).⁶² After 125 h and 20 min (**1e** and **3**) or after 61 h and 20 min (for **2** and **4a**) the moduli changed only slightly due to the stagnant network formation. The results of all rheology investigations are shown in Table 2, together with the viscosity of the polymer mixture at the beginning of the experiment (η_0), the gelation time and the kinetic data of the crosslinking reactions.

According to Fokin et al.⁶⁵ the rate law for kinetic controlled “click” reactions can be assumed as first order for the azide, as first to second order for the alkyne and at least as second order (x) for the copper resulting in an overall reaction rate $r_{\text{“click”}}$ of $r_{\text{“click”}} = k[\text{alkyne}]^{2,3}[\text{Cu(I)}]^x$ (assuming $[\text{azide}] = [\text{alkyne}]$). Thus, for higher concentrations of functional groups (azide/alkyne) higher reaction rates as well as a faster crossover and therefore a faster network formation should be expected.

To prove this assumption the crosslinking of polymers with decreasing

concentration of functional groups but with comparable molecular weight was studied (Table 2, entries 2, 5, 6 and 8, composition PA-*n*BA: 1:6, 1:12, 1:24, 1:36) comparing the kinetic behavior of **1b** (entry 2, 20.1 alkynes/chain), **1e** (entry 5, 11.4 alkynes/chain), **1f** (entry 6, 4.7 alkynes/chain) and **1h** (entry 8, 2.9 alkynes/chain) crosslinked with the three-arm star polymer **3**. The gelation time of **1b** with **3** corresponding to the highest concentration took the longest time (entry 2, 601 min), whereas the gelation time of **1f** with **3** was significantly shorter (entry 6, 328 min). An explanation for this behavior can be given by the strongly increased starting viscosity η_0 of the polymer mixtures with rising PA content (entry 6, **1f** + **3**: 59.1 Pa·s; entry 2, **1b** + **3**: 336.0 Pa·s), indicating that the gelation time in these cases is primarily dominated by the initial viscosity of the polymer mixture. A similar behavior could be observed by comparing the crosslinking of polymer mixtures **1c** (entry 3, 5.6 alkynes/chain), **1d** (entry 4, 7.4 alkynes/chain) and **1e** (entry 5, 11.4 alkynes/chain) with **3**, which displayed an equal concentration of functional groups (0.245 M, composition PA-*n*BA: 1: 12) but increasing viscosities due to their increasing molecular weights (entry 3, **1c** + **3**: 60.0 Pa·s; entry 4, **1d** + **3**: 73.8 Pa·s; entry 5, **1e** + **3**: 123.0 Pa·s).

Table 2 Results obtained *via in situ* rheology and kinetic data for crosslinking **1a–i** with **3** applying bromotris(triphenylphosphine)copper(I) and TBTA as catalytic system at 20 °C and by crosslinking **2** and **4a–d** applying bromotris(triphenylphosphine)copper(I) as catalyst at 20 °C.

Entry	Polymer mixture	c [M] ^a	η_0^b [Pa·s]	gel. time ^c [min]	c_{Cu} [M] (10^{-2})	k_0 [M ⁻³ ·min ⁻¹]	$k_{\text{crossover}}$ [M ⁻³ ·min ⁻¹]	r_0 [M·min ⁻¹] (10^{-3})
1	1a + 3	0.302	89.0	142	3.0	29.9	47.8	2.4
2	1b + 3	0.302	336.0	601	3.4	10.8	37.3	1.1
3	1c + 3	0.245	60.0	213	2.4	42.2	76.0	1.5
4	1d + 3	0.245	73.8	400	2.4	26.6	73.7	0.92
5	1e + 3	0.245	123.0	468	2.4	22.7	49.9	0.81
6	1f + 3	0.179	59.1	328	1.8	98.5	229.6	1.1
7	1g + 3	0.179	147.0	724	1.8	19.5	29.4	0.21
8	1h + 3	0.139	56.0	585	1.4	89.1	158.0	0.32
9	1i + 3	0.139	74.3	1940	1.5	33.0	91.1	0.14
10	2 + 4a	0.238	44.0	290	2.4	706.9	2676.8	23
11	2 + 4b	0.155	33.4	375	1.6	522.8	1889.2	3.2
12	2 + 4c	0.093	32.9	467	0.95	377.4	820.4	0.29
13	2 + 4d	0.076	30.8	855	0.81	323.0	686.5	0.13

^a Absolute concentration of functional groups (azide/alkyne) in the reaction mixture. ^b Absolute initial viscosity at 100 Hz. ^c Crossover, $G' = G''$.

In contrast for the crosslinking of the three-arm star alkyne-telechelic PIB **2** with the three-arm star azide-telechelic PIBs **4a–d** (Table 2, entries 10–13) the gelation time increased from 290 to 855 min with increasing molecular weights from 5500 g/mol to 30000 g/mol and with decreasing concentration of the reactive functional groups from 0.238 to 0.076 M. As this observation is in accordance to Fokin et al.⁶⁵ we assume a kinetically controlled “click” reaction when crosslinking **2** with **4a–d**. The increased gelation time for crosslinking **2** and **4d** (entry 13, 855 min) could be explained by the high molecular weight and the molecular weight distribution of **4d** (30000 g/mol), reaching the range of the entanglement molecular weight which is 17000 g/mol for linear PIB⁶⁷ assuming partial entanglement of **4d**.

In order to exclude viscosity effects in case of poly(acrylate)s the gelation times of crosslinking the polymers **1a**, **1c**, **1f**, and **1h** with polymer **3** (Table 2, entries 1, 3, 6 and 8) were compared. This series of poly(acrylate)s **1a** (entry 1, 7.6 alkynes/chain), **1c** (entry 3, 5.6 alkynes/chain), **1f** (entry 6, 4.7 alkynes/chain), and **1h** (entry 8, 2.9 alkynes/chain) showed decreasing concentrations of functional groups (composition PA-*n*BA: 1:6, 1:12, 1:24, 1:36) but comparable starting viscosities η_0 (56.0–89.0 Pa·s). Clearly the gelation times increased with decreasing concentrations of the reactive functional groups (entry 1, **1a** + **3**, 142 min; entry 8, **1h** + **3**, 585 min) and the expected behavior based on the mentioned kinetic law could thus be proven.

Autocatalysis during the Crosslinking Reactions.

When analyzing the development of the rate constants k as well as the dk values (derivative of the rate constant k with respect to time) as a function of time an autocatalytic effect of the herein described “click” reactions of multivalent poly-(acrylate)s and PIBs was observed. On the basis of the assumption of a pseudo-first reaction order near the gel point⁶² corresponding to Ampudia⁶⁸ and Barton⁶⁹ the rate constants k could be determined according

to eqn 1 (for mathematical derivation see Supporting Information).

$$k = \frac{e^{(k' \cdot t)} - 1}{t \cdot [A]_0} \quad (1)$$

By using eqn 1, the rate constant k_0 correlating to the first measurable value for the real part of the viscosity and the corresponding reaction rate r_0 as well as the rate constant $k_{crossover}$ at the gel-point were calculated. The values of k_0 , $k_{crossover}$, and r_0 are listed in Table 2 for all performed crosslinking reactions.

For the crosslinking reactions of the series **1c–e** with **3** characterized by increasing molecular weights of **1c–e** (Table 1, entries 3–5) the curves of the rate constants k were analyzed over time. The corresponding results for the crosslinking reaction of **1c–e** with **3** are shown in Figure 2.

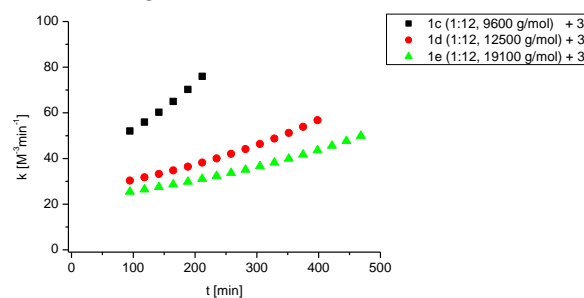


Fig. 2 Correlation of the rate constants k vs. time t for crosslinking **1c–e** with **3** applying bromotris(triphenylphosphine)copper(I) and TBTA as catalytic system at 20 °C.

As all rate constants k as well as the dk values (see Supporting Information, Figure S2) increased exponentially with increasing time a strong autocatalytic effect (of a factor up to 2.5) during the crosslinking reaction of **1c–e** with **3** can be assumed. Furthermore, the absolute values of the rate constants k decreased from **1c** and **3** to **1d** and **3** to for **1e** and **3**, thus following the trends of the observed gelation times corresponding to the starting viscosities of the polymer mixtures.

The autocatalytic behavior of poly(acrylate)s **1a–i** crosslinked with **3** was analyzed according to Figure 3 by incorporating the concentration of copper(I) catalyst.

Autocatalysis could be observed for crosslinking polymers **1a**, **1c**, **1f** and **1h** with

polymer **3**. As these polymer mixtures showed increasing gelation times with decreasing concentrations of functional groups (Table 2, entry 1, **1a** + **3**: 142 min; entry 8, **1h** + **3**: 585 min) the dk values proved this trend increasing stronger for **1a** and **3** than for **1c** and **3** than for **1f** with **3** than for **1h** with **3**.

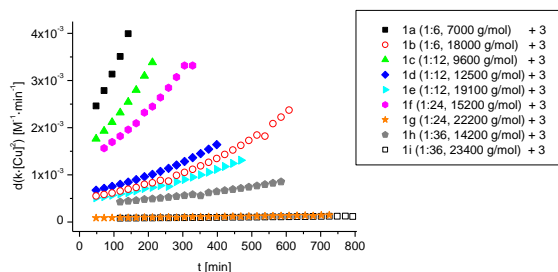


Fig. 3 Correlation of the derivative of the rate constants dk with respect to time t vs. time t for crosslinking **1a–i** with **3** applying bromotris(triphenylphosphine)copper(I) and TBTA as catalytic system at 20 °C incorporating the concentration of copper(I) catalyst.

When crosslinking the polymer mixtures with the same composition of PA to n BA but with a higher molecular weight a less pronounced autocatalytic effect could be observed due to the different starting viscosities of the polymer mixtures. (Table 2, entry 6, **1f** + **3**: 59.1 Pa·s; entry 7, **1g** + **3**: 147.0 Pa·s). Thus, for the polymer mixtures **1d** and **1e** with **3** displaying a lower concentration of functional groups (composition PA- n BA: 1:12) the increase of the dk values was comparable or even stronger than for crosslinking **1b** with **3** (composition PA- n BA: 1:6) due to the higher starting viscosity of this polymer mixture (Table 2, entry 2, **1b** + **3**: 336.0 Pa·s; entry 4, **1d** + **3**: 73.8 Pa·s; entry 5, **1e** + **3**: 123.0 Pa·s).

The same analysis of the rate constants k over time was done for crosslinking **2** with

4a–d as illustrated in Figure 4, determining the rate constant k independently from the used copper(I) concentrations.

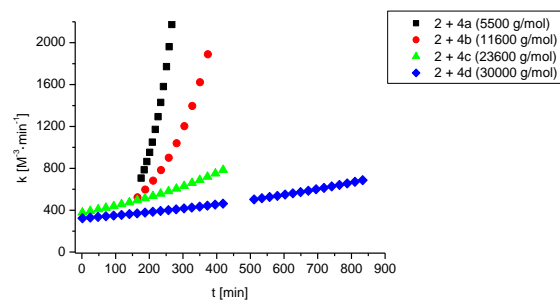


Fig. 4 Correlation of the rate constants k vs. time t for crosslinking **2** with **4a–d** applying bromotris(triphenylphosphine)copper(I) as catalyst at 20 °C.

For these polymer mixtures, the values of the rate constants k and the dk values (see Supporting Information, Figure S3) reflected the already discussed trends shown by *in situ* rheology experiments (see Table 2). The strongest increase of the rate constants k as well as the highest absolute values of the k values could be observed for crosslinking **2** with **4a** showing the shortest gelation time due to the highest concentration of functional groups (entry 10: 290 min, 0.238 M) and therefore the most prominent autocatalytic behavior of a factor of 3.8. Consequently the rate constants k increased stronger for the crosslinking reaction of **2** with **4b** (entry 11: 375 min, 0.155 M) in comparison to the reaction of **2** with **4c** (entry 12: 467 min, 0.093 M) and of **2** with **4d** (entry 13: 855 min, 0.076 M). The same trends were observed for the dk values. The absolute values of the rate constants k as well as the dk values for the “click” reactions of **2** with **4a–d** were one magnitude higher compared to crosslinking **1a–i** with **3**.

Scheme 3 Proposed mechanism of autocatalysis for crosslinking multivalent poly(acrylate)s and PIBs functionalized with alkyne or azide groups, respectively, applying bromotris(triphenylphosphine)copper(I) and a ligand as catalytic system at 20 °C.

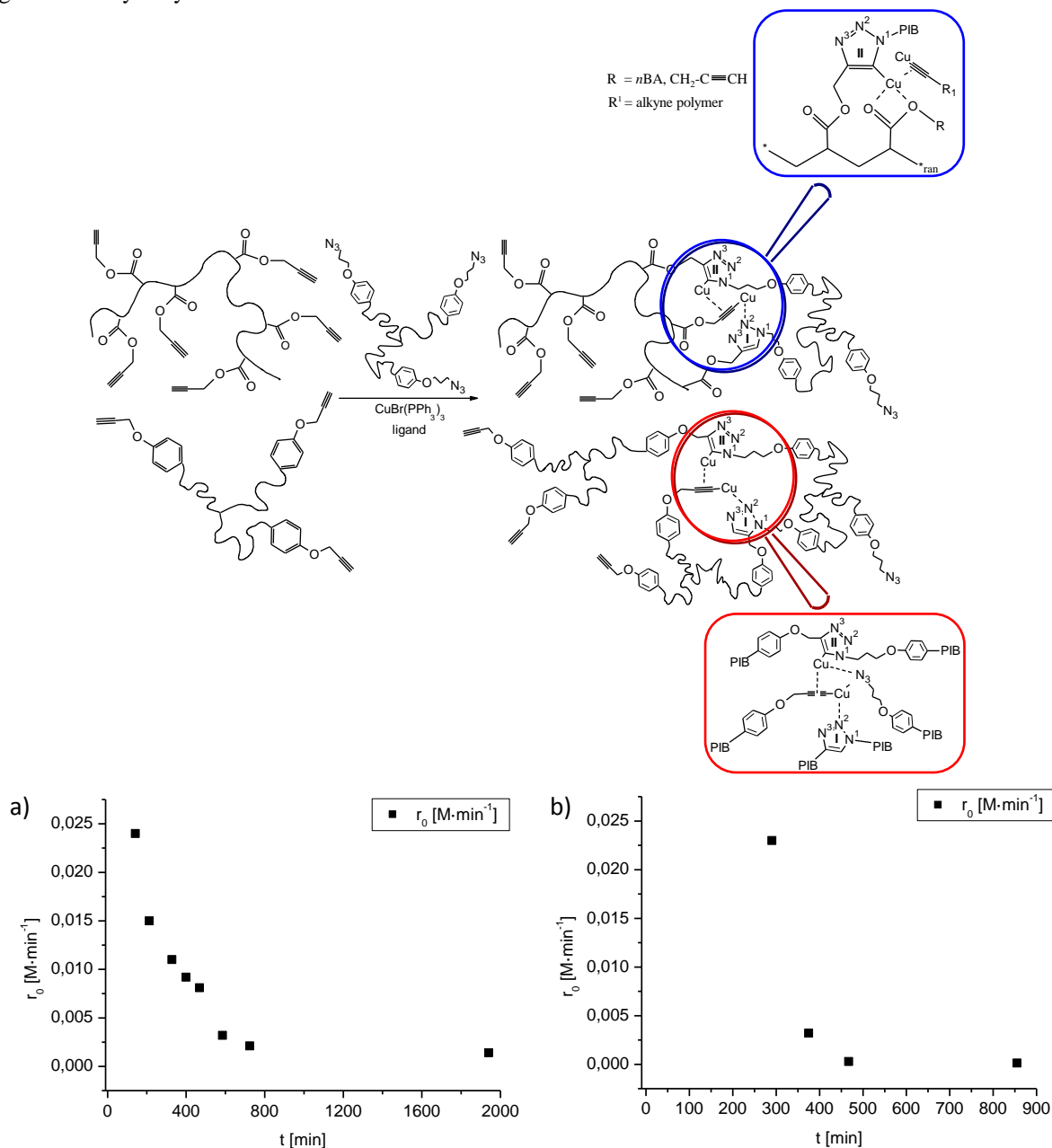


Fig. 5 Correlation of gelation time and reaction rate r_0 for crosslinking a) **1a–i** with **3** applying bromotris(triphenylphosphine)copper(I) and TBTA as catalytic system at 20 °C and b) **2** and **4a–d** applying bromotris(triphenylphosphine)copper(I) as catalyst at 20 °C.

On the basis of our results we proposed a mechanism to explain the observed autocatalytic behavior for crosslinking multivalent poly(acrylate)s and PIBs as shown in Scheme 3. According to Scheme 3 triazole rings with different functions could be identified. One triazole functionality (**I**) is assumed to act as **internal ligand** using either the N²-atom or the N³-atom of the triazole ring

as donor atom while forming the copper(I)–acetylide/ligand complex.⁷⁰ Additionally, it can be assumed that a second triazole functionality (**II**) can preorientate the functional groups (azide/alkyne) near the copper(I) center resulting in spatial proximity of all reaction components (shown in the blue and red framed image details). Thus, the formation of the next triazole ring is promoted

while retarding the cleavage of the Cu–C bond of the Cu triazolyl-intermediate in the proteolysis step as described by Fokin et al.⁶⁵

The calculated values of the rate constants k_0 and therefore also of the reaction rates r_0 were comparable to rate constants of DA reactions being in the range of $1.25 \times 10^{-5} \text{ M}^{-1}\cdot\text{s}^{-1}$ to $4.83 \times 10^{-5} \text{ M}^{-1}\cdot\text{s}^{-1}$ by assuming second-order kinetics.^{33,71,72} Correlations of the gelation times and the reaction rates r_0 are illustrated in Figure 5a for crosslinking **1a–i** with **3** and in Figure 5b for crosslinking **2** with **4a–d**.

The reaction rate r_0 decreased with increasing gelation time resulting in an exponential decay for crosslinking **1a–i** with **3** as well as for crosslinking **2** with **4a–d** as illustrated in Figure 5, parts a and b. According to the shown correlations the order of magnitudes of the reaction rate r_0 could be derived directly in case of performing further crosslinking experiments between the discussed multivalent polymers.

Calculation of Network Strand Densities.

Plateau moduli^{62,73} and network strand densities^{73,74} as a function of the absolute concentration of functional groups were explored to prove the suitability of the represented “click” reaction for self-healing purpose. The network strand density is an average value for the crosslinking points per volume segment providing information about

the completeness of the “click” reaction. The relationship between the observed plateau modulus G_N , the network strand density ν_x , the density of the polymer mixture ρ and the average molecular weight between two network points M_c and the molecular weight M_n is given according to eqn 2^{73,74}

$$G_N = \nu_x RT = \frac{\rho RT}{M_c} \left(1 - \frac{2M_c}{M_n}\right) \quad (2)$$

where R is the universal gas constant, $R = 8.3145 \text{ J}\cdot\text{mol}^{-1}\cdot\text{K}^{-1}$ and T the temperature, $T = 293.15 \text{ K}$. According to eqn 2 the maximum network strand densities $\nu_{x, \text{max}}$ could be calculated assuming complete crosslinking. Furthermore, the experimental network strand densities $\nu_{x, \text{exp}}$ were determined using the plateau moduli and the ratios between the two network strand densities were calculated to obtain an impression about the formed network points during the performed “click” reaction (see Table 3).

In the case of crosslinking polymer mixtures **1a–i** with **3**, the best values for the experimental network strand density were in the range of 100 mol/m^3 . CuAAC of polymer **3** with poly(acrylate)s with the same concentration of functional groups but with higher molecular weights resulted in higher network strand densities. Thus, the “click” reaction between **1a + 3** (entry 1, **1a**, 7000 g/mol, composition PA-*n*BA: 1:6) resulted in a network strand density of 69 mol/m^3 compared to 105 mol/m^3 for crosslinking **1b + 3** (entry 2,

Table 3 Obtained results based on eqn 2 for crosslinking **1a–i** with **3** applying bromotris(triphenylphosphine)copper(I) and TBTA as catalytic system at 20 °C and for crosslinking **2** and **4a–d** applying bromotris(triphenylphosphine)copper(I) as catalyst at 20 °C.

Entry	Polymer mixture	c [M] ^a	G_N^b [Pa] 10 ⁵	$\nu_{x, \text{max}}$ [mol/m ³]	$\nu_{x, \text{exp}}$ [mol/m ³]	$\frac{\nu_{x, \text{exp}}}{\nu_{x, \text{max}}}$ [%]
1	1a + 3	0.302	1.69	807	69	8.6
2	1b + 3	0.302	2.55	972	105	10.8
3	1c + 3	0.245	^c	385	^c	^c
4	1d + 3	0.245	2.11	431	87	20.2
5	1e + 3	0.245	2.68	485	110	22.7
6	1f + 3	0.179	2.42	179	99	55.3
7	1g + 3	0.179	1.40	220	57	25.9
8	1h + 3	0.139	0.89	71	37	52.1
9	1i + 3	0.139	0.38	125	16	12.8
10	2 + 4a	0.238	2.25	244	91	37.3
11	2 + 4b	0.155	0.13	158	6	3.8
12	2 + 4c	0.093	0.19	93	8	8.6
13	2 + 4d	0.076	0.078	77	3	3.9

^a Absolute concentration of functional groups (azide/alkyne) in the reaction mixture. ^b Constant value at 100 Hz. ^c Measurement finished after 1900 min.

1b: 18000 g/mol, composition PA-*n*BA: 1:6). The ratio between the experimental and the maximal network strand density varied between 8.6 and 55.3%, increasing with decreasing concentration of functional groups presumably due to steric hindrance. For crosslinking polymer **3** and poly(acrylate)s with a composition of PA to *n*BA of 1:6 or 1:12 higher ratios were observed for higher molecular weights (entry 1, **1a**, 7000 g/mol, 8.6%; entry 2, **1b**, 18000 g/mol, 10.8%). In contrast, a higher ratio between experimental and maximal network strand density could be achieved for the “click” reaction between polymer **3** and poly(acrylate)s with lower molecular weights and with a composition of PA to *n*BA of 1:24 or 1:36 (entry 6, **1f**, 15200 g/mol, 55.3%; entry 7, **1g**, 22200 g/mol, 25.9%).

For crosslinking polymer **2** with polymers **4a–d** the values of the maximal network strand density decreased with decreasing concentrations (entries 10–13, from 244 to 77 mol/m³), as less network points could be formed. The experimental determined network strand density showed this tendency as well (entries 10–13, 91–3 mol/m³). Therefore, the relation of the maximal and experimental network strand density varied between 37 and 4% implying that the experimentally determined network strand density decreased relatively and absolutely, the values, however, remaining within the limits observed for hydrogels.⁷⁵

Calculation of Activation Energies.

DSC experiments were performed for selected crosslinking reactions in order to determine their activation energies according to Kessler et al.⁷⁶ DSC measurements were run in a temperature range from 20 to 200 °C using heating rates of 2, 5, and 10 K/min. With increasing heating rate β a shift of the peak temperature T_p to higher temperatures could be observed. The activation energy E_a as well as the pre-exponential factor A could be calculated by applying Kissinger’s equation⁷⁶ which is shown in eqn 3

$$\ln\left(\frac{\beta}{T_p^2}\right) = \ln\left(\frac{AR}{E_a}\right) - \frac{E_a}{RT_p} \quad (3)$$

where R is the universal gas constant, $R = 8.3145 \text{ J}\cdot\text{mol}^{-1}\cdot\text{K}^{-1}$, β the given heating rate, and T_p the measured peak temperature. The so obtained results are illustrated in Table 4 for crosslinking **1a**, **1f**, and **1h** with **3** and for crosslinking **2** with **4a** and **4d**.

Table 4 Results obtained *via* DSC experiments for crosslinking **1a**, **1f** and **1h** with **3** applying bromotris(triphenylphosphine)copper(I) and TBTA as catalytic system and for crosslinking **2** and **4a** and **4d** applying bromotris(triphenylphosphine)copper(I) as catalyst.

Entry	Polymer mixture	E_a [kJ/mol]	$\ln A$
1	1a + 3	60.3	17.1
2	1f + 3	38.5	10.5
3	1h + 3	23.1	4.4
4	2 + 4a	41.7	13.2
5	2 + 4d	44.5	16.1

All determined activation energies were in the range of CuAAC reported by Kessler et al.⁷⁶ and Binauld et al.⁷⁷ as well as being located in between the activation energy of 32 and 96 kJ/mol described by Liu et al.³³ and Chen et al.²⁴ for DA-reactions of furan and maleimide compounds. This indicates clearly that the rate-determining step of the CuAAC remains unchanged by the observed autocatalysis.

The crosslinking reaction of the polymer mixtures **1a**, **1f** and **1h** with **3** followed the rate law of Fokin et al.⁶⁵ due to comparable starting viscosities (56.0–89.0 Pa·s). Therefore, with decreasing concentration of functional groups increased gelation times could be observed (see Table 2, entries 1, 6, and 8). Nevertheless, the activation energy displayed the highest value for the crosslinking reaction of **1a** with **3**, followed by the crosslinking of **1f** and **1h** with **3**. This aspect might be explained by an increased steric hindrance due to a higher concentration of functional groups within sample **1a** (0.302 M).

CONCLUSIONS

We have investigated autocatalytic effects in crosslinking processes based on the CuAAC, aiming at the design of generating polymeric networks for future self-healing materials without the need of an external stimulus like increased temperature. Specifically, we planned to take advantage of the 1,3-triazole rings formed during the CuAAC-based crosslinking, thus enabling to act as internal ligands in turn accelerating the reaction rate of subsequent “click”-reactions. To this effect, we have synthesized multivalent polymeric alkynes and azides (nine atactic random poly(propargyl acrylate-*co*-*n*-butyl acrylate)s, $M_n = 7000\text{--}23400$ g/mol) *via* NMP displaying alkyne-contents ranging from 2.7 mol % to 14.3 mol % per chain. Furthermore, five three-arm star azide-telechelic PIBs ($M_n = 5500\text{--}30000$ g/mol) and one three-arm star alkyne-telechelic PIB ($M_n = 6300$ g/mol) were prepared *via* LCCP with perfect end group-functionalization, thus studying the influence of functional group density, viscosity and molecular weight on the crosslinking process. Crosslinking reactions were studied *via in situ* melt-rheology and DSC, revealing increasing reaction rates with increasing concentration of functional groups (**1c** + **3**, composition PA-*n*BA, 1:12, $r_0 = 1.5 \times 10^{-3}$ M·min⁻¹; **1a** + **3**, composition PA-*n*BA, 1:6, $r_0 = 2.4 \times 10^{-3}$ M·min⁻¹). A kinetic analysis showed significant autocatalytic effects ranging from a factor of 1.6 to 4.3 for crosslinking the polymers **1a–i** with **3** and from a factor of 2.1 to 3.8 for crosslinking the polymers **2** with **4a–d** now enabling control of the catalytic effects. Therefore, it is assumed that clustering effects of the generated triazole rings prompted the catalysis of the CuAAC thus explaining the observed autocatalysis. Furthermore, a “click”-crosslinking concept acting at room temperature with very short gelation times (**1a** + **3**, 142 min; **2** + **4a**, 290 min), with experimental network strand densities about 100 mol/m³ (**1b** + **3**, 105 mol/m³; **2** + **4a**, 91 mol/m³) and ratios between experimental and maximal network strand densities up to 55.3% (**1f** + **3**) could be

achieved. Effects exerted by the molecular weight reacting five three-arm star azide-telechelic PIBs and one three-arm star alkyne-telechelic PIB on the crosslinking-reaction, linked molecular mobility to changes in CuAAC-reactivity featuring increased reaction rates with decreasing molecular weights (**2** + **4b** (11600 g/mol), $r_0 = 3.2 \times 10^{-3}$ M·min⁻¹; **2** + **4a** (5500 g/mol), $r_0 = 23 \times 10^{-3}$ M·min⁻¹). The now designable significant autocatalytic effects enabled the design of new, highly efficient and fast crosslinking systems acting at room temperature.

* Supporting Information

Derivation of eqn 1 and correlation of the derivative of the reaction rate k with respect to time t vs. time t for crosslinking **1c–e** with **3** and **2** with **4a–d**.

ACKNOWLEDGMENTS

We gratefully acknowledge Grant DFG BI 1337/8-1 (within the SPP 1568 “Design and Generic Principles of Self-Healing Materials”).

ABBREVIATIONS

CuAAC Copper(I)-catalyzed alkyne–azide “click” cycloaddition
 DA Diels–Alder
 DSC Differential scanning calorimetry
 LCCP Living carbocationic polymerization
 MeOH Methanol
*n*BA *N*-butyl acrylate
 NMP Nitroxide mediated polymerization
 PA Propargyl acrylate
 PIB Poly(isobutylene)
 TBTA Tris[(1-benzyl-1*H*-1,2,3-triazol-4-yl)methyl]amine
 T_g Glass transition temperature
 TIPNO 2,2,5-Trimethyl-4-phenyl-3-azahexane-3-nitroxide
 TMSPA 3-(Trimethylsilyl)prop-2-ynyl acrylate

REFERENCES

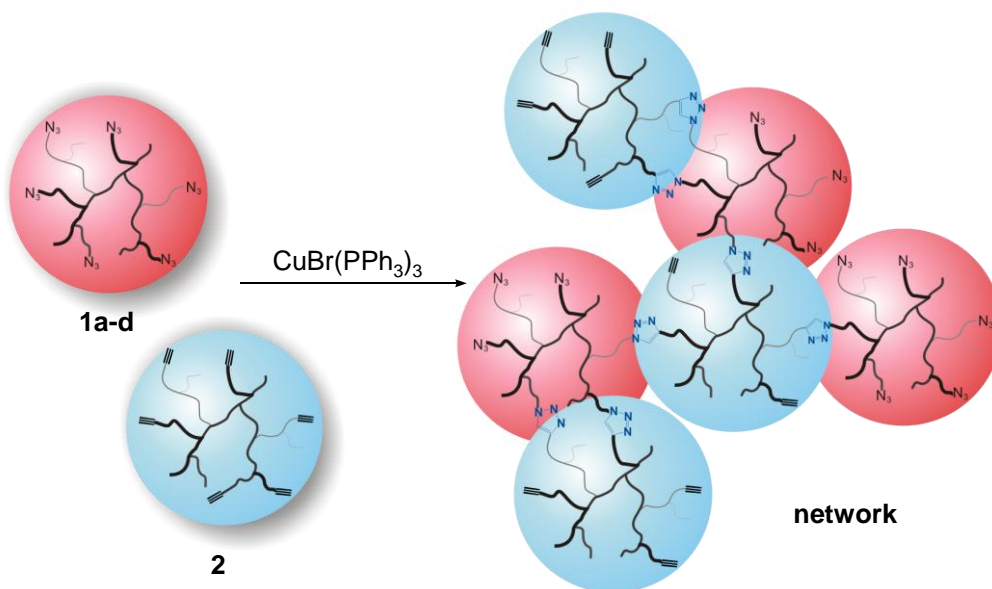
- (1) Kolb, H. C.; Finn, M. G.; Sharpless, K. B. *Angew. Chem., Int. Ed.* 2001, 40 (11), 2004–2021.
- (2) Tillet, G.; Boutevin, B.; Ameduri, B. *Prog. Polym. Sci.* 2011, 36, 191–217.

- (3) Binder, W. H.; Sachsenhofer, R. *Macromol. Rapid Commun.* 2007, 28 (1), 15–54.
- (4) Iha, R. K.; Wooley, K. L.; Nystrom, A. M.; Burke, D. J.; Kade, M. J.; Hawker, C. J. *Chem. Rev.* 2009, 109 (11), 5620–5686.
- (5) Binder, W. H.; Sachsenhofer, R. *Macromol. Rapid Commun.* 2008, 29 (12–13), 952–981.
- (6) Vestberg, R.; Malkoch, M.; Kade, M.; Wu, P.; Fokin, V. V.; Sharpless, K. B.; Drockenmuller, E.; Hawker, C. J. *J. Polym. Sci., Part A: Polym. Chem.* 2007, 45 (14), 2835–2846.
- (7) Malkoch, M.; Schleicher, K.; Drockenmuller, E.; Hawker, C. J.; Russell, T. P.; Wu, P.; Fokin, V. V. *Macromolecules* 2005, 38 (9), 3663–3678.
- (8) Blaiszik, B. J.; Kramer, S. L. B.; Olugebefola, S. C.; Moore, J. S.; Sottos, N. R.; White, S. R. *Annu. Rev. Mater. Res.* 2010, 40 (1), 179–211.
- (9) Weder, C. *Nature* 2009, 459, 45–46.
- (10) Blaiszik, B. J.; Caruso, M. M.; McIlroy, D. A.; Moore, J. S.; White, S. R.; Sottos, N. R. *Polymer* 2009, 50 (4), 990–997.
- (11) Wu, D. Y.; Meure, S.; Solomon, D. *Prog. Polym. Sci.* 2008, 33 (5), 479–522.
- (12) Guadagno, L.; Longo, P.; Raimondo, M.; Naddeo, C.; Mariconda, A.; Sorrentino, A.; Vittoria, V.; Iannuzzo, G.; Russo, S. *J. Polym. Sci., Part B: Polym. Phys.* 2010, 48 (23), 2413–2423.
- (13) Montarnal, D.; Tournilhac, F.; Hildago, M.; Leibler, L. *J. Polym. Sci., Part A: Polym. Chem.* 2010, 48, 2413–2423.
- (14) McIlroy, D. A.; Blaiszik, B. J.; Caruso, M. M.; White, S. R.; Moore, J. S.; Sottos, N. R. *Macromolecules* 2010, 43 (4), 1855–1859.
- (15) Jackson, A. C.; Bartelt, J. A.; Marczewski, K.; Sottos, N. R.; Braun, P. V. *Macromol. Rapid Commun.* 2011, 32 (1), 82–87.
- (16) Jones, A. S.; Rule, J. D.; Moore, J. S.; White, S. R.; Sottos, N. R. *Chem. Mater.* 2006, 18 (5), 1312–1317.
- (17) Brown, E. N.; White, S. R.; Sottos, N. R. *J. Mater. Sci.* 2004, 39, 1703–1710.
- (18) Blaiszik, B. J.; Baginska, M.; White, S. R.; Sottos, N. R. *Adv. Funct. Mater.* 2010, 20, 3547–3554.
- (19) Kessler, M. R.; Sottos, N. R.; White, S. R. *Compos. Part A: Appl. S.* 2003, 34 (8), 743–753.
- (20) Brown, E. N.; Kessler, M. R.; Sottos, N. R.; White, S. R. *J. Microencapsulation* 2003, 20 (6), 719–730.
- (21) White, S. R.; Sottos, N. R.; Geubelle, P. H.; Moore, J. S.; Kessler, M. R.; Sriram, S. R.; Brown, E. N.; Viswanathan, S. *Nature* 2001, 409 (6822), 794–797.
- (22) Hizal, G.; Tunca, U.; Sanyal, A. *J. Polym. Sci., Part A: Polym. Chem.* 2011, 49 (19), 4103–4120.
- (23) Chen, X.; Wudl, F.; Mal, A. K.; Shen, H.; Nutt, S. R. *Macromolecules* 2003, 36 (6), 1802–1807.
- (24) Chen, X.; Dam, M. A.; Ono, K.; Mal, A. K.; Shen, H.; Nutt, S. R.; Sheran, K.; Wudl, F. *Science* 2002, 295, 1698–1702.
- (25) Park, J. S.; Takahashi, K.; Guo, Z.; Wang, Y.; Bolanos, E.; Hamann-Schaffner, C.; Murphy, E.; Wudl, F.; Hahn, T. *J. Compos. Mater.* 2008, 42 (26), 2869–2881.
- (26) Murphy, E. B.; Bolanos, E.; Schaffner-Hamann, C.; Wudl, F.; Nutt, S. R.; Auad, M. L. *Macromolecules* 2008, 41 (14), 5203–5209.
- (27) Liu, Y. L.; Chen, Y. W. *Macromol. Chem. Phys.* 2007, 208, 224–232.
- (28) Kavitha, A. A.; Singha, N. K. *Macromolecules* 2010, 43 (7), 3193–3205.
- (29) Ishida, K.; Yoshie, N. *Macromolecules* 2008, 41 (13), 4753–4757.
- (30) Ishida, K.; Nishiyama, Y.; Michimura, Y.; Oya, N.; Yoshie, N. *Macromolecules* 2010, 43 (2), 1011–1015.
- (31) Ishida, K.; Weibel, V.; Yoshie, N. *Polymer* 2011, 52 (13), 2877–2882.
- (32) Ishida, K.; Yoshie, N. *Macromol. Biosci.* 2008, 8 (10), 916–922.
- (33) Liu, Y.-L.; Hsieh, C.-Y.; Chen, Y.-W. *Polymer* 2006, 47 (8), 2581–2586.
- (34) Kavitha, A. A.; Singha, N. K. *J. Polym. Sci., Part A: Polym. Chem.* 2007, 45, 4441–4449.
- (35) Kavitha, A. A.; Singha, N. K. *Macromol. Chem. Phys.* 2007, 208 (23), 2569–2577.

- (36) Adzima, B. J.; Aguirre, H. A.; Kloxin, C. J.; Scott, T. F.; Bowman, C. N. *Macromolecules* 2008, 41 (23), 9112–9117.
- (37) Nimmo, C. M.; Owen, S. C.; Shoichet, M. S. *Biomacromolecules* 2011, 12 (3), 824–830.
- (38) Wei, H.-L.; Yang, Z.; Chen, Y.; Chu, H.-J.; Zhu, J.; Li, Z.-C. *Eur. Polym. J.* 2010, 46 (5), 1032–1039.
- (39) Defize, T.; Riva, R.; Raquez, J.-M.; Dubois, P.; Jérôme, C.; Alexandre, M. *Macromol. Rapid Commun.* 2011, 32 (16), 1264–1269.
- (40) Raquez, J.-M.; Vanderstappen, S.; Meyer, F.; Verge, P.; Alexandre, M.; Thomassin, J.-M.; Jérôme, C.; Dubois, P. *Chem. Eur. J.* 2011, 17 (36), 10135–10143.
- (41) Schunack, M.; Gragert, M.; Döhler, D.; Michael, P.; Binder, W. H. *Macromol. Chem. Phys.* 2012, 213, 205–214.
- (42) Gragert, M.; Schunack, M.; Binder, W. H. *Macromol. Rapid Commun.* 2011, 32 (5), 419–425.
- (43) Ossipov, D. A.; Hilborn, J. *Macromolecules* 2006, 39 (5), 1709–1718.
- (44) Liu, J.; Jiang, X.; Xu, L.; Wang, X.; Hennink, W. E.; Zhuo, R. *Bioconjugate Chem.* 2010, 21 (10), 1827–1835.
- (45) Malkoch, M.; Vestberg, R.; Gupta, N.; Mespouille, L.; Dubois, P.; Mason, A. F.; Hedrick, J. L.; Liao, Q.; Frank, C. W.; Kingsbury, K.; Hawker, C. J. *Chem. Commun.* 2006, 26, 2774–2776.
- (46) Liu, S. Q.; Ee, P. L. R.; Ke, C. Y.; Hedrick, J. L.; Yang, Y. Y. *Biomaterials* 2009, 30 (8), 1453–1461.
- (47) Crescenzi, V.; Cornelio, L.; Di Meo, C.; Nardecchia, S.; Lamanna, R. *Biomacromolecules* 2007, 8 (6), 1844–1850.
- (48) Testa, G.; Di Meo, C.; Nardecchia, S.; Capitani, D.; Mannina, L.; Lamanna, R.; Barbetta, A.; Dentini, M. *Int. J. Pharm.* 2009, 378, 86–92.
- (49) Huerta-Angeles, G.; Šmejkalová, D.; Chládková, D.; Ehlová, T.; Buffa, R.; Velebný, V. *Carbohydr. Polym.* 2011, 84 (4), 1293–1300.
- (50) Díaz, D. D.; Punna, S.; Holzer, P.; McPherson, A. K.; Sharpless, K. B.; Fokin, V. V.; Finn, M. G. *J. Polym. Sci., Part A: Polym. Chem.* 2004, 42 (17), 4392–4403.
- (51) Filpponen, I.; Argyropoulos, D. S. *Biomacromolecules* 2010, 11 (4), 1060–1066.
- (52) van der Ende, A. E.; Harrell, J.; Sathiyakumar, V.; Meschievitz, M.; Katz, J.; Adcock, K.; Harth, E. *Macromolecules* 2010, 43 (13), 5665–5671.
- (53) Cengiz, H.; Aydogan, B.; Ates, S.; Acikalin, E.; Yagci, Y. *Des. Monomers. Polym.* 2011, 14, 69–78.
- (54) de Luzuriaga, A. R.; Ormategui, N.; Grande, H. J.; Odriozola, I.; Pomposo, J. A.; Loinaz, I. *Macromol. Rapid Commun.* 2008, 29 (12–13), 1156–1160.
- (55) Li, C.; Finn, M. G. *J. Polym. Sci., Part A: Polym. Chem.* 2006, 44 (19), 5513–5518.
- (56) Chan, T. R.; Hilgraf, R.; Sharpless, K. B.; Fokin, V. V. *Org. Lett.* 2004, 6 (17), 2853–2855.
- (57) Lang, A. S.; Neubig, A.; Sommer, M.; Thelakkat, M. *Macromolecules* 2010, 43 (17), 7001–7010.
- (58) Rother, M. Diploma Thesis, Martin-Luther-Universität Halle-Wittenberg, 2009.
- (59) Mishra, M. K.; Wang, B.; Kennedy, J. P. *Polym. Bull.* 1987, 17 (4), 307–314.
- (60) Morgan, D. L.; Martinez-Castro, N.; Storey, R. F. *Macromolecules* 2010, 43 (21), 8724–8740.
- (61) Lee, B.-Y.; Park, S. R.; Jeon, H. B.; Kim, K. S. *Tetrahedron Lett.* 2006, 47 (29), 5105–5109.
- (62) Mezger, T. G., *The Rheology Handbook: For users of rotational and oscillatory rheometers*, 2nd revised ed.; Vincentz Network: Hannover, Germany, 2006.
- (63) Binder, W. H.; Kunz, M. J.; Kluger, C.; Hayn, G.; Saf, R. *Macromolecules* 2004, 37 (5), 1749–1759.
- (64) Morgan, D. L.; Storey, R. F. *Macromolecules* 2009, 42 (18), 6844–6847.
- (65) Rodionov, V. O.; Fokin, V. V.; Finn, M. G. *Angew. Chem.* 2005, 117 (15), 2250–2255.
- (66) Hawker, C. J.; Bosman, A. W.; Harth, E. *Chem. Rev. (Washington, DC)* 2001, 101 (12), 3661–3688.
- (67) Fox, T. G.; Flory, P. J. *Further studies on the melt viscosity of polyisobutylene*; Research Laboratory of the Goodyear Tire and Rubber Company: Akron, OH, 1950; pp 221–234

- (68) Ampudia, J.; Larrauri, E.; Gil, E. M.; Rodríguez, M.; León, L. M. *J. Appl. Polym. Sci.* 1999, 71 (8), 1239–1245.
- (69) Barton, J. M.; Greenfield, D. C. L.; Hodd, K. A. *Polymer* 1992, 33 (6), 1177–1186.
- (70) Schweinfurth, D.; Deibel, N.; Weisser, F.; Sarkar, B. *Nachr. Chem.* 2011, 59 (10), 937–941.
- (71) Kavitha, A. A.; Singha, N. K. *ACS Appl. Mater. Interfaces* 2009, 1 (7), 1427–1436.
- (72) Goiti, E.; Heatley, F.; Huglin, M. B.; Rego, J. M. *Eur. Polym. J.* 2004, 40 (7), 1451–1460.
- (73) Feldman, K. E.; Kade, M. J.; Meijer, E. W.; Hawker, C. J.; Kramer, E. J. *Macromolecules* 2009, 42 (22), 9072–9081.
- (74) Müller, M.; Seidel, U.; Stadler, R. *Polymer* 1995, 36 (16), 3143–3150.
- (75) Goiti, E.; Huglin, M. B.; Rego, J. M. *Eur. Polym. J.* 2004, 40 (2), 219–226.
- (76) Sheng, X.; Mauldin, T. C.; Kessler, M. R. *J. Polym. Sci., Part A: Polym. Chem.* 2010, 48 (18), 4093–4102.
- (77) Binauld, S.; Boisson, F.; Hamaide, T.; Pascault, J.-P.; Drockenmuller, E.; Fleury, E. J. *Polym. Sci., Part A: Polym. Chem.* 2008, 46 (16), 5506–5517.

6.2. Hyperbranched poly(isobutylene)s for self-healing polymers



ABSTRACT

Hyperbranched azide- and alkyne-functionalized poly(isobutylene)s (PIBs, $M_n = 25\,200\text{--}35\,400\text{ g}\cdot\text{mol}^{-1}$) suitable for crosslinking at room temperature *via* the copper-catalyzed alkyne-azide "click" cycloaddition reaction (CuAAC) are reported, aiming at the design of improved crosslinking reactions for novel self-healing materials. Based on the low glass transition temperature (T_g) the high molecular mobility of the hyperbranched PIBs was linked with an efficient crosslinking chemistry while introducing reactive endgroups into the polymer and tuning molecular architecture *via* living carbocationic polymerization (LCCP). Hyperbranched PIBs were prepared by inimer-type LCCP followed by direct end quenching of living chain ends with either 3-(bromopropoxy)benzene (BPB) or trimethyl(3-phenoxy-1-propynyl)silane (TMPPS). Optimized quenching time conditions (6 hours quenching with BPB and 20 hours quenching with TMPPS) yielded the fully bromine- and trimethylsilyl-protected alkyne-functionalized hyperbranched PIBs with up to ≈ 9 endgroups, subsequently being converted into the respective fully azide- and alkyne-functionalized polymers. "Click" reactions between the azide and the alkyne group of hyperbranched PIBs linked the two spherical polymers resulting in fast gelation times of 30 to 50 minutes as investigated *via* melt rheology. Materials with high network densities were obtained due to the high amount of reactive endgroups and the architecture of the applied polymers. Thus, the concept of crosslinking hyperbranched azide- and alkyne-functionalized PIBs *via* "click" chemistry at room temperature towards self-healing polymers could be successfully proven.

INTRODUCTION

Self-healing materials and polymers^{1–3} have gained increased attention, as many of the basic self-repair mechanisms demand a thorough understanding and design of chemical reaction processes, catalysis as well as fundamental knowledge of chain dynamics.⁴ Besides supramolecular^{5,6} and mechanochemical⁷ healing concepts, the issue of encapsulated reagents and subsequent

catalytic healing is among the closest to technical realization.⁸ The central concept involves separate encapsulation (or enchanneling) of two potentially reactive components able to effect efficient crosslinking reactions, ideally acting at room temperature or below. Thus, a large variety of crosslinking concepts has been developed, many of them relying on catalytic reactions, such as ROMP,^{8–39} base catalyzed

epoxy-crosslinking,^{15,31,40,41} siloxane-based healing systems^{42–47} and thiol-maleimide healing systems.⁴⁸

Especially “click”-based reactions^{49–53} have gained interest, as these reactions are fast, efficient, and often catalytic and thus lead to efficient crosslinking reactions and chemistries, irrespective of the functional moieties used in other parts of the crosslinked molecules. Thus we^{54–56} and others⁵⁷ have recently developed a room-temperature self-healing concept devoid of external stimuli such as UV-irradiation or heat, using the copper-catalyzed alkyne-azide “click” cycloaddition reaction (CuAAC) based on appropriately azide/alkyne-functionalized polymers. Besides a favorable thermodynamics and kinetics of the underlying chemical reaction the molecular mobility of the components is crucial in enabling efficient crosslinking chemistry, the initial viscosity defines the molecular diffusion within the polymer mixture, thus favoring low glass transition (T_g)-polymers with lower molecular weights as components for crosslinking. We therefore had chosen PIB as a low T_g polymer in several of our healing concepts,^{54–56,58} which allows the tuning of molecular weights and molecular architecture of the polymers *via* living carbocationic polymerization (LCCP) together with the quantitative introduction of reactive endgroups. However, as high network densities could be only achieved for crosslinking star-shaped trivalent PIBs with a low molecular weight,⁵⁴ we envisioned to change the architecture of the PIB to a hyperbranched architecture in order to still benefit from the low T_g of the polymer backbone together with the presence of more functional groups per molecule to enable enhanced formation of triazole rings acting as network points.

Hyperbranched PIBs^{59,60} are conventionally prepared by inimer-type living carbocationic polymerization (LCCP)^{60–65} using 4-(1-hydroxy-1-methylethyl)styrene, 4-(1,2-oxirane-isopropyl)-styrene and 4-(2-methoxyisopropyl)styrene^{60,61,66} as inimers (initiator-monomers). As the T_g 's of these

polymers are around -60 to -70 °C (as described by a modified Fox-Flory equation) the hyperbranched PIBs are expected to provide lower viscosities in solution and bulk compared to their linear counterparts.^{60,66–69}

We thus decided to change the architecture of the initially used star-type polymers to PIBs with a hyperbranched structure, where the reactive endgroups are suitable for subsequent Cu(I)-catalyzed crosslinking reactions. Therefore a series of hyperbranched azide- (**1a-d**) and alkyne-functionalized PIBs (**2**) *via* inimer-type LCCP using 4-(2-methoxyisopropyl)styrene as an inimer has been prepared (see Fig. 1). Furthermore hyperbranched PIBs containing an ionic moiety (**4a,b**) are investigated as liquefiers for crosslinking azide- and alkyne-functionalized hyperbranched PIBs as their liquid-like character is well known in the literature.^{70,71} The prepared hyperbranched PIBs bear different amounts of endgroups in order to further increase network densities and to decrease gelation times during network formation as healing has to be faster than crack propagation.

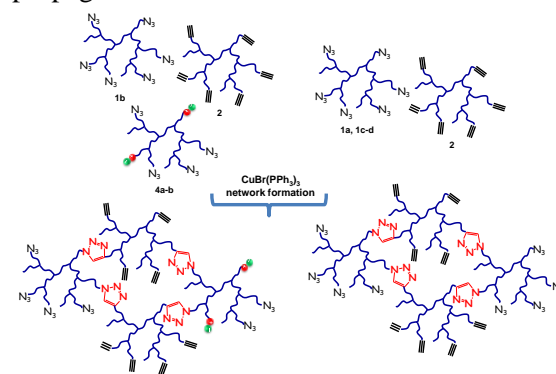


Fig. 1 CuAAC of azide- (**1a-d**) and alkyne-functionalized (**2**) hyperbranched PIBs with and without PIBs bearing an ionic moiety (**4a,b**) applying bromotris(triphenylphosphine)copper(I) as a catalyst at 20 °C.

EXPERIMENTAL SECTION

Materials

All materials were obtained from Sigma-Aldrich and used without further purification if not mentioned otherwise. *N,N,N*-Triethylamine and 1-methylpyrrolidine were freshly distilled over CaH_2 under a nitrogen atmosphere prior to use. *N*-Hexane was predried over KOH and

freshly distilled over sodium and KOH under a nitrogen atmosphere prior to use. Dichloromethane was predried over CaCl₂ and freshly distilled over CaH₂ under a nitrogen atmosphere prior to use.

Synthesis

The synthesis of ionic liquid containing alkynes **3a,b** was carried out according to the literature.⁷¹ 4-(2-Methoxyisopropyl)styrene (inimer-type initiator) was prepared according to the synthesis protocol of Puskas et al.⁶² Synthesis of trimethyl(3-phenoxy-1-propynyl)silane was done according to Storey et al.⁷²

General polymerization procedure

For the polymerization of isobutylene living carbocationic polymerization (LCCP) was used. The synthesis was carried out under a dry atmosphere of argon. A three-necked round-bottom flask equipped with a rubber septum, stopcock and mechanical stirrer was heated under vacuo and flushed with argon several times. Dry *n*-hexane and dry dichloromethane (v/v = 40/60) were added to the flask and the solution was cooled down to -80 °C using a methanol cooling bath and liquid nitrogen. During cooling D₇BP (0.008 mol L⁻¹) and the inimer-type initiator were added and condensed and dried isobutylene (2 mol·L⁻¹) was added at the final temperature. The polymerization was initiated by the addition of TiCl₄ (10 equiv. of inimer-type initiator). Polymerization reactions were run for one hour. As a quenching agent 3-(bromopropoxy)benzene (BPB, 26 equiv. of inimer-type initiator) was used to introduce bromine endgroups and trimethyl(3-phenoxy-1-propynyl)silane (TMPPS, 30 equiv. of inimer-type initiator) and a second portion of TiCl₄ (85 equiv. of inimer-type initiator) was used to introduce protected alkyne endgroups. The quenching time was varied in order to achieve complete functionalization of living chain ends. Additionally, allyltrimethylsilane (ATMS, 26 equiv. of inimer-type initiator) was used as a quenching agent to trap residual

cations which were not completely functionalized with bromine endgroups.

Synthesis of azide-functionalized hyperbranched PIBs (1a–d)

The synthesis was carried out under a dry atmosphere of nitrogen. In a two-necked flask equipped with a magnetic stirring bar, septum, reflux condenser and stopcock bromine-functionalized hyperbranched PIB (ca. 2.0 g) was dissolved in a 1 : 1 mixture of *n*-heptane (50.0 mL) and DMF (50.0 mL). To the reaction mixture sodium azide (20 equiv. of inimer-type initiator) was added and the resultant mixture was heated up to 90 °C for 20 hours. After the reaction mixture cooled down, the *n*-heptane-layer was separated and washed with water (five times 50.0 mL). The organic layer was separated and dried over Na₂SO₄ and the solvent was removed in vacuo. The crude polymer was dissolved in *n*-hexane and the resultant solution was precipitated into a ten to fifteen times excess of MeOH three times and dried at high vacuo. ¹H-NMR (400 MHz, CDCl₃) δ ppm: 7.28 (d, *J* = 8.8 Hz), 7.25–7.06 (m), 6.81 (d, *J* = 8.8 Hz), 4.03 (t, *J* = 6.0 Hz), 3.51 (t, *J* = 6.7 Hz), 2.04 (m), 1.53 (s), 1.42 (s), 1.11 (s), 0.89 (s).

Synthesis of alkyne-functionalized hyperbranched PIB (2).

The synthesis was carried out under a dry atmosphere of nitrogen. In a two-necked flask equipped with a magnetic stirring bar, stopcock and septum trimethyl-silyl protected alkyne-functionalized hyperbranched PIB (ca. 2.0 g) was dissolved in THF (15.0 mL) and TBAF (1.0 M solution in THF, 2.5 equiv. of trimethyl(3-phenoxy-1-propynyl)silane). The reaction mixture was stirred at room temperature for 72 hours. The polymer solution was washed with water (five times 50.0 mL). The organic layer was separated and dried over Na₂SO₄. The solvent was removed in vacuo. The crude polymer was dissolved in *n*-hexane, precipitated into a ten to fifteen time excess of MeOH three times and dried at high vacuo. ¹H-NMR (400 MHz, CDCl₃) δ ppm: 7.28 (d, *J* = 8.9 Hz), 7.21–7.03 (m), 6.88 (d, *J*

= 8.9 Hz), 4.66 (d, $J = 2.4$ Hz), 2.50 (t, $J = 2.4$ Hz), 1.56 (s), 1.41 (s), 1.11 (s), 0.80 (s).

General synthesis of hyperbranched PIBs (4a,b) containing an ionic moiety via “click” chemistry

The synthesis was carried out under a dry atmosphere of nitrogen. In a microwave vial azide-functionalized hyperbranched PIB (100 mg) and the ionic liquid containing alkyne **3a** or **3b** (0.6 mmol) were dissolved in a solvent mixture of toluene–water–isopropanol = 2/1/1 (4.0 mL). After addition of DIPEA (15 equiv.), the vial was closed with a septum and the solution was purged with nitrogen for 30 minutes. Then copper(I) iodide (5 mg) was added to the mixture, and the solution was again purged with nitrogen for 30 minutes. Subsequently, the vial was sealed, placed in a microwave reactor, and irradiated under 75W at 80 °C for 20 hours. After termination of the irradiation, the organic phase was separated and washed with saturated ammonium chloride solution (15.0 mL) and with water (three times 15.0 mL). The organic layer was separated and dried over Na_2SO_4 . The solvent was removed in vacuo. The crude polymer was purified by column chromatography (chloroform; chloroform–methanol = 15/1) followed by precipitation into a ten to fifteen time excess of MeOH and dried at high vacuo.

Kinetic investigations of inimer-type living carbocationic polymerization via inline FTIR-measurements

For *inline FTIR-measurements* a Bruker Vertex 70 MIR spectrometer equipped with an ATR-FTIR diamond probe was used. Therefore polymerization reactions were run in a Schlenk-tube equipped with a FTIR-probe, a rubber septum and a magnetic stirring bar (550 rpm). The collection of IR-spectra was started with the addition of TiCl_4 . IR-spectra were collected each 9 seconds (20 scans per spectrum, scans every 4 cm^{-1}). In order to determine the concentration of monomer the wag vibration of the isobutylene at 887 cm^{-1} was integrated over time. Opus 6.5 was used for analyzing data.

Differential scanning calorimetry (DSC) experiments were performed with a DSC 204 F1 Phoenix from NETZSCH. To determine the glass transition temperature (T_g) samples were first cooled to -90 °C and then heated up to 150 °C with a rate of $10\text{ K}\cdot\text{min}^{-1}$. T_g is taken upon heating from the amorphous glass state to the liquid state of the sample as midpoint of a small change in the heat capacity. Proteus-Thermal Analysis (V 5.2.1) from NETZSCH was used for analyzing data.

Rheology experiments were performed on an Anton Paar (Physica) MCR 301/SN 80753612 at 20 °C . For regulating the sample temperature thermoelectric cooling/heating in a Peltier chamber under dry oxygen was applied. For all measurements parallel plates with a diameter of 8 mm were used. Frequency measurements were performed within the LVE. For crosslinking experiments an azide-functionalized hyperbranched PIB (50.0 mg) and an alkyne-functionalized hyperbranched PIB (50.0 mg) were put in a vial and were mixed with a spatula. In some cases 10 wt% of **4a,b** (10.0 mg) was added additionally to study the influence of hyperbranched PIBs containing an ionic moiety. $\text{CuBr}(\text{PPh}_3)_3$ (5 wt%, 5.0 mg) was added to the vial as a stock solution (dissolved in 40.0 mL CHCl_3). Subsequently, the reaction mixture was mixed with a spatula and was immediately put on the rheometer plate. Crosslinking experiments were performed with a strain γ of 0.1% and with an angular frequency ω ranging from 100 to $1\text{ rad}\cdot\text{s}^{-1}$. A frequency sweep was performed every 5 minutes. The gelation time^{54,73} was determined as crossover of the storage (G') and loss moduli (G'') at $10\text{ rad}\cdot\text{s}^{-1}$. Each measurement was stopped when the values of the loss and storage moduli stayed constant (second decimal place) for at least 1 hour. This time is considered as the total time. The determined plateau moduli correspond to the storage moduli measured at this total time at 100 Hz. Frequency sweeps of hyperbranched PIBs containing an ionic moiety were performed with a strain γ of 2.0% and with an angular frequency ω ranging from 100 to $0.01\text{ rad}\cdot\text{s}^{-1}$.

Temperature sweep measurements were performed from $-10\text{ }^{\circ}\text{C}$ to $120\text{ }^{\circ}\text{C}$ with a strain γ of 2%, an angular frequency ω of $10\text{ rad}\cdot\text{s}^{-1}$ and a heating rate of $1^{\circ}\text{C}\cdot\text{min}^{-1}$. Before each measurement the sample was annealed for 30 minutes. For evaluation of data the RheoPlus/32 software (V 3.40) and OriginPro8 were used.

GPC spectra were recorded on a GPCmax VE 2001 from Viscotek™ equipped with a column set of a H_{HR}-H Guard-17369 column, a CLM30111 column and a G2500H_{HR}-17354 column in THF ($1\text{ mL}\cdot\text{min}^{-1}$) at $35\text{ }^{\circ}\text{C}$. For determination of absolute molecular weights a triple detection array (refractive index, viscosity, light scattering) TDA 302 from Viscotek™ was applied. For evaluation of data OmniSEC software (V 4.5.6) was used. Calibration was carried out using polystyrene standards provided by Viscotek™.

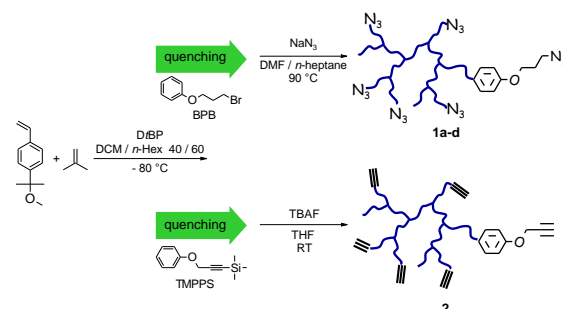
RESULTS AND DISCUSSION

Synthesis of azide- and alkyne-functionalized hyperbranched PIBs

Based on our recently developed synthetic route towards azide- and alkyne-functionalized three-arm-star PIBs (living carbocationic polymerization (LCCP) of isobutylene followed by direct end quenching of living chain ends^{72,74} with either 3-(bromopropoxy)benzene (BPB) or trimethyl(3-phenoxy-1-propynyl)silane (TMPPS))⁵⁴ this approach is now conceptually transferred to hyperbranched PIBs, taking into account that a fundamental investigation of the quenching conditions is required, as now a significantly large number of active centers require a quantitative quenching reaction.

As illustrated in Scheme 1 we used a combination of inimer-type LCCP⁶² and the quenching approaches with BPB or TMPPS to obtain the hyperbranched PIBs (**1a-d** or **2**, see Scheme 1). In this special case of LCCP the initiator contains both an initiating site for LCCP and a double bond active for cationic polymerization which can be copolymerized with IB. Consequently, each incorporated inimer unit ideally results in two branches

while the amount of introduced branching points can be tuned by varying the inimer to IB ratio (see Scheme 1).



Scheme 1 Synthetic route towards azide- (**1a-d**) and alkyne-functionalized (**2**) hyperbranched PIBs.

To achieve a complete endgroup functionalization we intensely studied the quenching of the inimer-type LCCP with BPB while varying the quenching time as well as the inimer to IB ratio. Additionally, allyltrimethylsilane (ATMS) was used as the second fast and quantitative quencher for LCCP to trap residual cations which were not completely functionalized with bromine endgroups, thus enabling the quantification of the quenching success of each individual reaction.

Details of the applied reaction conditions can be found in Table 1, with all conducted polymerization reactions running for 1 hour. In the first set of experiments (Table 1, entry 1–4) the quenching time of inimer-type LCCP with BPB was increased stepwise from 3 to 6 hours while applying a defined inimer to IB ratio of 0.008. Afterwards in a competitive quenching experiment, ATMS (26 equiv. of inimer) as an irreversible quencher was added in excess to terminate all still existing living chain ends thus introducing an allyl-group and enabling direct monitoring of the quenching efficiency of BPB. The endgroup distribution of the so-obtained polymers was analyzed *via* ¹H-NMR- spectroscopy as illustrated in Fig. 2. A complete quenching with BPB and accordingly a 100% functionalization with bromine endgroups could be observed after 6 hours of quenching (Table 1, entry 4, Fig. 2 (d) and (e)) as all other ¹H-NMR-spectra show resonances at 5.00 ppm and 5.84 ppm (Fig. 2

Table 1 Reaction conditions of quenching inimer-type LCCP either with BPB followed by ATMS or with TMPPS: $[IB]_0 = 2.0 \text{ mol}\cdot\text{L}^{-1}$; $[DzBP] = 0.008 \text{ mol}\cdot\text{L}^{-1}$; TiCl_4 : 10 equiv. of inimer; *n*-hexane–DCM = 60/40 v/v; $T = -80 \text{ }^\circ\text{C}$, molecular weights, amount of branches and amount of endgroups of hyperbranched bromine- and alkyne-functionalized PIBs.

Entry	Inimer/IB	Quencher	Quench time (hours)	M_n ($\text{g}\cdot\text{mol}^{-1}$)	M_w ($\text{g}\cdot\text{mol}^{-1}$)	M_w/M_n	Amount of branches (calc.) ^d	Integral of endgroup/integral of inimer	Amount of endgroups (calc.) ^e
1	0.008	BPB ^a , ATMS ^b	3	15 600	62 400	4.0	5.09	1.12/1.00	5.70
2	0.008	BPB ^a , ATMS ^b	4	16 300	65 100	4.0	5.37	1.15/1.00	6.17
3	0.008	BPB ^a , ATMS ^b	5	18 800	56 400	3.0	6.34	1.17/1.00	7.41
4	0.008	BPB ^a , ATMS ^b	6	21 500	98 000	4.6	7.39	1.18/1.00	8.72
5	0.006	BPB ^a , ATMS ^b	6	22 900	76 800	3.4	5.96	1.12/1.00	6.67
6	0.004	BPB ^a , ATMS ^b	6	23 500	70 000	3.0	3.95	0.95/1.00	3.75
7	0.006	TMPPS ^c	20	35 300	135 500	3.8	2.76	1.10/1.00	3.04

^a BPB (26 equiv. of inimer) was added first for the indicated quenching time. ^b After the indicated quenching time with BPB, ATMS (26 equiv. of inimer) was added and stirring was proceeded for 30 minutes. ^c 30 equiv. of inimer. ^d Amount of branches = $\frac{M_n}{M_{n,theoretic}} - 1$

(a)–(c)) resulting from the protons of the allyl group beside the resonances of the CH_2 -moieties of the desired bromine endgroup at 2.29 ppm, 3.58 ppm and 4.06 ppm.

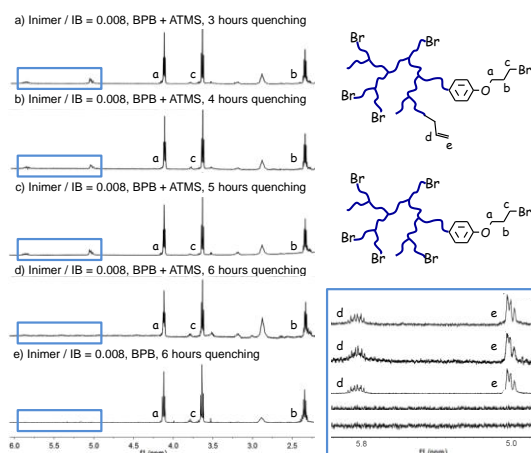


Fig. 2 Analysis of endgroup distribution of hyperbranched PIBs *via* $^1\text{H-NMR}$ -spectroscopy after quenching with BPB (26 equiv. with respect to inimer) followed by ATMS (26 equiv. with respect to inimer) or BPB only (26 equiv. with respect to inimer) applying different quenching times. Inimer/IB = 0.008: (a) BPB and ATMS, 3 hours quenching, (b) BPB and ATMS, 4 hours quenching, (c) BPB and ATMS, 5 hours quenching, (d) BPB and ATMS, 6 hours quenching, and (e) BPB, 6 hours quenching.

After the optimization of the necessary quenching time in the second step the inimer to IB ratio was varied between 0.008 and 0.004

(Table 1, entry 4–6) under optimized quenching conditions (quenching with BPB for 6 hours followed by the addition of ATMS for 30 minutes). As confirmed *via* $^1\text{H-NMR}$ -spectroscopy (see Fig. 1, ESI†) full endgroup functionalization was achieved. The concept of direct quenching of inimer-type LCCP was finally proven by running a polymerization reaction with an inimer to IB ratio of 0.006 while applying BPB as a quenching agent for 6 hours without the addition of ATMS. 100% conversion of living chain ends was achieved as illustrated in Fig. 2(e).

For synthesis of alkyne-functionalized hyperbranched PIB (2) TMPPS was used as a quenching agent for inimer-type LCCP (Table 1, entry 7). Quenching was proceeded for 20 hours as this time was assumed to be sufficient for endgroup functionalization based on the quenching of trivalent PIB chains with TMPPS.⁵⁴ The so-obtained TMS-protected alkyne-functionalized hyperbranched PIB was directly deprotected with tetrabutylammonium fluoride (TBAF) at room temperature. $^1\text{H-NMR}$ analysis indicated complete conversion during quenching and complete deprotection could be confirmed as no resonances from other endgroups (formed during incomplete

quenching processes such as *tert*-chlorine or endo- and exo-double bonds) were detected (see Fig. 2, ESI†).⁷⁵ Determination of absolute molecular weights with triple detection (refractive index, viscosity and light scattering) indicated values in the range between 16 000 and 35 000 g·mol⁻¹. Additionally, livingness of inimer-type living carbocationic polymerization was proven *via* inline FTIR-measurements by generating first-order kinetic plots and calculation of propagation rate constants (see Table 1, ESI†).

The amount of branches of the hyperbranched PIBs was calculated according to eqn (1),⁶²

$$\text{Amount of branches} = \frac{M_n}{M_{n,\text{theoretic}}} - 1 \quad (1)$$

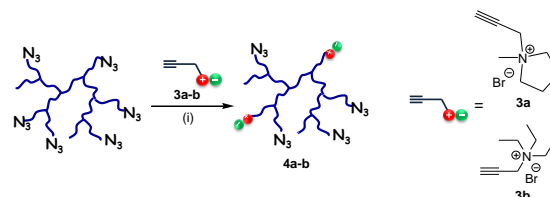
displaying branching degrees from 2.76 (Table 1, entry 7) up to 7.39 (Table 1, entry 4) with a calculated number of endgroups of the bromine-functionalized hyperbranched PIBs ranging from 3.75 (Table 1, entry 6) up to 8.72 (Table 1, entry 4).⁵⁴ For the hyperbranched polymer **2** quenched with TMPPS 3.04 endgroups per molecule (Table 1, entry 7) could be detected.

Endgroup modification of hyperbranched PIBs Subsequently the obtained bromine-functionalized hyperbranched PIBs were converted into the corresponding azide-functionalized hyperbranched polymers (**1a–d**) according to Scheme 1 using sodium azide in a DMF–*n*-heptane mixture at 90 °C for 20 hours. Alkyne-functionalized hyperbranched PIB (**2**) was obtained by treating the TMS-protected precursors with an excess of TBAF at room temperature for three days (Scheme 1).

Molecular weights of the investigated polymers ranged from 24 500 up to 35 400 g·mol⁻¹, with azide/alkyne-endgroups ranging from 3.04 (Table 2, entry 5) to 9.91 (Table 2, entry 2). Accordingly, this variety allowed us to study their influence on the network formation of hyperbranched PIBs intensely as the degree of functionality of the alkyne-modified hyperbranched PIB was kept

constant (Table 2, entry 5). Additionally hyperbranched PIBs **4a,b** partially containing an ionic moiety were prepared *via* a microwave-assisted CuAAC using Cu^(I)I as a catalyst (see Scheme 2) in order to study the influence of the ionic endgroup on the melt rheology of the hyperbranched PIBs.

Thus the hyperbranched PIB **1b** (9.91 azide-groups) was reacted with either 1-propargyl-1-methylpyrrolidinumbromide (**3a**) or *N*-propargyl-*N,N,N*-triethylammonium bromide (**3b**) to partially functionalize **1b** obtaining either 1-methylpyrrolidinium-functionalized hyperbranched PIB (**4a**) or *N,N,N*-triethylammonium-functionalized hyperbranched PIB (**4b**), both still containing a residual amount of azide-groups. An endgroup modification of ca. 20% could be achieved as confirmed *via* ¹HNMR-spectroscopy (see Fig. 3, ESI†).



Scheme 2 Synthetic route towards hyperbranched PIBs (**4a,b**) containing an ionic moiety *via* CuAAC. (i) Reaction conditions are given in the experimental section.

Melt rheology of the pure hyperbranched polymers **4a–b** and **1b**

Melt rheology and frequency sweep measurements were run in a broad frequency range in order to get deeper insights into the rheological behavior of hyperbranched PIBs **4a,b** compared to **1b**, before the reactive crosslinking was performed (see Fig. S4, ESI†). The observed slopes of the storage (G') and loss moduli (G'') (**1b**: 1.38 versus 0.90, **4a**: 0.61 versus 0.68, and **4b**: 0.68 versus 0.69) were indicative for a viscoelastic fluid with a more compact spherical topology. Furthermore values of the storage modulus of samples **4a,b** increased slower than for the structurally similar, but fully azide-functionalized hyperbranched PIB **1b** supporting the assumption of aggregation of the hyperbranched PIBs **4a,b** due to ionic cluster

formation. Unexpectedly the total values of the viscosity of all samples (see Table 2, 631.2 Pa·s (entry 2) up to 1120.3 Pa·s (entry 5)) were relatively high in comparison to linear/star-type PIBs of equal molecular weight^{60,66–69} explainable by the incorporation of aromatic core-structures into the PIB chain

Table 2 Results for hyperbranched PIBs (**1a–d**, **2** and **4a,b**), molecular weight data, amount of branches and amount of endgroups of hyperbranched azide-functionalized PIBs (**1a–d**), hyperbranched alkyne-functionalized PIB (**2**) and hyperbranched PIBs containing an ionic moiety (**4a,b**).

Entry	Polymer	Inimer/IB	M_n (g·mol ⁻¹)	M_w (g·mol ⁻¹)	M_w/M_n	Amount of branches (calc.) ^a	Integral of endgroup/ integral of inimer	Amount of endgroups (calc.) ^b
1	1a	0.010	34 600	241 300	7.0	5.18	0.89/1.00	4.61
2	1b	0.008	25 200	66 200	2.6	8.84	1.23/1.00	9.91
3	1c	0.008	35 400	109 600	3.1	4.06	1.50/1.00	6.09
4	1d	0.006	34 100	169 500	5.0	2.63	1.30/1.00	3.42
5	2	0.006	35 300	135 500	3.8	2.76	1.10/1.00	3.04
6	4a	0.008	24 500	43 600	1.8	8.57	1.24/1.00	9.92
7	4b	0.008	26 300	54 200	2.1	9.27	1.17/1.00	10.85

^a Amount of branches = $\frac{M_n}{M_{n,theoretic}} - 1$. ^b Amount of endgroups = amount of branches × integral of endgroup/integral of inimer.

Furthermore, temperature sweep measurements of samples **1b** and **4a,b** were conducted in a temperature range between -10 °C up to 120 °C to investigate flow properties of the pure hyperbranched PIBs (see Fig. 3).

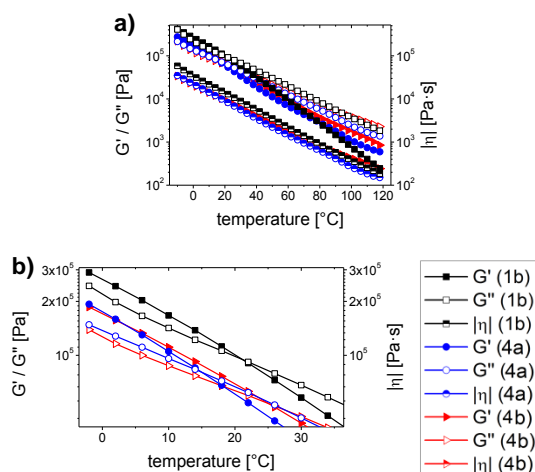


Fig. 3 Temperature sweep measurements of selected hyperbranched PIBs **1b** and **4a,b**: (a) whole temperature range between -10 and 120 °C, (b) enlargement: temperature range between -10 and 40 °C.

Roughly at room temperature terminal flow was observed for all polymers (**1b** and **4a,b**) and no additional order-to-disorder temperature or order-order transition temperature could be detected. Again the values of G' and G'' decreased for

due to the use of the inimer-type initiator. This assumption was confirmed by investigation of linear copolymers of IB with styrene to IB ratios similar to inimer to IB ratios applied in inimer-type LCCP showing similar viscosity values in the same frequency range (see ESI S5†).

hyperbranched PIBs **4a,b** at low temperatures whereas the value of the storage modulus of **1b** decreased much faster with increasing temperature thus additionally hinting at the existence of any partially structured ordering within hyperbranched PIBs containing an ionic moiety.

Melt rheology measurements of crosslinking hyperbranched PIBs

Crosslinking of the hyperbranched PIBs (see Fig. 1) *via* “click” chemistry was monitored by applying *in situ* melt rheology at 20 °C, using CuBr(PPh₃)₃ as a catalyst due to its high oxidation stability.^{54–56} While applying this technique the starting viscosity of the investigated polymer mixtures as well as the gelation time which was determined as the crossover of G' and G'' at 10 Hz was recorded. Furthermore, for all experiments the plateau moduli were measured at the total time, when the values of the storage and the loss modulus stayed constant at least for one hour. The so-obtained values were used to calculate the strand network densities of the formed networks according to eqn (2).

$$G_N = \nu_x RT \quad (2)$$

where R is the universal gas constant, $R = 8.3145 \text{ J mol}^{-1} \cdot \text{K}^{-1}$, and T is the

temperature, $T = 293.15$ K. The so-obtained results and the aforementioned parameters for the crosslinking reactions between hyperbranched PIBs can be found in Table 3.

In the first experiments we studied the crosslinking reaction of **1b** with **2** as **1b** displayed the highest amount of functional groups (9.91) within all synthesized azide-functionalized hyperbranched PIBs. Consequently, a crosslinking experiment of **1b** with **2** was conducted to yield gelation times of 39 minutes (Table 3, entry 1) which confirmed our choice to use azide- and alkyne-functionalized hyperbranched PIBs as suitable highly mobile components for network formation *via* “click” chemistry and thus, for self-healing applications. In order to further increase the fluidity within our system (and thus to decrease the gelation times) we additionally added 10 wt% of hyperbranched PIBs **4a,b** containing around 20% of an ionic moiety, expecting to observe a decreased gelation time due to the attached ionic liquid cations. Surprisingly, the detected gelation time for crosslinking **1b** with **2** and 10 wt% of **4a** was around 450 minutes and for crosslinking **1b** with **2** and 10 wt% of **4b** it was around 800 minutes (Table 3, entry 2 and 3) thus displaying even higher gelation times than the respective star-shaped trivalent azide- and alkyne-telechelic PIBs (290 minutes).⁵⁴ It is assumed that the low reactivity of polymer mixtures with an incorporated liquefying agent is due to the phase separation effects between the hydrophobic polymer backbone and the polar endgroups which were not expected to this extend due to the low degree of functionality of around 20%.

Therefore further crosslinking experiments without liquefying agent were performed to investigate the influence of the branching degree and therefore of the amount of endgroups on the kinetics of the network formation. The results obtained *via in situ* rheology measurements for crosslinking hyperbranched azide-functionalized PIBs **1a** and **1c–d** with hyperbranched alkyne-functionalized PIB **2** are summarized in Table 3.

We were especially interested in the impact of the degree of functionality on the gelation time and the experimentally determined network densities. Surprisingly, relatively short gelation times were recorded for all crosslinking reactions ranging between 30 and 50 minutes (Table 3, entry 4–6). Similar tendencies were observed for the network densities, which were in the range from $61 \text{ mol}\cdot\text{m}^{-3}$ (Table 3, entry 3) up to $98 \text{ mol}\cdot\text{m}^{-3}$ (Table 3, entry 6) and are therefore increased around 3 to 10 times in comparison to using star-PIBs as components for the crosslinking reactions.⁵⁴

A schematic picture of crosslinking the hyperbranched PIBs is imagined in Fig. 4, taking into account the molecular spherical architecture of hyperbranched PIBs and their thus limited crosslinking ability due to geometrical reasons. Thus autocatalytic behavior of the azide–alkyne-click-reaction can be ruled out, as the hindered molecular mobility disfavors the formation of catalytically active triazole-clusters needed for autocatalysis.

Table 3 Results obtained *via in situ* rheology and kinetic data for crosslinking hyperbranched PIBs: **1b** with **2** and 10 wt% **4a** and **1b** with **2** and 10 wt% **4b** and **1a–d** with **2** applying 5 wt% bromotris(triphenylphosphine)copper(I) as a catalyst at 20 °C.

Entry	Polymer mixture ^a	Starting viscosity at 100 Hz (Pa·s)	Gelation time at 10 Hz (min)	Total time (min)	G_N at 100 Hz $\times 10^5$ (Pa)	Network density (mol·m ⁻³)
1	1b + 2	1091.5	39	2350	2.30	93
2	1b + 2 + 4a ^b	975.8	445	2560	2.14	86
3	1b + 2 + 4b ^b	631.2	810	2750	1.51	61
4	1a + 2	685.7	50	4030	1.70	69
5	1c + 2	1120.3	35	3950	2.33	94
6	1d + 2	1097.6	33	4560	2.42	98

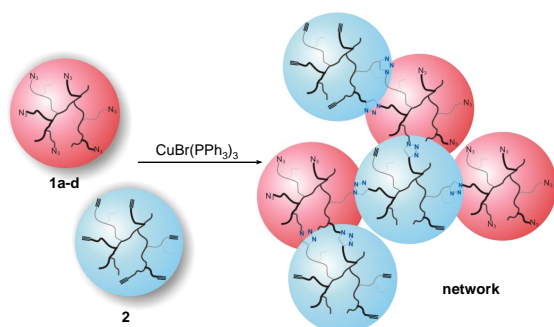


Fig. 4 Proposed mechanism for crosslinking hyperbranched azide- and alkyne-functionalized PIBs, applying bromotris(triphenylphosphine)copper(I) as a catalyst at 20 °C.

CONCLUSIONS

We report on a synthetic route towards hyperbranched azide- and alkyne-functionalized PIBs prepared by inimer-type living carbocationic polymerization of isobutylene applying 4-(2-methoxyisopropyl)styrene as an inimer followed by direct end quenching of living chain ends with either 3-(bromopropoxy) benzene (BPB) or trimethyl(3-phenoxy-1-propynyl)silane (TMPPS). After intensive investigation of the necessary quenching time and evaluation of the endgroup distribution *via* NMR-spectroscopy a series of bromine- and trimethylsilyl-protected alkyne-functionalized hyperbranched PIBs was obtained after 6 hours of quenching with BPB and after 20 hours of quenching with TMPPS. The so-prepared set of hyperbranched PIBs with different amounts of endgroups was converted into the corresponding hyperbranched azide- (**1a-d**) and alkyne-functionalized (**2**) PIBs *via* simple endgroup transformation suitable for “click” chemistry. The crosslinking reaction between hyperbranched azide- (**1a-d**) and alkyne-functionalized (**2**) polymers and the kinetics were studied *via in situ* melt rheology. Different parameters like gelation times, starting viscosities of the polymer mixtures and the final network densities were investigated depending on the amount of endgroups (varying from 3.04 (**2**) to 9.91 (**1b**)). Hyperbranched PIBs (**4a,b**) containing an ionic moiety were prepared to study their influence on the crosslinking process. The “click”

reaction of the respective azide- and alkyne-endgroups links the two hyperbranched, spherically shaped PIB molecules as proven *via* their fast gelation times (**1d** + **2**: 33 minutes), indicative of a fast crosslinking-reaction at room temperature. Higher network densities could be achieved as altogether more crosslinking points can be created in comparison to trivalent PIBs. Thus, both major drawbacks of the previously investigated star-shaped polymers could be overcome within this work and the concept of crosslinking hyperbranched azide- and alkyne-functionalized PIBs *via* “click” chemistry towards self-healing polymers acting at room temperature was successfully confirmed.

ABBREVIATIONS

CuAAC Copper(I)-catalyzed alkyne–azide “click” cycloaddition reaction
DtBP 2,6-Di-*tert*-butylpyridine
LCCP Living Carbocationic Polymerization
BPB 3-(Bromopropoxy)benzene
TMPPS Trimethyl(3-phenoxy-1-propynyl)silane
ATMS Allyltrimethylsilane
IB Isobutylene
PIB Poly(isobutylene)
DCM Dichloromethane
TBAF Tetrabutylammonium fluoride
DIPEA *N,N*-Diisopropylethylamine

ACKNOWLEDGEMENT

We gratefully acknowledge Grant DFG BI 1337/8-1 (within the SPP 1568 “Design and Generic Principles of Self-Healing Materials”).

NOTES AND REFERENCES

- (1) Self-Healing Polymers. From Principles to Applications, ed. W. H. Binder, Wiley-VCH Verlag GmbH & Co. KGaA, Weinheim, 2013.
- (2) E. B. Murphy and F. Wudl, *Prog. Polym. Sci.*, 2010, 35, 223–251.
- (3) B. J. Blaiszik, S. L. B. Kramer, S. C. Olugebefola, J. S. Moore, N. R. Sottos and S. R. White, *Annu. Rev. Mater. Res.*, 2010, 40, 179–211.
- (4) D. Döhler, P. Michael and W. H. Binder, in *Self Healing Polymers: from Principle to*

- Application, ed. W. H. Binder, Wiley-VCH Verlag GmbH & Co. KGaA, Weinheim, 2013.
- (5) F. Herbst and W. H. Binder, in *Self Healing Polymers: from Principles to Application*, ed. W. H. Binder, Wiley-VCH Verlag GmbH & Co. KGaA, Weinheim, 2013.
- (6) F. Herbst, D. Döhler, P. Michael and W. H. Binder, *Macromol. Rapid Commun.*, 2013, 34, 203–220.
- (7) M. M. Caruso, D. A. Davis, Q. Shen, S. A. Odom, N. R. Sottos, S. R. White and J. S. Moore, *Chem. Rev.*, 2009, 109, 5755–5798.
- (8) S. R. White, N. R. Sottos, P. H. Geubelle, J. S. Moore, M. R. Kessler, S. R. Sriram, E. N. Brown and S. Viswanathan, *Nature*, 2001, 409, 794–817.
- (9) T. C. Mauldin, J. Leonard, K. Earl, J. K. Lee and M. R. Kessler, *ACS Appl. Mater. Interfaces*, 2012, 4, 1831–1837.
- (10) R. T. M. Jakobs and R. P. Sijbesma, *Organometallics*, 2012, 31, 2476–2481.
- (11) N. Yoshie, M. Watanabe, H. Araki and K. Ishida, *Polym. Degrad. Stab.*, 2010, 95, 826–829.
- (12) G. O. Wilson, K. A. Porter, H. Weissman, S. R. White, N. R. Sottos and J. S. Moore, *Adv. Synth. Catal.*, 2009, 351, 1817–1825.
- (13) X. Sheng, J. K. Lee and M. R. Kessler, *Polymer*, 2009, 50, 1264–1269.
- (14) X. Liu, X. Sheng, J. K. Lee, M. R. Kessler and J. S. Kim, *Compos. Sci. Technol.*, 2009, 69, 2102–2107.
- (15) G. O. Wilson, J. S. Moore, S. R. White, N. R. Sottos and H. M. Andersson, *Adv. Funct. Mater.*, 2008, 18, 44–52.
- (16) J. K. Lee, X. Liu, S. H. Yoon and M. R. Kessler, *J. Polym. Sci., Part B: Polym. Phys.*, 2007, 45, 1771–1780.
- (17) J. D. Rule and J. S. Moore, *Macromolecules*, 2002, 35, 7878–7882.
- (18) E. N. Brown, N. R. Sottos and S. R. White, *Exp. Mech.*, 2002, 42, 372–379.
- (19) E. N. Brown, S. R. White and N. R. Sottos, *J. Mater. Sci.*, 2004, 39, 1703–1710.
- (20) E. N. Brown, S. R. White and N. R. Sottos, *Compos. Sci. Technol.*, 2005, 65, 2466–2473.
- (21) E. N. Brown, S. R. White and N. R. Sottos, *Compos. Sci. Technol.*, 2005, 65, 2474–2480.
- (22) J. D. Rule, N. R. Sottos and S. R. White, *Polymer*, 2007, 48, 3520–3529.
- (23) A. S. Jones, J. D. Rule, J. S. Moore, N. R. Sottos and S. R. White, *J. R. Soc. Interface*, 2007, 4, 395–403.
- (24) T. C. Mauldin, J. D. Rule, N. R. Sottos, S. R. White and J. S. Moore, *J. R. Soc. Interface*, 2007, 4, 389–393.
- (25) M. R. Kessler, N. R. Sottos and S. R. White, *Composites, Part A*, 2003, 34, 743–753.
- (26) M. R. Kessler and S. R. White, *Composites, Part A*, 2001, 32, 683–699.
- (27) A. J. Patel, N. R. Sottos, E. D. Wetzel and S. R. White, *Composites, Part A*, 2010, 41, 360–368.
- (28) J. D. Rule, E. N. Brown, N. R. Sottos, S. R. White and J. S. Moore, *Adv. Mater.*, 2005, 17, 205–208.
- (29) A. S. Jones, J. D. Rule, J. S. Moore, S. R. White and N. R. Sottos, *Chem. Mater.*, 2006, 18, 1312–1317.
- (30) G. O. Wilson, M. M. Caruso, N. T. Reimer, S. R. White, N. R. Sottos and J. S. Moore, *Chem. Mater.*, 2008, 20, 3288–3297.
- (31) J. M. Kamphaus, J. D. Rule, J. S. Moore, N. R. Sottos and S. R. White, *J. R. Soc. Interface*, 2008, 5, 95–103.
- (32) E. L. Kirkby, V. J. Michaud, J. A. E. Månson, N. R. Sottos and S. R. White, *Polymer*, 2009, 50, 5533–5538.
- (33) E. L. Kirkby, J. D. Rule, V. J. Michaud, N. R. Sottos, S. R. White and J.-A. E. Månson, *Adv. Funct. Mater.*, 2008, 18, 2253–2260.
- (34) K. S. Toohy, N. R. Sottos, J. A. Lewis, J. S. Moore and S. R. White, *Nat. Mater.*, 2007, 6, 581–585.
- (35) K. S. Toohy, N. R. Sottos and S. R. White, *Exp. Mech.*, 2009, 49, 707–717.
- (36) J. L. Moll, S. R. White and N. R. Sottos, *J. Compos. Mater.*, 2010, 44, 2573–2585.
- (37) T. C. Mauldin and M. R. Kessler, *J. Mater. Chem.*, 2010, 20, 4198–4206.
- (38) B. J. Blaiszik, M. Baginska, S. R. White and N. R. Sottos, *Adv. Funct. Mater.*, 2010, 20, 3547–3554.

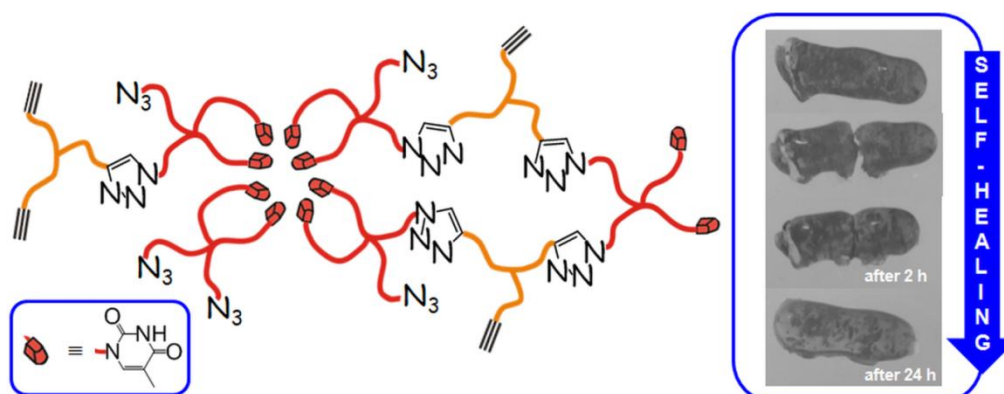
- (39) X. Liu, J. K. Lee, S. H. Yoon and M. R. Kessler, *J. Appl. Polym. Sci.*, 2006, 101, 1266–1272.
- (40) D. A. McIlroy, B. J. Blaiszik, M. M. Caruso, S. R. White, J. S. Moore and N. R. Sottos, *Macromolecules*, 2010, 43, 1855–1859.
- (41) M. M. Caruso, D. A. Delafuente, V. Ho, N. R. Sottos, J. S. Moore and S. R. White, *Macromolecules*, 2007, 40, 8830–8832.
- (42) C. L. Mangun, A. C. Mader, N. R. Sottos and S. R. White, *Polymer*, 2010, 51, 4063–4068.
- (43) S. H. Cho, H. M. Andersson, S. R. White, N. R. Sottos and P. V. Braun, *Adv. Mater.*, 2006, 18, 997–1000.
- (44) S. H. Cho, S. R. White and P. V. Braun, *Adv. Mater.*, 2009, 21, 645–649.
- (45) M. W. Keller, S. R. White and N. R. Sottos, *Adv. Funct. Mater.*, 2007, 17, 2399–2404.
- (46) M. W. Keller, S. R. White and N. R. Sottos, *Polymer*, 2008, 49, 3136–3145.
- (47) B. A. Beiermann, M. W. Keller and N. R. Sottos, *Smart Mater. Struct.*, 2009, 18, 085001.
- (48) S. Billiet, W. Van Camp, X. K. D. Hillewaere, H. Rahier and F. E. Du Prez, *Polymer*, 2012, 53, 2320–2326.
- (49) W. H. Binder and C. Kluger, *Curr. Org. Chem.*, 2007, 10, 1791.
- (50) W. H. Binder and R. Sachsenhofer, in *Click Chemistry for Biotechnology and Materials Science*, ed. J. Lahann, Wiley-Blackwell, 2009, pp. 119–175.
- (51) W. H. Binder and R. Sachsenhofer, *Macromol. Rapid Commun.*, 2007, 28, 15–54.
- (52) W. H. Binder and R. Sachsenhofer, *Macromol. Rapid Commun.*, 2008, 29, 952–981.
- (53) W. H. Binder and R. Zirbs, in *Encyclopedia of Polymer Science and Technology*, John Wiley & Sons, Inc, 2009, DOI: 10.1002/0471440264.pst0471440565.
- (54) D. Döhler, P. Michael and W. H. Binder, *Macromolecules*, 2012, 45, 3335–3345.
- (55) M. Gragert, M. Schunack and W. H. Binder, *Macromol. Rapid Commun.*, 2011, 32, 419–425.
- (56) M. Schunack, M. Gragert, D. Döhler, P. Michael and W. H. Binder, *Macromol. Chem. Phys.*, 2012, 213, 205–214.
- (57) X. Sheng, T. C. Mauldin and M. R. Kessler, *J. Polym. Sci., Part A: Polym. Chem.*, 2010, 48, 4093–4102.
- (58) F. Herbst, S. Seiffert and W. H. Binder, *Polym. Chem.*, 2012, 3, 3084–3092.
- (59) O. Nuyken, F. Gruber, S. D. Pask, A. Riederer and M. Walter, *Makromol. Chem.*, 1993, 194, 3415–3432.
- (60) J. E. Puskas and M. Grasmüller, *Macromol. Symp.*, 1998, 132, 117–126.
- (61) E. A. Foreman, J. E. Puskas and G. Kaszas, *J. Polym. Sci., Part A: Polym. Chem.*, 2007, 45, 5847–5856.
- (62) C. Paulo and J. E. Puskas, *Macromolecules*, 2001, 34, 734–739.
- (63) A. A. Albarran, M. Luebbers and J. E. Puskas, *Polym. Prepr.*, 2012, 53, 183–184.
- (64) J. E. Puskas, Y. Chen, K. Kulbaba, G. Kaszas and A. Soleymannezhad, *J. Polym. Sci., Part A: Polym. Chem.*, 2006, 44, 1770–1776.
- (65) J. E. Puskas, E. A. Foreman, L. M. Dos Santos and S. H. Soyta&scdil, *Macromol. Symp.*, 2008, 261, 85–90.
- (66) J. E. Puskas, Y. Kwon, P. Antony and A. K. Bhowmick, *J. Polym. Sci., Part A: Polym. Chem.*, 2005, 43, 1811–1826.
- (67) C. Gong and J. M. J. Fréchet, *J. Polym. Sci., Part A: Polym. Chem.*, 2000, 38, 2970–2978.
- (68) J. E. Puskas, P. Antony, Y. Kwon, M. Kovar and P. R. Norton, *Macromol. Symp.*, 2002, 183, 191–198.
- (69) P. Antony, Y. Kwon, J. E. Puskas, M. Kovar and P. R. Norton, *Eur. Polym. J.*, 2004, 40, 149–157.
- (70) A. Stojanovic, C. Appiah, D. Döhler, J. Akbarzadeh, P. Zare, H. Peterlik and W. H. Binder, *J. Mater. Chem. A*, 2013, 1, 12159–12169.
- (71) P. Zare, A. Stojanovic, F. Herbst, J. Akbarzadeh, H. Peterlik and W. H. Binder, *Macromolecules*, 2012, 45, 2074–2084.
- (72) D. L. Morgan, N. Martinez-Castro and R. F. Storey, *Macromolecules*, 2010, 43, 8724–8740.

(73) T. G. Metzger, *The Rheology Handbook: For users of rotational and oscillatory rheometers*, Vincentz Network, Hannover, 2006.

(74) D. L. Morgan and R. F. Storey, *Macromolecules*, 2009, 42, 6844–6847.

(75) J. Si and J. P. Kennedy, *J. Polym. Sci., Part A: Polym. Chem.*, 1994, 32, 2011–2021.

6.3. A dual crosslinked self-healing system: Supramolecular and covalent network formation of four-arm star polymers



ABSTRACT

Restoration of large volume damage together with mechanical stability of self-healing polymers requires fast and efficient reversible crosslinking processes together with the presence of a static network. We investigate four-arm star polymers as a dual self-healing material, equipped with hydrogen bonding moieties and azide endgroups applicable for crosslinking based on “click” cycloaddition reaction (CuAAC). The concept takes advantage of additional supramolecular network formation due to supramolecular cluster formation. To this effect four-arm star poly(isobutylene)s were prepared *via* living carbocationic polymerization (LCCP) in combination with simple endgroup transformation steps and microwave-assisted click-chemistry to introduce thymine moieties as supramolecular tie points. Four-arm star thymine-telechelic PIB was obtained as a tough rubbery material as proven *via* melt rheology and SAXS measurements with clusters of ≈ 10 hydrogen bonding moieties resulting in a self-healing response at room temperature. To enable the design of a doubly crosslinked self-healing system, four-arm star PIBs bearing an average of 1.7 azide groups and 2.3 thymine endgroups/polymer were crosslinked with a three-arm star alkyne-telechelic PIB. A weakly crosslinked covalent network reinforced by supramolecular hydrogen bonding interactions was obtained in which “click”-crosslinking reduces the number of clustered hydrogen bonds from ≈ 10 to ≈ 8 . Macroscopic self-healing studies of the double covalent and supramolecular network structure revealed fast and multiple self-healing at 20 °C within 24 h. The now designable four-arm star polymers enabled the design of a highly efficient self-healing system based on double network formation due to “click”-crosslinking and supramolecular cluster formation.

INTRODUCTION

The development and further improvement of self-healing polymers to effect faster self-healing systems operating at ambient conditions is attracting the interest of many materials scientists¹. Therefore, fast and efficient crosslinking reactions leading to subsequent network formation to generate complex architectures play a key role in order to impart mechanical stability within a material after the self-healing event². Network formation can be realized *via* chemical crosslinking based on Diels–Alder (DA)

chemistry³, disulfide exchange reactions⁴, curing of epoxides⁵, ROMP^{1c,d, 5a, 6} or “click”-type-reactions like the azide/alkyne-“click”-reaction (CuAAC)⁷, where the former reactions are exceptionally well-suited for tuning the timescale of the crosslinking reaction^{2a, 8}. The CuAAC in particular opens suitable pathways for crosslinking approaches not only for the design of self-healing materials⁹ but also for the preparation of polymer nanoparticles¹⁰, particle-like structures¹¹ or cellulose nanoplatelet gels¹². While using chemical

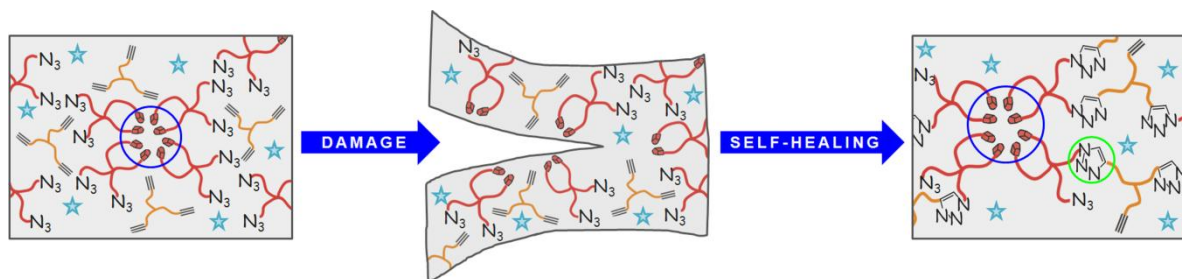


Fig. 1 Concept of a doubly crosslinked self-healing system based on supramolecular and covalent network formation *via* CuAAC (★ ≡ Cu(I)-catalyst, ● ≡ supramolecular moiety).

crosslinking concepts often reactive components are applied, which require encapsulation^{8a, 13} or are stored in an appropriate container within a (polymer) matrix in order to prevent their reaction or degradation before a damage event occurs¹⁴. However, the aforementioned systems are often just either working at elevated temperatures¹⁵ or can be applied for healing of a single damage event only. Another self-healing concept not showing these drawbacks is applying supramolecular interactions such as hydrogen bonds^{16a,b, 17}, ionomers¹⁸, π - π -stacking interactions¹⁹ or metal ligand interactions²⁰ where a multiple self-healing response can be realized *via* rebonding of supramolecular moieties. One of the first concepts based on hydrogen bonding was reported by Lehn^{16b}, who introduced the term “dynamers” (dynamic polymers) allowing reversible formation and exchange reactions within a polymeric material. The well known hydrogen bonds based on 2-ureido-4[1*H*]-pyrimidinones²¹ provide a good basis for the commercially available self-healing material SupraB^{TM21,22}. Although already several supramolecular polymers find application in self-healing materials, the final supramolecular networks are often soft and not shape-persistent. Therefore the generation of sufficient mechanical stability within such a polymeric material is still challenging. In order to reinforce the mechanical stability either multiphase systems with hard-soft-segments analogous to the creation of thermoplastic elastomers (TPEs)²³ or nanoparticles²⁴ can be introduced into the polymer. Other strategies rely on the formation of rubber-like self-healing materials^{16a, 25}, where the building

blocks themselves show sufficient high mobility and dynamics. We in the past^{2c} have investigated bivalent barbiturate-functionalized PIBs resulting in tough rubbery materials with increased thermal stability and self-healing abilities at room temperature due to dynamic supramolecular cluster formation^{2b,c, 26}. Overall, the generation of newly formed covalent or supramolecular bonds and thus network formation represents a key requirement for a successful healing response and for the restoration of mechanical properties, e.g. based on amphiphilic co-networks (APCN)²⁷.

To overcome the aforementioned disadvantages of covalent and supramolecular self-healing concepts, we have designed a self-healing system based on double network formation by combining a covalent network together with a supramolecular and therefore multiple self-healing concept based on hydrogen bonding moieties forming supramolecular clusters (see Fig. 1). If now a damage event is occurring the already existing supramolecular aggregates, formed *via* phase separation effects between the nonpolar polymer backbone and the polar supramolecular moiety will break, resulting in two newly generated surfaces with sticky supramolecular tie points. The now *via* an additional covalent network crosslinked polymer is reinforced and thus structurally stable, enabling self-healing *via* reformation of the supramolecular aggregates between the covalent tie points.

To enable a realization of this concept, star polymers functionalized with azide-endgroups and hydrogen bonding moieties simultaneously were prepared in

order to introduce both, the covalent tie points (*via* CuAAC) and the hydrogen bonding moieties acting as the supramolecular (reversible) network. Covalent crosslinking was effected by subsequent mixing with a second component, (a three-arm star alkyne-telechelic polymer) and a copper(I)-catalyst, in turn effecting subsequent covalent network formation *via* CuAAC.

EXPERIMENTAL SECTION

Instrumentation

NMR spectra were recorded on a Varian Gemini 2000 (400 MHz) at 27 °C. Deuterated chloroform (CDCl₃) was used as solvent. All chemical shifts were given in ppm. MestRec-C software (version 4.9.9.6) was used for interpretation of the NMR-spectra.

ATR-IR spectra were performed on a Bruker Tensor VERTEX 70 equipped with a Golden Gate Heated Diamond ATR Top-plate. Opus 6.5 was used for analyzing data.

Gel permeation chromatography (GPC) measurements were performed on a Viscotek GPCmax VE 2002 from Viscotek™ using a H_{HR}H Guard-17369 and a GMH_{HR}-N-18055 column in THF at 40 °C and *via* detection of the refractive index with a VE 3580 RI detector of Viscotek™. For external calibration PIB-standards (320 g/mol to 578,000 g/mol) from Viscotek™ were used. In case of PIBs functionalized with supramolecular moieties GPC spectra were recorded on a GPCmax VE 2001 from Viscotek™ equipped with a column set of a H_{HR}-H Guard-17369 column, a CLM30111 column and a G2500H_{HR}-17354 column in THF (1 mL/min) at 35 °C. For determination of absolute molecular weights a triple detection array (light scattering, viscosity, refractive index) was applied. Calibration was performed using PS-standards (1000 g/mol to 115,000 g/mol). For evaluation of data OmniSEC software (V 4.5.6) was used. The concentration of all samples was 3 mg/mL and the flow rate was 1 mL/min.

Differential scanning calorimetry (DSC) experiments were performed using a DSC 204 F1 Phoenix provided from

NETZSCH. In order to investigate the glass transition temperature (T_g) polymers were first cooled to -90 °C and then heated up to 160 °C with a heating rate of 10 K·min⁻¹. T_g 's were determined upon heating from the amorphous glass state of the polymers to the liquid state as midpoint of a small change within the heat capacity. For analyzing of data Proteus-Thermal Analysis (V5.2.1) from NETZSCH was applied.

Thermogravimetric analysis (TGA) was performed on a NETZSCH TG tarsus 209 instrument. Under a nitrogen atmosphere the sample was heated in a Pt pan over a temperature range of 25 °C up to 800 °C with a heating rate of 10 °C·min⁻¹. For analyzing of data OriginPro7 was used.

Matrix-assisted laser desorption/ionization time-of-flight mass spectrometry (MALDI-ToF-MS) experiments were performed on a Bruker Autoflex III system operating in linear mode. For data evaluation flexAnalysis software (version 3.0) was used. Ions were formed by laser desorption (smart beam laser at 355, 532, 808, and 1064 ± 6.5 nm; 3 ns pulse width; up to 2500 Hz repetition rate), accelerated by a voltage of 20 kV, and detected as positive ions. As matrix *trans*-2-[3-(4-*tert*-butylphenyl)-2-methyl-2-propenylidene]malononitrile (DCTB) was used dissolved in THF at a concentration of 20 mg·mL⁻¹. Four-arm star thymine-functionalized PIB and four-arm star PIB with azide and thymine endgroups as well as lithium trifluoroacetate (LiTFA) were dissolved in THF at a concentration of 20 mg·mL⁻¹. Solutions of the applied matrix, the polymer, and the salt were mixed in a volume ratio of 25:5:1. Smoothing and baseline subtraction of the recorded MALDI-ToF-MS spectrum was performed using a three point Savitzky–Golay algorithm.

Rheological measurements were performed on an oscillatory plate rheometer MCR 101 from Anton Paar (Physica). For all measurements a PP08 measuring system (parallel plated, diameter 8 mm) was used. For regulating the sample temperature thermoelectric cooling/heating in a Peltier

chamber under dry oxygen was applied. Frequency measurements were performed within the LVE. For evaluation of data the RheoPlus/32 software (V 3.40) and OriginPro7 was used.

Small-angle X-ray scattering (SAXS) experiments were performed with Cu-K α radiation (wavelength 0.1542 nm) from a microfocus source (Incoatec High Brilliance) using a pinhole camera system (Nanostar, Bruker AXS, equipped with a 2D position sensitive detector, Vantec 2000). SAXS investigations were performed at room temperature (23 °C) in a q -range of 0.2–2.8 nm⁻¹ and the samples were placed between commercial aluminum foils.

Abbreviations

LCCP	Living carbocationic polymerization
DtBP	2,6-Di- <i>tert</i> -butylpyridine
DMA	<i>N,N</i> -Dimethylacetamide
BPTCC	Biphenyl tetracumyl chloride
BPB	3-(Bromopropoxy)benzene
IB	Isobutylene
PIB	Poly(isobutylene)
DCM	Dichloromethane
CuAAC	Copper(I)-catalyzed alkyne-azide cycloaddition
DIPEA	<i>N,N</i> -Diisopropylethylamine
TBTA	Tris[(1-benzyl-1 <i>H</i> -1,2,3-triazol-4-yl)methyl]amine
SAXS	Small-angle X-ray scattering

Materials

All materials were obtained from Sigma-Aldrich and used without further purification if not mentioned otherwise. *N*-hexane was predried over KOH and freshly distilled over sodium and KOH under a nitrogen atmosphere prior to use. DCM was predried over CaCl₂ and freshly distilled over CaH₂ under nitrogen atmosphere prior to use.

Synthesis

The synthesis of biphenyl tetracumyl chloride (tetravalent initiator for LCCP) was carried out according to literature²⁸. Synthesis of TBTA was done according to Lee et al.²⁹ Three-arm star alkyne-telechelic PIB was prepared out of

trimethylsilyl-protected alkyne-telechelic PIB which was synthesized *via* LCCP^{2a}.

General polymerization procedure - synthesis of four-arm star bromide-telechelic PIB (1)

For the polymerization of isobutylene living carbocationic polymerization (LCCP) was used. The synthesis was carried out under a dry atmosphere of argon. A three-necked round-bottom flask equipped with rubber septum, stop cock and mechanical stirrer was heated under vacuo and flushed with argon several times. Dry *n*-hexane and dry DCM ($v/v = 40/60$) was added to the flask and the solution was started to cool down to -70 °C with a methanol cooling bath and liquid nitrogen. During cooling DtBP (0.005 mol·L⁻¹), DMA (0.005 mol·L⁻¹) and BPTCC (0.006 mol·L⁻¹, 80% activity) as initiator dissolved in dry DCM was added and condensed and dried isobutylene (1.000 mol·L⁻¹) was added at the final temperature. The reaction mixture was stirred at -70 °C for 10 minutes before the polymerization was started by the addition of TiCl₄ (0.100 mol·L⁻¹). Polymerizations were run for 90 minutes. As quenching agent 3-(bromopropoxy)benzene (BPB, 10 equ. of BPTCC) and a second portion of TiCl₄ (0.112 mol·L⁻¹) was used to introduce bromine endgroups. Quenching proceeded for 5 h in order to achieve complete functionalization of living chain ends. Therefore isopropyl alcohol and dry ice was used as cooling agent. After warming up to room temperature the solvent was removed in vacuo. The crude polymer was dissolved in *n*-hexane and was precipitated into a ten to fifteen excess of MeOH for three times and dried at high vacuo. ¹H-NMR (CDCl₃, 400 MHz): δ 7.26 (d, 8H, Ar-*H* of quenching agent, ³J_{H,H} = 8.6 Hz), 7.10–6.88 (m, 6H, Ar-*H* of initiator), 6.82 (d, 8H, Ar-*H* of quenching agent, ³J_{H,H} = 8.6 Hz), 4.09 (t, 8H, O-CH₂, ³J_{H,H} = 6.4 Hz), 3.59 (t, 8H, CH₂-Br, ³J_{H,H} = 5.9 Hz), 2.32 (q, 8H, CH₂-CH₂-CH₂, ³J_{H,H} = 6.1 Hz), 1.42 (s, CH₂ of repetitive unit), 1.11 (s, CH₃ of repetitive unit), 0.80 (s, 24H, CH₃ of initiator part).

Synthesis of four-arm star azide-telechelic PIB (2)

The synthesis was carried out under a dry atmosphere of nitrogen. In a two-necked flask equipped with magnetic stirring bar, septum, reflux condenser and stop cock PIB **1** (1 equ., 200.0 mg, 24.7 mmol) was dissolved in a 1: 1 mixture of *n*-heptane (10.0 mL) and DMF (10.0 mL). To the reaction mixture sodium azide (40 equ., 64.3 mg, 987.6 mmol) was added and heated up to 90 °C for 65 h. After the reaction mixture cooled down, the *n*-heptane-layer was separated and washed with water (five times 25.0 mL). The organic layer was separated and dried over Na₂SO₄ and after filtration the solvent was removed in vacuo. The crude polymer was dissolved in *n*-hexane and was precipitated into a ten to fifteen excess of MeOH for three times and dried at high vacuo. ¹H-NMR (CDCl₃, 400 MHz): δ 7.26 (d, 8H, Ar-*H* of quenching agent, ³J_{H,H} = 8.6 Hz), 7.10–6.88 (m, 6H, Ar-*H* of initiator), 6.81 (d, 8H, Ar-*H* of quenching agent, ³J_{H,H} = 8.7 Hz), 4.03 (t, 8H, O-CH₂, ³J_{H,H} = 5.9 Hz), 3.51 (t, 8H, CH₂-N₃, ³J_{H,H} = 6.6 Hz), 2.04 (q, 8H, CH₂-CH₂-CH₂, ³J_{H,H} = 6.2 Hz), 1.42 (s, CH₂ of repetitive unit), 1.11 (s, CH₃ of repetitive unit), 0.80 (s, 24H, CH₃ of initiator part).

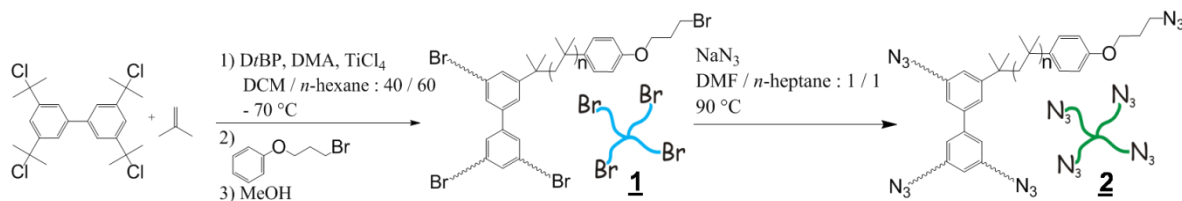
Synthesis of four-arm star thymine-functionalized PIB (3)

The synthesis was carried out under a dry atmosphere of argon. In a one-necked flask equipped with magnetic stirring bar PIB **2** (1.0 equ., 300.0 mg, 38.5 mmol) was dissolved in toluene (5.0 mL). Isopropanol (2.0 mL), water (2.0 mL), DIPEA (8.0 equ., 55.1 mL, 308.0 mmol) and TBTA (0.2 equ., 4.1 mg, 7.7 mmol) were added and the reaction mixture was purged with argon for 40 minutes. CuBr(PPh₃)₃ (0.2 equ., 7.1 mg, 7.7 mmol) was added followed by purging with argon for 5 minutes and then alkyne-functionalized thymine (8.0 equ., 51.0 mg, 308.0 mmol) was added to the reaction mixture. After a final purging with argon for 5 minutes the flask was sealed with a rubber septum and placed in a microwave oven. Irradiation conditions: 100

W, 90 °C, ΔT = 10 °C, SPS method (“pulse – no pulse – pulse”), 32 h. After the reaction was finished (R_f (CHCl₃) = 0.05) the crude reaction mixture was diluted with chloroform (50.0 mL). The organic layer was washed with saturated NH₄Cl-solution (two times 50.0 mL) and with water (50.0 mL). The organic layer was separated and dried over Na₂SO₄ and after filtration the solvent was removed in vacuo. The crude polymer was purified *via* column chromatography (SiO₂, *n*-hexane/CHCl₃ (v:v = 1:2) followed by CHCl₃, CHCl₃/MeOH (v:v = 100:2) and CHCl₃/MeOH (v:v = 100:3)). The so obtained polymer was finally purified *via* dialysis in THF and dried at high vacuo. ¹H-NMR (CDCl₃, 400 MHz): δ 8.15 (s, 4H, N-*H*), 7.69 (s, 4H, CH of thymine endgroup), 7.33 (s, 4H, CH of triazole ring), 7.26 (d, 8H, Ar-*H* of quenching agent, ³J_{H,H} = 8.6 Hz), 7.10–6.87 (m, 6H, Ar-*H* of initiator), 6.78 (d, 8H, Ar-*H* of quenching agent, ³J_{H,H} = 8.7 Hz), 4.94 (s, 8H, C-CH₂-N), 4.57 (t, 8H, O-CH₂, ³J_{H,H} = 7.0 Hz), 3.97 (t, 8H, CH₂-CH₂-N, ³J_{H,H} = 5.6 Hz), 2.38 (q, 8H, CH₂-CH₂-CH₂, ³J_{H,H} = 6.3 Hz), 1.41 (s, CH₂ of repetitive unit), 1.11 (s, CH₃ of repetitive unit), 0.79 (s, 24H, CH₃ of initiator part).

Synthesis of four-arm star PIBs with azide and thymine endgroups (4a, 4b)

The synthesis was carried out under a dry atmosphere of argon. In a one-necked flask equipped with magnetic stirring bar PIB **2** (1.0 equ., 300.0 mg, 38.5 mmol) was dissolved in toluene (5.0 mL). Isopropanol (2.0 mL), water (2.0 mL), DIPEA (8.0 equ., 55.1 mL, 308.0 mmol) and TBTA (0.2 equ., 4.1 mg, 7.7 mmol) were added and the reaction mixture was purged with argon for 40 minutes. CuBr(PPh₃)₃ (0.2 equ., 7.1 mg, 7.7 mmol) was added followed by purging with argon for 5 minutes and then alkyne-functionalized thymine (1.1 equ., 7.0 mg, 42.4 mmol) was added to the reaction mixture. After a final purging with argon for 5 minutes the flask was sealed with a rubber septum and placed in a microwave oven. Irradiation conditions: 100 W, 90 °C, ΔT = 10 °C, SPS method (“pulse – no pulse – pulse”), 17 h.



Scheme 1 Synthetic route towards four-arm star bromide- **1** and azide-telechelic **2** PIBs.

After irradiation the crude reaction mixture was diluted with chloroform (20.0 mL). The organic layer was washed with saturated NH_4Cl -solution (two times 25.0 mL) and with water (25.0 mL). The organic layer was separated and dried over Na_2SO_4 and after filtration the solvent was removed in vacuo. The crude polymer was purified *via* column chromatography (SiO_2 , solvent gradient: *n*-hexane/ CHCl_3 (v:v = 1:1), CHCl_3 , $\text{CHCl}_3/\text{MeOH}$ (v:v = 100:1), $\text{CHCl}_3/\text{MeOH}$ (v:v = 100:2) and $\text{CHCl}_3/\text{MeOH}$ (v:v = 100:5)). Thus, two polymer fractions (R_{f1} = 0.08–0.36, R_{f2} = 0.03–0.13) were obtained and were finally purified separately *via* dialysis in THF and dried at high vacuo. $^1\text{H-NMR}$ (CDCl_3 , 400 MHz): δ 8.01 (s, N-H), 7.68 (s, CH of thymine endgroup), 7.33 (s, CH of triazole ring), 7.26 (d, 8H, Ar-H of quenching agent, $^3J_{\text{H,H}}$ = 8.6 Hz), 7.09–6.88 (m, 6H, Ar-H of initiator), 6.78 (d, 8H, Ar-H of quenching agent, $^3J_{\text{H,H}}$ = 8.7 Hz), 4.94 (s, C- CH_2 -N), 4.57 (t, O- CH_2 of thymine endgroup, $^3J_{\text{H,H}}$ = 7.0 Hz), 4.03 (t, O- CH_2 of azide endgroup, $^3J_{\text{H,H}}$ = 6.1 Hz), 3.97 (t, CH_2 - CH_2 -N of thymine endgroup, $^3J_{\text{H,H}}$ = 5.7 Hz), 3.51 (t, CH_2 - CH_2 -N of azide endgroup, $^3J_{\text{H,H}}$ = 6.6 Hz), 2.38 (q, CH_2 - CH_2 - CH_2 of thymine endgroup, $^3J_{\text{H,H}}$ = 6.3 Hz), 2.04 (q, CH_2 - CH_2 - CH_2 of azide endgroup, $^3J_{\text{H,H}}$ = 6.3 Hz), 1.41 (s, CH_2 of repetitive unit), 1.11 (s, CH_3 of repetitive unit), 0.79 (s, 24H, CH_3 of initiator part).

RESULTS AND DISCUSSION

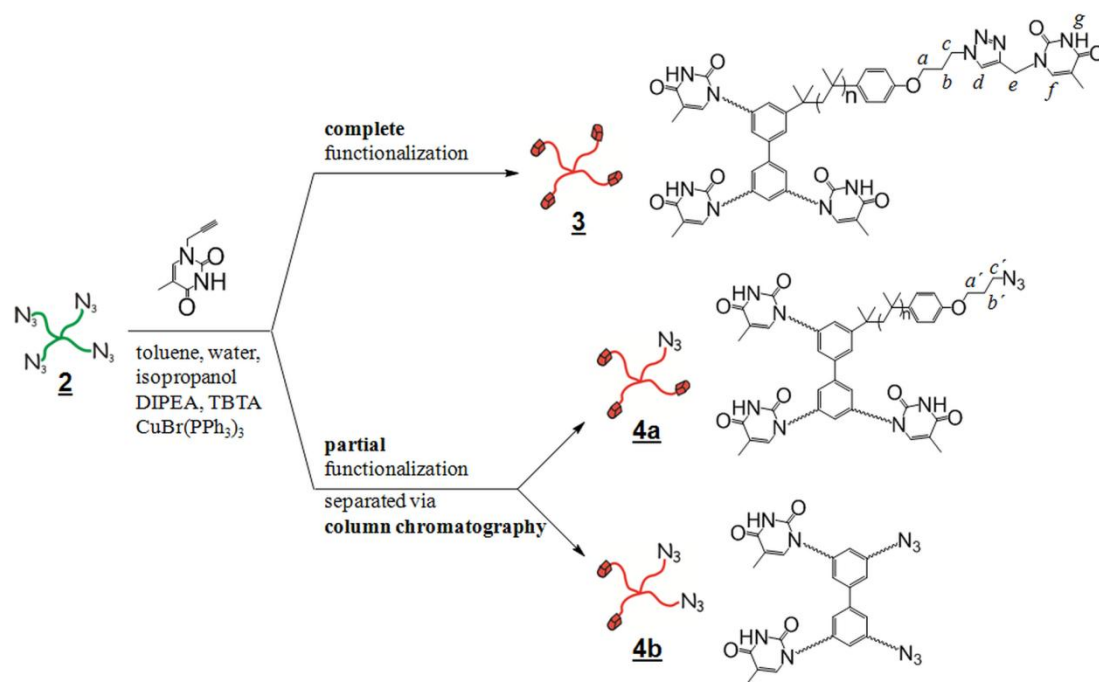
Synthesis and characterization of four-arm star PIBs

We have planned the self-healing system based on supramolecular and covalent network

formation of star polymers based on the preparation of four-arm star polymers (poly(isobutylene)s (PIBs)) bearing thymine- and azide-endgroups, the latter enabling covalent crosslinking *via* a CuAAC process in combination with a three-arm star alkyne-telechelic polymer (see Fig. 1). The basic architecture is generated *via* the four-arm star PIB (**2**), able to be subsequently functionalized *via* “click”-based chemistry. Four-arm star bromide-telechelic PIB **1** was prepared *via* living carbocationic polymerization (LCCP, see Scheme 1) using biphenyl tetracumyl chloride (BPTCC) as initiator and 3-(bromopropoxy)benzene (BPB) as quencher^{28, 30}.

In order to achieve the desired architecture as well as complete endgroup functionalization the polymerization was conducted for 90 minutes followed by a quenching period of 5 h combined with repeated addition of TiCl_4 to force the equilibrium towards four-arm star bromide-telechelic PIB **1**^{28, 30}. Complete endgroup functionalization of PIB **1** was proven *via* $^1\text{H-NMR}$ -analysis as the resonances of the six aromatic protons of the quenching unit and the resonances of the methyl groups of the initiator part (24 protons) are in relation of one to four (see Fig. S1 Supporting Information).

For the preparation of four-arm star azide-telechelic PIB **2** a simple endgroup transformation methodology using sodium azide and heating in a 1: 1 mixture of *n*-heptane and DMF at 90 °C for 65 h was applied (see Scheme 1). In order to synthesize



Scheme 2 Synthetic route towards four-arm star thymine-telechelic **3** PIB and four-arm star PIBs with azide and thymine endgroups **4a** and **4b** via copper(I)-catalyzed alkyne-azide cycloaddition (CuAAC) of four-arm star azide-telechelic PIB **2** with alkyne-functionalized thymine.

four-arm star thymine-telechelic PIB **3** via a microwave-assisted copper(I)-catalyzed alkyne-azide cycloaddition (CuAAC) reaction^{26a} (see Scheme 2), polymer **2** was treated with alkyne-functionalized thymine in a solvent mixture of toluene, water and isopropanol.

Additionally, *N,N*-diisopropylethylamine (DIPEA, 8.0 equ.), tris[(1-benzyl-1*H*-1,2,3-triazol-4-yl)methyl]amine (TBTA, 0.2 equ.) and $\text{CuBr}(\text{PPh}_3)_3$ (0.2 equ.) were added and reacted under microwave irradiation.

The desired polymer **3** was obtained via column chromatography followed by dialysis. In a similar manner four-arm star PIBs with both, azide- and thymine-endgroups **4a** and **4b** were synthesized (see Scheme 2). The already optimized reaction conditions of the microwave-assisted CuAAC reaction were adapted and the reaction time was decreased from 32 to 17 hours with respect to the functional endgroups of polymer **2**. Furthermore, the amount of alkyne-functionalized thymine was reduced from 8.0 to 1.1 equivalents. Following the aforementioned work-up strategy two

polymers **4a** and **4b** with different endgroup compositions were separated via column chromatography and further cleaned up via dialysis. The complete endgroup transformation within the four-arm star azide-telechelic PIB **2** and thymine-telechelic PIB **3** after click-reaction as well as the endgroup composition of partially thymine-functionalized PIBs **4a** and **4b** was investigated and proven via FTIR- and ¹H-NMR-spectroscopy (see Fig. 2a and b).

According to the FTIR-spectra displayed in Fig. 2a the stretching vibration of the azide group is visible at 2097 cm^{-1} in case of polymer **3**. Consequently, no azide group was detected in PIB **3** after complete conversion of all azide groups with alkyne-functionalized thymine. Instead, the carbonyl stretching vibration of the attached thymine moiety was observed at 1690 cm^{-1} . The ¹H-NMR-analysis of the four-arm star azide-telechelic PIB **2** clearly revealed a shift of the resonances of the CH_2 -groups of the quencher part to higher field in comparison to four-arm star bromide-telechelic PIB **1** (e.g.

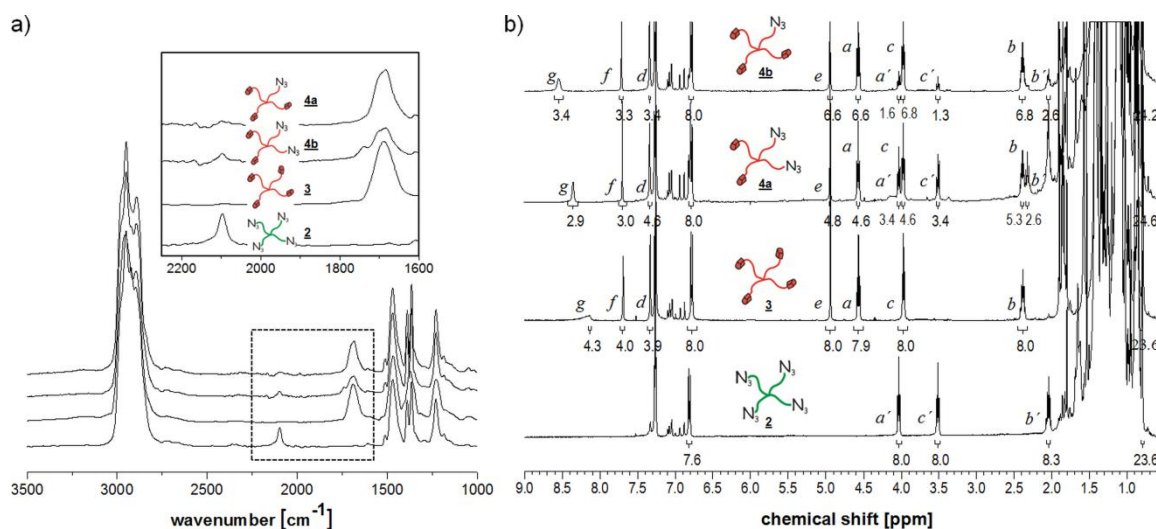


Fig. 2 a) FTIR-spectra of four-arm star PIBs **2**, **3**, **4a** and **4b**, b) $^1\text{H-NMR}$ -spectra of four-arm star PIBs **2**, **3**, **4a** and **4b**.

Table 1 Results for the synthesis of four-arm star PIBs **1** - **4b**, molecular weight data, polydispersities, glass transition temperatures (T_g), decomposition temperatures and azide endgroups of four-arm star PIBs **2** - **4b**.

Entry	Polymer	$M_{n, \text{theor.}}$ [g/mol]	M_n , NMR ^a [g/mol]	M_n , GPC [g/mol]	M_w / M_n ^b	Amount of azide endgroups ^c	T_g [°C]	T_{decay} ^d [°C]
1	PIB-Br ₄ 1	8,000	7,400	8,500	1.55	-	- 58.2	325.0
2	PIB-(N ₃) ₄ 2	8,000	7,500	8,400	1.52	4.0	- 59.7	301.4
3	PIB-thymine ₄ 3	8,700	8,100	9,300	1.48	0.0	- 59.0	360.3
4	PIB-thymine ₃ -(N ₃) 4a	8,500	8,000	11,300	1.76	0.7	- 59.8	350.4
5	PIB-thymine ₂ -(N ₃) ₂ 4b	8,300	8,800	10,500	1.98	1.7	- 58.5	295.2

^a determined via $^1\text{H-NMR}$ -spectroscopy: integration of resonances of initiator at 0.79 ppm to 0.80 ppm and of polymer at 1.11 ppm or at 1.40 ppm to 1.42 ppm. ^b determined via GPC. ^c determined via $^1\text{H-NMR}$ -spectroscopy. ^d determined at 5 % weight loss.

from 2.32 ppm to 2.04 ppm for $\text{CH}_2\text{-CH}_2\text{-CH}_2$), followed by an even more prominent low-field shift (e.g. from 2.04 ppm (b') to 2.38 ppm (b) for $\text{CH}_2\text{-CH}_2\text{-CH}_2$) for four-arm star thymine-telechelic PIB **3**.

Additionally, the resonances of the amine proton (g) and the CH proton of the thymine group (f) as well as the resonance of the click proton (d) were observed indicating a successful click reaction and a complete functionalization with the supramolecular moieties (see Fig. 2b).

The FTIR-spectra of PIBs **4a** and **4b** after partial functionalization with thymine groups after the click reaction show both, the stretching vibration of the azide group and the carbonyl stretching vibration of the supramolecular moiety proving qualitatively the presence of both desired endgroups. A

quantitative analysis of the endgroup composition within polymers **4a** and **4b** was accomplished via NMR-analysis. The resonances of the CH_2 -moieties of the quencher part bearing either the azide group or the thymine endgroup were used for the quantification, obtaining 0.7 azide groups per four-arm star PIB **4a** and 1.7 azide groups per four-arm star polymer **4b** (see Fig. 2b and Table 1).

Furthermore, polymers **3** and **4b** were additionally characterized via MALDI-ToF mass spectrometry (see Figs. S2 and S3 Supporting Information). In case of four-arm star thymine-telechelic PIB **3** one series with a distance of 56.1 Da correlating to one isobutylene unit was observed matching to the sodium adduct of the desired structure, with all four labile hydrogen atoms of the NH groups

within the thymine moiety exchanged against sodium-ions. In contrast, for polymer **4b** a sodium and a lithium series were detected whereas both series reflect the structure of the polymer with one labile NH proton exchanged either against sodium- or lithium-ions.

Table 1 summarizes the molecular weight data, polydispersities, glass transition temperatures (T_g), and the decomposition temperatures of four-arm star PIBs **1–4b**.

Molecular weights determined *via* GPC and NMR are in good agreement with the theoretical molecular weight projected to 8000 g/mol, corresponding to 2000 g/mol per

polymer arm. The obtained polydispersities indicate the living character of the polymerization. In case of polymers **4a** and **4b** containing the different endgroups a slight increase in the molecular weight as well as in the polydispersity was observed, which can be attributed to the superposition of several molecular weight distributions. The glass transition temperature of all prepared polymers is in the range of -58.0 °C to -60.0 °C, thus contributing to their high diffusion mobility under ambient conditions; with thermogravimetric analysis proving their thermal stability up to 295 °C (see Table 1).

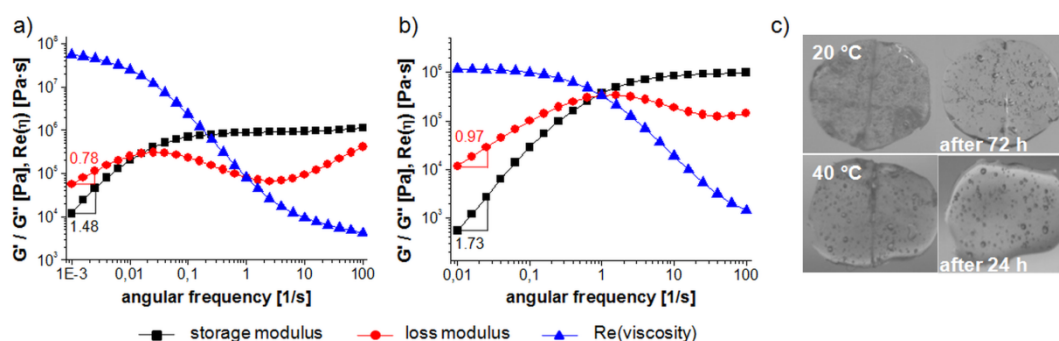


Fig. 3: Frequency sweeps of four-arm star thymine-telechelic PIB **3** a) at 20 °C, b) at 40 °C and c) macroscopic self-healing experiments of a cut specimen at 20 °C (upper part) and 40 °C (lower part).

Macroscopic self-healing studies

The dynamics and the self-healing ability of four-arm star thymine-telechelic PIB **3** were investigated *via* melt rheology^{2a, 2c}, performing frequency sweep measurements at 20 °C and 40 °C over a broad frequency range (see Fig. 3a and b).

At 20 °C a prominent rubbery plateau with a plateau modulus G_N of 1.1 E6 Pa at high frequencies as well as an extremely high viscosity η of 5.6 E7 Pa·s at low frequency was observed (see Fig. 3a). Both phenomena can only be explained by the presence of a supramolecular network due to the formation of supramolecular junction points built up by thymine moieties. The approximate lifetime of the supramolecular aggregates was estimated *via* the crossover time of G' and G'' according to Feldman et al.³¹ Thus, a bond lifetime of around 67 s was calculated indicating open supramolecular aggregates due to the dissociation of hydrogen bonds at low frequencies and a closed state of

supramolecular clusters at higher frequencies, explaining the rubber-like behavior of the four-arm star thymine-telechelic PIB **3** at room temperature. Similar observations were reported by Herbst et al.^{2c} who investigated bivalent barbiturate-functionalized PIBs showing self-healing due to the ability of rearrangement within the dynamic supramolecular aggregates.

In contrast, the bond lifetime of the junction points within polymer **3** decreased from 67 s at 20 °C to approximately 1 s at 40 °C. Terminal flow at low frequencies was observed by the determined slopes of G' and G'' in this frequency range (see Fig. 3b). Nevertheless, even at this moderately increased temperature, higher values for the plateau modulus ($G_N = 9.8$ E5 Pa) and for the viscosity ($\eta = 1.2$ E6 Pa·s) were recorded than ever reported for linear high molecular weight PIB³². All results obtained by frequency and thus time dependent oscillatory rheology measurements support the presence of a

supramolecular network due to phase separation effects between the non-polar polymer backbone and the polar thymine moieties, resulting in supramolecular cluster formation as already described by us previously^{2c, 26b} for the bivalent polymers. Consequently, macroscopic self-healing studies were performed to investigate the self-

healing performance of four-arm star thymine-telechelic PIB **3**. Polymer films with a thickness of around 1 mm were cut with a razor blade. After bringing the freshly generated and sticky surfaces into contact again photos were taken in defined time intervals (see photos in Fig. 3c).

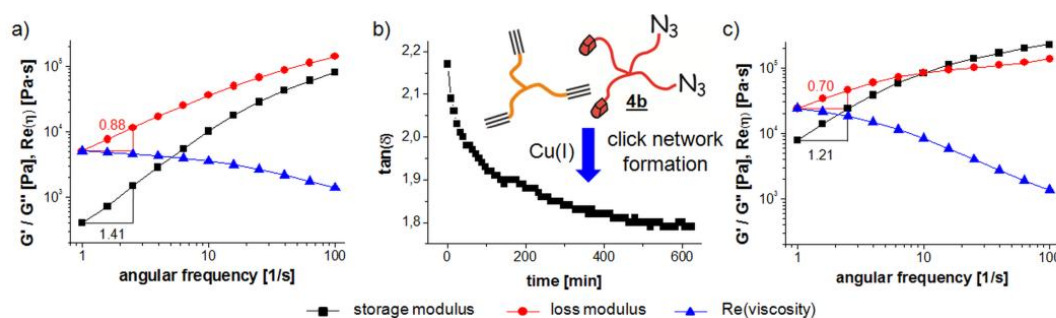


Fig. 4 a) Frequency sweep of four-arm star PIB **4b** at 40 °C. Rheological investigation of a polymer mixture composed of three-arm star alkyne-telechelic PIB and four-arm star PIB **4b**: b) development of the loss factor $\tan(\delta)$ during the progress of the CuAAC at 40 °C, c) frequency sweep at 40 °C after CuAAC.

At 20 °C complete self-healing was achieved after 72 h whereas the intersection of the former cut is still partially visible. On the contrary, at 40 °C complete closure of the damaged region was observed within 24 h due to the higher mobility at this temperature as evidenced by the frequency sweep measurement.

For the creation of a self-healing system based on double network formation the four-arm star PIB **4b** bearing 1.7 azide groups and 2.3 thymine endgroups per one molecule was crosslinked with a three-arm star alkyne-telechelic PIB (the final product being referred as **crosslinked 4b**) thus combining a covalent but single-time crosslinking concept with the supramolecular and thus multiple self-healing concept *via* hydrogen bonding interactions. Therefore, an equimolar polymer mixture with respect to the azide-/alkyne-ratio was prepared by simple mixing and subsequently investigated *via* melt rheology before adding a Cu(I)-catalyst required for covalent network formation *via* click reaction (see Fig. 4a).

A frequency sweep measurement of the four-arm star PIB **4b** at 40 °C demonstrated the presence of supramolecular aggregation although just 2.3 thymine moieties per molecule are attached (see Fig. 4a). In contrast,

the investigation of a neat equimolar polymer mixture (with respect to the endgroups) composed of the four-arm star polymer **4b** and the three-arm star alkyne-telechelic PIB before “click”-crosslinking revealed a liquid-like behavior as the loss modulus is larger than the storage modulus over the whole investigated frequency range (see Fig. S4 Supporting Information). “Click”-crosslinking was started by the addition of $\text{CuBr}(\text{PPh}_3)_3$ to the polymer mixture at 40 °C. The reaction was monitored over a timeframe of 70 h where every 10 minutes a frequency sweep measurement was performed. During the first 600 minutes the change of the loss factor $\tan(\delta)$ with time at 10 1/s was investigated (see Fig. 4b) showing a decrease from 2.2 to 1.8 whereas the temporal changes became less prominent with increasing time. After 70 h the value of the loss factor $\tan(\delta)$ became less than one indicating the formation of covalent network points. In order to further force the crosslinking process *via* click chemistry to completeness a temperature sweep measurement from -10 °C to 150 °C with a heating rate of 1 °C/min was conducted. Afterwards the frequency measurement at 40 °C was repeated displaying a crossover of G' and G'' at around 10 1/s as well as a rough approximation of the slopes of

G' and G'' vs. angular frequency ω (see Fig. 4c). Furthermore, an increase in G' of around 190% and in G'' of around 50% was noticed (see Fig. S4 Supporting Information for comparison). Thus, the formation of a weakly crosslinked covalent network reinforced by supramolecular hydrogen bonding interaction can be proven. In contrast, crosslinking experiments of polymer **4a** bearing only 0.7 azide groups per four-arm star polymer **4a** with a three-arm star alkyne-telechelic PIB was not sufficient to form even a weakly crosslinked covalent network.

Macroscopic self-healing studies of the final covalent and supramolecular network composed of polymer **4b** and three-arm star alkyne-telechelic PIB (**crosslinked 4b**) reveal fast self-healing at room temperature within 24 hours, whereas already after 2 hours a significant reduction of the depth of the former cut was observed (see Fig. 5).



Fig. 5 Macroscopic self-healing experiments of a cut specimen of **crosslinked 4b** after CuAAC at 20 °C

Moreover this self-healing process could be repeated several times due to the presence of supramolecular interactions proving the

reliability of our double crosslinked self-healing system.

SAXS investigations of supramolecular polymer networks

In order to further confirm supramolecular aggregation providing the basis for the self-healing response of the polymers SAXS measurements were conducted. Therefore, PIB **3** as well as the polymer mixture composed of polymer **4b** and three-arm star alkyne-telechelic PIB were investigated in a q -range of 0.2–2.8 nm^{-1} at room temperature (see Fig. 6a) and the so obtained results are summarized in Table 2.

SAXS data were analyzed assuming spheres with a Gaussian size distribution with a structure factor derived from a hard sphere model (Percus–Yevick model as described in literature^{2c, 26b} and in the Supporting Information). The strongest difference is observed in the hard sphere volume fraction, which decreases from 0.39 for the four-arm star thymine-telechelic PIB **3** to 0.23 for the **crosslinked 4b**. As the hard sphere volume fraction is a measure for the probability to find a neighboring supramolecular cluster, crosslinking reduces this probability and thus the cluster–cluster aggregation. Additionally, the typical distance of the supramolecular clusters (twice the value of the hard-sphere-radius) is $d = 2 \cdot R_2 = 6.7$ nm for PIB **3** and decreases to $d = 6.3$ nm for the **crosslinked 4b**.

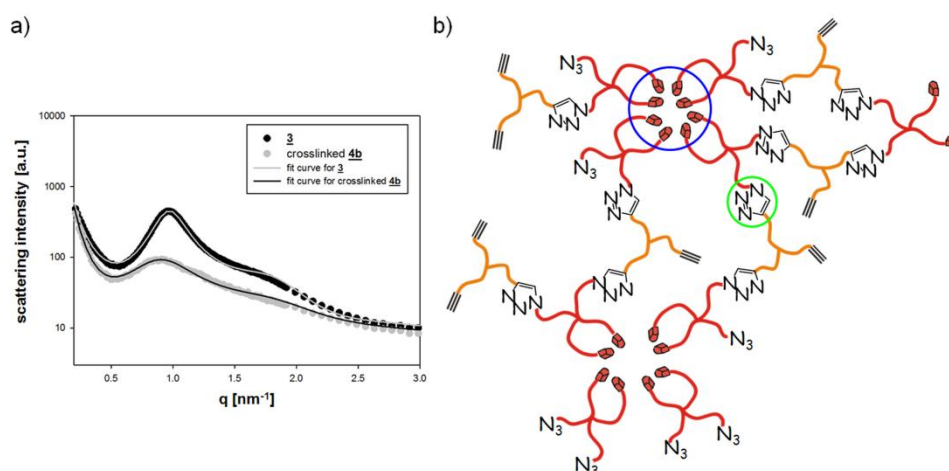


Fig. 6 a) SAXS profiles of four-arm star thymine-telechelic PIB **3** (black curve) and of **crosslinked 4b** (grey curve) after covalent network formation *via* CuAAC. In red: fitting of SAXS data (Gaussian distribution). b) proposed structure of the obtained double network (**crosslinked 4b**) composed of a weakly crosslinked covalent polymer network reinforced by supramolecular aggregation of thymine moieties.

Table 2 SAXS-results of PIB **3**, and of the **crosslinked 4b** after covalent "click"-crosslinking *via* CuAAC.

Entry	Sample	Hard sphere radius R_2^a [nm]	Hard sphere volume fraction	Aggregation number N^b
1	PIB-thymine ₄ 3	3.33	0.39	≈ 10
2	crosslinked 4b	3.15	0.23	≈ 8

^a SAXS-data were fitted and further analyzed assuming spheres with a Gaussian size distribution with a structure factor from a hard sphere model according to Percus-Yevick (PY model, for more information see Supporting Information)^[139, 196]. ^b calculated according to equation 1: $N = (4\pi R_2^3 \rho N_A)/(3M)$ (eq. 1).

From the hard sphere radius, the aggregation number N of the respective system (representing the amount of hydrogen bonding moieties within supramolecular clusters) was calculated, which decreases from ≈ 10 to ≈ 8 from PIB **3** to the **crosslinked 4b**. Thus, "click" crosslinking reduces the number of clustered hydrogen bonds implying that four four-arm star polymers **4b** are forming one supramolecular cluster, connected to the three-arm star alkyne-telechelic PIB *via* triazole-ring formation due to click-chemistry (see Fig. 6b). Furthermore, it is proposed that not all alkyne-groups will participate in the CuAAC reaction due to their restricted and additionally decreasing mobility during the progress of the click-reaction as well as due to the presence of supramolecular tie points.

SUMMARY

We have investigated multivalent star-shaped polymers which can form reversible as well as irreversible crosslinking points aiming at the design of a doubly crosslinked self-healing system based on two separate networks: one *via* supramolecular clustering of hydrogen bonds, the second *via* covalent "click"-crosslinking, thus generating polymeric networks for multiple self-healing applications acting under ambient conditions. To this effect, we have synthesized four-arm star bromide-telechelic PIBs *via* living carbocationic polymerization (LCCP), which were further converted to four-arm star azide-telechelic PIBs *via* simple endgroup transformation. Furthermore, four-arm star thymine-telechelic PIB as well as four-arm star polymers carrying both, azide-moieties (for covalent network formation) and

thymine-moieties (acting as supramolecular tie points) were prepared *via* microwave-assisted CuAAC reaction. All prepared polymers were completely characterized *via* ¹H-NMR-investigations, FTIR-investigations and MALDI-ToF mass spectrometry in case of four-arm star supramolecular polymers. Four-arm star thymine-telechelic PIB **3** was investigated *via* melt-rheology showing a prominent rubbery plateau with a plateau modulus G_N of 1.1 E6 Pa as well as an extremely high viscosity η of 5.6 E7 Pa·s at 20 °C which is attributed to supramolecular cluster formation due to phase separation effects between the polar thymine endgroups and the non-polar polymer backbone. Supramolecular network formation was additionally proven *via* SAXS investigations revealing a strong scattering peak at 0.97 nm⁻¹ corresponding to a distance of supramolecular clusters built up by ≈ 10 thymine moieties of 6.5 nm in real space. Macroscopic self-healing studies were performed by simple cutting of polymer films, observing a complete self-healing of the four-arm star thymine-telechelic PIB **3** after 72 hours at 20 °C and after 24 hours at 40 °C, respectively. For the creation of the dual crosslinked self-healing system the four-arm star PIB **4b** bearing 1.7 azide groups and 2.3 thymine endgroups per one molecule, was crosslinked with a three-arm star alkyne-telechelic PIB at 40 °C, catalyzed by Cu(I)-addition. After 70 hours a weakly crosslinked covalent network reinforced by supramolecular hydrogen bonding interaction was obtained as proven *via* melt rheology and SAXS measurements: in rheology the decrease of the loss factor $\tan(\delta)$ as well as an increase in G' of around 190%

and in G'' of around 50% in comparison to the neat polymer mixture clearly indicates the formation of the covalent network, whereas SAXS proves the presence of supramolecular clusters. Macroscopic self-healing studies of the so obtained double covalent and supramolecular network structure revealed fast and multiple self-healing at 20 °C within 24 hours, whereas already after 2 hours a significant reduction of the depth of the former cut was observed. Thus, the here presented four-arm star polymers bearing hydrogen bonding moieties enabled the design of a doubly crosslinked self-healing system based on two separate networks due to “click”-crosslinking and supramolecular cluster formation.

ACKNOWLEDGEMENT

We gratefully acknowledge Grant DFG BI 1337/8-2 (within the SPP 1568 “Design and Generic Principles of Self-Healing Materials”) and the grant IASS from the EU within FP 7.

APPENDIX A. Supplementary data

Supplementary data related to this article can be found at <http://dx.doi.org/10.1016/j.polymer.2015.01.073>.

REFERENCES

- (a) Binder, W. H., *Self-Healing Polymers. From Principles to Applications*. Wiley-VCH: Weinheim, 2013; p 440; (b) Blaiszik, B. J.; Kramer, S. L. B.; Olugebefola, S. C.; Moore, J. S.; Sottos, N. R.; White, S. R., Self-Healing Polymers and Composites. *Annu. Rev. Mater. Res.* **2010**, *40* (1), 179-211; (c) White, S. R.; Sottos, N. R.; Geubelle, P. H.; Moore, J. S.; Kessler, M. R.; Sriram, S. R.; Brown, E. N.; Viswanathan, S., Autonomic healing of polymer composites. *Nature* **2001**, *409* (6822), 794-797; (d) Akbarzadeh, J.; Puchegger, S.; Stojanovic, A.; Kirchner, H. O. K.; Binder, W. H.; Bernstorff, S.; Zioupos, P.; Peterlik, H., Timescales of self-healing in human bone tissue and polymeric ionic liquids. *Bioinspired, Biomimetic and Nanobiomaterials* **2014**, *3* (3), 123-130.
- (a) Döhler, D.; Michael, P.; Binder, W. H., Autocatalysis in the Room Temperature Copper(I)-Catalyzed Alkyne-Azide “Click” Cycloaddition of Multivalent Poly(acrylate)s and Poly(isobutylene)s. *Macromolecules* **2012**, *45* (8), 3335-3345; (b) Herbst, F.; Döhler, D.; Michael, P.; Binder, W. H., Self-Healing Polymers via Supramolecular Forces. *Macromol. Rapid Commun.* **2013**, *34* (3), 203-220; (c) Herbst, F.; Seiffert, S.; Binder, W. H., Dynamic supramolecular poly(isobutylene)s for self-healing materials. *Polym. Chem.* **2012**, *3* (11), 3084-3092.
- (a) Hizal, G.; Tunca, U.; Sanyal, A., Discrete macromolecular constructs via the Diels–Alder “Click” reaction. *J. Polym. Sci. Part A: Polym. Chem.* **2011**, *49* (19), 4103-4120; (b) Chen, X.; Dam, M. A.; Ono, K.; Mal, A.; Shen, H.; Nutt, S. R.; Sheran, K.; Wudl, F., A Thermally Re-mendable Cross-Linked Polymeric Material. *Science* **2002**, *295*, 1698-1702; (c) Chen, X.; Wudl, F.; Mal, A. K.; Shen, H.; Nutt, S. R., New Thermally Remendable Highly Cross-Linked Polymeric Materials. *Macromolecules* **2003**, *36* (6), 1802-1807; (d) Liu, Y.-L.; Chen, Y.-W., Thermally Reversible Cross-Linked Polyamides with High Toughness and Self-Repairing Ability from Maleimide- and Furan-Functionalized Aromatic Polyamides. *Macromol. Chem. Phys.* **2007**, *208* (2), 224-232; (e) Murphy, E. B.; Bolanos, E.; Schaffner-Hamann, C.; Wudl, F.; Nutt, S. R.; Auad, M. L., Synthesis and Characterization of a Single-Component Thermally Remendable Polymer Network: Staudinger and Stille Revisited. *Macromolecules* **2008**, *41* (14), 5203-5209; (f) Park, J. S.; Takahashi, K.; Guo, Z.; Wang, Y.; Bolanos, E.; Hamann-Schaffner, C.; Murphy, E.; Wudl, F.; Hahn, H. T., Towards Development of a Self-Healing Composite using a Mendable Polymer and Resistive Heating. *J. Compos. Mater.* **2008**, *42* (26), 2869-2881.
- Amamoto, Y.; Kamada, J.; Otsuka, H.; Takahara, A.; Matyjaszewski, K., Repeatable Photoinduced Self-Healing of Covalently Cross-Linked Polymers through Reshuffling of

Trithiocarbonate Units. *Angew. Chem. Int. Ed.* **2011**, *50* (7), 1660-1663.

5. (a) Blaiszik, B. J.; Caruso, M. M.; McIlroy, D. A.; Moore, J. S.; White, S. R.; Sottos, N. R., Microcapsules filled with reactive solutions for self-healing materials. *Polymer* **2009**, *50* (4), 990-997; (b) Guadagno, L.; Longo, P.; Raimondo, M.; Naddeo, C.; Mariconda, A.; Sorrentino, A.; Vittoria, V.; Iannuzzo, G.; Russo, S., Cure Behavior and Mechanical Properties of Structural Self-Healing Epoxy Resins. *J. Polym. Sci. Part B: Polym. Phys.* **2010**, *48* (23), 2413-2423; (c) Guadagno, L.; Raimondo, M.; Naddeo, C.; Longo, P.; Mariconda, A., Self-healing materials for structural applications. *Polym. Eng. Sci.* **2014**, *54* (4), 777-784; (d) McIlroy, D. A.; Blaiszik, B. J.; Caruso, M. M.; White, S. R.; Moore, J. S.; Sottos, N. R., Microencapsulation of a Reactive Liquid-Phase Amine for Self-Healing Epoxy Composites. *Macromolecules* **2010**, *43* (4), 1855-1859; (e) Montarnal, D.; Tournilhac, F.; Hidalgo, M.; Leibler, L., Epoxy-based networks combining chemical and supramolecular hydrogen-bonding crosslinks. *J. Polym. Sci. Part A: Polym. Chem.* **2010**, *48* (5), 1133-1141; (f) Yuan, L.; Liang, G.; Xie, J.; Li, L.; Guo, J., Preparation and characterization of poly(urea-formaldehyde) microcapsules filled with epoxy resins. *Polymer* **2006**, *47*, 5338-5349; (g) Yuan, Y. C.; Rong, M. Z.; Zhang, M. Q.; Yang, G. C.; Zhao, J. Q., Self-healing of fatigue crack in epoxy materials with epoxy/mercaptan system *Express polym. lett.* **2011**, *5* (1), 47-59.

6. (a) Brown, E. N.; Kessler, M. R.; Sottos, N. R.; White, S. R., In situ poly(urea-formaldehyde) microencapsulation of dicyclopentadiene. *J. Microencapsulation* **2003**, *20* (6), 719 - 730; (b) Jones, A. S.; Rule, J. D.; Moore, J. S.; White, S. R.; Sottos, N. R., Catalyst Morphology and Dissolution Kinetics of Self-Healing Polymers. *Chem. Mater.* **2006**, *18* (5), 1312-1317; (c) Kessler, M. R.; Sottos, N. R.; White, S. R., Self-healing structural composite materials. *Compos. Part A-Appl. S.* **2003**, *34* (8), 743-753; (d) Toohey, K. S.; Sottos, N. R.; Lewis, J. A.; Moore, J. S.;

White, S. R., Self-healing materials with microvascular networks. *Nat. Mater.* **2007**, *6* (8), 581-585; (e) Jackson, A. C.; Bartelt, J. A.; Marczewski, K.; Sottos, N. R.; Braun, P. V., Silica-Protected Micron and Sub-Micron Capsules and Particles for Self-Healing at the Microscale. *Macromol. Rapid Commun.* **2011**, *32* (1), 82-87; (f) Brown, E. N.; White, S. R.; Sottos, N. R., Microcapsule induces toughening in a self-healing polymer composite. *J. Mater. Sci.* **2004**, *39*, 1703-1710; (g) Blaiszik, B. J.; Baginska, M.; White, S. R.; Sottos, N. R., Autonomic Recovery of Fiber/Matrix Interfacial Bond Strength in a Model Composite. *Adv. Funct. Mater.* **2010**, *20* (20), 3547-3554.

7. (a) Binder, W. H.; Sachsenhofer, R., 'Click' Chemistry in Polymer and Materials Science. *Macromol. Rapid Commun.* **2007**, *28* (1), 15-54; (b) Binder, W. H.; Sachsenhofer, R., 'Click' Chemistry in Polymer and Material Science: An Update. *Macromol. Rapid Commun.* **2008**, *29* (12-13), 952-981; (c) Kolb, H. C.; Finn, M. G.; Sharpless, K. B., Click Chemistry: Diverse Chemical Function from a Few Good Reactions. *Angew. Chem. Int. Ed.* **2001**, *40* (11), 2004-2021; (d) Tillet, G.; Boutevin, B.; Ameduri, B., Chemical reactions of polymer crosslinking and post-crosslinking at room and medium temperature. *Prog. Polym. Sci.* **2011**, *36* (2), 191-217; (e) Vestberg, R.; Malkoch, M.; Kade, M.; Wu, P.; Fokin, V. V.; Sharpless, K. B.; Drockenmuller, E.; Hawker, C. J., Role of Architecture and Molecular Weight in the Formation of Tailor-Made Ultrathin Multilayers Using Dendritic Macromolecules and Click Chemistry. *J. Polym. Sci. Part A: Polym. Chem.* **2007**, *45* (14), 2835-2846; (f) Iha, R. K.; Wooley, K. L.; Nyström, A. M.; Burke, D. J.; Kade, M. J.; Hawker, C. J., Applications of Orthogonal "Click" Chemistries in the Synthesis of Functional Soft Materials. *Chem. Rev.* **2009**, *109* (11), 5620-5686; (g) Malkoch, M.; Schleicher, K.; Drockenmuller, E.; Hawker, C. J.; Russell, T. P.; Wu, P.; Fokin, V. V., Structurally Diverse Dendritic Libraries: A Highly Efficient Functionalization Approach

- Using Click Chemistry. *Macromolecules* **2005**, *38* (9), 3663-3678.
8. (a) Gragert, M.; Schunack, M.; Binder, W. H., Azide/Alkyne-“Click”-Reactions of Encapsulated Reagents: Toward Self-Healing Materials. *Macromol. Rapid Commun.* **2011**, *32* (5), 419-425; (b) Schunack, M.; Gragert, M.; Döhler, D.; Michael, P.; Binder, W. H., Low-Temperature Cu(I)-Catalyzed “Click” Reactions for Self-Healing Polymers. *Macromol. Chem. Phys.* **2012**, *213* (2), 205-214.
9. (a) Sheng, X.; Mauldin, T. C.; Kessler, M. R., Kinetics of Bulk Azide/Alkyne “Click” Polymerization. *J. Polym. Sci. Part A: Polym. Chem.* **2010**, *48* (18), 4093-4102; (b) Sheng, X.; Rock, D. M.; Mauldin, T. C.; Kessler, M. R., Evaluation of different catalyst systems for bulk polymerization through “click” chemistry. *Polymer* **2011**, *52* (20), 4435-4441.
10. (a) de Luzuriaga, A. R.; Ormategui, N.; Grande, H. J.; Odriozola, I.; Pomposo, J. A.; Loinaz, I., Intramolecular Click Cycloaddition: An Efficient Room-Temperature Route towards Bioconjugable Polymeric Nanoparticles. *Macromol. Rapid Commun.* **2008**, *29* (12-13), 1156-1160; (b) van der Ende, A. E.; Harrell, J.; Sathiyakumar, V.; Meschievitz, M.; Katz, J.; Adcock, K.; Harth, E., “Click” Reactions: Novel Chemistries for Forming Well-defined Polyester Nanoparticles. *Macromolecules* **2010**, *43* (13), 5665-5671.
11. Cengiz, H.; Aydogan, B.; Ates, S.; Acikalin, E.; Yagci, Y., Intramolecular Cross-linking of Polymers Using Difunctional Acetylenes via Click Chemistry. *Des. Monomers. Polym.* **2011**, *14*, 69-78.
12. Filpponen, I.; Argyropoulos, D. S., Regular Linking of Cellulose Nanocrystals via Click Chemistry: Synthesis and Formation of Cellulose Nanoplatelet Gels. *Biomacromolecules* **2010**, *11* (4), 1060-1066.
13. Zhao, Y.; Döhler, D.; Lv, L.-P.; Binder, W. H.; Landfester, K.; Crespy, D., Facile Phase-Separation Approach to Encapsulate Functionalized Polymers in Core-Shell Nanoparticles. *Macromol. Chem. Phys.* **2014**, *215* (2), 198-204.
14. White, S. R.; Moore, J. S.; Sottos, N. R.; Krull, B. P.; Santa Cruz, W. A.; Gergely, R. C. R., Restoration of Large Damage Volumes in Polymers. *Science* **2014**, *344* (6184), 620-623.
15. (a) Ossipov, D. A.; Hilborn, J., Poly(vinyl alcohol)-Based Hydrogels Formed by “Click Chemistry”. *Macromolecules* **2006**, *39* (5), 1709-1718; (b) Liu, J.; Jiang, X.; Xu, L.; Wang, X.; Hennink, W. E.; Zhuo, R., Novel Reduction-Responsive Cross-Linked Polyethylenimine Derivatives by Click Chemistry for Nonviral Gene Delivery. *Bioconjugate Chem.* **2010**, *21* (10), 1827-1835; (c) Malkoch, M.; Vestberg, R.; Gupta, N.; Mespouille, L.; Dubois, P.; Mason, A. F.; Hedrick, J. L.; Liao, Q.; Frank, C. W.; Kingsbury, K.; Hawker, C. J., Synthesis of well-defined hydrogel networks using Click chemistry. *Chem. Commun.* **2006**, (26), 2774-2776; (d) Liu, S. Q.; Ee, P. L. R.; Ke, C. Y.; Hedrick, J. L.; Yang, Y. Y., Biodegradable poly(ethylene glycol)-peptide hydrogels with well-defined structure and properties for cell delivery. *Biomaterials* **2009**, *30* (8), 1453-1461; (e) Crescenzi, V.; Cornelio, L.; Di Meo, C.; Nardecchia, S.; Lamanna, R., Novel Hydrogels via Click Chemistry: Synthesis and Potential Biomedical Applications. *Biomacromolecules* **2007**, *8* (6), 1844-1850; (f) Huerta-Angeles, G.; Šmejkalová, D.; Chládková, D.; Ehlová, T.; Buffa, R.; Velebný, V., Synthesis of highly substituted amide hyaluronan derivatives with tailored degree of substitution and their crosslinking via click chemistry. *Carbohydr. Polym.* **2011**, *84* (4), 1293-1300; (g) Testa, G.; Di Meo, C.; Nardecchia, S.; Capitani, D.; Mannina, L.; Lamanna, R.; Barbetta, A.; Dentini, M., Influence of dialkyne structure on the properties of new click-gels based on hyaluronic acid *Int. J. Pharm.* **2009**, *378*, 86-92; (h) Díaz, D. D.; Rajagopal, K.; Strable, E.; Schneider, J.; Finn, M. G., “Click” Chemistry in a Supramolecular Environment: Stabilization of Organogels by Copper(I)-Catalyzed Azide-Alkyne [3 + 2] Cycloaddition. *J. Am. Chem. Soc.* **2006**, *128* (18), 6056-6057.

16. (a) Cordier, P.; Tournilhac, F.; Soulie-Ziakovic, C.; Leibler, L., Self-healing and thermoreversible rubber from supramolecular assembly. *Nature* **2008**, *451*, 977-980; (b) Lehn, J.-M., Dynamers: dynamic molecular and supramolecular polymers. *Prog. Polym. Sci.* **2005**, *30*, 814-831; (c) Wojtecki, R. J.; Meador, M. A.; Rowan, S. J., Using the dynamic bond to access macroscopically responsive structurally dynamic polymers. *Nat. Mater.* **2011**, *10* (1), 14-27.
17. (a) Courtois, J.; Baroudi, I.; Nouvel, N.; Degrandi, E.; Pensec, S.; Ducouret, G.; Chanéac, C.; Bouteiller, L.; Creton, C., Supramolecular Soft Adhesive Materials. *Adv. Funct. Mater.* **2010**, *20* (11), 1803-1811; (b) Müller, M.; Dardin, A.; Seidel, U.; Balsamo, V.; Iván, B.; Spiess, H. W.; Stadler, R., Junction Dynamics in Telechelic Hydrogen Bonded Polyisobutylene Networks. *Macromolecules* **1996**, *29* (7), 2577-2583; (c) Sivakova, S.; Bohnsack, D. A.; Mackay, M. E.; Suwanmala, P.; Rowan, S. J., Utilization of a Combination of Weak Hydrogen-Bonding Interactions and Phase Segregation to Yield Highly Thermosensitive Supramolecular Polymers. *J. Am. Chem. Soc.* **2005**, *127*, 18202-18211; (d) Hackethal, K.; Döhler, D.; Tanner, S.; Binder, W. H., Introducing Polar Monomers into Polyisobutylene by Living Cationic Polymerization: Structural and Kinetic Effects. *Macromolecules* **2010**, *43* (4), 1761-1770.
18. (a) Döhler, D.; Zare, P.; Binder, W. H., Hyperbranched polyisobutylenes for self-healing polymers. *Polym. Chem.* **2014**, *5* (3), 992-1000; (b) Stojanovic, A.; Appiah, C.; Döhler, D.; Akbarzadeh, J.; Zare, P.; Peterlik, H.; Binder, W. H., Designing melt flow of poly(isobutylene)-based ionic liquids. *J. Mater. Chem. A* **2013**, *1*, 12159-12169; (c) Zare, P.; Stojanovic, A.; Herbst, F.; Akbarzadeh, J.; Peterlik, H.; Binder, W. H., Hierarchically Nanostructured Polyisobutylene-Based Ionic Liquids. *Macromolecules* **2012**, *45* (4), 2074-2084; (d) Kalista, S. J.; Pflug, J. R.; Varley, R. J., Effect of ionic content on ballistic self-healing in EMAA copolymers and ionomers. *Polym. Chem.* **2013**, *4* (18), 4910-4926; (e) Rahman, M. A.; Penco, M.; Peroni, I.; Ramorino, G.; Grande, A. M.; Di Landro, L., Self-Repairing Systems Based on Ionomers and Epoxidized Natural Rubber Blends. *ACS Appl. Mater. Interfaces* **2011**, *3* (12), 4865-4874; (f) Rahman, M. A.; Spagnoli, G.; Grande, A. M.; Di Landro, L., Role of Phase Morphology on the Damage Initiated Self-healing Behavior of Ionomer Blends. *Macromol. Mater. Eng.* **2013**, *298* (12), 1350-1364.
19. (a) Burattini, S.; Colquhoun, H. M.; Greenland, B. W.; Hayes, W., A novel self-healing supramolecular polymer system. *Faraday Discuss.* **2009**, *143*, 251-264; (b) Burattini, S.; Greenland, B. W.; Chappell, D.; Colquhoun, H. M.; Hayes, W., Healable polymeric materials: a tutorial review. *Chem. Soc. Rev.* **2010**, *39* (6), 1973-1985; (c) Burattini, S.; Greenland, B. W.; Hermida Merino, D.; Weng, W.; Seppala, J.; Colquhoun, H. M.; Hayes, W.; Mackay, M. E.; Hamley, I. W.; Rowan, S. J., A Healable Supramolecular Polymer Blend Based on Aromatic *p-p*- Stacking and Hydrogen-Bonding Interactions. *J. Am. Chem. Soc.* **2010**, *132* (34), 12051-12058; (d) Greenland, B. W.; Bird, M. B.; Burattini, S.; Cramer, R.; O'Reilly, R. K.; Patterson, J. P.; Hayes, W.; Cardin, C. J.; Colquhoun, H. M., Mutual binding of polymer end-groups by complementary p-p-stacking: a molecular "Roman Handshake". *Chem. Commun.* **2013**, *49* (5), 454-456.
20. Burnworth, M.; Tang, L.; Kumpfer, J. R.; Duncan, A. J.; Beyer, F. L.; Fiore, G. L.; Rowan, S. J.; Weder, C., Optically healable supramolecular polymers. *Nature* **2011**, *472*, 334-337.
21. Bosman, A. W.; Sijbesma, R. P.; Meijer, E. W., Supramolecular polymers at work. *Mater. today* **2004**, *7* (4), 34-39.
22. www.suprapolix.com.
23. (a) Chen, Y.; Kushner, A. M.; Williams, G. A.; Guan, Z., Multiphase design of autonomic self-healing thermoplastic elastomers. *Nat. Chem.* **2012**, *4*, 467-472; (b) Holden, G.; Kricheldorf, H. R.; Quirk, R. P., *Thermoplastic Elastomers*. 3rd edn ed.;

- Hanser: 2004; (c) Hentschel, J.; Kushner, A. M.; Ziller, J.; Guan, Z., Self-Healing Supramolecular Block Copolymers. *Angew. Chem. Int. Ed.* **2012**, n/a-n/a.
24. Chen, Y.; Guan, Z., Self-assembly of core-shell nanoparticles for self-healing materials. *Polym. Chem.* **2013**, (4), 4885-4889.
25. (a) Stukalin, E. B.; Cai, L.-H.; Kumar, N. A.; Leibler, L.; Rubinstein, M., Self-Healing of Unentangled Polymer Networks with Reversible Bonds. *Macromolecules* **2013**, *46* (18), 7525-7541; (b) Tournilhac, F.; Cordier, P.; Montarnal, D.; Soulié-Ziakovic, C.; Leibler, L., Self-Healing Supramolecular Networks. *Macromol. Symp.* **2010**, 291-292 (1), 84-88.
26. (a) Herbst, F.; Schröter, K.; Gunkel, I.; Gröger, S.; Thurn-Albrecht, T.; Balbach, J.; Binder, W. H., Aggregation and Chain Dynamics in Supramolecular Polymers by Dynamic Rheology: Cluster Formation and Self-Aggregation. *Macromolecules* **2010**, *43* (23), 10006-10016; (b) Yan, T.; Schröter, K.; Herbst, F.; Binder, W. H.; Thurn-Albrecht, T., Nanostructure and Rheology of Hydrogen-Bonding Telechelic Polymers in the Melt: From Micellar Liquids and Solids to Supramolecular Gels. *Macromolecules* **2014**, *47* (6), 2122-2130.
27. (a) Kali, G.; Vavra, S.; László, K.; Iván, B., Thermally Responsive Amphiphilic Conetworks and Gels Based on Poly(N-isopropylacrylamide) and Polyisobutylene. *Macromolecules* **2013**, *46* (13), 5337-5344; (b) Domján, A.; Mezey, P.; Varga, J., Behavior of the Interphase Region of an Amphiphilic Polymer Conetwork Swollen in Polar and Nonpolar Solvent. *Macromolecules* **2012**, *45* (2), 1037-1040; (c) Kali, G.; Georgiou, T. K.; Iván, B.; Patrickios, C. S., Anionic amphiphilic end-linked conetworks by the combination of quasiliving carbocationic and group transfer polymerizations. *J. Polym. Sci. Part A: Polym. Chem.* **2009**, *47* (17), 4289-4301; (d) Toman, L.; Janata, M.; Spěváček, J.; Brus, J.; Sikora, A.; Horský, J.; Vlček, P.; Látalová, P., Amphiphilic conetworks. IV. Poly(methacrylic acid)-1-polyisobutylene and poly(acrylic acid)-1-polyisobutylene based hydrogels prepared by two-step polymer procedure. New pH responsive conetworks. *J. Polym. Sci. Part A: Polym. Chem.* **2009**, *47* (5), 1284-1291; (e) Erdodi, G.; Kennedy, J. P., Amphiphilic conetworks: Definition, synthesis, applications. *Prog. Polym. Sci.* **2006**, *31* (1), 1-18.
28. Taylor, S. J.; Storey, R. F., Tetrafunctional initiators for cationic polymerization of olefins. *J. Polym. Sci. Part A: Polym. Chem.* **2004**, *42* (23), 5942-5953.
29. Lee, B.-Y.; Park, S. R.; Jeon, H. B.; Kim, K. S., A new solvent system for efficient synthesis of 1,2,3-triazoles. *Tetrahedron Lett.* **2006**, *47* (29), 5105-5109.
30. (a) Morgan, D. L.; Martinez-Castro, N.; Storey, R. F., End-Quenching of TiCl₄-Catalyzed Quasiliving Polyisobutylene with Alkoxybenzenes for Direct Chain End Functionalization. *Macromolecules* **2010**, *43* (21), 8724-8740; (b) Morgan, D. L.; Storey, R. F., End-Quenching of Quasi-Living Isobutylene Polymerizations with Alkoxybenzene Compounds. *Macromolecules* **2009**, *42* (18), 6844-6847.
31. Feldman, K. E.; Kade, M. J.; Meijer, E. W.; Hawker, C. J.; Kramer, E. J., Model Transient Networks from Strongly Hydrogen-Bonded Polymers. *Macromolecules* **2009**, *42* (22), 9072-9081.
32. (a) Aharoni, S. M., Correlations between chain parameters and the plateau modulus of polymers. *Macromolecules* **1986**, *19* (2), 426-434; (b) Fetters, L. J.; Lohse, D. J.; Richter, D.; Witten, T. A.; Zirkel, A., Connection between Polymer Molecular Weight, Density, Chain Dimensions, and Melt Viscoelastic Properties. *Macromolecules* **1994**, *27* (17), 4639-4647.
33. (a) Kinning, D. J.; Thomas, E. L., Hard-sphere interactions between spherical domains in diblock copolymers. *Macromolecules* **1984**, *17* (9), 1712-1718; (b) Schwab, M.; Stühn, B., Thermotropic Transition from a State of Liquid Order to a Macrolattice in Asymmetric Diblock Copolymers. *Phys. Rev. Lett.* **1996**, *76* (6), 924-927.

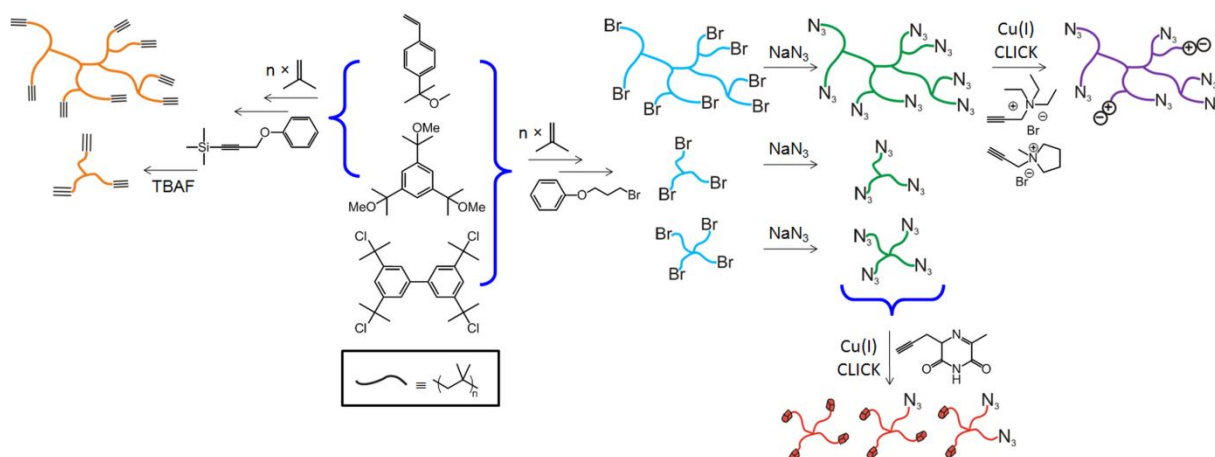
7. SUMMARY AND OUTLOOK

In the scope of this thesis embedded in the DFG SPP 1568 "Design and Generic Principles of Self-Healing Materials" the synthesis of liquid poly(isobutylene)s (PIBs) with various architectures, molecular weights and varying amounts of reactive endgroups suitable for click-crosslinking and / or supramolecular clustering enabling the design of room temperature based self-healing polymers was developed by combining living carbocationic polymerization (LCCP) techniques with direct end-quenching approaches and subsequent endgroup modification steps.

4-(2-Methoxyisopropyl)styrene was used as inimer-type initiator in combination with 3-(bromopropoxy)benzene (BPB) or trimethyl(3-phenoxy-1-propynyl)silane (TMPPS) as quenching moieties while applying optimized quenching conditions in order to create hyperbranched bromide- or TMS-protected alkyne-functionalized PIBs, which were subsequently converted into the corresponding hyperbranched azide- and alkyne-functionalized PIBs ($M_n = 25200 - 35400$ g/mol, up to 10 endgroups) in the presence of sodium azide or tetrabutylammonium fluoride (TBAF), respectively. Similarly, three-arm star azide- and alkyne-telechelic PIBs ($M_n = 5500 - 30000$ g/mol) as well as four-arm star azide-telechelic PIBs were prepared while applying 1,3,5-tris(2-methoxy-2-propyl)benzene or biphenyl tetracumyl chloride, respectively as initiator for LCCP.

Hyperbranched PIBs functionalized with ionic moieties were obtained by a microwave-assisted CuAAC reaction converting hyperbranched azide-functionalized PIB with *N*-propargyl-*N,N,N*-triethylammonium bromide or 1-propargyl-1-methylpyrrolidinium bromide.

In a similar approach, four-arm star thymine-functionalized PIBs with complete or partial endgroup functionalization ($M_n = 7400 - 8800$ g/mol) were synthesized *via* a microwave-assisted CuAAC reaction in the presence of an alkyne-functionalized thymine-moiety (see Scheme 3).

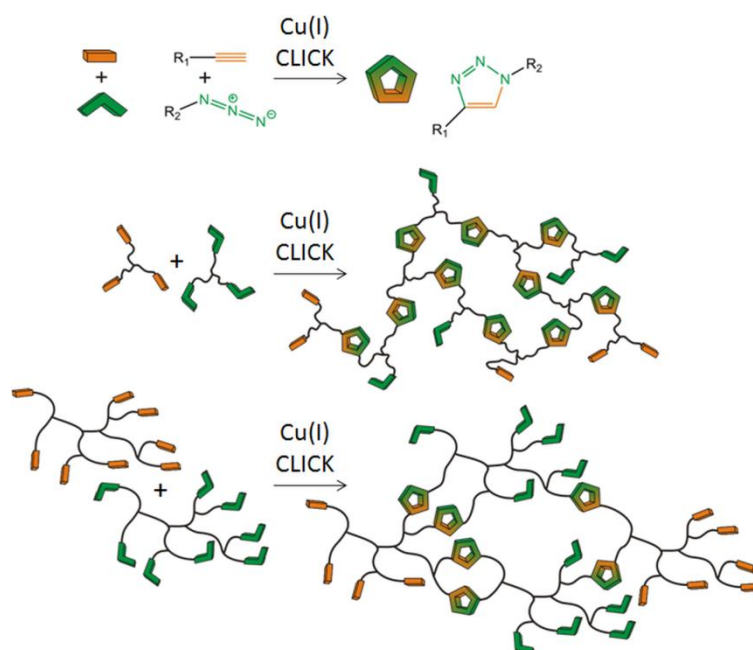


Scheme 3: Synthesis of TMS-protected alkyne-functionalized three-arm star and hyperbranched PIBs and bromide-functionalized three-arm star, four-arm-star and hyperbranched PIBs *via* living carbocation polymerization followed by subsequent endgroup modification to obtain hyperbranched and three-arm star alkyne-functionalized PIBs and hyperbranched, three-arm star and four-arm star azide-functionalized PIBs. Synthesis of hyperbranched PIBs functionalized with ionic moieties and of four-arm star thymine-functionalized PIBs was performed *via* microwave-assisted CuAAC reaction in the presence of *N*-propargyl-*N,N,N*-triethylammonium bromide, 1-propargyl-1-methylpyrrolidinium bromide or an alkyne-functionalized thymine-moiety, respectively.

Thus, several four-arm star PIBs carrying both, azide-moieties suitable for covalent network formation and thymine-motifs acting as supramolecular tie points towards the design of multiple self-healing polymers with an interwoven network structure, were prepared and separated *via* column chromatography.

All synthesized polymers were fully characterized by NMR-spectroscopy, IR-spectroscopy and mass spectrometry methods.

Click-crosslinking of three-arm star azide- and alkyne-telechelic PIBs and of hyperbranched azide- and alkyne-functionalized polymers was investigated *via* melt rheology and DSC measurements while applying bromotris(triphenylphosphine)copper(I) as catalyst at 20 °C, enabling covalent network formation, and therefore a room temperature once-a-time self-healing approach without the need of an external stimulus like heat, light or pressure (see Scheme 4).



Scheme 4: Schematic representation of the CuAAC reaction and click-crosslinking of three-arm star azide- and alkyne-telechelic PIBs and of hyperbranched azide- and alkyne-functionalized polymers *via* the CuAAC reaction applying bromotris(triphenylphosphine)copper(I) as catalyst at 20 °C enabling the design of a room temperature once-a-time self-healing approach *via* covalent network formation.

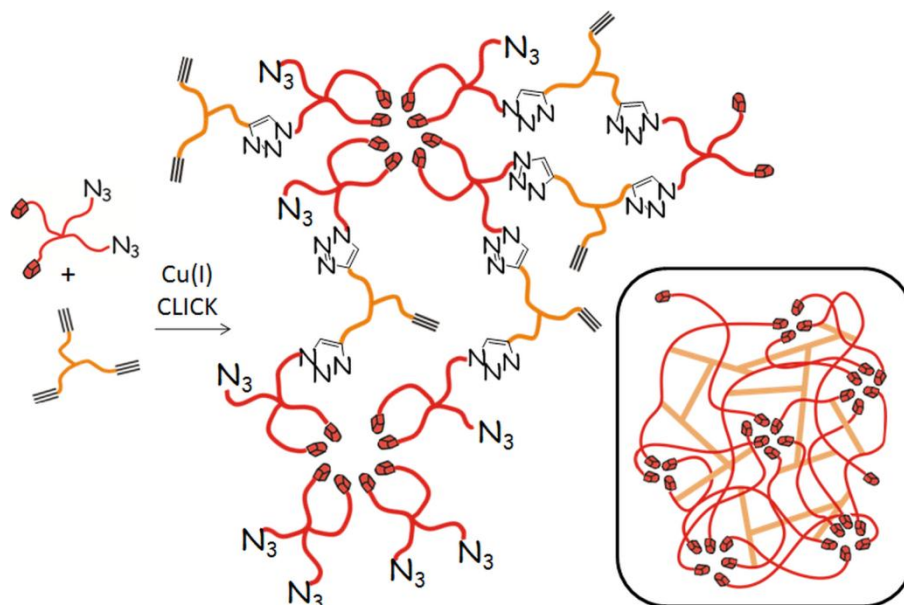
While preparing equimolar polymer mixtures of three-arm star azide-functionalized PIBs with varying molecular weights ($M_n = 5500 - 30000$ g/mol) and a three-arm star alkyne-functionalized PIB ($M_n = 6300$ g/mol) the influence of the molecular weight related to the concentration of the attached functional groups and to the starting viscosity of the polymer mixture on the kinetics of the CuAAC crosslinking approach was investigated *via* differential scanning calorimetry (DSC) and melt rheology aiming at a deeper understanding of the CuAAC reactivity linked to the molecular mobility of studied polymers. Click-crosslinking proceeded very fast at room temperature resulting in gelation times in the magnitude of hours. Thus, a significant autocatalytic effect up to a factor of 3.8 was observed in the CuAAC crosslinking reaction due to subsequent formation of 1,3-triazole rings acting as internal ligands, consequently accelerating the reaction rate of further click-reactions by preorientation of functional groups near to the active copper(I) centers. Accordingly, increased reaction rates were observed with increasing concentration of functional groups revealing the fastest network formation and the highest strand network density within the final polymer network for crosslinking three-arm

star azide-functionalized PIB with the lowest molecular weight (gelation time: 290 minutes, $r_0 = 23 \times 10^{-3} \text{ M}\cdot\text{min}^{-1}$, network strand density of 91 mol/m^3 , autocatalytic factor of 3.8). Furthermore, by promoting the CuAAC reaction due to clustering effects of generated triazole rings the control of catalytic effects and therefore the design of a fast and highly efficient covalent crosslinking system working at room temperature was enabled.

Improved strand network densities and an even faster gelation was observed for click-crosslinking of spherical hyperbranched azide- and alkyne-functionalized PIBs with varying amounts of reactive endgroups ranging from 3.04 up to 9.91 while applying bromotris(triphenylphosphine)copper(I) as catalyst at $20 \text{ }^\circ\text{C}$. Performed room temperature melt rheology experiments investigating the kinetics of the click crosslinking approach have shown gelation times in the range of 30 to 50 minutes indicating a very fast crosslinking process of more readily available reaction partners while linking spherical polymers with a complex architecture, therefore easily forming even more complex polymer networks. Thus, it was pointed out that covalent network formation of hyperbranched reactive PIBs was nearly independent on the starting viscosity of the polymer mixture as well as on the amount of functional groups.

Furthermore, hyperbranched functionalized PIBs partially modified with ionic moieties (20 %) were prepared to increase the fluidity of polymer mixtures and to study the influence of ionic clustering on the covalent network formation proceeding *via* CuAAC click-crosslinking. Due to unexpected strong microphase separation between attached ionic moieties and the unpolar polymer backbone, click-crosslinking of hyperbranched azide- and alkyne-functionalized PIBs mixed with 10 wt% of hyperbranched functionalized PIBs with attached ionic moieties was disturbed resulting in decreased reaction rates while displaying even higher gelation times than observed for click-crosslinking the respective three-arm star azide- and alkyne-telechelic PIBs. Nevertheless, both major drawbacks of crosslinking three-arm star polymers were overcome while changing the polymer architecture to a hyperbranched architecture resulting in faster gelation times at $20 \text{ }^\circ\text{C}$ and higher strand network densities of finally obtained polymer networks.

For the design of a dual crosslinked multiple self-healing system based on interwoven network structure providing both sufficient chain dynamics as well as mechanical integrity, fast and efficient room temperature click-crosslinking as well as supramolecular clustering was combined. Thus, three-arm star alkyne-telechelic PIB was converted at $40 \text{ }^\circ\text{C}$ with a partially modified four-arm star polymer containing 1.7 azide groups and 2.3 thymine-moieties acting as supramolecular tie points while applying bromotris(triphenylphosphine)copper(I) as catalyst (see Scheme 5).



Scheme 5: Design of a dual crosslinking system based on an interwoven network structure *via* covalent network formation due to click-crosslinking and *via* supramolecular network formation due to clustering of thymine-moieties suitable for multiple self-healing at room temperature. Click-crosslinking of four-arm star PIB with azide- and thymine-endgroups and three-arm star alkyne-telechelic PIB proceeded at 40 ° while applying bromotris(triphenylphosphine)copper(I) as catalyst.

Click-crosslinking – investigated *via* melt rheology – proceeded for 70 hours while a decrease of the loss factor $\tan(\delta)$ as well as an increase in G'' of around 50 % and in G' of around 190 % was observed, indicating the formation of covalent network points due to the proceeding click-crosslinking reaction. SAXS investigations of so obtained dual network structures reinforced *via* hydrogen bonding interactions proved the presence of supramolecular clusters, whereas the amount of involved hydrogen bonding moieties decreased from ≈ 10 to ≈ 8 in comparison to pure four-arm star thymine-telechelic PIB. Macroscopic self-healing studies of dual crosslinked polymer networks have shown multiple self-healing within 24 hours at 20 °C, whereas a significant reduction in the depth of the formerly present cut was already observed after two hours. Thus, the available synthesis of four-arm star PIBs bearing azide-endgroups as well as supramolecular tie points, namely thymine-moieties, enabled the design of a dual crosslinked room temperature self-healing system based on click-crosslinking and supramolecular cluster formation.

Furthermore, four-arm star thymine-telechelic PIB was investigated *via* melt rheology and SAXS measurements proving a prominent rubbery plateau with an outstanding high viscosity of 56 MPa·s and a plateau modulus of 1.1 MPa at 20 °C related to supramolecular clustering of thymine-moieties due to phase separation effects between the unpolar polymer backbone and the polar thymine-endgroups. Thus, SAXS investigations revealed a strong scattering peak at 0.97 nm^{-1} related to formed supramolecular clusters of ≈ 10 thymine-moieties with a distance of 6.5 nm in real space. Cut polymer films showed complete self-healing within 72 hours at 20 °C and within 24 hours at 40 °C thus highlighting the multiple self-healing potential of neat four-arm star thymine-telechelic PIBs.

The preparation of four-arm star azide-functionalized PIBs and their complete or partial modification with various supramolecular moieties *via* microwave-assisted click chemistry offers a wonderful playground for the development of supramolecular self-healing polymers as well as self-healing

polymers based on dual network formation. Due to the present interwoven network structures based on click-crosslinking and supramolecular clustering or based on two independent supramolecular network structures the dynamics and therefore the timescale of self-healing can be freely tuned by choosing the introduced supramolecular moiety. Thus, further investigations with other supramolecular motifs as well as more sophisticated self-healing investigations are ongoing in our laboratories as well as in collaboration within the DFG SPP 1568 "Design and Generic Principles of Self-Healing Materials".

8. REFERENCES

- [1] a)W. H. Binder, Wiley-VCH, Weinheim, **2013**, p. 440; b)B. J. Blaiszik, S. L. B. Kramer, S. C. Olugebefola, J. S. Moore, N. R. Sottos, S. R. White, *Annu. Rev. Mater. Res.* **2010**, *40*, 179; c)S. R. White, B. J. Blaiszik, *Spektrum der Wissenschaft* **2012**, *3*, 82; d)S. J. Garcia, *Eur. Polym. J.* **2014**, *53*, 118; e)H. Fischer, *Natural Science* **2010**, *2*, 873; f)M. Zhu, M. Z. Rong, M. Q. Zhang, *Polym. Int.* **2014**, *63*, 1741.
- [2] S. van der Zwaag, in *Self Healing Materials, An Alternative Approach to 20 Centuries of Materials Science, Vol. 100* (Ed.: S. van der Zwaag), Springer Netherlands, **2007**, pp. 1.
- [3] J.-M. Lehn, *Angew. Chem. Int. Ed.* **2015**, *54*, 3276.
- [4] a)S. Hoffmann, *P.M. Magazin* **2014**, *1*, 32; b)P. Fratzl, R. Weinkamer, in *Self Healing Materials, An Alternative Approach to 20 Centuries of Materials Science., Vol. 100* (Ed.: S. van der Zwaag), Springer Netherlands, **2007**, pp. 323.
- [5] a)Q. Liu, E. Schlangen, Á. García, M. van de Ven, *Constr. Build. Mater.* **2010**, *24*, 1207; b)Q. Liu, W. Yu, E. Schlangen, G. van Bochove, *Constr. Build. Mater.* **2014**, *71*, 152; c)Q. Liu, Á. García, E. Schlangen, M. v. d. Ven, *Constr. Build. Mater.* **2011**, *25*, 3746; d)E. Schlangen, in *Self Healing Asphalt, Vol. 2015*.
- [6] a)L. Lucas, in *Biom mineralization: Key to Self-Healing Concrete, Vol. 2015*, **2012**; b)H. Jonkers, in *Self-healing of Concrete by Bacterial Mineral Precipitation, Vol. 2015* (Ed.: H. Jonkers); c)H. M. Jonkers, A. Thijssen, G. Muyzer, O. Copuroglu, E. Schlangen, *Ecol. Eng.* **2010**, *36*, 230; d)A. Bertron, *Mater. Struct.* **2014**, *47*, 1787.
- [7] a)<http://www.materialscience.bayer.com/>, *Vol. 2015*; b)<http://www.ruehl-ag.de/>, *Vol. 2015*; c)<http://www.nissan-global.com/EN/TECHNOLOGY/OVERVIEW/scratch.html>, *Vol. 2015*; d)O. Fleck, S. Nowak, U. Meier-Westhuis, *Eur. Coat. J.* **2009**, *4*, 106.
- [8] a)R. P. Wool, K. M. O'Connor, *J. Appl. Phys.* **1981**, *52*, 5953; b)R. P. Wool, K. M. O'Connor, *J. Polym. Sci. Pol. Lett.* **1982**, *20*, 7; c)M. Q. Zhang, M. Z. Rong, *J. Polym. Sci. Part B: Polym. Phys.* **2012**, *50*, 229; d)T. Ge, M. O. Robbins, D. Perahia, G. S. Grest, *Phys. Rev. E* **2014**, *90*, 012602.
- [9] a)Z. Erno, A. M. Asadirad, V. Lemieux, N. R. Branda, *Org. Biomol. Chem.* **2012**, *10*, 2787; b)C. Zeng, H. Seino, J. Ren, K. Hatanaka, N. Yoshie, *Polymer* **2013**, *54*, 5351; c)C. Zeng, H. Seino, J. Ren, K. Hatanaka, N. Yoshie, *Macromolecules* **2013**, *46*, 1794; d)S. D. Bergman, F. Wudl, *J. Mater. Chem.* **2008**, *18*, 41; e)X. Chen, M. A. Dam, K. Ono, A. Mal, H. Shen, S. R. Nutt, K. Sheran, F. Wudl, *Science* **2002**, *295*, 1698; f)X. Chen, F. Wudl, A. K. Mal, H. Shen, S. R. Nutt, *Macromolecules* **2003**, *36*, 1802; g)E. B. Murphy, E. Bolanos, C. Schaffner-Hamann, F. Wudl, S. R. Nutt, M. L. Auad, *Macromolecules* **2008**, *41*, 5203; h)Y. Chujo, K. Sada, T. Saegusa, *Macromolecules* **1990**, *23*, 2636; i)S. Dumitrescu, M. Grigoras, A. Natansohn, *J. Polym. Sci. Pol. Lett.* **1979**, *17*, 553; j)A. Gandini, *Polím.: Ciênc. Tecnol.* **2005**, *15*, 95; k)K. M. Wiggins, J. N. Brantley, C. W. Bielawski, *Chem. Soc. Rev.* **2013**, *42*, 7130; l)K. M. Wiggins, T. W. Hudnall, A. G. Tennyson, C. W. Bielawski, *J. Mater. Chem.* **2011**, *21*, 8355; m)J. R. Jones, C. L. Liotta, D. M. Collard, D. A. Schiraldi, *Macromolecules* **1999**, *32*, 5786; n)S. A. Canary, M. P. Stevens, *J. Polym. Sci. Part A: Polym. Chem.* **1992**, *30*, 1755; o)A. J. Inglis, L. Nebhani, O. Altintas, F. G. Schmidt, C. Barner-Kowollik, *Macromolecules* **2010**, *43*, 5515; p)P. Reutenauer, E. Buhler, P. J. Boul, S. J. Candau, J.-M. Lehn, *Chem. Eur. J.* **2009**, *15*, 1893; q)A. J. Inglis, S. Sinnwell, M. H. Stenzel, C. Barner-Kowollik, *Angew. Chem. Int. Ed.* **2009**, *48*, 2411; r)N. Yoshie, S. Saito, N. Oya, *Polymer* **2011**, *52*, 6074; s)B. J. Adzima, H. A. Aguirre, C. J. Kloxin, T. F. Scott, C. N. Bowman, *Macromolecules* **2008**, *41*, 9112; t)A. M. Asadirad, S. Boutault, Z. Erno, N. R. Branda, *J. Am. Chem. Soc.* **2014**, *136*, 3024; u)J. Ax, G. Wenz, *Macromol. Chem. Phys.* **2012**, *213*, 182; v)M. J. Barthel, T. Rudolph, A. Teichler, R. M. Paulus, J. Vitz, S. Hoepfener, M. D. Hager, F. H. Schacher, U. S. Schubert,

- Adv. Funct. Mater.* **2013**, *23*, 4921; w)R. K. Bose, J. Kötteritzsch, S. J. Garcia, M. D. Hager, U. S. Schubert, S. van der Zwaag, *J. Polym. Chem. Part A: Polym. Chem.* **2014**, *52*, 1669; x)J. Kötteritzsch, M. D. Hager, U. S. Schubert, *Polymer* **2015**, doi:10.1016/j.polymer.2015.03.027; y)J. Kötteritzsch, S. Stumpf, S. Hoepfener, J. Vitz, M. D. Hager, U. S. Schubert, *Macromol. Chem. Phys.* **2013**, *214*, 1636; z)J. Canadell, H. Fischer, G. De With, R. A. T. M. van Benthem, *J. Polym. Sci. Part A: Polym. Chem.* **2010**, *48*, 3456; aa)X. Cheng, C. Peng, D. Zhang, S. Liu, A. Zhang, H. Huang, J. Lian, *J. Polym. Sci Part A: Polym. Chem.* **2013**, *51*, 1205; ab)E. Goiti, F. Heatley, M. B. Huglin, J. M. Rego, *Eur. Polym. J.* **2004**, *40*, 1451; ac)E. Goiti, M. B. Huglin, J. M. Rego, *Polymer* **2001**, *42*, 10187; ad)E. Goiti, M. B. Huglin, J. M. Rego, *Macromol. Rapid Commun.* **2003**, *24*, 692; ae)E. Goiti, M. B. Huglin, J. M. Rego, *Eur. Polym. J.* **2004**, *40*, 219; af)C. Goussé, A. Gandini, P. Hodge, *Macromolecules* **1998**, *31*, 314; ag)J. He, Y. Zhang, E. Y. X. Chen, *J. Polym. Sci Part A: Polym. Chem.* **2013**, *51*, 2793; ah)K. Ishida, Y. Nishiyama, Y. Michimura, N. Oya, N. Yoshie, *Macromolecules* **2010**, *43*, 1011; ai)K. Ishida, V. Weibel, N. Yoshie, *Polymer* **2011**, *52*, 2877; aj)K. Ishida, N. Yoshie, *Macromol. Biosci.* **2008**, *8*, 916; ak)K. Ishida, N. Yoshie, *Macromolecules* **2008**, *41*, 4753; al)A. A. Kavitha, N. K. Singha, *J. Polym. Sci. Part A: Polym. Chem.* **2007**, *45*, 4441; am)A. A. Kavitha, N. K. Singha, *Macromol. Chem. Phys.* **2007**, *208*, 2569; an)A. A. Kavitha, N. K. Singha, *ACS Appl. Mater. Interfaces* **2009**, *1*, 1427; ao)A. A. Kavitha, N. K. Singha, *Macromolecules* **2010**, *43*, 3193; ap)Y.-L. Liu, Y.-W. Chen, *Macromol. Chem. Phys.* **2007**, *208*, 224; aq)Y.-L. Liu, T.-W. Chuo, *Polym. Chem.* **2013**, *4*, 2194; ar)H. Mallek, C. Jegat, N. Mignard, M. Abid, S. Abid, M. Taha, *J. Appl. Polym. Sci.* **2013**, *129*, 954; as)K. K. Oehlenschlaeger, J. O. Mueller, J. Brandt, S. Hilf, A. Lederer, M. Wilhelm, R. Graf, M. L. Coote, F. G. Schmidt, C. Barner-Kowollik, *Adv. Mater.* **2014**, *26*, 3561; at)T. A. Plaisted, S. Nemat-Nasser, *Acta Mater.* **2007**, *55*, 5684; au)G. Postiglione, S. Turri, M. Levi, *Prog. Org. Coat.* **2015**, *78*, 526; av)N. B. Pramanik, G. B. Nando, N. K. Singha, *Polymer* **2015**, doi:10.1016/j.polymer.2015.01.023; aw)H. Sun, C. P. Kabb, B. S. Sumerlin, *Chem. Sci.* **2014**, *5*, 4646; ax)J. A. Syrett, G. Mantovani, W. R. S. Barton, D. Price, D. M. Haddleton, *Polym. Chem.* **2010**, *1*, 102; ay)M. Watanabe, N. Yoshie, *Polymer* **2006**, *47*, 4946; az)H.-L. Wei, Z. Yang, Y. Chen, H.-J. Chu, J. Zhu, Z.-C. Li, *Eur. Polym. J.* **2010**, *46*, 1032; ba)Z. Wei, J. H. Yang, X. J. Du, F. Xu, M. Zrinyi, Y. Osada, F. Li, Y. M. Chen, *Macromol. Rapid Commun.* **2013**, *34*, 1464; bb)N. Yoshie, M. Watanabe, H. Araki, K. Ishida, *Polym. Degrad. Stabil.* **2010**, *95*, 826; bc)J. J. Intemann, W. Huang, Z. Jin, Z. Shi, X. Yang, J. Yang, J. Luo, A. K. Y. Jen, *ACS Macro Lett.* **2013**, *2*, 256.
- [10] a)R. J. Varley, B. Dao, C. Pillsbury, S. J. Kalista, F. R. Jones, *J. Intel. Mat. Syst. Str.* **2014**, *25*, 107; b)T. Siva, K. Kamaraj, S. Sathiyarayanan, *Prog. Org. Coat.* **2014**, *77*, 1095; c)L. Guadagno, M. Raimondo, C. Naddeo, P. Longo, A. Mariconda, *Polym. Eng. Sci.* **2014**, *54*, 777; d)L. Guadagno, M. Raimondo, C. Naddeo, P. Longo, A. Mariconda, W. H. Binder, *Smart Mater. Struct.* **2014**, *23*, 045001; e)M. Raimondo, L. Guadagno, *AIP Conf. Proc.* **2012**, *1459*, 223; f)Q. Tian, Y. C. Yuan, M. Z. Rong, M. Q. Zhang, *J. Mater. Chem.* **2009**, *19*, 1289; g)Y. C. Yuan, M. Z. Rong, M. Q. Zhang, G. C. Yang, *eXpress Polym. Lett.* **2011**, *5*, 47; h)T. S. Coope, U. F. J. Mayer, D. F. Wass, R. S. Trask, I. P. Bond, *Adv. Funct. Mater* **2011**, *21*, 4624; i)L. Guadagno, P. Longo, M. Raimondo, C. Naddeo, A. Mariconda, A. Sorrentino, V. Vittoria, G. Iannuzzo, S. Russo, *J. Polym. Sci Part B: Polym. Phys.* **2010**, *48*, 2413; j)M. A. M. Rahmathullah, G. R. Palmese, *J. Appl. Polym. Sci.* **2009**, *113*, 2191; k)E. N. Brown, S. R. White, N. R. Sottos, *Compos. Sci. Technol.* **2005**, *65*, 2474; l)M. M. Caruso, D. A. Delafuente, V. Ho, N. R. Sottos, J. S. Moore, S. R. White, *Macromolecules* **2007**, *40*, 8830; m)G. O. Wilson, J. S. Moore, S. R. White, N. R. Sottos, H. M. Andersson, *Adv. Funct. Mater* **2008**, *18*, 44; n)M. Z. Rong, M. Q. Zhang, W. Zhang, *Adv. Compos. Lett.* **2007**, *16*, 167; o)T. Yin, M. Z. Rong, M. Q. Zhang, G. C. Yang, *Compos. Sci. Technol.* **2007**, *67*, 201; p)M. Zako, N. Takano,

- J. Intel. Mat. Syst. Str.* **1999**, *10*, 836; q)H. Jin, C. L. Mangun, A. S. Griffin, J. S. Moore, N. R. Sottos, S. R. White, *Adv. Mater.* **2014**, *26*, 282; r)H. Jin, C. L. Mangun, D. S. Stradley, J. S. Moore, N. R. Sottos, S. R. White, *Polymer* **2012**, *53*, 581; s)J. M. Kamphaus, J. D. Rule, J. S. Moore, N. R. Sottos, S. R. White, *J. Roy. Soc. Interface* **2008**, *5*, 95; t)H. Jin, G. M. Miller, S. J. Pety, A. S. Griffin, D. S. Stradley, D. Roach, N. R. Sottos, S. R. White, *Int. J. Adhes. Adhes.* **2013**, *44*, 157; u)H. Jin, G. M. Miller, N. R. Sottos, S. R. White, *Polymer* **2011**, *52*, 1628; v)N. W. Khun, D. W. Sun, M. X. Huang, J. L. Yang, C. Y. Yue, *Wear* **2014**, *313*, 19; w)M. A. Rahman, L. Sartore, F. Bignotti, L. Di Landro, *ACS Appl. Mater. Interfaces* **2013**, *5*, 1494; x)D. S. Xiao, Y. C. Yuan, M. Z. Rong, M. Q. Zhang, *Polymer* **2009**, *50*, 2967; y)Y. C. Yuan, M. Z. Rong, M. Q. Zhang, J. Chen, G. C. Yang, X. M. Li, *Macromolecules* **2008**, *41*, 5197; z)H. Zhang, J. Wang, X. Liu, Z. Wang, S. Wang, *Ind. Eng. Chem. Res.* **2013**, *52*, 10172; aa)T. S. Coope, D. F. Wass, R. S. Trask, I. P. Bond, *Macromol. Mater. Eng.* **2014**, 299, 208; ab)A. M. Peterson, R. E. Jensen, G. R. Palmese, *ACS Appl. Mater. Interfaces* **2009**, *1*, 992; ac)F. I. Altuna, V. Pettarin, R. J. J. Williams, *Green Chem.* **2013**, *15*, 3360.
- [11] a)P. Espeel, F. Goethals, F. E. Du Prez, *J. Am. Chem. Soc.* **2011**, *133*, 1678; b)M. T. Gokmen, J. Brassinne, R. A. Prasath, F. E. Du Prez, *Chem. Commun.* **2011**, *47*, 4652; c)R. A. Prasath, M. T. Gokmen, P. Espeel, F. E. Du Prez, *Polym. Chem.* **2010**, *1*, 685; d)M. J. Kade, D. J. Burke, C. J. Hawker, *J. Polym. Sci. A: Polym. Chem.* **2010**, *48*, 743; e)H. B. Yue, J. P. Fernandez-Blazquez, D. F. Beneito, J. J. Vilatela, *J. Mater. Chem. A* **2014**, *2*, 3881; f)B.-S. Chiou, S. A. Khan, *Macromolecules* **1997**, *30*, 7322; g)A. E. van der Ende, J. Harrell, V. Sathiyakumar, M. Meschievitz, J. Katz, K. Adcock, E. Harth, *Macromolecules* **2010**, *43*, 5665; h)D. Döhler, P. Michael, W. H. Binder, *Macromolecules* **2012**, *45*, 3335; i)M. Gragert, M. Schunack, W. H. Binder, *Macromol. Rapid Commun.* **2011**, *32*, 419; j)M. Schunack, M. Gragert, D. Döhler, P. Michael, W. H. Binder, *Macromol. Chem. Phys.* **2012**, *213*, 205; k)S. Vasiliu, B. Kampe, F. Theil, B. Dietzek, D. Döhler, P. Michael, W. H. Binder, J. Popp, *Appl. Spectrosc.* **2014**, *68*, 541; l)X. Sheng, T. C. Mauldin, M. R. Kessler, *J. Polym. Sci. Part A: Polym. Chem.* **2010**, *48*, 4093; m)X. Sheng, D. M. Rock, T. C. Mauldin, M. R. Kessler, *Polymer* **2011**, *52*, 4435; n)S. Kantheti, R. Narayan, K. V. S. N. Raju, *RSC Adv.* **2015**, *5*, 3687; o)H. Cengiz, B. Aydogan, S. Ates, E. Acikalın, Y. Yagci, *Des. Monomers. Polym.* **2011**, *14*, 69; p)A. R. de Luzuriaga, N. Ormategui, H. J. Grande, I. Odriozola, J. A. Pomposo, I. Loinaz, *Macromol. Rapid Commun.* **2008**, *29*, 1156; q)M. Meldal, *Macromol. Rapid Commun.* **2008**, *29*, 1016; r)D. D. Díaz, S. Punna, P. Holzer, A. K. McPherson, K. B. Sharpless, V. V. Fokin, M. G. Finn, *J. Polym. Sci. Part A: Polym. Chem.* **2004**, *42*, 4392; s)Y. Liu, D. D. Díaz, A. A. Accurso, K. B. Sharpless, V. V. Fokin, M. G. Finn, *J. Polym. Sci. Part A: Polym. Chem.* **2007**, *45*, 5182; t)N. L. Baut, D. D. Díaz, S. Punna, M. G. Finn, H. R. Brown, *Polymer* **2007**, *48*, 239; u)C. Li, M. G. Finn, *J. Polym. Sci. Part A: Polym. Chem.* **2006**, *44*, 5513; v)S. Q. Liu, P. L. R. Ee, C. Y. Ke, J. L. Hedrick, Y. Y. Yang, *Biomaterials* **2009**, *30*, 1453; w)M. Malkoch, R. Vestberg, N. Gupta, L. Mespouille, P. Dubois, A. F. Mason, J. L. Hedrick, Q. Liao, C. W. Frank, K. Kingsbury, C. J. Hawker, *Chem. Commun.* **2006**, 2774; x)D. A. Ossipov, J. Hilborn, *Macromolecules* **2006**, *39*, 1709; y)J. Liu, X. Jiang, L. Xu, X. Wang, W. E. Hennink, R. Zhuo, *Bioconjugate Chem.* **2010**, *21*, 1827; z)J. A. Johnson, D. R. Lewis, D. D. Díaz, M. G. Finn, J. T. Koberstein, N. J. Turro, *J. Am. Chem. Soc.* **2006**, *128*, 6564; aa)G. Testa, C. Di Meo, S. Nardecchia, D. Capitani, L. Mannina, R. Lamanna, A. Barbeta, M. Dentini, *Int. J. Pharm.* **2009**, *378*, 86; ab)A. R. Katritzky, N. K. Meher, S. Hanci, R. Gyanda, S. R. Tala, S. Mathai, R. S. Duran, S. Bernard, F. Sabri, S. K. Singh, J. Doskocz, D. A. Ciaramitaro, *J. Polym. Sci. Part A: Polym. Chem.* **2008**, *46*, 238; ac)G. Huerta-Angeles, D. Šmejkalová, D. Chládková, T. Ehlová, R. Buffa, V. Velebný, *Carbohydr. Polym.* **2011**, *84*, 1293; ad)Q. Wei, J. Wang, X. Shen, X. A. Zhang, J. Z. Sun, A. Qin, B. Z. Tang, *Sci. Rep.* **2013**, *3*, 1; ae)S. Billiet, W. Van Camp, X. K. D. Hillewaere, H. Rahier, F. E. Du Prez,

- Polymer* **2012**, *53*, 2320; af)M.-H. Yao, J. Yang, M.-S. Du, J.-T. Song, Y. Yu, W. Chen, Y.-D. Zhao, B. Liu, *J. Mater. Chem. B* **2014**, *2*, 3123.
- [12] a)Z. Zhang, Y. Hu, Z. Liu, T. Guo, *Polymer* **2012**, *53*, 2979; b)A. C. Schüssele, F. Nübling, Y. Thomann, O. Carstensen, G. Bauer, T. Speck, R. Mülhaupt, *Macromol. Mater. Eng.* **2012**, *297*, 411; c)Y. Bai, Y. Chen, Q. Wang, T. Wang, *J. Mater. Chem. A* **2014**, *2*, 9169; d)J. Yang, M. W. Keller, J. S. Moore, S. R. White, N. R. Sottos, *Macromolecules* **2008**, *41*, 9650; e)T. Dikić, W. Ming, R. A. T. M. van Benthem, A. C. C. Esteves, G. de With, *Adv. Mater.* **2012**, *24*, 3701.
- [13] a)S. R. White, N. R. Sottos, P. H. Geubelle, J. S. Moore, M. R. Kessler, S. R. Sriram, E. N. Brown, S. Viswanathan, *Nature* **2001**, *409*, 794; b)G. E. Larin, N. Bernklau, M. R. Kessler, J. C. DiCesare, *Polym. Eng. Sci.* **2006**, *46*, 1804; c)J. K. Lee, X. Liu, S. H. Yoon, M. R. Kessler, *J. Polym. Sci. Part B: Polym. Phys.* **2007**, *45*, 1771; d)X. Sheng, J. K. Lee, M. R. Kessler, *Polymer* **2009**, *50*, 1264; e)M. R. Kessler, N. R. Sottos, S. R. White, *Compos. Part A-Appl. S.* **2003**, *34*, 743; f)J. D. Rule, J. S. Moore, *Macromolecules* **2002**, *35*, 7878; g)X. Liu, J. K. Lee, S. H. Yoon, M. R. Kessler, *J. Appl. Polym. Sci.* **2006**, *101*, 1266; h)T. C. Mauldin, J. Leonard, K. Earl, J. K. Lee, M. R. Kessler, *ACS Appl. Mater. Interfaces* **2012**, *4*, 1831; i)M. Aldridge, C. Shankar, Changgua Zhen, Lang Sui, J. Kieffer, M. Caruso, J. Moore, *J. Compos. Mater.* **2010**, *44*, 2605; j)A. S. Jones, J. D. Rule, J. S. Moore, N. R. Sottos, S. R. White, *J. Roy. Soc. Interface* **2007**, *4*, 395; k)A. S. Jones, J. D. Rule, J. S. Moore, S. R. White, N. R. Sottos, *Chem. Mater.* **2006**, *18*, 1312; l)T. C. Mauldin, J. D. Rule, N. R. Sottos, S. R. White, J. S. Moore, *J. Roy. Soc. Interface* **2007**, *4*, 389; m)G. O. Wilson, M. M. Caruso, N. T. Reimer, S. R. White, N. R. Sottos, J. S. Moore, *Chem. Mater.* **2008**, *20*, 3288; n)D. M. Chipara, M. Flores, A. Perez, N. Puente, K. Lozano, M. Chipara, *Adv. Polym. Tech.* **2013**, *32*, E505; o)M. D. Chipara, M. Chipara, E. Shansky, J. M. Zaleski, *Polym. Adv. Technol.* **2009**, *20*, 427; p)M. R. Kessler, S. R. White, *J. Polym. Sci. A: Polym. Chem.* **2002**, *40*, 2373; q)X. Liu, X. Sheng, J. K. Lee, M. R. Kessler, J. S. Kim, *Compos. Sci. Technol.* **2009**, *69*, 2102; r)J. Lee, S. Hong, X. Liu, S. Yoon, *Macromol. Res.* **2004**, *12*, 478; s)M. Majchrzak, P. J. Hine, E. Khosravi, *Polymer* **2012**, *53*, 5251.
- [14] a)R. Groote, R. T. M. Jakobs, R. P. Sijbesma, *Polym. Chem.* **2013**, *4*, 4846; b)M. M. Caruso, D. A. Davis, Q. Shen, S. A. Odom, N. R. Sottos, S. R. White, J. S. Moore, *Chem. Rev.* **2009**, *109*, 5755; c)D. A. Davis, A. Hamilton, J. Yang, L. D. Cremar, D. Van Gough, S. L. Potisek, M. T. Ong, P. V. Braun, T. J. Martínez, S. R. White, J. S. Moore, N. R. Sottos, *Nature* **2009**, *459*, 68; d)C. R. Hickenboth, J. S. Moore, S. R. White, N. R. Sottos, J. Baudry, S. R. Wilson, *Nature* **2007**, *446*, 423.
- [15] Z. S. Kean, S. L. Craig, *Polymer* **2012**, *53*, 1035.
- [16] a)B. A. Beiermann, S. L. B. Kramer, J. S. Moore, S. R. White, N. R. Sottos, *ACS Macro Lett.* **2012**, *1*, 163; b)C. M. Kingsbury, P. A. May, D. A. Davis, S. R. White, J. S. Moore, N. R. Sottos, *J. Compos. Mater.* **2011**, *21*, 8381; c)M. J. Kryger, A. M. Munaretto, J. S. Moore, *J. Am. Chem. Soc.* **2011**, *133*, 18992; d)J. M. Lenhardt, A. L. Black, B. A. Beiermann, B. D. Steinberg, F. Rahman, T. Samborski, J. Elsagr, J. S. Moore, N. R. Sottos, S. L. Craig, *J. Mater. Chem.* **2011**, *21*, 8454; e)S. L. Potisek, D. A. Davis, N. R. Sottos, S. R. White, J. S. Moore, *J. Am. Chem. Soc.* **2007**, *129*, 13808; f)H. M. Klukovich, Z. S. Kean, S. T. Iacono, S. L. Craig, *J. Am. Chem. Soc.* **2011**, *133*, 17882; g)H. M. Klukovich, T. B. Kouznetsova, Z. S. Kean, J. M. Lenhardt, S. L. Craig, *Nat. Chem.* **2013**, *5*, 110; h)J. M. Lenhardt, A. L. Black, S. L. Craig, *J. Am. Chem. Soc.* **2009**, *131*, 10818.
- [17] a)S. Karthikeyan, S. L. Potisek, A. Piermattei, R. P. Sijbesma, *J. Am. Chem. Soc.* **2008**, *130*, 14968; b)J. M. J. Paulusse, J. P. J. Huijbers, R. P. Sijbesma, *Chem. Eur. J.* **2006**, *12*, 4928; c)J. M. J. Paulusse, R. P. Sijbesma, *Angew. Chem. Int. Ed.* **2004**, *43*, 4460; d)A. Piermattei, S. Karthikeyan, R. P. Sijbesma, *Nat. Chem.* **2009**, *1*, 133.

- [18] a)Y.-K. Song, Y.-H. Jo, Y.-J. Lim, S.-Y. Cho, H.-C. Yu, B.-C. Ryu, S.-I. Lee, C.-M. Chung, *ACS Appl. Mater. Interfaces* **2013**, *5*, 1378; b)X. F. Lei, Y. Chen, H. P. Zhang, X. J. Li, P. Yao, Q. Y. Zhang, *ACS Appl. Mater. Interfaces* **2013**, *5*, 10207; c)S. H. Cho, S. R. White, P. V. Braun, *Adv. Mater.* **2009**, *21*, 645; d)S. H. Cho, S. R. White, P. V. Braun, *Chem. Mater.* **2012**, *24*, 4209; e)K. Takeda, M. Tanahashi, H. Unno, *Sci. Technol. Adv. Mat.* **2003**, *4*, 435; f)K. Takeda, H. Unno, M. Zhang, *J. Appl. Polym. Sci.* **2004**, *93*, 920; g)S. H. Cho, H. M. Andersson, S. R. White, N. R. Sottos, P. V. Braun, *Adv. Mater.* **2006**, *18*, 997; h)F. W. van Der Weij, *Makromol. Chem.* **1980**, *181*, 2541; i)X. Y. Fu, Z. P. Fang, H. T. Yang, L. F. Tong, *Chinese Chem. Lett.* **2008**, *19*, 655; j)M. W. Keller, S. R. White, N. R. Sottos, *Adv. Funct. Mater.* **2007**, *17*, 2399; k)M. W. Keller, S. R. White, N. R. Sottos, *Polymer* **2008**, *49*, 3136.
- [19] a)B. T. Michal, C. A. Jaye, E. J. Spencer, S. J. Rowan, *ACS Macro Lett.* **2013**, *2*, 694; b)J. A. Yoon, J. Kamada, K. Koynov, J. Mohin, R. Nicolaÿ, Y. Zhang, A. C. Balazs, T. Kowalewski, K. Matyjaszewski, *Macromolecules* **2011**, *45*, 142; c)M. Pepels, I. Filot, B. Klumperman, H. Goossens, *Polym. Chem.* **2013**, *4*, 4955; d)R. Martin, A. Rekondo, A. Ruiz de Luzuriaga, G. Cabanero, H. J. Grande, I. Odriozola, *J. Mater. Chem. A* **2014**, *2*, 5710; e)A. Rekondo, R. Martin, A. Ruiz de Luzuriaga, G. Cabanero, H. J. Grande, I. Odriozola, *Mater. Horiz.* **2014**, *1*, 237; f)Z. Q. Lei, H. P. Xiang, Y. J. Yuan, M. Z. Rong, M. Q. Zhang, *Chem. Mater.* **2014**, *26*, 2038; g)B. Gyarmati, Á. Némethy, A. Szilágyi, *Eur. Polym. J.* **2013**, *49*, 1268; h)J. J. Griebel, N. A. Nguyen, A. V. Astashkin, R. S. Glass, M. E. Mackay, K. Char, J. Pyun, *ACS Macro Lett.* **2014**, *3*, 1258; i)N. V. Tsarevsky, K. Matyjaszewski, *Macromolecules* **2002**, *35*, 9009; j)Y. Chujo, K. Sada, A. Naka, R. Nomura, T. Saegusa, *Macromolecules* **1993**, *26*, 883; k)J. Canadell, H. Goossens, B. Klumperman, *Macromolecules* **2011**, *44*, 2536; l)A. P. Bapat, J. G. Ray, D. A. Savin, B. S. Sumerlin, *Macromolecules* **2013**, *46*, 2188; m)U. Lafont, H. van Zeijl, S. van der Zwaag, *ACS Appl. Mater. Interfaces* **2012**, *4*, 6280; n)Y. Amamoto, H. Otsuka, A. Takahara, K. Matyjaszewski, *Adv. Mater.* **2012**, *24*, 3975.
- [20] a)F. Wang, M. Z. Rong, M. Q. Zhang, *J. Mater. Chem.* **2012**, *22*, 13076; b)K. N. Long, M. L. Dunn, T. F. Scott, L. P. Turpin, H. J. Qi, *J. Appl. Phys.* **2010**, *107*, 053519; c)T. F. Scott, A. D. Schneider, W. D. Cook, C. N. Bowman, *Science* **2005**, *308*, 1615; d)T. Ono, T. Nobori, J.-M. Lehn, *Chem. Commun.* **2005**, 1522; e)G. Moad, *Polym. Int.* **2015**, *64*, 15; f)L. Yao, M. Z. Rong, M. Q. Zhang, Y. C. Yuan, *J. Mater. Chem.* **2011**, *21*, 9060; g)L. Yao, Y. C. Yuan, M. Z. Rong, M. Q. Zhang, *Polymer* **2011**, *52*, 3137; h)Y. Amamoto, M. Kikuchi, H. Masunaga, S. Sasaki, H. Otsuka, A. Takahara, *Macromolecules* **2009**, *42*, 8733; i)S. Telitel, Y. Amamoto, J. Poly, F. Morlet-Savary, O. Soppera, J. Lalevee, K. Matyjaszewski, *Polym. Chem.* **2014**, *5*, 921; j)C. e. Yuan, M. Z. Rong, M. Q. Zhang, Z. P. Zhang, Y. C. Yuan, *Chem. Mater.* **2011**, *23*, 5076; k)C. e. Yuan, M. Q. Zhang, M. Z. Rong, *J. Mater. Chem. A* **2014**, *2*, 6558; l)Z. P. Zhang, M. Z. Rong, M. Q. Zhang, *Polymer* **2014**, *55*, 3936; m)Z. P. Zhang, M. Z. Rong, M. Q. Zhang, C. e. Yuan, *Polym. Chem.* **2013**, *4*, 4648.
- [21] a)S. Burattini, B. W. Greenland, D. Chappell, H. M. Colquhoun, W. Hayes, *Chem. Soc. Rev.* **2010**, *39*, 1973; b)J.-M. Chang, J. J. Aklonis, *J. Polym. Sci. Pol. Lett.* **1983**, *21*, 999; c)Y. Chujo, K. Sada, R. Nomura, A. Naka, T. Saegusa, *Macromolecules* **1993**, *26*, 5611; d)L. A. Connal, R. Vestberg, C. J. Hawker, G. G. Qiao, *Adv. Funct. Mater.* **2008**, *18*, 3315; e)M. Coursan, J. P. Desvergne, A. Deffieux, *Makromol. Chem. Phys.* **1996**, *197*, 1599; f)P. Froimowicz, H. Frey, K. Landfester, *Makromol. Rapid Commun.* **2011**, *32*, 468; g)J. Matsui, Y. Ochi, K. Tamaki, *Chem. Lett.* **2006**, *35*, 80; h)T. Torii, H. Ushiki, K. Horie, *Polym. J.* **1993**, *25*, 173; i)Y. Zheng, M. Micic, S. V. Mello, M. Mabrouki, F. M. Andreopoulos, V. Konka, S. M. Pham, R. M. Leblanc, *Macromolecules* **2002**, *35*, 5228; j)Y. Chen, J.-L. Geh, *Polymer* **1996**, *37*, 4481; k)Y. Chujo, K. Sada, T. Saegusa, *Macromolecules* **1990**, *23*, 2693; l)S. R. Trenor, A. R. Shultz, B. J. Love, T. E. Long, *Chem. Rev.* **2004**, *104*, 3059; m)W. L. Dilling, *Chem. Rev.* **1983**, *83*, 1; n)C. M. Chung, Y. S. Roh, S. Y. Cho, J. G. Kim, *Chem. Mater.* **2004**,

- 16, 3982; o)S. Banerjee, R. Tripathy, D. Cozzens, T. Nagy, S. Keki, M. Zsuga, R. Faust, *ACS Appl. Mater. Interfaces* **2015**, *7*, 2064; p)C. Cardenas-Daw, A. Kroeger, W. Schaertl, P. Froimowicz, K. Landfester, *Macromol. Chem. Phys.* **2012**, *213*, 144; q)P. Froimowicz, D. Klinger, K. Landfester, *Chem. Eur. J.* **2011**, *17*, 12465; r)D. Habault, H. Zhang, Y. Zhao, *Chem. Soc. Rev.* **2013**, *42*, 7244; s)L. Hu, X. Cheng, A. Zhang, *J. Mater. Sci.* **2015**, *50*, 2239; t)B. Kiskan, Y. Yagci, *J. Polym. Sci Part A: Polym. Chem.* **2014**, *52*, 2911; u)Y.-K. Song, C.-M. Chung, *Polym. Chem.* **2013**, *4*, 4940; v)Y.-K. Song, K.-H. Lee, W.-S. Hong, S.-Y. Cho, H.-C. Yu, C.-M. Chung, *J. Mater. Chem.* **2012**, *22*, 1380.
- [22] a)W. H. Binder, R. Sachsenhofer, *Macromol. Rapid Commun.* **2007**, *28*, 15; b)W. H. Binder, R. Sachsenhofer, *Macromol. Rapid Commun.* **2008**, *29*, 952; c)W. H. Binder, R. Zirbs, in *Encyclopedia of Polymer Science and Technology*, John Wiley & Sons Inc., **2009**.
- [23] H. C. Kolb, M. G. Finn, K. B. Sharpless, *Angew. Chem. Int. Ed.* **2001**, *40*, 2004.
- [24] a)P. J. Flory, *J. Am. Chem. Soc.* **1952**, *74*, 2718; b)P. J. Flory, *J. Am. Chem. Soc.* **1941**, *63*, 3083; c)W. H. Stockmayer, *J. Chem. Phys.* **1943**, *11*, 45.
- [25] J. Ampudia, E. Larrauri, E. M. Gil, M. Rodríguez, L. M. León, *J. Appl. Polym. Sci.* **1999**, *71*, 1239.
- [26] a)H. H. Winter, M. Mours, *Adv. Polym. Sci.* **1997**, *134*, 165; b)C. Chassenieux, L. Bouteiller, in *Supramolecular Chemistry: From Molecules to Nanomaterials, Vol. 2* (Eds.: J. W. Steed, P. A. Gale), Wiley, **2012**, p. 517.
- [27] J. H. Daly, D. Hayward, R. A. Pethrick, *Macromolecules* **2013**, *46*, 3621.
- [28] F. Xia, L. Jiang, *Adv. Mater.* **2008**, *20*, 2842.
- [29] V. Lemieux, S. Gauthier, N. R. Branda, *Angew. Chem. Int. Ed.* **2006**, *45*, 6820.
- [30] a)E. A. Appel, J. del Barrio, X. J. Loh, O. A. Scherman, *Chem. Soc. Rev.* **2012**, *41*, 6195; b)W. Binder, R. Zirbs, in *Hydrogen Bonded Polymers*, **2007**, pp. 1; c)W. H. Binder, C. Enders, F. Herbst, K. Hackethal, *Synthesis and Self-Assembly of Hydrogen-Bonded Supramolecular Polymers*, John Wiley & Sons (Asia) Pte Ltd, **2011**; d)T. Aida, E. W. Meijer, S. I. Stupp, *Science* **2012**, *335*, 813; e)H. Hofmeier, U. S. Schubert, *Chem. Commun.* **2005**, 2423; f)J. S. Moore, *Curr. Opin. Coll. Interfac. Sci.* **1999**, *4*, 108; g)M. Zigon, G. Ambrozic, *Materiali in Tehnologije* **2003**, *37*, 231; h)J.-M. Lehn, *Polym. Int.* **2002**, *51*, 825; i)S. Burattini, H. M. Colquhoun, B. W. Greenland, W. Hayes, in *Supramolecular Chemistry*, John Wiley & Sons, Ltd, **2012**; j)H. M. Colquhoun, *Nat. Chem.* **2012**, *4*, 435.
- [31] a)J. Cortese, C. Soulié-Ziakovic, M. Cloitre, S. Tencé-Girault, L. Leibler, *J. Am. Chem. Soc.* **2011**, *133*, 19672; b)J. Cortese, C. Soulié-Ziakovic, S. Tencé-Girault, L. Leibler, *J. Am. Chem. Soc.* **2012**, *134*, 3671.
- [32] a)D. G. Kurth, M. Higuchi, *Soft Matter* **2006**, *2*, 915; b)P. R. Andres, U. S. Schubert, *Adv. Mater.* **2004**, *16*, 1043; c)S. Bode, R. K. Bose, S. Matthes, M. Ehrhardt, A. Seifert, F. H. Schacher, R. M. Paulus, S. Stumpf, B. Sandmann, J. Vitz, A. Winter, S. Hoepfener, S. J. Garcia, S. Spange, S. van der Zwaag, M. D. Hager, U. S. Schubert, *Polym. Chem.* **2013**, *4*, 4966; d)S. Bode, L. Zedler, F. H. Schacher, B. Dietzek, M. Schmitt, J. Popp, M. D. Hager, U. S. Schubert, *Adv. Mater.* **2013**, *25*, 1634; e)M. Enke, S. Bode, J. Vitz, F. H. Schacher, M. J. Harrington, M. D. Hager, U. S. Schubert, *Polymer* **2015**, doi:10.1016/j.polymer.2015.03.068; f)H. Hofmeier, U. S. Schubert, *Chem. Soc. Rev.* **2004**, *33*, 373; g)S. Kupfer, L. Zedler, J. Guthmuller, S. Bode, M. D. Hager, U. S. Schubert, J. Popp, S. Grafe, B. Dietzek, *Phys. Chem. Chem. Phys.* **2014**, *16*, 12422; h)U. S. Schubert, C. Eschbaumer, *Angew. Chem. Int. Ed.* **2002**, *41*, 2892; i)G. R. Whittell, M. D. Hager, U. S. Schubert, I. Manners, *Nat. Mater.* **2011**, *10*, 176; j)J. Brassinne, C.-A. Fustin, J.-F. Gohy, *J. Inorg. Organomet. Polym.* **2013**, *23*, 24; k)J. Brassinne, F. Jochum, C.-A. Fustin, J.-F. Gohy, *Int. J. Mol. Sci.* **2015**, *16*, 990; l)M. Burnworth, L. Tang, J. R. Kumpfer, A. J. Duncan, F. L. Beyer, G. L. Fiore, S. J. Rowan, C. Weder, *Nature* **2011**, *472*, 334; m)D. E. Fullenkamp, L. He, D. G. Barrett, W. R. Burghardt, P.

- B. Messersmith, *Macromolecules* **2013**, *46*, 1167; n)Y. Gao, D. Rajwar, A. C. Grimsdale, *Macromol. Rapid Commun.* **2014**, *35*, 1727; o)A. I. Gasnier, G. Royal, P. Terech, *Langmuir* **2009**, *25*, 8751; p)M. J. Harrington, H. S. Gupta, P. Fratzl, J. H. Waite, *J. Struct. Biol.* **2009**, *167*, 47; q)M. J. Harrington, A. Masic, N. Holten-Andersen, J. H. Waite, P. Fratzl, *Science* **2010**, *328*, 216; r)M. J. Harrington, J. H. Waite, *J. Exp. Biol.* **2007**, *210*, 4307; s)M. J. Harrington, J. H. Waite, *Biomacromolecules* **2008**, *9*, 1480; t)M. J. Harrington, J. H. Waite, *Adv. Mater.* **2009**, *21*, 440; u)N. Holten-Andersen, M. J. Harrington, H. Birkedal, B. P. Lee, P. B. Messersmith, K. Y. C. Lee, J. H. Waite, *P. Natl. Acad. Sci. USA* **2011**, *108*, 2651; v)N. Holten-Andersen, A. Jaishankar, M. J. Harrington, D. E. Fullenkamp, G. DiMarco, L. He, G. H. McKinley, P. B. Messersmith, K. Y. C. Lee, *J. Mater. Chem. B* **2014**, *2*, 2467; w)S. Krauss, T. H. Metzger, P. Fratzl, M. J. Harrington, *Biomacromolecules* **2013**, *14*, 1520; x)G. Hong, H. Zhang, Y. Lin, Y. Chen, Y. Xu, W. Weng, H. Xia, *Macromolecules* **2013**, *46*, 8649; y)B. J. Kim, D. X. Oh, S. Kim, J. H. Seo, D. S. Hwang, A. Masic, D. K. Han, H. J. Cha, *Biomacromolecules* **2014**, *15*, 1579; z)M. Krogsgaard, M. A. Behrens, J. S. Pedersen, H. Birkedal, *Biomacromolecules* **2013**, *14*, 297; aa)M. Martínez-Calvo, O. Kotova, M. E. Möbius, A. P. Bell, T. McCabe, J. J. Boland, T. Gunnlaugsson, *J. Am. Chem. Soc.* **2015**, *137*, 1983; ab)D. Mozhdzhi, S. Ayala, O. R. Cromwell, Z. Guan, *J. Am. Chem. Soc.* **2014**, *136*, 16128; ac)L. Qu, J. Fan, Y. Ren, K. Xiong, M. Yan, X. Tuo, P. Terech, G. Royal, *Mater. Chem. Phys.* **2015**, *153*, 54; ad)G. Schwarz, I. Haßlauer, D. G. Kurth, *Adv. Colloid. Interfac.* **2014**, *207*, 107; ae)P. Sun, J. Wang, X. Yao, Y. Peng, X. Tu, P. Du, Z. Zheng, X. Wang, *ACS Appl. Mater. Interfaces* **2014**, *6*, 12495; af)S. Varghese, A. Lele, R. Mashelkar, *J. Polym. Sci. Part A: Polym. Chem.* **2006**, *44*, 666; ag)M. Vatankhah-Varnoosfaderani, A. GhavamiNejad, S. Hashmi, F. J. Stadler, *Chem. Commun.* **2013**, *49*, 4685; ah)M. Vatankhah-Varnoosfaderani, S. Hashmi, A. GhavamiNejad, F. J. Stadler, *Polym. Chem.* **2014**, *5*, 512; ai)Z. Wei, J. He, T. Liang, H. Oh, J. Athas, Z. Tong, C. Wang, Z. Nie, *Polym. Chem.* **2013**, *4*, 4601; aj)B. Yang, H. Zhang, H. Peng, Y. Xu, B. Wu, W. Weng, L. Li, *Polym. Chem.* **2014**, *5*, 1945; ak)P. S. Yavvari, A. Srivastava, *J. Mater. Chem. B* **2015**, *3*, 899; al)J. Yuan, X. Fang, L. Zhang, G. Hong, Y. Lin, Q. Zheng, Y. Xu, Y. Ruan, W. Weng, H. Xia, G. Chen, *J. Mater. Chem.* **2012**, *22*, 11515; am)J. Yuan, H. Zhang, G. Hong, Y. Chen, G. Chen, Y. Xu, W. Weng, *J. Mater. Chem. B* **2013**, *1*, 4809; an)M. L. Zheludkevich, J. Tedim, C. S. R. Freire, S. C. M. Fernandes, S. Kallip, A. Lisenkov, A. Gandini, M. G. S. Ferreira, *J. Mater. Chem.* **2011**, *21*, 4805; ao)J. Zhou, G. R. Whittell, I. Manners, *Macromolecules* **2014**, *47*, 3529; ap)R. Dobrawa, F. Würthner, *J. Polym. Sci. Part A: Polym. Chem.* **2005**, *43*, 4981; aq)B. Schulze, C. Friebe, S. Hoeppe, G. M. Pavlov, A. Winter, M. D. Hager, U. S. Schubert, *Macromol. Rapid Commun.* **2012**, *33*, 597; ar)B. Sandmann, B. Happ, S. Kupfer, F. H. Schacher, M. D. Hager, U. S. Schubert, *Macromol. Rapid Commun.* **2015**, *36*, 604.
- [33] a)A. Aboudzadeh, M. Fernandez, M. E. Muñoz, A. Santamaría, D. Mecerreyes, *Macromol. Rapid Commun.* **2014**, *35*, 460; b)M. A. Aboudzadeh, M. E. Muñoz, A. Santamaría, R. Marcilla, D. Mecerreyes, *Macromol. Rapid Commun.* **2012**, *33*, 314; c)J. Akbarzadeh, S. Puchegger, A. Stojanovic, H. O. K. Kirchner, W. H. Binder, S. Bernstorff, P. Zioupos, H. Peterlik, *Bioinsp. Biomim.* **2014**, *3*, 123; d)A. Stojanovic, C. Appiah, D. Döhler, J. Akbarzadeh, P. Zare, H. Peterlik, W. H. Binder, *J. Mater. Chem. A* **2013**, *1*, 12159; e)R. K. Bose, N. Hohlbein, S. J. Garcia, A. M. Schmidt, S. van der Zwaag, *Phys. Chem. Chem. Phys.* **2015**, *17*, 1697; f)R. K. Bose, N. Hohlbein, S. J. Garcia, A. M. Schmidt, S. van der Zwaag, *Polymer* **2015**, doi:10.1016/j.polymer.2015.03.049; g)A. Francesconi, C. Giacomuzzo, A. M. Grande, T. Mudric, M. Zaccariotto, E. Etemadi, L. Di Landro, U. Galvanetto, *Adv. Space Res.* **2013**, *51*, 930; h)T. Haase, I. Rohr, K. Thoma, *J. Intel. Mat. Syst. Str.* **2014**, *25*, 25; i)E. Hsiao, A. Barthel, S. Kim, *Tribol. Lett.* **2011**, *44*, 287; j)E. Hsiao, L. Bradley, S. Kim, *Tribol. Lett.* **2011**, *41*, 33; k)Y. Huang, P. G. Lawrence, Y. Lapitsky, *Langmuir* **2014**, *30*, 7771; l)N.

- Huebsch, C. J. Kearney, X. Zhao, J. Kim, C. A. Cezar, Z. Suo, D. J. Mooney, *PNAS* **2014**, *111*, 9762; m)S. J. Kalista, J. R. Pflug, R. J. Varley, *Polym. Chem.* **2013**, *4*, 4910; n)R. J. Varley, S. Shen, S. van der Zwaag, *Polymer* **2010**, *51*, 679; o)R. J. Varley, S. van der Zwaag, *Acta Mater.* **2008**, *56*, 5737; p)R. J. Varley, S. van der Zwaag, *Polym. Test.* **2008**, *27*, 11; q)R. J. Varley, S. van der Zwaag, *Polym. Int.* **2010**, *59*, 1031; r)S. J. Kalista, T. C. Ward, *J. Roy. Soc. Interface* **2007**, *4*, 405; s)S. J. Kalista, T. C. Ward, Z. Oyetunji, *Mech. Adv. Mater. Struct.* **2007**, *14*, 391; t)R. Krieg, M. Rohwerder, S. Evers, B. Schuhmacher, J. Schauer-Pass, *Corros. Sci.* **2012**, *65*, 119; u)J. Lu, S.-G. Kim, S. Lee, I.-K. Oh, *J. Control. Release* **2011**, *152*, 229; v)M. A. Rahman, M. Penco, I. Peroni, G. Ramorino, A. M. Grande, L. Di Landro, *ACS Appl. Mater. Interfaces* **2011**, *3*, 4865; w)M. A. Rahman, M. Penco, G. Spagnoli, A. M. Grande, L. Di Landro, *Macromol. Mater. Eng.* **2011**, *296*, 1119; x)M. A. Rahman, G. Spagnoli, A. M. Grande, L. Di Landro, *Macromol. Mater. Eng.* **2013**, *298*, 1350; y)J. M. Vega, A. M. Grande, S. van der Zwaag, S. J. Garcia, *Eur. Polym. J.* **2014**, *57*, 121; z)H. Kuroki, I. Tokarev, D. Nykypanchuk, E. Zhulina, S. Minko, *Adv. Funct. Mater.* **2013**, *23*, 4593; aa)T. E. Dirama, V. Varshney, K. L. Anderson, J. A. Shumaker, J. A. Johnson, *Mech. Time-Depend. Mater.* **2008**, *12*, 205.
- [34] a)F. J. M. Hoeben, P. Jonkheijm, E. W. Meijer, A. P. H. J. Schenning, *Chem. Rev.* **2005**, *105*, 1491; b)S. Burattini, H. M. Colquhoun, J. D. Fox, D. Friedmann, B. W. Greenland, P. J. F. Harris, W. Hayes, M. E. Mackay, S. J. Rowan, *Chem. Commun.* **2009**, 6717; c)S. Burattini, H. M. Colquhoun, B. W. Greenland, W. Hayes, *Faraday Discuss.* **2009**, *143*, 251; d)S. Burattini, B. W. Greenland, W. Hayes, M. E. Mackay, S. J. Rowan, H. M. Colquhoun, *Chem. Mater.* **2011**, *23*, 6; e)J. Fox, J. J. Wie, B. W. Greenland, S. Burattini, W. Hayes, H. M. Colquhoun, M. E. Mackay, S. J. Rowan, *J. Am. Chem. Soc.* **2012**, *134*, 5362; f)B. W. Greenland, S. Burattini, W. Hayes, H. M. Colquhoun, *Tetrahedron* **2008**, *64*, 8346; g)L. R. Hart, J. L. Harries, B. W. Greenland, H. M. Colquhoun, W. Hayes, *Polym. Chem.* **2013**, *4*, 4860; h)L. R. Hart, J. H. Hunter, N. A. Nguyen, J. L. Harries, B. W. Greenland, M. E. Mackay, H. M. Colquhoun, W. Hayes, *Polym. Chem.* **2014**, *5*, 3680; i)L. R. Hart, N. A. Nguyen, J. L. Harries, M. E. Mackay, H. M. Colquhoun, W. Hayes, *Polymer* **2015**, doi:10.1016/j.polymer.2015.03.028.
- [35] a)L. Brunsveld, B. J. B. Folmer, E. W. Meijer, R. P. Sijbesma, *Chem. Rev.* **2001**, *101*, 4071; b)T. F. A. de Greef, E. W. Meijer, *Nature* **2008**, *453*, 171.
- [36] a)R. Berger, K. Binder, G. Diezemann, J. Gauss, M. Helm, H. P. Hsu, A. Janshoff, T. Metzroth, I. Mey, A. Milchev, W. Paul, V. G. Rostiasvili, T. A. Vilgis, in *From Single Molecules to Nanoscopically Structured Materials, Vol. 260* (Eds.: T. Basché, K. Müllen, M. Schmidt), Springer International Publishing, **2014**, pp. 1; b)T. Haino, *Polym. J.* **2013**, *45*, 363.
- [37] J.-M. Lehn, *Angew. Chem. Int. Ed.* **1988**, *27*, 89.
- [38] G. Armstrong, M. Buggy, *J. Mater. Sci.* **2005**, *40*, 547.
- [39] X. Yan, F. Wang, B. Zheng, F. Huang, *Chem. Soc. Rev.* **2012**, *41*, 6042.
- [40] G. M. L. van Gemert, J. W. Peeters, S. H. M. Söntjens, H. M. Janssen, A. W. Bosman, *Macromol. Chem. Phys.* **2012**, *213*, 234.
- [41] a)F. Herbst, D. Döhler, P. Michael, W. H. Binder, *Macromol. Rapid Commun.* **2013**, *34*, 203; b)W. Knoblen, N. A. M. Besseling, L. Bouteiller, M. A. Cohen-Stuart, *Phys. Chem. Chem. Phys.* **2005**, *7*, 2390.
- [42] W. C. Yount, D. M. Loveless, S. L. Craig, *Angew. Chem. Int. Ed.* **2005**, *44*, 2746.
- [43] L. Yang, X. Tan, Z. Wang, X. Zhang, *Chem. Rev.* **2015**, doi: 10.1021/cr500633b.
- [44] J.-M. Lehn, *Chem. Soc. Rev.* **2007**, *36*, 151.
- [45] D. R. Lippits, S. Rastogi, G. W. H. Hohne, B. Mezari, P. C. M. M. Magusin, *Macromolecules* **2007**, *40*, 1004.

- [46] a)F. Herbst, S. Seiffert, W. H. Binder, *Polym. Chem.* **2012**, *3*, 3084; b)D. Döhler, H. Peterlik, W. H. Binder, *Polymer* **2015**, 10.1016/j.polymer.2015.01.073; c)T. Rossow, A. Habicht, S. Seiffert, *Macromolecules* **2014**, *47*, 6473.
- [47] L. Bouteiller, in *Hydrogen Bonded Polymers, Vol. 207* (Ed.: W. Binder), Springer Berlin Heidelberg, **2007**, pp. 79.
- [48] a)F. Herbst, W. H. Binder*, in *Self Healing Polymers: from Principles to Application* (Ed.: W. H. Binder), Wiley-VCH Verlag GmbH & Co. KGaA, Weinheim, **2013**, pp. 275; b)A. W. Bosman, R. P. Sijbesma, E. W. Meijer, *Mater. Today* **2004**, *7*, 34.
- [49] a)T. C. B. McLeish, S. T. Milner, *Vol. 143*, Springer Berlin / Heidelberg, **1999**, pp. 195; b)S. Seiffert, J. Sprakel, *Chem. Soc. Rev.* **2012**, *41*, 909; c)M. J. Serpe, S. L. Craig, *Langmuir* **2007**, *23*, 1626.
- [50] a)D. Vlassopoulos, T. Pakula, G. Fytas, M. Pitsikalis, N. Hadjichristidis, *J. Chem. Phys.* **1999**, *111*, 1760; b)D. Vlassopoulos, M. Pitsikalis, N. Hadjichristidis, *Macromolecules* **2000**, *33*, 9740.
- [51] T. Park, S. C. Zimmerman, S. Nakashima, *J. Am. Chem. Soc.* **2005**, *127*, 6520.
- [52] L. G. Baxandall, *Macromolecules* **1989**, *22*, 1982.
- [53] E. B. Stukalin, L.-H. Cai, N. A. Kumar, L. Leibler, M. Rubinstein, *Macromolecules* **2013**, *46*, 7525.
- [54] W. C. Yount, D. M. Loveless, S. L. Craig, *J. Am. Chem. Soc.* **2005**, *127*, 14488.
- [55] M. E. Cates, *Macromolecules* **1987**, *20*, 2289.
- [56] W. E. Wallace, D. A. Fischer, K. Efimenko, W.-L. Wu, J. Genzer, *Macromolecules* **2001**, *34*, 5081.
- [57] a)M. S. Green, A. V. Tobolsky, *J. Chem. Phys.* **1946**, *14*, 80; b)P. G. De Gennes, *J. Chem. Phys.* **1971**, *55*, 572.
- [58] a)L. Leibler, M. Rubinstein, R. H. Colby, *Macromolecules* **1991**, *24*, 4701; b)S. Hackelbusch, T. Rossow, P. van Assenbergh, S. Seiffert, *Macromolecules* **2013**, *46*, 6273.
- [59] G. V. Kolmakov, K. Matyjaszewski, A. C. Balazs, *ACS Nano* **2009**, *3*, 885.
- [60] a)B. V. S. Iyer, I. G. Salib, V. V. Yashin, T. Kowalewski, K. Matyjaszewski, A. C. Balazs, *Soft Matter* **2013**, *9*, 109; b)B. V. S. Iyer, V. V. Yashin, M. J. Hamer, T. Kowalewski, K. Matyjaszewski, A. C. Balazs, *Prog. Polym. Sci.* **2015**, *40*, 121; c)B. V. S. Iyer, V. V. Yashin, T. Kowalewski, K. Matyjaszewski, A. C. Balazs, *Polym. Chem.* **2013**, *4*, 4927.
- [61] I. G. Salib, G. V. Kolmakov, C. N. Gnegy, K. Matyjaszewski, A. C. Balazs, *Langmuir* **2011**, *27*, 3991.
- [62] a)A. C. Balazs, T. Emrick, T. P. Russell, *Science* **2006**, *314*, 1107; b)A. C. Balazs, *Mater. Today* **2007**, *10*, 18; c)J. Y. Lee, G. A. Buxton, A. C. Balazs, *J. Chem. Phys.* **2004**, *121*, 5531.
- [63] A. C. Balazs, *Nat. Mater.* **2007**, *6*, 94.
- [64] R. Verberg, A. T. Dale, P. Kumar, A. Alexeev, A. C. Balazs, *J. Roy. Soc. Interface* **2007**, *4*, 349.
- [65] Y. Chen, A. M. Kushner, G. A. Williams, Z. Guan, *Nat. Chem.* **2012**, *4*, 467.
- [66] Y. Chen, Z. Guan, *Polym. Chem.* **2013**, 4885.
- [67] J. Hentschel, A. M. Kushner, J. Ziller, Z. Guan, *Angew. Chem. Int. Ed.* **2012**, *51*, 10561.
- [68] A. W. Bosman, L. Brunsveld, B. J. B. Folmer, R. P. Sijbesma, E. W. Meijer, *Macromol. Symp.* **2003**, *201*, 143.
- [69] a)S. H. M. Söntjens, R. P. Sijbesma, M. H. P. van Genderen, E. W. Meijer, *J. Am. Chem. Soc.* **2000**, *122*, 7487; b)M. Rubinstein, A. N. Semenov, *Macromolecules* **1998**, *31*, 1386; c)D. Xu, S. L. Craig, *Macromolecules* **2011**, *44*, 5465.
- [70] a)E. Buhler, S.-J. Candau, E. Kolomiets, J.-M. Lehn, *Phys. Rev. E* **2007**, *76*, 061804; b)M. Rubinstein, A. N. Semenov, *Macromolecules* **2001**, *34*, 1058.
- [71] R. J. Composto, E. J. Kramer, D. M. White, *Macromolecules* **1992**, *25*, 4167.

- [72] a)F. H. Beijer, H. Kooijman, A. L. Spek, R. P. Sijbesma, E. W. Meijer, *Angew. Chem. Int. Ed.* **1998**, *37*, 75; b)F. H. Beijer, R. P. Sijbesma, H. Kooijman, A. L. Spek, E. W. Meijer, *J. Am. Chem. Soc.* **1998**, *120*, 6761.
- [73] J. A. Kaitz, C. M. Possanza, Y. Song, C. E. Diesendruck, A. J. H. Spiering, E. W. Meijer, J. S. Moore, *Polym. Chem.* **2014**, *5*, 3788.
- [74] R. P. Sijbesma, F. H. Beijer, L. Brunsveld, B. J. B. Folmer, J. H. K. K. Hirschberg, R. F. M. Lange, J. K. L. Lowe, E. W. Meijer, *Science* **1997**, *278*, 1601.
- [75] a)N. E. Botterhuis, D. J. M. van Beek, G. M. L. van Gemert, A. W. Bosman, R. P. Sijbesma, *J. Polym. Sci. A: Polym. Chem.* **2008**, *46*, 3877; b)J. H. K. K. Hirschberg, F. H. Beijer, H. A. van Aert, P. C. M. M. Magusin, R. P. Sijbesma, E. W. Meijer, *Macromolecules* **1999**, *32*, 2696.
- [76] C.-H. Wong, W.-S. Chan, C.-M. Lo, H.-F. Chow, T. Ngai, K.-W. Wong, *Macromolecules* **2010**, *43*, 8389.
- [77] S. Bobade, Y. Wang, J. Mays, D. Baskaran, *Macromolecules* **2014**, *47*, 5040.
- [78] P. Y. W. Dankers, T. M. Hermans, T. W. Baughman, Y. Kamikawa, R. E. Kiełtyka, M. M. C. Bastings, H. M. Janssen, N. A. J. M. Sommerdijk, A. Larsen, M. J. A. van Luyn, A. W. Bosman, E. R. Popa, G. Fytas, E. W. Meijer, *Adv. Mater.* **2012**, *24*, 2703.
- [79] T. V. Chirila, H. H. Lee, M. Odon, M. M. L. Nieuwenhuizen, I. Blakey, T. M. Nicholson, *J. Appl. Polym. Sci.* **2014**, *131*, 39932/1.
- [80] C. L. Elkins, T. Park, M. G. McKee, T. E. Long, *J. Polym. Sci. Part A: Polym. Chem.* **2005**, *43*, 4618.
- [81] A. Faghijnejad, K. E. Feldman, J. Yu, M. V. Tirrell, J. N. Israelachvili, C. J. Hawker, E. J. Kramer, H. Zeng, *Adv. Funct. Mater.* **2014**, *24*, 2322.
- [82] K. E. Feldman, M. J. Kade, E. W. Meijer, C. J. Hawker, E. J. Kramer, *Macromolecules* **2009**, *42*, 9072.
- [83] C. L. Lewis, K. Stewart, M. Anthamatten, *Macromolecules* **2014**, *47*, 729.
- [84] I. Schnell, B. Langer, S. H. M. Söntjens, R. P. Sijbesma, M. H. P. v. Genderenb, H. W. Spiess, *Phys. Chem. Chem. Phys.* **2002**, *4*, 3750.
- [85] B. J. B. Folmer, R. P. Sijbesma, R. M. Versteegen, J. A. J. van der Rijt, E. W. Meijer, *Adv. Mater.* **2000**, *12*, 874.
- [86] a)H. Kautz, D. J. M. van Beek, R. P. Sijbesma, E. W. Meijer, *Macromolecules* **2006**, *39*, 4265; b)H. M. Keizer, R. van Kessel, R. P. Sijbesma, E. W. Meijer, *Polymer* **2003**, *44*, 5505.
- [87] T. Mes, M. M. E. Koenigs, V. F. Scalfani, T. S. Bailey, E. W. Meijer, A. R. A. Palmans, *ACS Macro Lett.* **2011**, 105.
- [88] S. H. M. Söntjens, R. A. E. Renken, G. M. L. van Gemert, T. A. P. Engels, A. W. Bosman, H. M. Janssen, L. E. Govaert, F. P. T. Baaijens, *Macromolecules* **2008**, *41*, 5703.
- [89] N. Oya, T. Ikezaki, N. Yoshie, *Polym. J.* **2013**, *45*, 955.
- [90] X. Fang, H. Zhang, Y. Chen, Y. Lin, Y. Xu, W. Weng, *Macromolecules* **2013**, *46*, 6566.
- [91] A. M. Kushner, J. D. Vossler, G. A. Williams, Z. Guan, *J. Am. Chem. Soc.* **2009**, *131*, 8766.
- [92] L. R. Rieth, R. F. Eaton, G. W. Coates, *Angew. Chem. Int. Ed.* **2001**, *40*, 2153.
- [93] G. Li, J. J. Wie, N. A. Nguyen, W. J. Chung, E. T. Kim, K. Char, M. E. Mackay, J. Pyun, *J. Polym. Sci. Part A: Polym. Chem.* **2013**, *51*, 3598.
- [94] D. J. M. van Beek, A. J. H. Spiering, G. W. M. Peters, K. te Nijenhuis, R. P. Sijbesma, *Macromolecules* **2007**, *40*, 8464.
- [95] J.-L. Wietor, D. J. M. van Beek, G. W. Peters, E. Mendes, R. P. Sijbesma, *Macromolecules* **2011**, *44*, 1211.
- [96] K. E. Feldman, M. J. Kade, T. F. A. de Greef, E. W. Meijer, E. J. Kramer, C. J. Hawker, *Macromolecules* **2008**, *41*, 4694.

- [97] K. E. Feldman, M. J. Kade, E. W. Meijer, C. J. Hawker, E. J. Kramer, *Macromolecules* **2010**, *43*, 5121.
- [98] H. Ohkawa, G. B. W. L. Ligthart, R. P. Sijbesma, E. W. Meijer, *Macromolecules* **2007**, *40*, 1453.
- [99] G. B. W. L. Ligthart, H. Ohkawa, R. P. Sijbesma, E. W. Meijer, *J. Am. Chem. Soc.* **2004**, *127*, 810.
- [100] F. Lortie, S. Boileau, L. Bouteiller, C. Chassenieux, F. Lauprêtre, *Macromolecules* **2005**, *38*, 5283.
- [101] R. F. M. Lange, M. Van Gorp, E. W. Meijer, *J. Polym. Sci. Part A: Polym. Chem.* **1999**, *37*, 3657.
- [102] a)D. W. Kuykendall, C. A. Anderson, S. C. Zimmerman, *Org. Lett.* **2008**, *11*, 61; b)T. Park, E. M. Todd, S. Nakashima, S. C. Zimmerman, *J. Am. Chem. Soc.* **2005**, *127*, 18133.
- [103] Y. Li, T. Park, J. K. Quansah, S. C. Zimmerman, *J. Am. Chem. Soc.* **2011**, *133*, 17118.
- [104] T. Park, S. C. Zimmerman, *J. Am. Chem. Soc.* **2006**, *128*, 13986.
- [105] T. Park, S. C. Zimmerman, *J. Am. Chem. Soc.* **2006**, *128*, 11582.
- [106] C. A. Anderson, A. R. Jones, E. M. Briggs, E. J. Novitsky, D. W. Kuykendall, N. R. Sottos, S. C. Zimmerman, *J. Am. Chem. Soc.* **2013**, *135*, 7288.
- [107] X. Callies, C. Fonteneau, C. Véchambre, S. Pensec, J. M. Chenal, L. Chazeau, L. Bouteiller, G. Ducouret, C. Creton, *Polymer* **2015**, doi:10.1016/j.polymer.2014.12.053.
- [108] O. Colombani, C. Barioz, L. Bouteiller, C. Chanéac, L. Fompérie, F. Lortie, H. Montès, *Macromolecules* **2005**, *38*, 1752.
- [109] N. Roy, E. Buhler, J.-M. Lehn, *Chem. Eur. J.* **2013**, *19*, 8814.
- [110] P. J. Woodward, D. Hermida Merino, B. W. Greenland, I. W. Hamley, Z. Light, A. T. Slark, W. Hayes, *Macromolecules* **2010**, *43*, 2512.
- [111] Y. Ni, F. Becquart, J. Chen, M. Taha, *Macromolecules* **2013**, *46*, 1066.
- [112] a)T. Shikata, T. Nishida, B. Isare, M. Linares, R. Lazzaroni, L. Bouteiller, *J. Phys. Chem. B* **2008**, *112*, 8459; b)P. Woodward, A. Clarke, B. W. Greenland, D. Hermida Merino, L. Yates, A. T. Slark, J. F. Miravet, W. Hayes, *Soft Matter* **2009**, *5*, 2000; c)F. Lortie, S. Boileau, L. Bouteiller, *Chem.-Eur. J.* **2003**, *9*, 3008.
- [113] a)P. Ribagnac, C. Cannizzo, R. Meallet-Renault, G. Clavier, P. Audebert, R. B. Pansu, L. Bouteiller, *J. Phys. Chem. B* **2013**, *117*, 1958; b)S. Pensec, N. Nouvel, A. Guilleman, C. Creton, F. Boué, L. Bouteiller, *Macromolecules* **2010**, *43*, 2529.
- [114] J. Courtois, I. Baroudi, N. Nouvel, E. Degrandi, S. Pensec, G. Ducouret, C. Chanéac, L. Bouteiller, C. Creton, *Adv. Funct. Mater.* **2010**, *20*, 1803.
- [115] R. M. Versteegen, D. J. M. van Beek, R. P. Sijbesma, D. Vlassopoulos, G. Fytas, E. W. Meijer, *J. Am. Chem. Soc.* **2005**, *127*, 13862.
- [116] Y. Chen, W. Wu, T. Himmel, M. H. Wagner, *Macromol. Mater. Eng.* **2013**, *298*, 876.
- [117] a)P. Cordier, F. Tournilhac, C. Soulié-Ziakovic, L. Leibler, *Nature* **2008**, *451*, 977; b)D. Montarnal, P. Cordier, C. Soulié-Ziakovic, F. Tournilhac, L. Leibler, *J. Polym. Sci. A: Polym. Chem.* **2008**, *46*, 7925; c)D. Montarnal, F. Tournilhac, M. Hidalgo, J.-L. Couturier, L. Leibler, *J. Am. Chem. Soc.* **2009**, *131*, 7966; d)F. Tournilhac, P. Cordier, D. Montarnal, C. Soulié-Ziakovic, L. Leibler, *Macromol. Symp.* **2010**, *291-292*, 84.
- [118] F. Maes, D. Montarnal, S. Cantournet, F. Tournilhac, L. Corte, L. Leibler, *Soft Matter* **2012**, *8*, 1681.
- [119] R. Zhang, T. Yan, B.-D. Lechner, K. Schröter, Y. Liang, B. Li, F. Furtado, P. Sun, K. Saalwächter, *Macromolecules* **2013**, *46*, 1841.
- [120] A. Zhang, L. Yang, Y. Lin, L. Yan, H. Lu, L. Wang, *J. Appl. Polym. Sci.* **2013**, *129*, 2435.
- [121] K. Chino, M. Ashiura, *Macromolecules* **2001**, *34*, 9201.
- [122] C.-C. Peng, V. Abetz, *Macromolecules* **2005**, *38*, 5575.

- [123] C. B. St.Pourcain, A. C. Griffin, *Macromolecules* **1995**, *28*, 4116.
- [124] a)C. Hilger, R. Stadler, *Polymer* **1991**, *32*, 3244; b)C. Hilger, R. Stadler, L. Liane, d. L. Freitas, *Polymer* **1990**, *31*, 818.
- [125] a)M. Müller, U. Seidel, R. Stadler, *Polymer* **1995**, *36*, 3143; b)R. Stadler, L. de Lucca Freitas, *Colloid Polym. Sci.* **1986**, *264*, 773.
- [126] R. Stadler, M. A. de Araujo, M. Kuhrau, J. Rösch, *Makromol. Chem.* **1989**, *190*, 1433.
- [127] A. Vidyasagar, K. Handore, K. M. Sureshan, *Angew. Chem. Int. Ed.* **2011**, *50*, 8021.
- [128] Q. Wei, C. Schlaich, S. Prévost, A. Schulz, C. Böttcher, M. Gradzielski, Z. Qi, R. Haag, C. A. Schalley, *Adv. Mater.* **2014**, *26*, 7358.
- [129] C. P. Lillya, R. J. Baker, S. Hutte, H. H. Winter, Y. G. Lin, J. Shi, L. C. Dickinson, J. C. W. Chien, *Macromolecules* **1992**, *25*, 2076.
- [130] a)M. Müller, A. Dardin, U. Seidel, V. Balsamo, B. Iván, H. W. Spiess, R. Stadler, *Macromolecules* **1996**, *29*, 2577; b)M. Schirle, I. Hoffmann, T. Pieper, H.-G. Kilian, R. Stadler, *Polym. Bull.* **1996**, *36*, 95.
- [131] V. Berl, M. Schmutz, M. J. Krische, R. G. Khoury, J.-M. Lehn, *Chem. Eur. J.* **2002**, *8*, 1227.
- [132] E. Kolomiets, E. Buhler, S. J. Candau, J. M. Lehn, *Macromolecules* **2006**, *39*, 1173.
- [133] K. P. Nair, V. Breedveld, M. Weck, *Macromolecules* **2008**, *41*, 3429.
- [134] K. P. Nair, V. Breedveld, M. Weck, *Soft Matter* **2011**, *7*, 553.
- [135] K. Fuchs, T. Bauer, R. Thomann, C. Wang, C. Friedrich, R. Mülhaupt, *Macromolecules* **1999**, *32*, 8404.
- [136] I.-H. Lin, C.-C. Cheng, Y.-C. Yen, F.-C. Chang, *Macromolecules* **2010**, *43*, 1245.
- [137] J. H. K. K. Hirschberg, L. Brunsveld, A. Ramzi, J. A. J. M. Vekemans, R. P. Sijbesma, E. W. Meijer, *Nature* **2000**, *407*, 167.
- [138] a)S. J. Rowan, P. Suwanmala, S. Sivakova, *J. Polym. Sci. Part A: Polym. Chem.* **2003**, *41*, 3589; b)S. Sivakova, D. A. Bohnsack, M. E. Mackay, P. Suwanmala, S. J. Rowan, *J. Am. Chem. Soc.* **2005**, *127*, 18202.
- [139] T. Yan, K. Schröter, F. Herbst, W. H. Binder, T. Thurn-Albrecht, *Macromolecules* **2014**, *47*, 2122.
- [140] P. Michael, D. Döhler, W. H. Binder, *Polymer* **2015**, doi:10.1016/j.polymer.2015.01.041.
- [141] R. Long, H. J. Qi, M. L. Dunn, *Soft Matter* **2013**, *9*, 4083.
- [142] F. Herbst, K. Schröter, I. Gunkel, S. Gröger, T. Thurn-Albrecht, J. Balbach, W. H. Binder, *Macromolecules* **2010**, *43*, 10006.
- [143] a)L. Huang, N. Yi, Y. Wu, Y. Zhang, Q. Zhang, Y. Huang, Y. Ma, Y. Chen, *Adv. Mater.* **2013**, *25*, 2224; b)J. R. McKee, E. A. Appel, J. Seitsonen, E. Kontturi, O. A. Scherman, O. Ikkala, *Adv. Funct. Mater.* **2014**, *24*, 2706; c)Y.-T. Liu, M. Zhong, X.-M. Xie, *J. Mater. Chem. B* **2015**, *3*, 4001; d)M. Prajer, X. Wu, S. J. Garcia, S. van der Zwaag, *Compos. Sci. Technol.* **2015**, *106*, 127; e)N. Zhong, W. Post, *Compos. Part A: Appl. S.* **2015**, *69*, 226; f)R. S. Trask, C. J. Norris, I. P. Bond, *J. Intel. Mat. Syst. Str.* **2014**, *25*, 87; g)R. Peng, Y. Yu, S. Chen, Y.-K. Yang, Y. Tang, *RSC Adv.* **2014**, *4*, 35149; h)J. Liu, G. Song, C. He, H. Wang, *Makromol. Rapid Commun.* **2013**, *34*, 1002; i)H.-P. Cong, P. Wang, S.-H. Yu, *Chem. Mater.* **2013**, *25*, 3357; j)T. J. Swait, A. Rauf, R. Grainger, P. B. S. Bailey, A. D. Lafferty, E. J. Fleet, R. J. Hand, S. A. Hayes, *Plast. Rubber Compos.* **2012**, *41*, 215; k)A. Ciferri, *Polym. Chem.* **2013**, *4*, 4980; l)A. Das, G. R. Kasaliwal, R. Jurk, R. Boldt, D. Fischer, K. W. Stöckelhuber, G. Heinrich, *Compos. Sci. Technol.* **2012**, *72*, 1961; m)S. J. Picken, S. D. Mookhoek, H. R. Fischer, S. van der Zwaag, in *Optimization of Polymer Nanocomposite Properties*, Wiley-VCH Verlag GmbH & Co. KGaA, **2010**, pp. 261; n)X. Xiao, T. Xie, Y.-T. Cheng, *J. Mater. Chem.* **2010**, *20*, 3508.
- [144] a)M. Yamaguchi, S. Ono, K. Okamoto, *Mater. Sci. Eng. B* **2009**, *162*, 189; b)M. Yamaguchi, S. Ono, M. Terano, *Mater. Lett.* **2007**, *61*, 1396.

- [145] S. R. White, J. S. Moore, N. R. Sottos, B. P. Krull, W. A. Santa Cruz, R. C. R. Gergely, *Science* **2014**, *344*, 620.
- [146] P. A. May, J. S. Moore, *Chem. Soc. Rev.* **2013**, *42*, 7497.
- [147] C. J. Hansen, W. Wu, K. S. Toohey, N. R. Sottos, S. R. White, J. A. Lewis, *Adv. Mater.* **2009**, *21*, 4143.
- [148] A. Lendlein, S. Kelch, *Angew. Chem. Int. Ed.* **2002**, *41*, 2034.
- [149] B. J. Sparks, E. F. T. Hoff, L. P. Hayes, D. L. Patton, *Chem. Mater.* **2012**, *24*, 3633.
- [150] a)B. Ghosh, K. V. Chellappan, M. W. Urban, *J. Mater. Chem.* **2011**, *21*, 14473; b)B. Ghosh, M. W. Urban, *Science* **2009**, *323*, 1458.
- [151] B. Ghosh, K. V. Chellappan, M. W. Urban, *J. Mater. Chem.* **2012**, *22*, 16104.
- [152] B. de Ruiter, A. El-ghayoury, H. Hofmeier, U. S. Schubert, M. Manea, *Prog. Org. Coat.* **2006**, *55*, 154.
- [153] Q. Chen, L. Zhu, H. Chen, H. Yan, L. Huang, J. Yang, J. Zheng, *Adv. Funct. Mater.* **2015**, *25*, 1598.
- [154] H. M. Keizer, R. P. Sijbesma, J. F. G. A. Jansen, G. Pasternack, E. W. Meijer, *Macromolecules* **2003**, *36*, 5602.
- [155] a)J. Brancart, G. Scheltjens, T. Muselle, B. Van Mele, H. Teryn, G. Van Assche, *J. Intel. Mat. Syst. Str.* **2014**, *25*, 40; b)G. Scheltjens, J. Brancart, I. De Graeve, B. Van Mele, H. Teryn, G. Van Assche, *J. Therm. Anal. Calorim.* **2011**, *105*, 805; c)G. Scheltjens, M. M. Diaz, J. Brancart, G. Van Assche, B. Van Mele, *React. Funct. Polym.* **2013**, *73*, 413; d)N. Bai, K. Saito, G. P. Simon, *Polym. Chem.* **2013**, *4*, 724; e)N. Bai, G. P. Simon, K. Saito, *RSC Adv.* **2013**, *3*, 20699.
- [156] a)P. A. Pratama, A. M. Peterson, G. R. Palmese, *Macromol. Chem. Phys.* **2012**, *213*, 173; b)P. A. Pratama, A. M. Peterson, G. R. Palmese, *Polym. Chem.* **2013**, *4*, 5000; c)A. M. Peterson, R. E. Jensen, G. R. Palmese, *ACS Appl. Mater. Interfaces* **2010**, *2*, 1141.
- [157] M. Wouters, E. Craenmehr, K. Tempelaars, H. Fischer, N. Stroeks, J. van Zanten, *Prog. Org. Coat.* **2009**, *64*, 156.
- [158] G. O. Wilson, M. M. Caruso, S. R. Schelkopf, N. R. Sottos, S. R. White, J. S. Moore, *ACS Appl. Mater. Interfaces* **2011**, *3*, 3072.
- [159] D. Döhler, P. Zare, W. H. Binder, *Polym. Chem.* **2014**, *5*, 992.
- [160] D. D. Díaz, K. Rajagopal, E. Strable, J. Schneider, M. G. Finn, *J. Am. Chem. Soc.* **2006**, *128*, 6056.
- [161] O. S. Taskin, B. Kiskan, Y. Yagci, *Macromolecules* **2013**, *46*, 8773.
- [162] S. Billiet, K. De Bruycker, F. Driessen, H. Goossens, V. Van Speybroeck, J. M. Winne, F. E. Du Prez, *Nat. Chem.* **2014**, *6*, 815.
- [163] a)J. Ling, M. Z. Rong, M. Q. Zhang, *J. Mater. Chem.* **2011**, *21*, 18373; b)J. Ling, M. Z. Rong, M. Q. Zhang, *Polymer* **2012**, *53*, 2691.
- [164] G. Deng, F. Li, H. Yu, F. Liu, C. Liu, W. Sun, H. Jiang, Y. Chen, *ACS Macro Lett.* **2012**, *1*, 275.
- [165] P. Zhang, F. Deng, Y. Peng, H. Chen, Y. Gao, H. Li, *RSC Adv.* **2014**, *4*, 47361.
- [166] N. Roy, E. Buhler, J.-M. Lehn, *Polym. Int.* **2014**, *63*, 1400.
- [167] J. A. Neal, D. Mozhdghi, Z. Guan, *J. Am. Chem. Soc.* **2015**, *137*, 4846.
- [168] L. M. Meng, Y. C. Yuan, M. Z. Rong, M. Q. Zhang, *J. Mater. Chem.* **2010**, *20*, 6030.
- [169] D. Montarnal, F. Tournilhac, M. Hildago, L. Leibler, *J. Polym. Sci. Part A: Polym. Chem.* **2010**, *48*, 1133.
- [170] S. P. Khor, R. J. Varley, S. Z. Shen, Q. Yuan, *J. Appl. Polym. Sci.* **2013**, *128*, 3743.
- [171] S. Yu, R. Zhang, Q. Wu, T. Chen, P. Sun, *Adv. Mater.* **2013**, *25*, 4912.
- [172] J. Zhang, L. Wang, Y. Zhao, *Mater. Design* **2013**, *51*, 648.
- [173] J. K. Mishra, Y.-W. Chang, D.-K. Kim, P. L. Nayak, *Polym.-Plast. Technol.* **2007**, *46*, 585.

- [174] F. R. Kersey, D. M. Loveless, S. L. Craig, *J. Roy. Soc. Interface* **2007**, *4*, 373.
- [175] F. Ding, S. Wu, S. Wang, Y. Xiong, Y. Li, B. Li, H. Deng, Y. Du, L. Xiao, X. Shi, *Soft Matter* **2015**, *11*, 3971.
- [176] H. Ying, Y. Zhang, J. Cheng, *Nat. Commun.* **2014**, *5*, 1.
- [177] S. Burattini, B. W. Greenland, D. Hermida Merino, W. Weng, J. Seppala, H. M. Colquhoun, W. Hayes, M. E. Mackay, I. W. Hamley, S. J. Rowan, *J. Am. Chem. Soc.* **2010**, *132*, 12051.
- [178] Z. Xu, J. Peng, N. Yan, H. Yu, S. Zhang, K. Liu, Y. Fang, *Soft Matter* **2013**, *9*, 1091.
- [179] J. Liu, Y. Feng, Z.-X. Liu, Z.-C. Yan, Y.-M. He, C.-Y. Liu, Q.-H. Fan, *Chem.-Asian J.* **2013**, *8*, 572.
- [180] a)D. G. Barrett, D. E. Fullenkamp, L. He, N. Holten-Andersen, K. Y. C. Lee, P. B. Messersmith, *Adv. Funct. Mater.* **2013**, *23*, 1111; b)H. Ceylan, M. Urel, T. S. Erkal, A. B. Tekinay, A. Dana, M. O. Guler, *Adv. Funct. Mater.* **2013**, *23*, 2081.
- [181] S. Huang, L. Yang, M. Liu, S. L. Phua, W. A. Yee, W. Liu, R. Zhou, X. Lu, *Langmuir* **2013**, *29*, 1238.
- [182] U. Mansfeld, A. Winter, M. D. Hager, R. Hoogenboom, W. Gunther, U. S. Schubert, *Polym. Chem.* **2013**, *4*, 113.
- [183] a)J. M. Pollino, K. P. Nair, L. P. Stubbs, J. Adams, M. Weck, *Tetrahedron* **2004**, *60*, 7205; b)J. M. Pollino, L. P. Stubbs, M. Weck, *J. Am. Chem. Soc.* **2004**, *126*, 563.
- [184] H. Liu, C. Xiong, Z. Tao, Y. Fan, X. Tang, H. Yang, *RSC Adv.* **2015**, *5*, 33083.
- [185] a)Y. Lei, T. P. Lodge, *Soft Matter* **2012**, *8*, 2110; b)A. Noro, Y. Matsushita, T. P. Lodge, *Macromolecules* **2008**, *41*, 5839.
- [186] a)F. Wang, J. Zhang, X. Ding, S. Dong, M. Liu, B. Zheng, S. Li, L. Wu, Y. Yu, H. W. Gibson, F. Huang, *Angew. Chem. Int. Ed.* **2010**, *49*, 1090; b)X. Yan, D. Xu, J. Chen, M. Zhang, B. Hu, Y. Yu, F. Huang, *Polym. Chem.* **2013**, *4*, 3312; c)J. Zhan, M. Zhang, M. Zhou, B. Liu, D. Chen, Y. Liu, Q. Chen, H. Qiu, S. Yin, *Macromol. Rapid Commun.* **2014**, *35*, 1424.
- [187] Z. Walsh, E.-R. Janeček, J. T. Hodgkinson, J. Sedlmair, A. Koutsioubas, D. R. Spring, M. Welch, C. J. Hirschmugl, C. Toprakcioglu, J. R. Nitschke, M. Jones, O. A. Scherman, *PNAS* **2014**, *111*, 17743.
- [188] G. C. Huang, J. K. Lee, M. R. Kessler, *Macromol. Mater. Eng.* **2011**, *296*, 965.
- [189] J.-M. Lehn, *Prog. Polym. Sci.* **2005**, *30*, 814.
- [190] a)W. G. Skene, J.-M. P. Lehn, *Proc. Natl. Acad. Sci. USA* **2004**, *101*, 8270; b)E. Kolomiets, J.-M. Lehn, *Chem. Commun.* **2005**, 1519.
- [191] Y.-X. Lu, Z. Guan, *J. Am. Chem. Soc.* **2012**, *134*, 14226.
- [192] O. A. Scherman, G. B. W. L. Lighthart, R. P. Sijbesma, E. W. Meijer, *Angew. Chem. Int. Ed.* **2006**, *45*, 2072.
- [193] H. Y. Atay, L. E. Doğan, E. Çelik, *J. Mater.* **2013**, *2013*, 7.
- [194] a)R. J. Puddephatt, *J. Inorg. Organomet. P.* **2005**, *15*, 371; b)E. Degtyar, M. J. Harrington, Y. Politi, P. Fratzl, *Angew. Chem. Int. Ed.* **2014**, *53*, 12026; c)Z. Shafiq, J. Cui, L. Pastor-Pérez, V. San Miguel, R. A. Gropeanu, C. Serrano, A. del Campo, *Angew. Chem. Int. Ed.* **2012**, *51*, 4332.
- [195] R. Dong, Y. Pang, Y. Su, X. Zhu, *Biomater. Sci.* **2015**, doi: 10.1039/C4BM00448E
- [196] a)D. J. Kinning, E. L. Thomas, *Macromolecules* **1984**, *17*, 1712; b)M. Schwab, B. Stühn, *Phys. Rev. Lett.* **1996**, *76*, 924.

9. APPENDIX

9.1. Preparation of initiators and quenching agents for living carbocationic polymerization of isobutylene and preparation of supramolecular moieties

Synthesis of trivalent initiator

1,3,5-tris(2-methoxy-2-propyl)benzene^{1,2,3} was synthesized in three steps.

In the first step 1,3,5-benzene-tricarboxylic acid (55.0 mmol, 12.2 g) and MeOH (350.0 mL) were put in a two-necked round-bottom flask which was equipped with a reflux condenser, a dropping funnel and a magnetic stir bar. After dissolving the starting material concentrated sulphuric acid (251.0 mmol, 13.4 mL) was added dropwise to the reaction mixture which was heated to reflux for 48 hours. The reaction progress was monitored *via* TLC (MeOH / CHCl₃ = 3 / 2, R_f = 0.9) and after cooling down to room temperature the reaction mixture was stored in a fridge overnight. Afterwards the formed precipitate was filtered and washed with distilled water to remove traces of acid. Multiple recrystallization in MeOH yielded 1,3,5-tris(2-methoxy-2-propyl)benzene as white solid in a yield of 95 % (52.3 mmol, 13.2 g).

¹H-NMR (CDCl₃, 400 MHz): δ 8.83 (s, 3H, Ar-CH), 3.96 (s, 9H, CH₃)

¹³C-NMR (CDCl₃, 100 MHz): δ 165.3 (CO), 134.5 (Ar-C), 131.2 (Ar-CH), 52.7 (CH₃)

In the second step a Grignard-reaction was performed under a dry atmosphere of nitrogen. Therefore, a three-necked round-bottom flask which was equipped with dropping funnel with septum, reflux condenser with stop cock, septum and magnetic stir bar was loaded with magnesium (205.7 mmol, 5.0 g) and dry diethyl ether (500.0 mL) in a counterflow of nitrogen. Iodomethane (205.7 mmol, 12.8 mL) was added dropwise to form CH₃MgI *in situ*. After stirring for 48 hours at room temperature the progress of the reaction was monitored *via* TLC (MeOH / DCM = 3 / 1, R_f = 0.79). For work-up a mixture of ammonium chloride (8.0 g) and crushed ice (200.0 g) were added. The organic layer was separated while the aqueous phase was extracted several times with diethyl ether (150.0 mL portions). After unifying the organic layers they were dried over Na₂SO₄. After filtering off the drying agent the solvent was removed and pure 1,3,5-tris(2-hydroxy-2-propyl)benzene was obtained as white to pale yellow crystals after multiple recrystallization in EA in a yield of 40 % (9.5 mmol, 2.4 g).

¹H-NMR (CDCl₃, 400 MHz): δ 7.49 (s, 3H, Ar-CH), 1.58 (s, 18H, CH₃)

¹³C-NMR (CDCl₃, 100 MHz): δ 149.0 (Ar-C), 118.9 (Ar-CH), 72.8 (COH), 31.9 (CH₃)

In the third step 1,3,5-tris(2-hydroxy-2-propyl)benzene (4.5 mmol, 1.1 g) was dissolved in dry MeOH (26.4 mL) and was converted with concentrated sulphuric acid (12.8 μmol, 125.7 μg) under a dry atmosphere of nitrogen. Therefore a stock solution in MeOH (26.4 mL) was prepared and added dropwise. The reaction mixture was heated up to reflux and the progress of the reaction was monitored by TLC (MeOH / n-hexane = 1 / 9, R_f = 0.65). After the reaction has finished the reaction mixture was allowed to cool down to room temperature. *N*-Hexane (60 mL) was added and stirring proceeded for fifteen minutes followed by the addition of water (12.0 mL) and additional stirring for further ten minutes. After separating the organic layer it was washed with water (five times 40.0 mL) and dried overnight over MgSO₄. After filtering off the drying agent the solvent was removed at room temperature. 1,3,5-Tris(2-hydroxy-2-propyl)benzene was obtained as white crystals in a yield of 63 % (2.8 mmol, 0.8 g) and was stored under nitrogen atmosphere in the freezer.

¹H-NMR (CDCl₃, 400 MHz): δ 7.26 (s, 3H, Ar-H), 3.01 (s, 9H, OCH₃), 1.47 (s, 18H, CH₃)

Synthesis of inimer-type initiator

4-(2-Methoxyisopropyl)styrene (inimer-type initiator)⁴ was synthesized in two steps.

The synthesis was done under a dry atmosphere of nitrogen. A three-necked round-bottom flask was equipped with a dropping funnel with septum, a thermometer, a stop-cock and a magnetic stir bar. The flask was loaded with activated magnesium (213.9 mmol, 5.2 g), an iodine crystal and dry THF (80.0 mL). In the dropping funnel a degassed mixture of 4-bromostyrene (27.3 mmol, 3.6 mL) and dry THF (20.0 mL) was added. This mixture was added dropwise to the reaction mixture at room temperature while gently stirring. During the addition the temperature was kept below 30 °C by cooling with an ice bath. After complete addition of the 4-bromostyrene / THF mixture stirring was proceeded at room temperature for 4 hours and the reaction mixture became brown-black. Afterwards, a mixture of dry acetone (81.7 mmol, 6.0 mL) in dry THF (5.0 mL) was added to the dropping funnel. This solvent mixture was added dropwise to the reaction mixture whereas the temperature was kept below 30 °C. The reaction mixture turned gray and stirring was proceeded at room temperature for further 4 hours. Afterwards, the reaction mixture was decanted from unreacted magnesium and poured into a mixture consisting of NH₄Cl (46.7 mmol, 2.5 g) and 200 g of ice. After separating the phased the aqueous phase was extracted with diethyl ether (three times 200 mL). The combined organic phases were washed with water (500 mL) and were concentrated. *N*-pentane was added dropwise to precipitate possibly formed polymer. Furthermore the organic phase was dried over MgSO₄ and all solid content was filtered off. The residual solvent was removed in vacuo.

The so obtained crude product of 4-(2-hydroxyisopropyl)styrene was directly converted in the second reaction step under a dry atmosphere of nitrogen. Therefore, a three-necked round-bottom flask was equipped with a dropping funnel with septum, a thermometer, a stop-cock and a magnetic stir bar. The flask was loaded with sodium hydride (66.7 mmol, 1.6 g) and with dry THF (20.0 mL). Crude 4-(2-hydroxyisopropyl)styrene (ca. 3.0 g) was dissolved in dry THF (15.0 mL), was degassed and was added to the dropping funnel. This mixture was added dropwise to the reaction mixture while keeping the temperature below 0 °C. After complete addition stirring was proceeded for 1 hour at 0 °C. Afterwards, methyl iodide (10.6 mmol, 6.6 mL) was added dropwise whereas the temperature was kept below 0 °C during the whole addition in order to control the evolution of hydrogen. Again stirring was proceeded for 1 hour at 0 °C and the color of the reaction mixture turned faint yellow. *N*-pentane (30.0 mL) was added to the reaction mixture and stirring was proceeded overnight at room temperature. Formed sodium iodide was filtered off under vacuum and then the solvents were concentrated under vacuum. *N*-pentane (10.0 mL) was added dropwise to precipitate possibly formed polymer. This mixture was centrifuged to remove remaining solids. Afterwards, the solution was separated from the precipitate and the solvent was removed in vacuo. 4-(2-Methoxyisopropyl)styrene was obtained as colorless liquid in a yield of 48 % (8.9 mmol, 1.6 g) and was stored under nitrogen atmosphere in the freezer.

¹H-NMR (CDCl₃, 400 MHz): δ 7.39 (d, 4H, Ar-CH, $J = 3.8$ Hz), 6.76 - 6.68 (dd, 1H, CH, $J = 17.6$ Hz, $J = 10.9$ Hz), 5.77 - 5.72 (dd, 1H, CH₂, $J = 5.8$ Hz, $J = 2.8$ Hz), 5.25 - 5.22 (dd, 1H, CH₂, $J = 5.8$ Hz, $J = 2.8$ Hz), 3.07 (s, 3H, OCH₃), 1.53 (s, 6H, CH₃)

Synthesis of alkyne quencher⁵

The synthesis was done under a dry atmosphere of nitrogen. Therefore a three-necked round-bottom flask which was equipped with a dropping funnel with septum, a septum, a stop cock and a magnetic stir bar and was loaded with phenyl propargyl ether (38.8 mmol, 5.0 mL) and dry THF (25.0 mL). After cooling down to $-30\text{ }^{\circ}\text{C}$ methyllithium (1.6 M solution in diethyl ether, 43.1 mmol, 26.8 mL) was added dropwise. After stirring for fifteen minutes at $-30\text{ }^{\circ}\text{C}$ chlorotrimethylsilane (76.8 mmol, 9.8 mL) was added dropwise as well. Stirring of the reaction mixture proceeded overnight. Afterwards the reaction mixture was filtered and the solvent was removed in vacuo. Final purification was done *via* vacuum distillation from CaH_2 ($p = 0.033\text{ mbar}$, $v = 55.0\text{ }^{\circ}\text{C}$) and trimethyl(3-phenoxy-1-propynyl)silane was obtained as colorless oil in a yield of 83 %.

$^1\text{H-NMR}$ (CDCl_3 , 400 MHz): δ 7.32 – 7.28 (m, 2H, Ar-*H*), 7.01 – 6.97 (m, 3H, Ar-*H*), 4.68 (s, 2H, CH_2), 0.18 (s, 9H, CH_3)

$^{13}\text{C-NMR}$ (CDCl_3 , 100 MHz): δ 157.8 (Ar-*C*), 129.4 (Ar-*C*), 121.4 (Ar-*C*), 115.0 (Ar-*C*), 100.2 (CH_2 -*C*), 92.6 (*C*-Si), 56.7 (CH_2), -0.3 (Si- CH_3)

Synthesis of alkyne-functionalized thymine-moiety

1-(prop-2-ynyl)-5-methylpyrimidine-2,4(1*H*,3*H*)-dione^{6,7} was synthesized in two steps.

The synthesis was done under a dry atmosphere of argon. In the first step a two-necked round-bottom flask was equipped with a reflux condenser with stop cock, a septum and a magnetic stir bar. The flask was loaded with thymine (7.9 mmol, 1.0 g), trimethylchlorosilane (1.6 mmol, 0.2 mL), hexamethyldisilazane (21.7 mmol, 4.5 mL) and anhydrous $(\text{NH}_4)_2\text{SO}_4$ (0.4 mmol, 0.05 g). The reaction mixture was heated under reflux for 24 hours. Afterwards, excess of hexamethyldisilazane was removed in vacuo and crude silylated thymine was obtained as a pale orange solid which was used without purification.

The second step was performed under a dry atmosphere of argon. A two-necked round-bottom flask was equipped with a reflux condenser with stop cock, a septum and a magnetic stir bar. The flask was loaded with crude silylated thymine (ca. 0.9 g) and with propargyl bromide (9.9 mmol, 1.1 mL, 80 wt% in toluene). The reaction mixture was stirred at room temperature for 9 days. Afterwards water (40.0 mL) was added and the reaction mixture was extracted with chloroform (five times 40.0 mL). The combined organic layers were dried over Na_2SO_4 . After filtering off the drying agent the solvent was removed in vacuo and 1-(prop-2-ynyl)-5-methylpyrimidine-2,4(1*H*,3*H*)-dione was obtained as a white powder in a yield of 70 % (3.7 mmol, 0.6 g).

$^1\text{H-NMR}$ (CDCl_3 , 400 MHz): δ 8.38 (s, 1H, *NH*), 7.22 (q, 1H, Ar-*CH*, $J = 1.3\text{ Hz}$), 4.51 (d, 2H, CH_2 , $J = 2.6\text{ Hz}$), 2.45 (t, 1H, *CH*, $J = 2.6\text{ Hz}$), 1.94 (d, 3H, CH_3 , $J = 1.2\text{ Hz}$).

$^{13}\text{C-NMR}$ (CDCl_3 , 100 MHz): δ 163.4 (CO), 150.1 (CO), 138.2 (Ar-*CH*), 111.5 (Ar-*C*), 109.9 (*C*-*CH*), 75.1 (*C*-*CH*), 36.7 (CH_2), 12.4 (CH_3).

[1] M. K. Mishra, B. Wang, J. P. Kennedy, *Polym. Bull.* **1987**, 17, 307.

[2] M. Rother, Diploma Thesis, Martin-Luther-Universität Halle-Wittenberg (Halle (Saale)), **2009**.

[3] M. Schunack, Diploma Thesis, Martin-Luther-Universität Halle-Wittenberg (Halle (Saale)), **2010**.

[4] C. Paulo, J. E. Puskas, *Macromolecules* **2001**, 34, 734.

[5] D. L. Morgan, N. Martinez-Castro, R. F. Storey, *Macromolecules* **2010**, 43, 8724.

[6] H. Griengl, W. Hayden, E. Schindler, E. Wanek, *Archiv der Pharmazie* **1983**, 316, 146.

[7] W. Edward Lindsell, C. Murray, P. N. Preston, T. A. J. Woodman, *Tetrahedron* **2000**, 56, 1233.

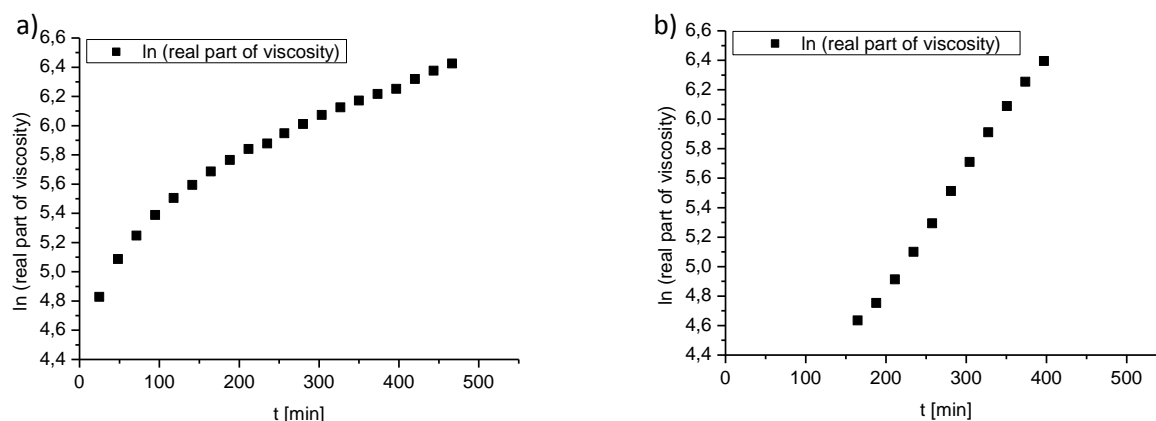
9.2. Autocatalysis in the room temperature copper(I)-catalyzed alkyne-azide "click" cycloaddition of multivalent poly(acrylate)s and poly(isobutylene)s

Derivation of eqn. 3 (eqn. 1 in main text)

The real part of the viscosity of each polymer mixture which was determined *via in situ* rheology experiments was used to evaluate the kinetics of the performed "click" reactions. To derive eqn. 3 equal concentration of reactants (azide; alkyne) at the beginning of the reaction $[A]_0 = [B]_0$ as well as during the reaction ($[A] = [B]$), together with an unchanged Cu(I)-concentration were assumed. Near the gel point a pseudo-first reaction order was postulated in accordance with Ampudia¹ and Barton² as shown in eqn. 1

$$\ln(\eta) = \ln(\eta_0) + k' \cdot t \quad (1)$$

By plotting $\ln(\eta)$ against time t an apparent rate constant k' could be determined as slope as illustrated in Figure S1a and S1b for crosslinking **1e** and **3** and for crosslinking **2** and **4a**.



S1 Graph obtained according to eqn. 1 for crosslinking a) **1e** (1:12, 19100 g/mol) with **3** applying bromotris(triphenylphosphine)copper(I) and TBTA as catalytic system at 20 °C, b) **2** and **4a** (5500 g/mol) applying bromotris(triphenylphosphine)copper(I) as catalyst at 20 °C.

According to Figure S1 a linearization of the data could be performed resulting in k' values of 0.003 min^{-1} in case of crosslinking **1e** and **3** and of 0.016 min^{-1} in the case of crosslinking **2** and **4a**. The apparent rate constants k' were used to determine the rate constants k of the performed crosslinking reactions. Therefore the rate law of first order at the gelation point could be described as

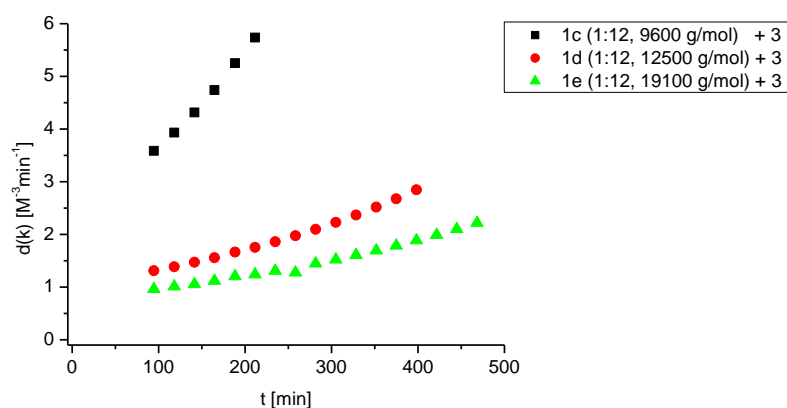
$$-\frac{d\alpha}{dt} = k'(1 - \alpha) \quad \text{by using the conversion which is defined as } \alpha = \frac{[A]_0 - [A]}{A_0} = 1 - \frac{[A]}{[A]_0}. \quad \text{By assuming}$$

a second order kinetics of the "click" reaction itself according to eqn. 2

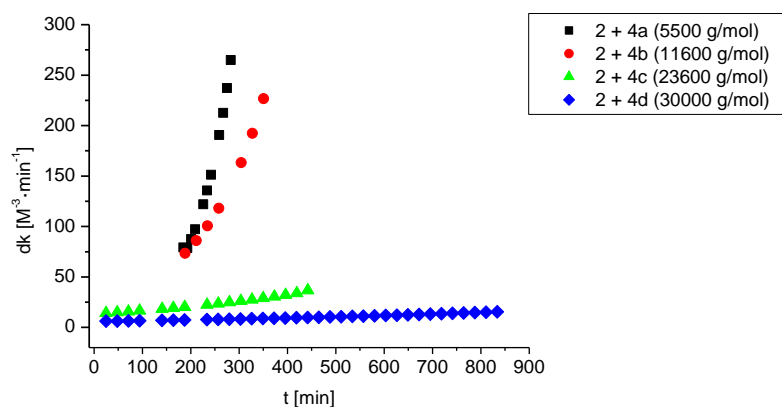
$$-\frac{d[A]}{dt} = k \cdot [A] \cdot [B] \quad (2)$$

the rate constant could be calculated as shown in eqn. 3

$$k = \frac{e^{(k' \cdot t)} - 1}{t \cdot [A]_0} \quad (3)$$

Autocatalysis during crosslinking reactions

S2 Correlation of the derivative of the reaction rate k with respect to time t vs. time t for crosslinking **1c–e** with **3** applying bromotris(triphenylphosphine)copper(I) and TBTA as catalytic system at 20 °C.



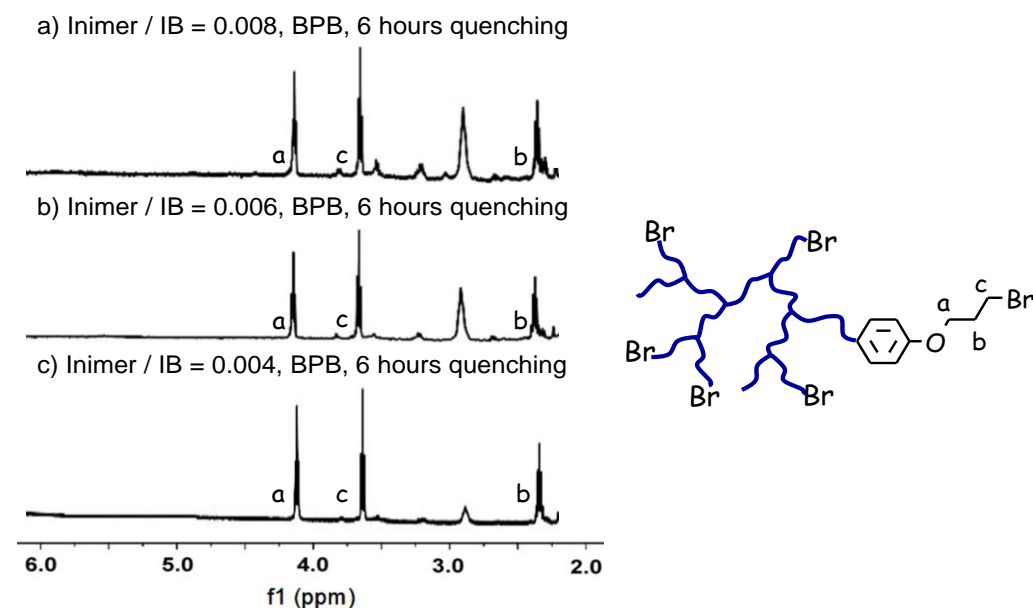
S3 Correlation of the derivative of the reaction rate k with respect to time t vs. time t for crosslinking **2** with **4a–d** applying bromotris(triphenylphosphine)copper(I) as catalyst at 20 °C.

[1] J. Ampudia, E. Larrauri, E. M. Gil, M. Rodríguez, L. M. León, J. Appl. Polym. Sci. 1999, 71, 1239.

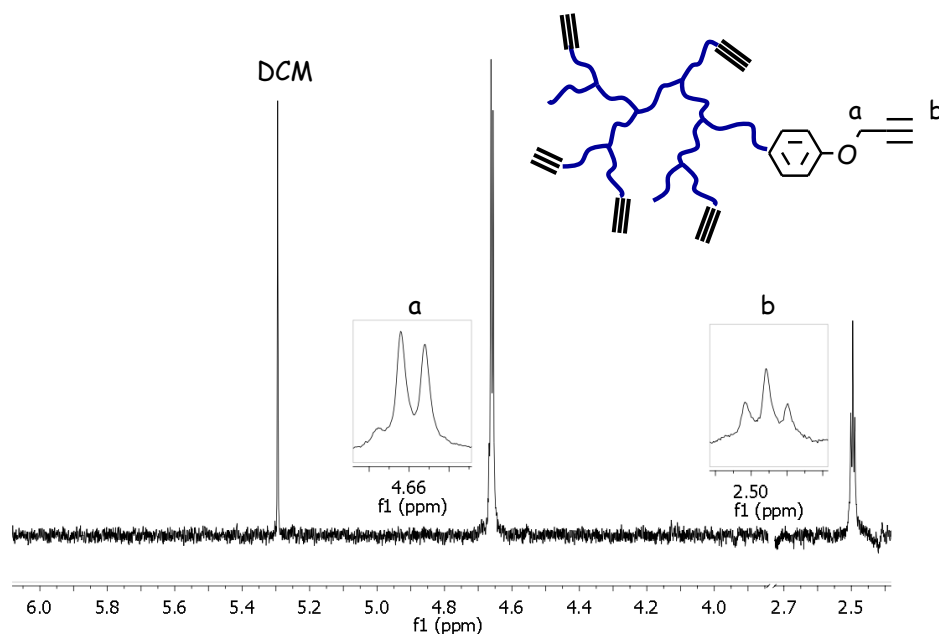
[2] J. M. Barton, D. C. L. Greenfield, K. A. Hodd, Polymer 1992, 33, 1177.

9.3. Characterization of hyperbranched poly(isobutylene)s and kinetic investigations of inimer-type living carbocationic polymerization *via* inline FTIR measurements

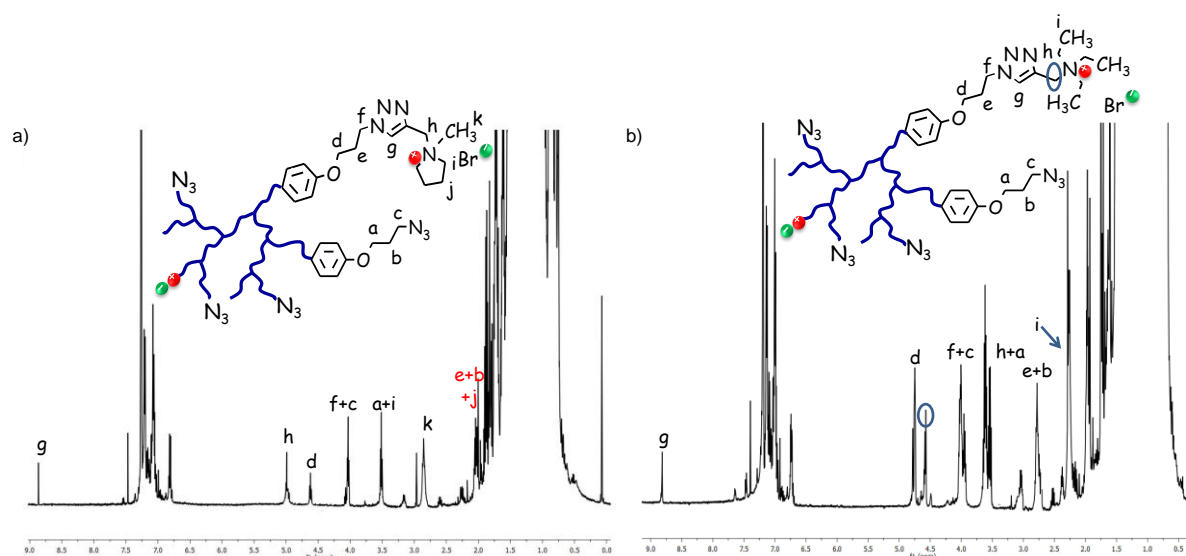
Characterization *via* $^1\text{H-NMR}$ -spectroscopy



S1 Analysis of endgroup distribution of hyperbranched PIBs *via* $^1\text{H-NMR}$ -spectroscopy after 6 hours quenching with BPB (26 equ. of inimer) followed by ATMS (26 equ. with respect to inimer) applying different inimer to isobutylene ratios. IM / IB = 0.008: a) Inimer / IB = 0.008, BPB and ATMS, 6 hours quenching, b) Inimer / IB = 0.006, BPB and ATMS, 6 hours quenching, c) Inimer / IB = 0.004, BPB and ATMS, 6 hours quenching.



S2 $^1\text{H-NMR}$ -spectrum of hyperbranched alkyne-functionalized PIB (2) after 20 hours quenching with TMPPS (30 equ. of inimer). IM / IB = 0.006.



S3 ^1H -NMR-spectrum of hyperbranched PIBs containing an ionic moiety: a) **4a**, b) **4b**.

Kinetic investigations of inimer-type living carbocationic polymerization via inline FTIR-measurements.

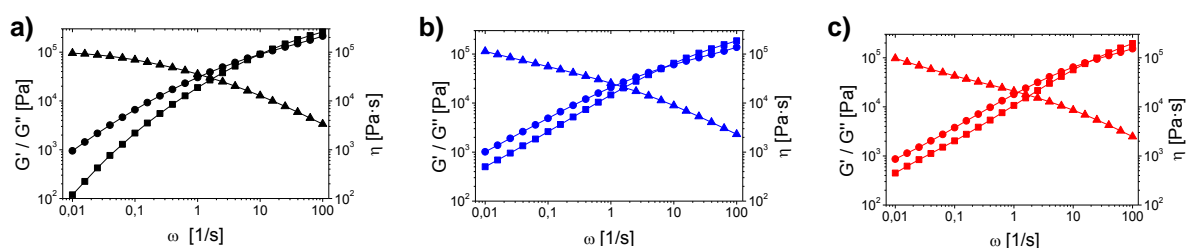
Table S1 Kinetic investigations of inimer-type living carbocationic polymerization via inline FTIR-measurements: determination of k_{app} out of first-order kinetic plots and calculation of the propagation constant k_p and the run number (RN).

Entry	inimer / IB	$[\text{IB}]_0$ ($\text{mol}\cdot\text{L}^{-1}$)	k_{app} (10^2 s^{-1}) ^a	k_p ($10^8 \text{ s}^{-1}\text{M}^{-1}$) ^b	RN ^c
1	0.010	2.30	2.03	1.27	3.88
2	0.006	1.91	0.92	2.65	6.73
3	0.004	2.00	0.34	3.37	8.98

^a Determined by inline FTIR-spectroscopy $\ln[M]_0/[M]_t$ plot. ^b Determined by calculation $k_i = 7.5 \cdot 10^7 \text{ 1/s}$, $k_i = 15 \text{ 1/(s M}^2\text{)}^1$ with k_p determined by combination of following equations: $\ln[M]_0/[M]_t = k_{app}t$ and $k_{app} = k_p K_{eq} I_0 [LA]_0^2$ with respect to the dimeric form of the LA²

^c Determined by calculation $RN = (k_p [P_n + Ti_2Cl_6^-] [M]) / (k_i [P_n + Ti_2Cl_6^-]) = k_p [M] / k_i$.

Rheology investigations of the pure hyperbranched polymers 4a-4b and 1b.



S4 Frequency sweep measurements of selected hyperbranched PIBs at 20°C a) **1b**, b) **4a** and c) **4b**.

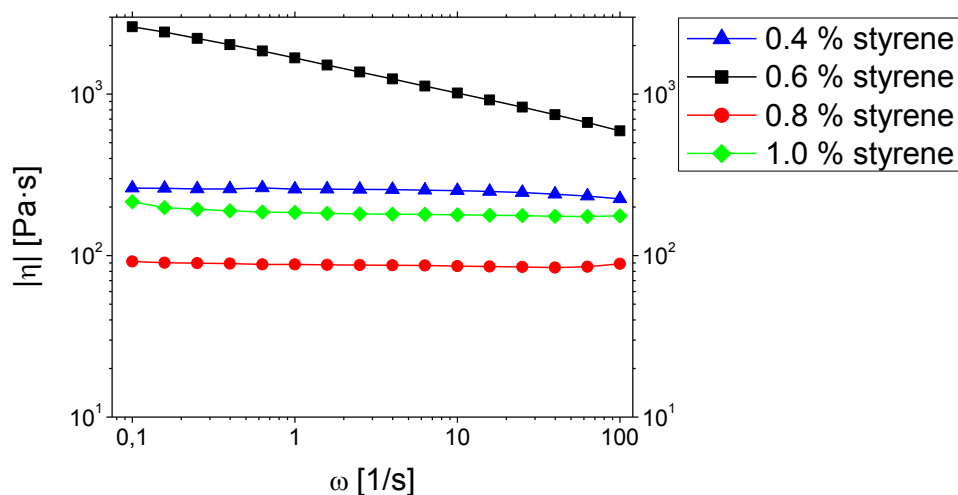
Rheology investigations of poly(isobutylene-co-styrene)s prepared via LCCP³

0.4 % styrene ($M_n = 13,200$ g/mol, $M_w/M_n = 1.34$)

0.6 % styrene ($M_n = 11,700$ g/mol, $M_w/M_n = 1.33$)

0.8 % styrene ($M_n = 10,900$ g/mol, $M_w/M_n = 1.30$)

1.0 % styrene ($M_n = 7,300$ g/mol, $M_w/M_n = 1.23$)



S5 Absolute value of the viscosity versus frequency of containing 0.4 % styrene (blue), 0.6 % styrene (black), 0.8 % styrene (red) and 1.0 % styrene (green).

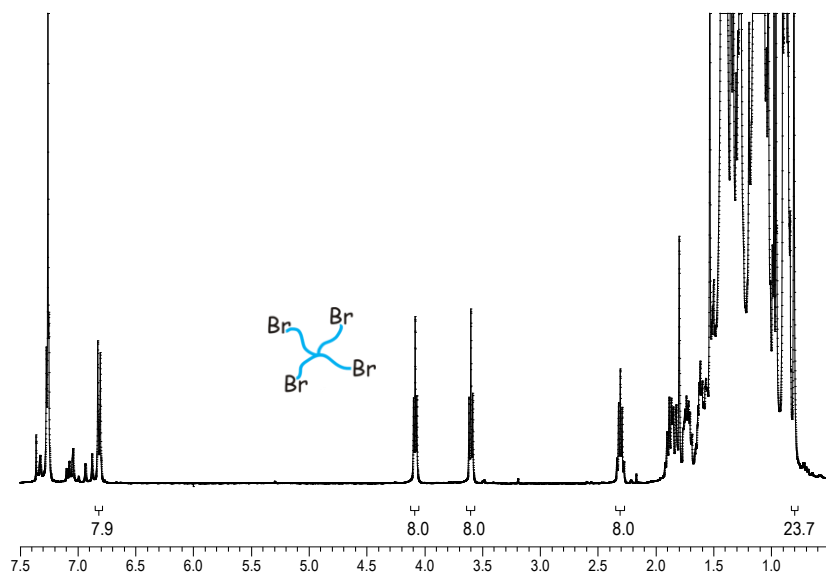
[1] R. F. Storey and Q. A. Thomas, *Macromolecules*, 2003, **36**, 5065-5071.

[2] J. E. Puskas, S. W. P. Chan, K. B. McAuley, S. Shaikh and G. Kaszas, *J. Polym. Sci. Part A: Polym. Chem.*, 2005, **43**, 5394-5413.

[3] G. Kaszas, J. E. Puskas, J. P. Kennedy and W. G. Hager, *J. Polym. Sci. Part A: Polym. Chem.*, 1991, **27**, 427-435.

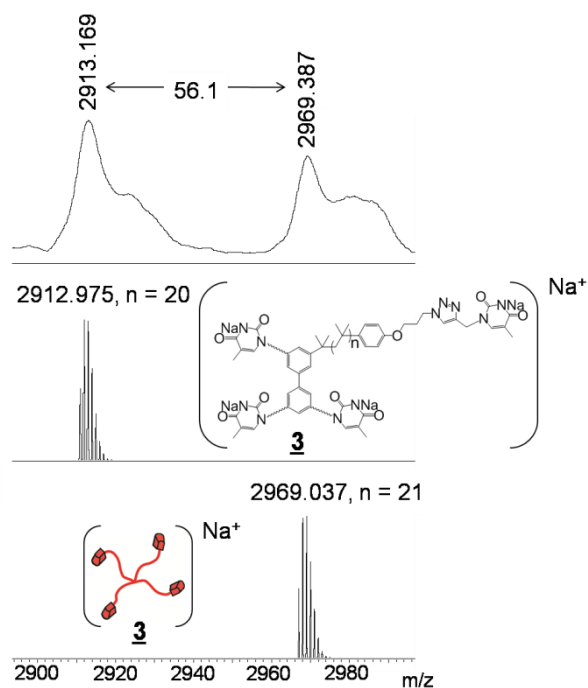
9.4. Characterization of four-arm star poly(isobutylene)s and analysis of SAXS-data according to the Percus-Yevick model

¹H-NMR-spectrum of four-arm star bromide-telechelic PIB 1.

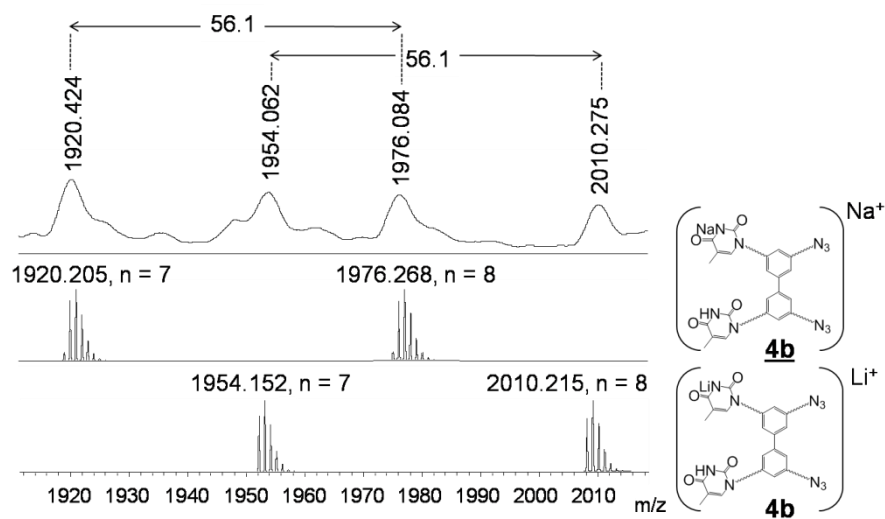


S1 ¹H-NMR-spectrum of four-arm star bromide-telechelic PIB 1.

MALDI- ToF-mass spectrum of four-arm star thymine-telechelic PIB 3 and of four-arm star PIB 4b.

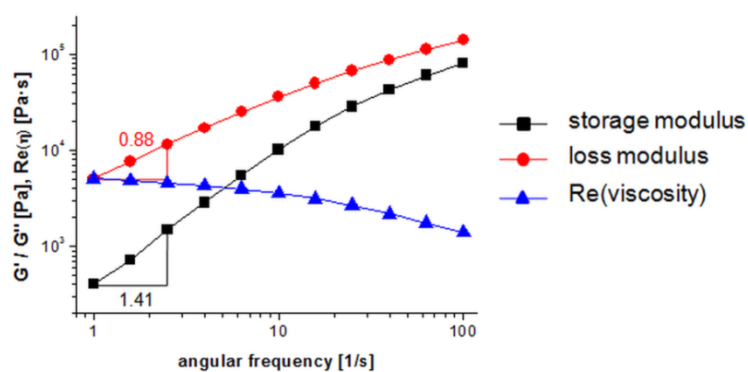


S2 MALDI-ToF-mass spectrum of four-arm star thymine-telechelic PIB 3.



S3 MALDI-ToF-mass spectrum of four-arm star PIB **4b**.

*Rheology investigation of the polymer mixture composed of trivalent alkyne-telechelic PIB and four-arm star PIB **4b**.*



S4 Rheological investigation of an equimolar polymer mixture with respect to the azide- / alkyne-ratio composed of tri-arm star alkyne-telechelic PIB and four-arm star PIB **4b**.

Analysis of SAXS-data according to the Percus-Yevick model¹⁻³

The total scattering intensity can be calculated according to equation 1 whereas a structure factor is multiplied by a form factor and added to a flat background.

$$I(q) = KS(qR_2) \int_0^\infty dR_1 \phi(qR_1) f_p(q, R_1, \overline{R_1}, \sigma) V^2(R_1) + C + aq^{-n} \quad (\text{Eq. 1})$$

$K \equiv$ *contrast factor*, depending on the differences of the electron density between the matrix C and hard particles

$S(qR_2) \equiv$ *structure factor* according to the hard sphere model, depending on the radius R_2 of hard spheres and on the scattering vector q

$\Phi(q) \equiv$ *form factor of the scattering objects*, depending on the scattering from the core of formed spherical objects with radius R_1

$V \equiv$ *volume of the sample*

$C + aq^{-n} \equiv$ *scattering background + power law background* due to large objects and grain boundaries

[1] D. J. Kinning, E. L. Thomas, *Macromolecules* **1984**, *17*, 1712.

[2] M. Schwab, B. Stühn, *Phys. Rev. Lett.* **1996**, *76*, 924.

[3] T. Yan, K. Schröter, F. Herbst, W. H. Binder, T. Thurn-Albrecht, *Macromolecules* **2014**, *47*, 2122.

DIANA DÖHLER (M. Sc.)
WALDMEISTERSTRASSE 19
06120 HALLE (SAALE)
TELEFON: 0 17 3 / 8 23 23 48
E-MAIL: DIANA.DOEHLER@CHEMIE.UNI-HALLE.DE
WWW.MACROCHEM.UNI-HALLE.DE

CURRICULUM VITAE

Geburtsdatum: 01-03-1988
Geburtsort: Werdau
Nationalität: Deutsch
Familienstand: ledig



AUSBILDUNG

seit 12/2011 Promotionsstudium am Institut für Chemie / Technische und Makromolekulare Chemie, Martin-Luther-Universität Halle-Wittenberg unter der Leitung von Prof. Dr. Wolfgang Binder

Thema: „Vernetzungsmethoden für selbstheilende Polymere: “Klick”-Vernetzung und Supramolekulare Clusterbildung“ – ”Crosslinking Approaches towards Self-Healing Polymers: “Click”-Crosslinking and Supramolecular Clustering“

09/2011 Abschluss des Master-Studiengangs Chemie (M. Sc.; Gesamtprädikat: sehr gut).

04/2011 – 09/2011 Masterarbeit: „Flüssige Polyisobutylene als Polymere für selbstheilende Materialien“ – ”Liquid Polyisobutylenes as Polymers for Self-Healing Materials“ (Bewertung: sehr gut).

2009 – 2011 Master-Studiengang Chemie
Martin-Luther-Universität Halle-Wittenberg.

09/2009 Abschluss des Bachelor-Studiengangs Chemie (B. Sc.; Gesamtprädikat: sehr gut).

04/2009 – 07/2009 Bachelorarbeit: „Kinetik der Copolymerisation von Polyisobutylen mit substituierten Styrolderivaten“ – ”Kinetics of Copolymerisation of Polyisobutylene with substituted Styrene Derivatives“ (Bewertung: sehr gut).

2006 – 2009 Bachelor-Studiengang Chemie
Martin-Luther-Universität Halle-Wittenberg.

1998 – 2006 Gymnasium, Werdau (Abiturnote: 1.1).

1994 – 1998 Grundschule, Werdau.

SPRACHKENNTNISSE

Deutsch (Muttersprache)
 Englisch (Fließend in Wort und Schrift)
 Russisch (Grundkenntnisse)

PUBLIKATIONEN

- Shaygan Nia, A.; Rana, S.; Döhler, D.; Jirsa, F.; Meister, A.; Guadagno, L.; Koslowski, E.; Bron, M.; Binder, W. H., Carbon Supported Copper Nanomaterials: Recyclable Catalysts for Huisgen [3+2] Cycloaddition Reactions. *Chem. Eur. J.* **2015**, DOI: 10.1002/chem.201501217.
- Döhler, D.; Michael, P.; Neumann, S.; Binder, W. H., Biomimetische Materialien / Selbstheilende Polymere. *Chem. Unserer Zeit* **2015**, DOI: 10.1002/ciuz.201500686.
- Michael, P.; Döhler, D.; Binder, W. H., Improving Autonomous Self Healing via Combined Chemical / Physical Principles. *Polymer* **2015**, doi:10.1016/j.polymer.2015.01.041.
- Döhler, D.; Peterlik, H.; Binder, W. H., A dual crosslinked self-healing system: Supramolecular and covalent network formation of four-arm star polymers. *Polymer* **2015**, 10.1016/j.polymer.2015.01.073.
- Shaygan Nia, A.; Rana, S.; Döhler, D.; Noirfalise, X.; Belfiore, A.; Binder, W. H., Click chemistry promoted by graphene supported copper nanomaterials. *Chem. Commun.* **2014**, 50 (97), 15374-15377.
- Vasiliu, S.; Kampe, B.; Theil, F.; Dietzek, B.; Döhler, D.; Michael, P.; Binder, W. H.; Popp, J., Insights into the Mechanism of Polymer Coating Self-Healing Using Raman Spectroscopy. *Appl. Spectrosc.* **2014**, 68 (5), 541-548.
- Döhler, D.; Zare, P.; Binder, W. H., Hyperbranched Polyisobutylenes for Self-Healing Polymers. *Polym. Chem.* **2014**, 5, 992-1000.
- Zhao, Y.; Döhler, D.; Lv, L.-P.; Binder, W. H.; Landfester, K.; Crespy, D., Facile Phase-Separation Approach to Encapsulate Functionalized Polymers in Core-Shell Nanoparticles. *Macromol. Chem. and Phys.* **2014**, 215, 198-204.
- Stojanovic, A.; Appiah, C.; Döhler, D.; Akbarzadeh, J.; Zare, P.; Peterlik, H.; Binder, W. H., Designing melt flow of poly(isobutylene)-based ionic liquids. *J. Mater. Chem. A* **2013**, 1, (39), 12159-12169.
- Herbst, F.; Döhler, D.; Michael, P.; Binder, W. H., Self-healing polymers via supramolecular forces. *Macromol. Rapid. Commun.* **2013**, 34, (3), 203-220.
- Döhler, D.; Michael, P.; Binder, W. H., in *Self Healing Polymers: from Principle to Application*, ed. W. H. Binder, Wiley-VCH Verlag GmbH & Co. KGaA, Weinheim, 2013, pp. 7-60.
- Döhler, D.; Michael, P.; Binder, W. H., Autocatalysis in the room temperature copper(I)-catalyzed alkyne-azide "click" cycloaddition of multivalent poly(acrylate) and poly(isobutylene)s. *Macromolecules* **2012**, 45, (8), 3335-3345.
- Schunack, M.; Gragert, M.; Döhler, D.; Michael, P.; Binder, W. H., Low-Temperature Cu(I)-Catalyzed "Click" Reactions for Self-Healing Polymers. *Macromol. Chem. Phys.* **2012**, 213, (2), 205-214.
- Hackethal, K.; Döhler, D.; Tanner, S.; Binder, W. H., Introducing Polar Monomers into Polyisobutylene by Living Cationic Polymerization: Structural and Kinetic Effects. *Macromolecules* **2010**, 43, (4), 1761-1770.

PRÄSENTATIONEN AUF KONFERENZEN

D. Döhler, P. Michael, S. Neumann, W. H. Binder: Mechanochemical and Supramolecular Self-Healing Polymers; Kick-off Meeting of Priority Programme SPP 1568 "Design and Generic Principles of Self-Healing Materials", März 23-24 2015, Jena, Deutschland. Poster Präsentation.

D. Döhler, P. Michael, W. H. Binder: Mechanochemical and Supramolecular Self-Healing Polymers; Meeting of Priority Programme SPP 1568 "Design and Generic Principles of Self-Healing Materials", Dezember 11-12 2014, Jena, Deutschland. Vortrag.

W. H. Binder, F. Herbst, P. Michael, D. Döhler, P. Zare, A. Stojanovic: Self-healing by hydrogen bonding and click reactions; Dutch German symposium on Self Healing Materials, September 30-Oktober 1 2013, Gouda, Niederlande. Vortrag.

D. Döhler, P. Michael, W. H. Binder: Investigation of autocatalytic crosslinking reactions based on room temperature "click" chemistry as versatile tool for designing self-healing polymers; ICSHM 2013, Juni 16-20 2013, Ghent, Belgien. Vortrag.

F. Herbst, A. Stojanovic, P. Zare, P. Michael, D. Döhler, W. H. Binder: Combined Supramolecular and Covalent Self-Healing Polymers; Meeting of Priority Programme SPP 1568 "Design and Generic Principles of Self-Healing Materials", April 8-9 2013, Weimar, Deutschland. Vortrag.

D. Döhler, P. Michael, W. H. Binder: Self-healing polymers; Polymeric Materials 2012 (P 2012), September 12-14 2012, Halle (Saale), Deutschland. Vortrag.

P. Michael, D. Döhler, W. H. Binder: Autocatalytic Effects in Copper(I)-catalyzed Alkyne-azide-click Reactions (CuAAC); Meeting of Priority Programme SPP 1568 "Design and Generic Principles of Self-Healing Materials", August 1-2 2012, Jena, Deutschland. Vortrag.

D. Döhler, P. Michael, W. H. Binder: Autocatalysis in the room temperature copper(I)-catalyzed alkyne-azide "click" cycloaddition: a strategy for self-healing polymeric materials; Junior Euromat 2012, Juli 23-27 2012, Lausanne, Schweiz. Poster Präsentation.

D. Döhler, P. Michael, M. Malke, P. Zare, A. Stojanovic, F. Herbst, W. Binder: Self-healing Polymers by Shear Induced Crosslinking of Liquid Polymers; Expertentreff "Neue Materialien", März 20 2012, Halle (Saale), Deutschland. Poster Präsentation.

W. Binder, P. Michael, D. Döhler: Liquid Polyisobutylenes as Polymers for Self-Healing Materials and their Investigation via *in situ* Rheology; Kick-off Meeting of Priority Programme SPP 1568 "Design and Generic Principles of Self-Healing Materials", Oktober 13-14 2011, Jena, Deutschland. Vortrag.

W. Binder, M. Schunack, D. Döhler and P. Michael: Liquid Biocompatible Polymers as Reactants in Self-Healing Materials; Euromat 2011, September 11-15 2011, Montpellier, Frankreich. Vortrag.

Halle (Saale), 16.06.2015

Diana Döhler

EIGENSTÄNDIGKEITSERKLÄRUNG

Ich erkläre an Eides statt, dass ich die vorliegende Dissertation mit dem Titel "Crosslinking Approaches towards Self-Healing Polymers: "Click" Crosslinking and Supramolecular Clustering" selbstständig und ohne fremde Hilfe verfasst, keine anderen als die von mir angegebenen Quellen und Hilfsmittel benutzt und die den zitierten Werken wörtlich oder inhaltlich entnommenen Stellen als solche kenntlich gemacht habe.

Außerdem erkläre ich, dass ich die vorliegende Dissertation an keiner anderen wissenschaftlichen Einrichtung zur Erlangung eines akademischen Grades eingereicht zu haben.

Halle (Saale), 16.06.2015

Diana Döhler